Millet growth in windbreak-shielded fields in the Sahel

Experiment and Model

Propositions

1   Reintroduction of trees in Sahelian agroecosystems is beneficial even when crop yields are not enhanced.
    This thesis

2   Agroforestry systems illustrate that progress not necessarily derives from the change of a single dominating factor, but can be the result of the combined action of several small modifications.
    This thesis

3   In Sahelian agroforestry systems, water is the most competitive factor early in the season and light is the most competitive factor late in the growing season.
    This thesis

4   Restricting the description of competition between species in a model with a high resolution in time and space to the most growth-limiting factor is too simple.
    This thesis

5   Fragmentary knowledge of spatial and temporal distribution of roots and their resource uptake is a major constraint of agroecosystem simulation models.
    Livesley, S.J., Gregory, P.J. and Buresh, R.J., 1997. Approaches to modelling root growth and the uptake of water and nutrients. Agroforestry Forum 8(2): 24-27.
    This thesis

6   In semi-arid regions the growing season should be characterised in terms of favourable and unfavourable rainfall distribution rather than in terms of total annual rainfall.
    This thesis

7   To guarantee sustainable food production in the Sahel introduction of external fertilisers is indispensable.
    Breman, H., 1998. Soil Fertility Improvement in Africa, A Tool for a By-product of sustainable production. African Fertilizer Market 11(5).

8   The central position of soil in the software system for model development APSIM witnesses the importance it deserves.

McCown, R.L. et al. 1996. APSIM: A novel software system for model development, model testing, and simulation in agricultural research. Agricultural System 50: 255-271.

9   Kunst lebt durch den Ausstausch zwischen Künstler und Betrachter; Natur lebt sich selbst.

10   Es gibt nur eine Warheit, aber immer zwei Möglichkeiten und unendlich viele Ansichten.

11   Ohne die Suche nach Wahrheit und die Freiheit des Spiels verkümmert Wissenschaft.

12   Der Grund warum wir trotz internationaler Hilfe Afrika noch Entwicklungsland nennen findet sich in gleichzeitiger Anstrengung es als solches zu erhalten.

13   More than 2500 dissertations show that love is not all we need.

Martina Mayus
"Millet growth in windbreak-shielded fields in the Sahel"
Wageningen, 2 November, 1998

Millet growth in windbreak-shielded fields in the Sahel

Experiment and Model

Martina Mayus

Cover design: Ernst van Cleef.

Acknowledgements

CONTENTS

Part A - EXPERIMENT
The effect of windbreaks on microclimate, growth resources, and crop growth

1 INTRODUCTION

1.1   Environmental setting

The Sahelian zone of Africa belongs to the poorest and most fragile agricultural areas of the world, while its population is highly dependent on agriculture. In the last three decades, agricultural production has lagged behind the population growth (ca. 3%) (Jayne et al., 1989). Farmers, usually of low purchasing power, have to produce under rainfed, traditional farming systems with little or no external inputs. Consequently, yields per hectare are low. This, in combination with rapid growth of the population and the extreme drought years from 1968 - 1977 has led to conflicts between sufficient food production in the short-term and traditional farming practices that preserve soil fertility. Decreasing lengths of fallow periods, cultivation of marginal lands, overgrazing, and deforestation, led to soil degradation and decreased the already low average production per hectare. Future food supply for Sahelian people is insecure due to increasing soil degradation, to which wind erosion contributes an important part (Sterk, et al., 1996). There is an urgent need to develop land use and cropping systems that stop soil degradation, and enhance production in a sustainable way at low costs.
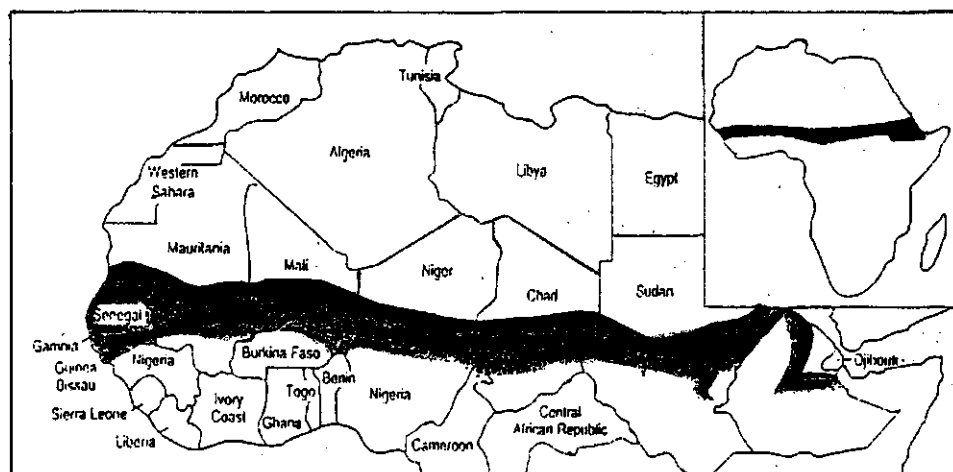
Figure 1.1   Geographical extent of the Sahelian zone between the 100 - 600 mm isohyetes (Source: Tauer and Humborg, 1992).

The Sahel, a semi-arid region between the Sahara desert (ca. 16° N latitude) in the north and the more humid Sudanian zone in the south, stretches from Senegal to Ethiopia (Fig. 1.1). The zone has no distinct boundaries with the Sahara or the Sudan (Tauer and Humborg, 1992), but is often defined as the region between the 100 mm and the 600 mm isohyetes (Le Houérou, 1989). From north to south temperature decreases. The region is characterized by a single short rainy season of three to four months between May and October and a dry period in the remainder of the year. Rains are caused by monsoon winds coming from the Gulf of Guinea and by the northern movement of the Intertropical Convergence Zone (Le Houérou, 1989). Between years, as well as within a rainy season, fluctuations in precipitation are high, and periodic droughts are a common feature, so that agricultural production is very unstable (Sivakumar et al., 1993). Individual showers are often short and intense, triggering runoff and soil loss (Hoogmoed and Stroosnijder, 1984).

Important soil types of the Sahel are Arenosols and Luviosols (FAO taxonomy). These soils are sandy, acidic, deficient in most nutrients (particularly in phosphorus and nitrogen), low in organic matter content and have a low nutrient- and water-holding capacity (Sivakumar, 1992). Soils are susceptible to form crusts, which hamper infiltration and facilitate runoff (Hoogmoed and Stroosnijder, 1984) and contribute to the general high variability of soils over short distances (Brouwer et al., 1993).

Livelihood changes from north to south with increasing rainfall. In the north, where the climate is too dry for crop production, only nomadic pastoralism exists (Tauer and Humborg, 1992). Sedentary rainfed farming is widespread where rainfall exceeds 400 mm. Many farmers keep small livestock for milk and meat. Proceeding to the more humid south, cropping and husbandry more and more co-exist at shorter distances, up to regions where populations undertake both (Tauer and Humborg, 1992). The principal food crop millet (*Pennisetum glaucum* (L.) R.Br.) is followed by sorghum (*Sorghum biocolor* (L.) Moench) in better regions. These cereals are often intercropped with a legume, usually cowpea (*Vigna unguicultata* (L.) Walp.) or groundnut (*Arachais hypogaea* L.). Vegetables and fruits are grown in small gardens close to the villages or near streams (Tauer and Humborg, 1992).

In the north Sahel, water deficiency is the prime constraint to crop production, but towards the south low soil fertility, for phosphorus in particular, becomes generally more growth limiting than low and variable rainfall (Penning de Vries and Djitèye, 1982; Bley, 1990; Payne et al., 1991a; Hafner et al., 1992). Traditionally, farmers tried to sustain the fertility of the soil by rotating cropping periods with fallow periods. In recent decades, however, the increased demand for food, concurrent with a general decline in yields per hectare due to droughts and incipient soil degradation, have forced farmers to extend the agricultural area (Jayne et al., 1989). Fallow periods were shortened or even eliminated, and poor marginal and communal

grazing lands were cultivated (Jayne et al., 1989; Tauer and Humborg, 1992). This has led to a reduction in bush and tree cover, additionally to trees killed by drought and more frequently cut as a result of the growing demand for wood for fuel and construction. Furthermore, the increasing number of livestock has led to heavy overgrazing of pastures (Tauer and Humborg, 1992). Overall, the decline in natural vegetation has increased the soil area exposed to erosion by water and wind (Sivakumar and Wallace, 1991; Michels et al., 1993).

Wind erosion is a further constraint for crop productivity (Michels et al., 1993). During the onset of the rainy season, strong eastern monsoon winds of 10 to 30 minutes duration (Sterk, 1997) reaching maximum speeds up to 100 km h^{-1}, may precede rainfall. At that time of year the soils are dry, loose, and bare, so that storms easily cause sand transport near the soil surface. Thus, storms may damage the crop by abrasion and burial, and contribute to a reduction in soil fertility and soil degradation. A well known wind erosion control measure is the use of windbreaks that reduce the wind velocity near the soil surface and, hence, protect soil and crops which often results in increased agricultural production. But there is another reason why windbreaks are interesting for the Sahel: Windbreaks consisting of trees or shrubs can spread farmers risks by providing extra income through useful byproducts such as livestock feed and the highly valued wood (Lamers, 1995). In this thesis, the term windbreak (WB) is used for a living barrier consisting of trees or shrubs if not explicitly mentioned otherwise.

Since arable land can hardly be expanded, higher crop production must result from improved yields per unit area. In on-stage trials significant increases in yield have been achieved through the use of external inputs, e.g. chemical fertilizers (Christianson et al, 1990b; Payne, 1991a; van Duivenbooden and Cissé 1992; Rebafka, 1993). However, under the prevailing conditions of environment, farmers' resources, marketing systems, and agricultural price policies, it is not realistic to expect dramatic yield increases based on technological improvements. Instead, cropping systems have to be developed that use nutrient and soil water resources as efficiently as possible (Sivakumar and Wallace, 1991) with management practices that (mainly based on natural resources and low costs) reduce soil degradation, enhance production in a sustainable way and reduce farmers' risks. An agroforestry system might be one of the options.

1.2   Millet

Pearl millet (*Pennisetum glaucum* (L.) R.Br.), a C4 tropical cereal, is particularly adapted to conditions of high temperatures, nutrient-poor soils and low rainfall. Pearl millet is the most drought tolerant of all domestic cereals and probably originated in the West African savanna (Konaté, 1984). It is grown mainly in the semi-arid tropics where annual rainfall ranges

between 200 - 800 mm, primarily as grain and secondary as a forage crop, but millet stalks are also used as mulch, fuel and construction material (Lamers and Feil, 1995). More than 95% of the world's millet crop is grown in Africa and South Asia, principally in the Sahelian-Sudanian zones of West Africa and in semi-arid regions east and southeast of the Thar desert in India (Huda et al., 1984). Crops are grown at low plant densities to limit intraspecific competition for water and nutrients: 5,000 - 10,000 plants per ha in the African Sahel and 30,000 - 100,000 plants per ha in India (Pearson, 1985).

In the Sahel, more than half of the area cropped with millet is situated in Niger (FAO, 1992), where average grain yields are among the lowest, varying from 2000 kg ha^{-1} in the south (Maradi, Gaya) to complete crop failure in unfavorable years in regions north of Tillabari (Fechter, 1993). Abiotic constraints to millet production include low natural soil fertility, low and erratic rainfall, high intensity rains, sand storms, high air and soil temperatures as well as traditional management practices such as low densities and no fertilization. Biotic constraints include the low genetic yield potential of local landraces, diseases such as millet head caterpillar (*Heliocheilus albipunctuella*), the parasitic weed *Striga*, and grain eating birds (Spencer and Sivakumar, 1987). In Table 1.1 grain yields for Sahelian countries are shown for 1989 and 1992, which have been a rather dry and a wet growing season, respectively for, e.g. Niger (Niamey: 462 and 586 mm rain y^{-1}) and Burkina Faso (Ougadougu: 680 and 760 mm rain y^{-1}).

Table 1.1 Millet grain yields at 8 Sahelian countries. 1989 was a rather dry and 1992 a rather wet growing season for Niger and Burkina (Source: FAO, 1992).

Country	Grain yield (kg ha^{-1})	
	1989	1992
Burkina Faso	508	667
Chad	342	490
Ethiopia	955	963
Mali	777	773
Mauritania	496	333
Niger	374	423
Senegal	670	642
Sudan	103	275

In rainfed agricultural systems with a short growing season the timing of sowing is one of the important factors determining a good harvest or crop failure. Sowing can only take place after a

minimum amount of rainfall, because germination and plant establishment are strongly related to soil moisture content and the occurrence of sufficient rainfall after sowing is uncertain. Moreover, a significant relation between the date of onset of the rainy season and the length of the growing season was found by Sivakumar (1988). If the onset of the rains is delayed, the growing season is generally shorter, and vice versa. Generally, there is a positive relationship between yield and length of growing season, which is less than 120 days for large parts of the Sahel (Sivakumar, 1989). As an adaptation to regional differences in the length of the growing season, early, middle and late millet varieties exist: long (120 - 140 days), middle (ca. 115 days) and short (80 - 90 days) cycle millet, respectively. Furthermore, cultivars are improved for production and response to fertilizer. Breeding programs are still developing cultivars and improved genetic material with stable and high yielding potential under improved management (ICRISAT Annual Report, 1994).

Since the late 1970's much research on millet (physiology, phenology, ecology, soil and crop management, production) has been carried out, mainly in India, but also in several West African countries under local, and under a range of controlled growth conditions and management practices (Maiti and Bidinger, 1981; Pearson, 1985; Ong and Monteith, 1985; Mahalakshmi et al., 1987; Christianson et al., 1990a; Wallace et al., 1990; Payne et al,. 1990; Hafner et al., 1992). However, knowledge of root growth and tillering, in particular for detailed simulation models, is still insufficient. There is evidence that improved and stabilized yields can be expected from application of fertilizer and crop residues, improved varieties, better management of pest and diseases, and also from intercropping (e.g. millet/cowpea, Ntare et al., 1989), alley-cropping (Leucaena/millet, Corlett et al., 1992) and by windbreak-cropping systems. For the Sahel the study on the response to windbreak effects, started by Long and Persaud (1988), Banzhaf (1988) and Brenner (1991), will be continued in this thesis.

1.3   Windbreaks

In the vegetation zones where trees and shrubs were growing spontaneously, agroforestry systems, an association of tree, crops and/or animals, are probably as old as farming. According to the ICRAF definition, agroforestry systems are not simply farming systems where both trees and crops or animals give useful products to the farmer, but systems where tree and crop (and/or animal) production interact (Lundgren and Raintree, 1982; Nair, 1993). Many forms of agroforestry systems do exist differentiated according to their functions, and ecological, cultural and social environment, in temperate and tropical regions (Smith, 1995). In the Sahel the main type of agroforestry is parkland: trees, e.g. *Faidherbia albida* dispersed in cropped fields extended over large areas (Vandenbeldt and Williams, 1992). Trees can have

multiple benefits, i.e. provide shade for the people and their cattle, fodder for animals during the dry season, fruits and seeds, and valuable wood and protect the soil from wind erosion (Lamers, 1995). With the reduction in tree cover these advantages have diminished and soil degradation enhanced. When the erosion problem was additionally aggravated by the severe droughts in the early 1970's, agroforestry systems were recognized as systems that meet the demand of local people for tree products, and improve sustainability of crop production (den Heijer, 1990; Smith, 1995). Reforestation started, and development projects reinforced windbreaks, trees planted in rows perpendicular to the prevailing wind direction during storms (den Heijer, 1990; Michels, 1994). Windbreaks (WBs) in the Sahel have the prime objective of reducing wind speed and, consequently, wind erosion.

Wind erosion events, occurring during the dry season by strong northeastern winds ('Harmattan') and at the onset of the rainy season due to strong eastern winds, cause an enormous amount of eolian transport and deposition over short (within a field) and long distances (Sterk, 1997). Hence, in the source areas soil fertility decreases through loss of nutrient-rich top soil (Sterk et al., 1996). The direct effect of wind erosion on the crop is abrasion and burial of seedlings. Abrasion delays crop development and growth, but usually plants such as millet recover soon, so that final yields are often not reduced (Michels et al., 1993). A more serious problem occurs when seedlings are covered, for a period of several dry days, so that the leaves burn and die under the hot sand. It happens, especially in the north of the Sahel, that whole fields have to be resown (Michels et al., 1993). The most commonly used erosion control measure is mulching of millet stalks and to a lesser extent tree branches. Its application, however, is limited by insufficient availability of these materials (Michels et al., 1994; Sterk and Spaan, 1997).

A long list of research reports, from all over the world, demonstrate that windbreaks can increase yields (Kort, 1988), not only by reducing the mechanical damage of strong winds, but also through a change in the microclimate, that results, though not always, in more favorable temperature, moisture and humidity conditions for crop growth (Rosenberg, 1974; McNaughton, 1988, Brenner et al., 1995b). In the vicinity of the windbreak, crop growth might be enhanced by improved soil fertility because of nitrogen fixation by leguminous trees, capture and cycling of nutrients by deep-rooted trees and higher soil organic matter contents resulting from litter production by trees (Ong et al, 1991; van Noordwijk et al., 1996) or reduced when between species allelopathic interactions and severe competition for light, water and nutrients occur. In addition, trees can harbour pests and crop pathogens or attract wild animals that may diminish potential WB benefits. In temperate regions the overall effect of windbreaks on crop production potential is generally beneficial, whereas in the Sahel experiences are less convincing. Experiments in the African semi-arid regions show that the effects of windbreaks on millet growth can be significant or elusive (Bognetteau-Verlinden,

1980; Ujah and Adeoye, 1984; Long, 1989; Banzhaf et al., 1992; Leihner at al., 1993; Brenner et al., 1995b). The results vary because weather, soil, WB characteristics and management practices all influence (in a more or less interactive way) WB effects and finally crop growth and yield.

To understand crop responses to windbreaks, it is necessary to consider the factors influencing the pattern of air flow in the lee of such tree rows. Windbreaks modify wind speed and turbulence as a function of distance from the windbreak, hence their effects on microclimate vary in space (Rosenberg, 1974; Ujah and Adeoye, 1984; McNaughton, 1988; Long, 1989; Brenner, 1991) (Fig.1.3B). The horizontal extent of most WB effects are assumed to be proportional to WB height; therefore, the distance from windbreaks is conventionally expressed as multiples of the height of the windbreak (H). Windbreaks force the air flow to be displaced, creating a short zone of wind speed reduction at the windward side of the windbreak and increased wind speed above it. At the lee side there is a shelter zone in which velocity of wind is reduced for at least 20% (van Eimern et al., 1964). At a certain distance, between 3 - 6 H (Brenner, 1995a), a point of minimum wind speed exists, after which the air flow returns back to the upwind scale. The effect of windbreaks on turbulence can be distinguished into the 'quiet' zone (2 - 8 H, Brenner, 1995a) with reduced turbulence, creating a warmer and more humid microclimate, and the subsequent 'wake' zone (8 - 15 H, Brenner 1995a), where turbulence is increased (Fig. 1.2) (McNaughton, 1988). WB height and length, orientation, porosity, field width (WB spacing), angle of the wind direction with the windbreak and turbulence of the approaching wind are major characteristics in determining the spatial air flow pattern and thus microclimate effects on crops (van Eimern et al., 1964, Sturrock, 1975). Microclimate effects are found to be opposite for the quiet and wake zone (van Eimern et al., 1964; McNaughton, 1988).

Crop yield as a function of distance from a windbreak reveals to a certain degree the microclimate and other factors that played a role in crop growth. A summary of possible modifications of yield levels with distance from the windbreak relative to the yield level under unshielded conditions is presented in Figure 1.3A. We might find the following yield pattern:

1. a *region of yield increases*, due to the decreasing impact of trees on competition with crops for resources of light, nutrients and soil water. Furthermore, depending on tree species, allelopathy could play a role. The yield pattern, however, could also be opposite: trees might ameliorate microclimate by lower temperatures and enhance soil fertility. An example is the leguminous tree *Faidherbia albida,* which competes only minimally, since it defoliates before the rainy season while it improves soil fertility and microclimate (Vandenbeldt and Williams, 1992; Kessler, 1992). For *Faidherbia albida* yield increases were commonly observed under
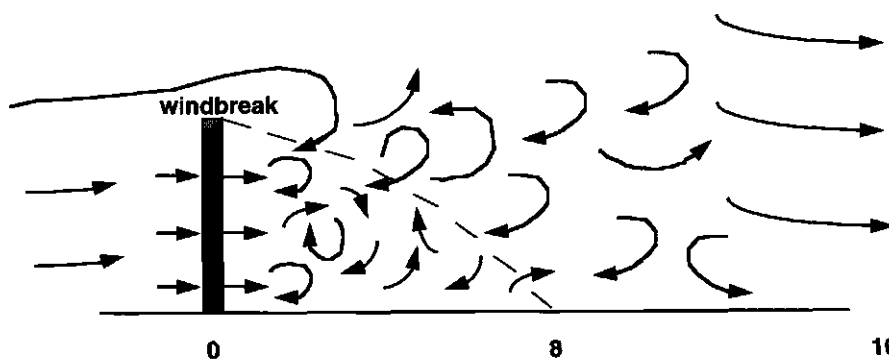
Figure 1.2 Turbulent flow in the quite and wake zone behind a windbreak (after McNaughton, 1988).
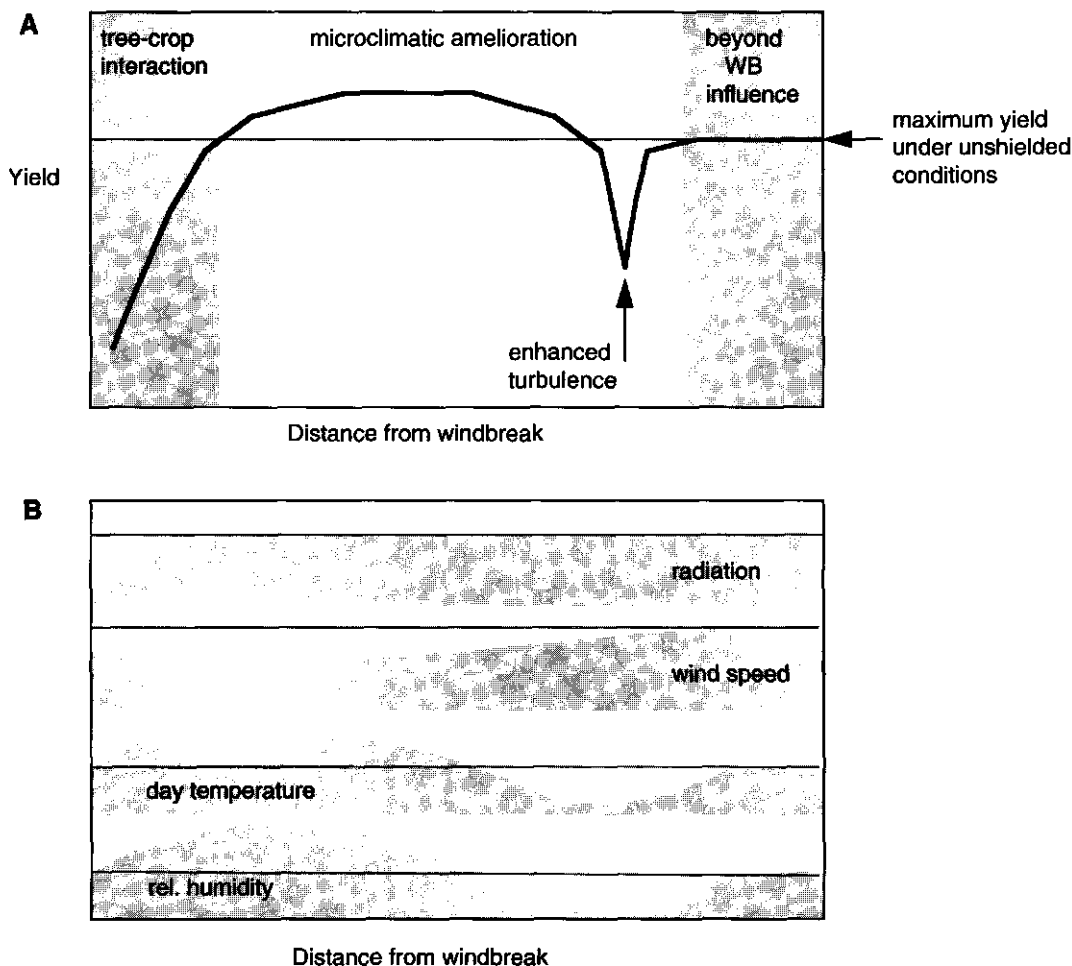
Figure 1.3 Yield (**A**) and microclimate (**B**) pattern as a function of distance from the windbreak. The dotted line indicates the normal level under unshielded conditions.

the canopy of scattered trees (Vandenbeldt and Williams, 1992; Kessler, 1992) and close to trees in windbreaks (Michels, 1994). In the Sahel, windbreaks of other tree species usually reduce the yield close to the shelter (up to 2 - 3 H) due to competition especially for soil water and light (Kessler, 1992; Brenner et al., 1993; Onyewotu et al., 1994).

2. a *region of maximum yield, possibly above the normal potential growth for that region,* due to the positive effect of the windbreaks on growth conditions (Ujah and Adeoye, 1984; Long and Persuad, 1988; Brenner, 1991; Bernardes, ESALQ/USP-Brazil, pers. comm., 1996). Positive influences in an *Azadirachta indica* millet field have been attributed to a larger crop leaf area and a more efficient conversion of solar radiation into dry matter as a result of higher air temperature and lower water vapour pressure deficit (Brenner et al., 1995b).

3. a *point of sharp yield decline,* due to locally increased water stress. The reasons for this can be locally enhanced turbulence and temperatures (at a point of minimum wind speed) and thus higher evapotranspiration usually at a distance exceeding 5 H (Onyewotu, pers. comm, 1996; McNaughton, 1988; Brenner et al., 1995a). In the lee of a 6 m high *Azadirachta indica,* growth rate of millet was lower at 6 H than at 10 H in the beginning of the season, attributed to a combination of high temperatures and water stress (Brenner et al., 1995a).

4. a *region of production level equal to the maximum yield of an unshielded crop field.* This region exists when the field length is long enough for the air flow to return to its original form, generally at a distance beyond 15 H (Ujah and Adeoye, 1984). In agroforestry systems with narrow spacing between windbreaks, there is an additional effect, namely the interference between two adjacent WB lines (McNaughton, DSIR and Jacobs, WAU, pers. comm., 1992).

All crop growth factors are interacting and it is impossible to predict intuitively the net effect of a windbreak on any single factor. Moreover, the horizontal extent of the individual factors may vary in dependence of external factors in a different way, which complicates the analysis of the tree-crop interactions. Very difficult to integrate into the analysis is wind erosion, because it is highly variable in space and time. Hence, for understanding of the tree-crop interactions in a windbreak-cropping system the dynamic and spatial aspects of interfering components have to be integrated in relation to external factors, most appropriately in a model.

1.4   Simulation models

Modelling is an effective approach to integrate knowledge of various processes or parts of a system. Models differ in level of detail and complexity and in their capability to explain and predict the behavior of such systems. Here, we focus on dynamic explanatory simulation models for agriculture related disciplines. Explanatory simulation models have a mechanistic structure; that means they describe the system on several integration levels, and thus, attempt to explain the system, e.g. crop growth, from underlying physiological processes. In this way explanatory models differ from descriptive models. Computation of the various processes can be done in specific time-intervals, which are largest for the level to explain. In biology, models are never purely mechanistic but also contain empirical functions, that describe, but do not explain, the relation between components. Such empirical relationships require local calibration, and validation for the environment, to which they are to be applied. The same is true for parameters, i.e. properties of system components, because their values (coefficients) are also experimentally derived under specific environmental conditions. Generally, the more complex a model, the more parameters it contains and the more calibration is required in response to environmental conditions (Spitters and van Keulen, 1990). Thus, prior to a simulation run, much experimental information is necessary. However, it is impossible to derive and calibrate all internal and external parameters (biophysical environment) of a system and estimates are necessarily inaccurate and uncertain (Spitters, 1990; Monteith, 1997). The more parameters that are very sensitive to external conditions, the lower the quality of the model. Therefore, next to purpose, also the quantity and quality of the available/ required data limit the degree of detail and size of a simulation model (van Keulen, 1976).

Since models answer easily and quickly 'what if' questions, they can help in organizing thoughts and in executing systematic and efficient research. Integrating the current level of experimental knowledge, simulations complement experiments. For instance, models can be used to screen various alternatives for experimental WB-designs, thereby saving time and costs. In short, they can act as a guide for experimental research, identify gaps in knowledge and thus be of use in the prioritisation of research. Besides their benefits for research, they are of practical use too. Models provide a means to predict the response of a cropping system to external conditions such as weather and soil properties. They enable evaluation of the effects of management strategies (e.g. date of sowing, irrigation schemes, use of windbreaks, WB pruning regimes) on crop variables in a reasonable time (< 1 day). In addition they may provide insights in long term effects, e.g. of windbreaks on soil fertility. All this highlights the advantages of simulation studies, especially for very complex systems such as agroforestry systems (see also Muetzefeldt and Sinclair, 1993).

At the time that this study started, no windbreak-cropping system model was available. Only models describing one or more components of an agroforestry system were available. The wind erosion model WEPS[1] (Hagen, 1991) and the erosion impact calculator model EPIC[2] (Williams et al., 1990) both focus on the erosion process, while crop growth is described rather simplistically, lacking the detail required to integrate effects, other than erosion, on crop growth. Growth models that account for interspecific interactions with respect to light, water and nutrients, exist, for example, for the presence of single trees or weeds, RECAFS[3] (Conijn, 1995) and INTERCOM[4] (Kropff and Van Laar, 1993), respectively. RECAFS describes tree growth in a simple way, whereas de Reffye et al. (1995) developed a model that simulates the architecture of trees in detail and that can be used for the description of light interception and water and nutrient uptake in tree-cropping systems.

When modelling semi-arid agroforestry systems, the soil water balance is of particular importance. Examples of mechanistic soil water models are the one-dimensional SWATRER[5] (Dierckx et al., 1986), and the two-dimensional FUSSIM2[6] (Heinen and de Willigen, 1992). Bley (1990) calibrated SWATRER for a millet field in Niger. Fechter (1993) continued his work by linking SWATRER to a growth model that was calibrated for millet varieties in the Sahel (SUCROS[7], Jansen and Gosseye, 1986) and compared the results with simulations of the CERES-Millet[8] model (Godwin et al., 1984; Jones et al., 1986), that calculates the soil water balance but also millet growth potential. Both models gave satisfactory simulations, but SWATRER simulated the soil water contents, and CERES-Millet plant growth more accurately under water deficit conditions. A further interesting model for millet in the Sahel is CP-BKF3[9] (Verberne et al., 1995), which provides insight in the dynamic interrelations between weather, soil nutrients, soil water and crop growth. Existing crop growth models tend to be detailed in process description, but simple in spatial patterns, assuming a homogeneous minimum representative area, with a one-dimensional variation between soil layers (van Noordwijk and

---

[1] WEPS: Wind Erosion Prediction System

[2] EPIC: Erosion Productivity Impact Calculator

[3] RECAFS: model for REsource Competition and cycling in AgroForestry Systems

[4] INTERCOM: simulation model for crop-weed INTERspecific COMpetition

[5] SWATRER: Soil Water and Actual TRanspiration simulation Extended

[6] FUSSIM2: a two (2)-dimensional SImulation Model for Flow of water in Unsaturated Soil

[7] SUCROS: Simple and Universal CROp growth Simulator

[8] CERES: Crop Environmental and REsource Simulation

[9] CP-BKF3: Cultures Pluviales Burkina Faso

Lusiana, 1997). In the case of agroforestry studies the spatial aspect is crucial and should be simulated either in detail (WIMISA[10], this thesis) or by zoning (RECAFS and WaNuLCAS[11]). In recent years there has been a rapid development of models in agroforestry systems, thanks to growing interest in agroforestry practices (Ong and Sinclair, 1997; Bergez et al., 1997), increasing knowledge of tree-crop interactions (Ong, 1996), and improving computer capacity (McCown et al., 1996). The development of such models has been driven by the general recognition that a system approach is needed to meet the challenges presented by complexities, uncertainties and conflicts in agricultural production systems (McCown et al., 1996). Concurrently, model structure and modularity (model design) have become important in obtaining computationally-efficient models with the required flexibility for modifications and extensions (linking of models that describe complementary systems' components) to keep track of the progressive understanding of complex systems.

Today, two trends in agroforestry modelling co-exists: (i) the development of more holistic models, that are multidisciplinary, but generally less process-oriented, in response to the demand for guidance from system managers (farmers, land use planners) and policy makers. Many of those models cover large scales, i.e. a farm or even a landscape. For instance the 'Multi agent model' analyses dynamics between forest and agroforestry land use at region level (Proton et al., 1997), (ii) in biophysiological research, models become still more complex and detailed, for evaluation of interactions between system components; e.g. WaNuLCAS, a process-oriented model for light, water and nutrient capture in agroforestry systems, is presently under development for the description of below- and above-ground temporal and spatial interactions to allow evaluation of competition and complementarity between trees and crops (van Noordwijk and Lusiana, 1997).

1.5   Aim and outline of the study

The aim of this study is to extend the insights in positive and negative influences of windbreaks on millet production in the Sahel. In particular the effects of *Bauhinia rufescens* within a narrowly spaced, short tree WB-design are investigated. Special attention is given to millet yields in the area of tree-crop interactions in relation to local conditions of light, soil water and wind speed.

---

[10] WIMISA: WIndbreak-MIllet SAhel

[11] WaNuLCAS: model for Light, Water and Nutrient CApture in agoroforestry Systems

The review of windbreak studies, presented above, illustrates various benefits as well as negative impacts of windbreaks on crop growth. Actual yield in a given situation depends on many interacting factors, e.g. climate, soil properties and WB-design. The few studies performed in semi-arid regions give insufficient insights to develop generally applicable rules that allow extrapolation of experimental results to other locations or from one WB-design to another. More quantitative data on the interactions between the various components, i.e. windbreak, crop, soil, weather and microclimate are required. A model is helpful to integrate knowledge and formulate hypotheses on the interacting components and thus to analyse a complex agroforestry system or parts of it. It allows a quantitative description of key processes that can be used to estimate crop growth and yield in windbreak shielded fields under various conditions. However, when starting this study, no windbreak-cropping system model was available. Existing crop models lacked spatial heterogeneity, which hampers the incorporation of WB effects.

The present study comprises a combination of experimental work (Part A) and simulation analysis (Part B). Agroforestry field experiments were conducted at the Sahelian Center of ICRISAT (International Crops Research Institute for the Semi-Arid Tropics), in southwest Niger in 1991, 1992 and 1993 (Chapter 2). The experimental results (Chapter 3), completed by literature data, were used for simulation analyses of tree-crop interactions in a windbreak-millet system (Chapter 6). For this purpose the model WIMISA (WIndbreak-MIllet SAhel) was developed by means of new methods, and methods from existing crop growth, soil water and root water uptake competition models (Chapter 4 and 5). Results of simulations and experiments are linked and discussed in Chapter 7. The specific objectives of the study were:

- to determine the effects of windbreaks on microclimate and millet growth,
- to quantify the effects of windbreaks on soil water, nutrient, and light resources in the tree-crop interface and assess possible competition between trees and crops,
- to determine microclimate, windbreak, and millet specific input data for a windbreak-millet crop growth model,
- to develop and evaluate a process-oriented simulation model that integrates tree-crop interactions of a windbreak-millet cropping system with a high resolution in time and space,
- to analyse the individual effects of competition between crops and trees for light and water and to quantify their relative importance in dry and wet years.

PART A - EXPERIMENT

The effect of windbreaks on microclimate, growth resources and crop growth

"Agroforestry has its parts to play in the spectrum of sensible, sustainable land use options, but it is up to us to provide credible information about the biological opportunities and, above all, the feasibility of the choices."

Peter Huxley, 1996

Abstract

In the Sahel, wind erosion is one of the major constraints to millet production systems. A possible control measure is the use of windbreaks; however, there is little and contradictory information on the effects of windbreaks on crop growth in the Sahel. An experiment was performed at the ICRISAT Sahelian Center, southwest Niger to study the effects of low, narrow spaced windbreaks, in particular those of *Bauhinia rufescens*, on microclimate, light, water and nutrient resources in the windbreak-crop interface, and the growth of pearl millet (*Pennisetum glaucum*). Radiation, wind speed, relative humidity, and air temperatures were continuously and soil temperatures occasionally measured in Bauhinia plots. To assess competition between crop and windbreak (2 - 3 m high), soil water and nutrient status were observed in the windbreak-crop interface and in control plots. Crop yields adjacent to seven windbreak species and in control plots were determined at maturity, whereas measurements of crop growth parameters were confined to Bauhinia and control plots. In two rather wet years of experiments it was found that the overall yield in windbreak plots was slightly (mostly not significantly) higher than in the control plots. However, up to 2.5 H (with H the windbreak height) from windbreaks lower yields were measured than in the middle of the plots. The zone of severe yield reduction (0.5 - 1.5 H) corresponded to that of the strongest reduction in radiation and soil moisture, indicating at competition effects. The windbreak canopy also lowered soil temperatures, but this had no impact on crop establishment and development. Although the Bauhinia windbreak reduced wind velocity up to 5 H, relative humidity and air temperature at the top of the sheltered crop appeared to be unaffected. Consequently, the influence of Bauhinia at the tree-crop zone from 0 - 5 H was most evident and is introduced into a windbreak-millet system model for further analyses, as described in Part B of this thesis.

Photo 1   Windbreak-millet field (top) and millet westwards of *Bauhinia rufescens* (bottom) at ISC, Niger, 1991.

2 MATERIALS AND METHODS

2.1   Introduction

In the Sahel, wind erosion is one of the major constraints to millet production. Windbreaks are recommended for wind erosion control, and thus crop protection and soil conservation (Chepil and Woodruff, 1963; Tibke, 1988; Banzhaf et al., 1992; Michels, 1994), to increase in the short- and long-term agricultural productivity. Furthermore, windbreaks may improve crop production through amelioration of the microclimate (McNaughton, 1988; Kort, 1988; Brenner, 1995b) or by improved soil fertility (Kessler, 1992; van Noordwijk et al., 1996). However, yields are not always higher in windbreak-cropping systems than in pure crop stands (Long and Persaud, 1988; Banzhaf et al., 1992; Renard and Vandenbeldt, 1990; Brenner, 1995b). There are several reasons for this as we have seen in Subsection 1.3. One point is that microclimate modifications can also have a negative impact on production, e.g. an increase in temperature could be a disadvantage for the crop when a certain threshold value is passed. A further important issue is competition for light, soil moisture, nutrients and land occupied by the windbreak, that may outweigh WB benefits. In general, windbreaks influence multiple crop growth factors to a degree that is very much dependent on windbreak system-characteristics, e.g. species and height, whereas the magnitude of the change in crop production is determined mainly by incident environmental conditions and crop species. Thus, any positive WB effect could be counteracted by negative influences. The interactions among the various components are not yet fully understood and more basic research is needed to explore the conditions under which windbreak-cropping systems are beneficial and to enable optimum windbreak-cropping systems design.

For the semi-arid regions in particular, more data on the effects of windbreak heights and spacings, as well as on the influence of different tree/shrub species on crop yields, are needed. In Nigeria, Ujah and Adeoye (1984) and Onewatoyu et al. (1994) worked with *Eucalyptus camaldulensis* and in Niger, Long (1989), and Brenner (1995a,b) studied systems with *Azadirachta indica* , where all windbreak heights were 6 m or more (10 and 12 m), whereas Banzhaf et al. (1992) studied the effects of natural bush savanna left in a line as windbreaks, and Renard and Vandenbeldt (1990) those of an alley-cropping system with *Andropogon gayanus*, both lower than 1 m on millet crop performance. Only in the study with the low savanna windbreaks several spacings were screened and narrow spacings (6, 20, 40 m) were included, while the high windbreaks had distances of at least 100 m.

Although alley-cropping systems illustrate the importance of competition and complementarity between trees and crops, this aspect has received little attention in windbreak cropping systems in the Sahel. No reports on nutrient aspects are yet available. Furthermore, quantitative information on the interactions of the various microclimatic factors is available in detail only from Brenner (1995a), over two years of measurements in Niger. For a fair understanding of the tree-crop interactions, all relevant factors should be included in the analysis of a windbreak-cropping system. This is a difficult task, because many factors are involved and they are not easy to separate. None of the reported Sahelian windbreak studies explored all possible effects, e.g. Brenner (1991) left out wind erosion and soil chemical analysis, whereas Banzhaf (1988) combined wind profile studies and sand transport, but paid no attention to relative humidity and air temperature.

When a basic understanding of windbreak-cropping systems is gained, a model such as WIMISA (Part B) could be helpful in testing different WB-designs in various environments and for several crops. For this, system characteristic data are required.

The objectives of this study were to investigate the effects of rather low, narrowly spaced windbreaks of (i) 7 species on yields of pearl millet, (ii) *Bauhinia rufescens* and *Andropogon gayanus* on soil water and nutrient resources in the tree-crop interface, (iii) *Bauhinia rufescens*, on microclimate including light reduction, and on the development and growth of millet. All studies included controls. Additionally, (iv) specific growth characteristics of millet were determined beyond the windbreak influence for model input parameters. The field experiments were conducted in 1991, 1992 and 1993 at the Sahelian Center of ICRISAT, Sadoré (Photo 1). At the same site, in an accompanying study by Michels (1994), Smith (1995) and Lamers (1995), knowledge was obtained on wind erosion effects on crop growth, water use of windbreaks and production of the experimental windbreaks. These results were used for discussion of the experimental results (Chapter 3 and 7) and for model development (Part B).

2.2   Experimental site

The research station ICRISAT Sahelian Center (ISC) at Sadoré (13° 16 ' N , 2° 21 ' E, altitude 221 m), is located 45 km south-east of Niamey in southwestern Niger. The rainy season, usually between May and October, has a long term mean annual rainfall of 545 mm at Niamey (Sivakumar et al., 1993). Potential evapotranspiration can reach 9 mm d^{-1} and 2500 mm y^{-1} (Bley, 1990). Average annual temperature is 29 °C with an average monthly minimum of 15 °C in January and an average monthly maximum of 42 °C in April (Fig. 2.1).
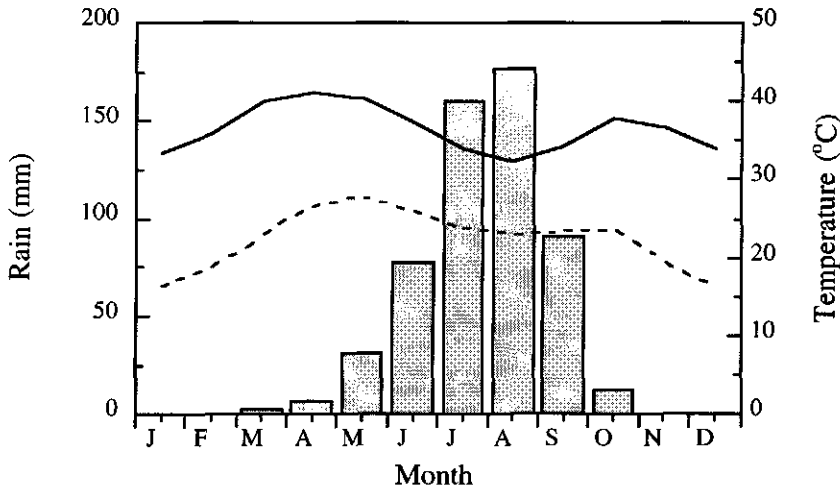
Figure 2.1   Climate at Niamey, Niger, showing monthly means of rainfall (bars) and maximum (—) and minimum (····) temperatures (after Sivakumar et al., 1993).

During the rainy season the prevailing winds come from the southwest, while the direction of the short sudden thunderstorms is usually east. The soil at the experimental site is classified as a sandy, siliceous, and isohyperthermic "Psammentic Paleustalf of the Labucheri soil series" according to the USDA taxonomy (West et. al., 1984) which extends down to a layer of hard laterite at a depth of about 4 m. Within the profile there are no root growth restricting layers or cracks (West et al., 1984). The water table is found at a depth of 35 m. Detailed soil analysis data from Sadoré Research Center location have been published (West et al., 1984; Bley, 1990).

2.3   Experimental setup of the windbreak-millet system

Windbreak fields were established in August 1988. Three lines of windbreaks were planted parallel to each other in north-south direction (Fig. 2.2). Over these lines various windbreaks and control plots (no windbreak), each 50 m long, were arranged in a randomized block design. The distance between two lines of windbreaks was 30 m, cropped by millet. Each windbreak

consisted of a single species of trees/shrubs planted in a staggered configuration of two rows. The distance between the windbreak plants was 3 and 1.5 m within and between the rows, respectively. Windbreak plants were pruned to a height of 2 and 1 m sideways (fieldwards) from the main stem before the onset of each rainy season.

The experiment was a split plot design with three replications of a control and of the following seven shelter species: the perennial grass *Andropogon gayanus* Kunth, five tree species native to Africa: *Bauhinia rufescens* Lam., *Faidherbia albida* Del., *Azadirachta indica* A.Juss., *Acacia nilotica* ssp. *adstringens* (Schumach. & Thonn.) Roberty, *Acacia senegal* (l.) Willd and the exotic (Australian) *Acacia holosericea* A. Cunn. ex G. Don, which has recently been introduced in Africa. The main plots were 50 x 30 m divided into 2 subplots, one covered with 2000 kg ha^{-1} millet crop residues (+CR) and one without crop residues (-CR). The crop residues were applied to investigate their efficacy as an additional wind erosion control measure and were studied by Michels (1994).

To the west of each windbreak pearl millet (*Pennisetum glaucum* (L.) R. Br.) cv. CIVT (Composite Inter-Variétal de Tarna) was sown in the traditionally way, i.e. 50 -100 seeds were thrown manually in ca. 5 cm deep holes ("pockets"), spaced 1 by 1 m. CIVT, an improved local variety, has a development cycle of 90 - 120 growing days depending on the photoperiod (Lambert, 1983). The first row of millet was planted at a distance of 1 m from the stem of the nearest row of windbreak plants. Phosphorus was applied before sowing (45 kg P_2O_5 ha^{-1}) as single super phosphate. Nitrogen was applied in each pocket as calcium-ammonium nitrate at tillering (30 kg N ha^{-1}) and during stem elongation (15 kg N ha^{-1}). Three weeks after sowing the pockets were manually thinned to three plants per pocket (30.000 plants ha^{-1}). Weeding was performed 3 and 10 weeks after sowing. Seed losses by birds were controlled by "hunters" during the last two weeks before final harvest. These cultural practices were applied uniformly on all plots. Time schedule of sowing, harvest and other operations are given for the three cropping seasons in Table 2.1.

Final millet yields were determined for the seven replicated windbreaks and the control plots. Detailed crop, soil and microclimatic measurements were restricted to the Bauhinia, Andropogon and/or control plots. Table 2.2 summarizes the locations of measurement and sampling in the various WB plots. For comparison with other studies, the distance from the windbreak is also expressed in terms of its height (H) at the onset of the season (note that after pruning the windbreak height continuously increased throughout the season). For convenience the plots are named after the bordering WB species in the east, (crop) rows refer to crop lines parallel to the windbreak and transects refer to lines perpendicular to the windbreaks.
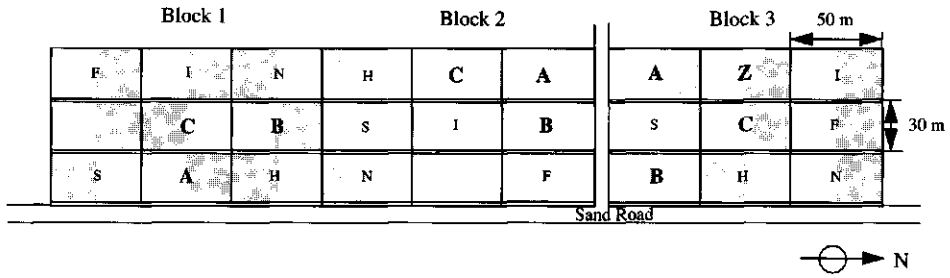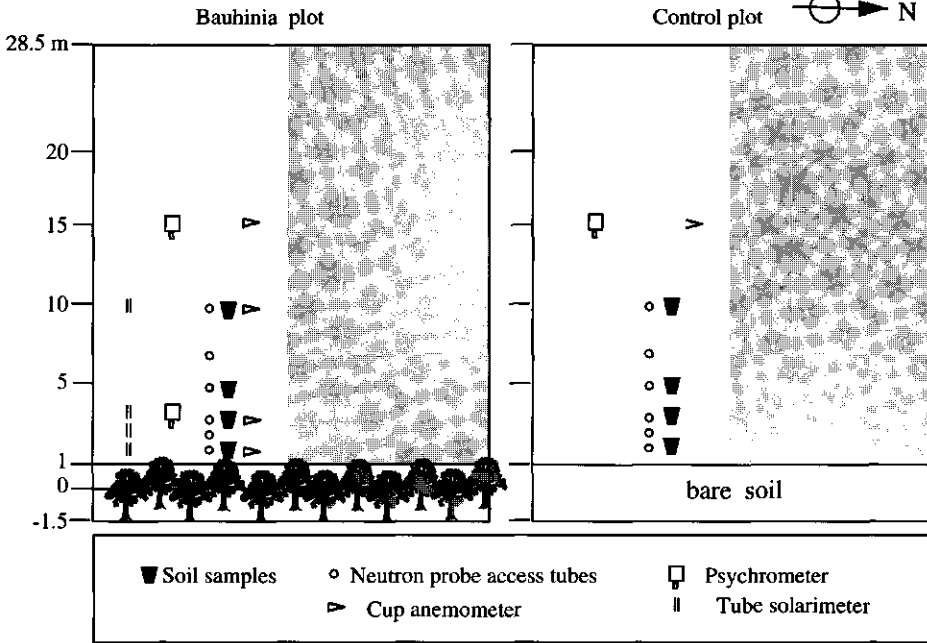
Figure 2.2 Field layout of the windbreak-millet system at ISC, Niger and the locations of instruments (configuration II) and sampling positions in Bauhinia (**B**) and control (**C**) plots. Detailed measurements were performed in plots of **B**, **C** and **A**; the other plots were used for determination of yields at maturity only.
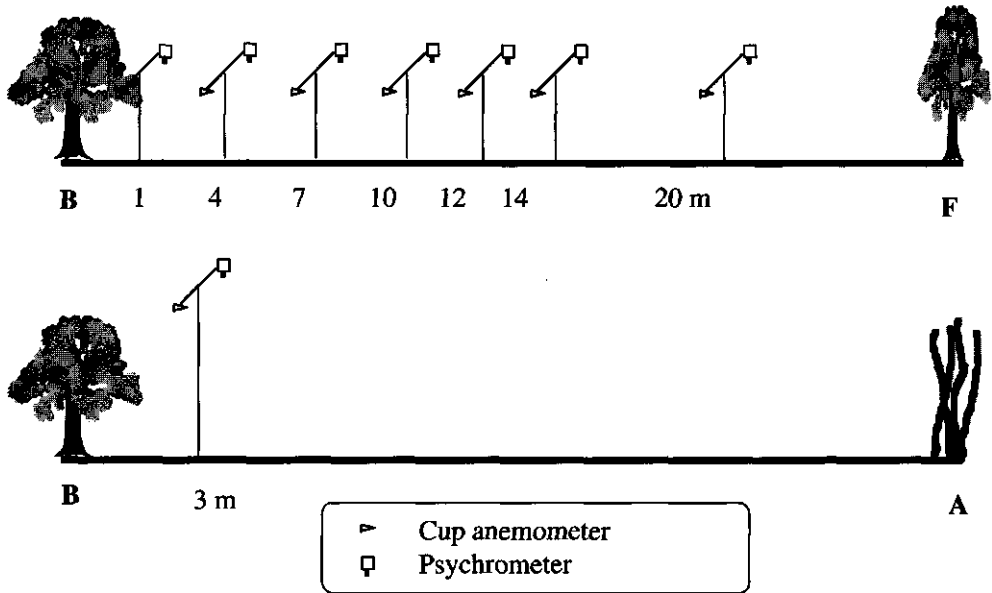
Figure 2.3   Configuration I of instrumentation in the east (top) and west (bottom) of a
Bauhinia WB (B) at ISC, Niger in 1992. F and A indicate the windbreak
Faidherbia albida and *Andropogon gayanus*, respectively.

Table 2.1   Time schedule of the operations in the growing seasons of 1991, 1992 and
1993 at ISC, Niger. DOY and DAE indicate day of year and day after
emergence.

Operation		1991			1992			1993		
		Date	DOY	DAE	Date	DOY	DAE	Date	DOY	DAE
Sowing		15.06	166		26.05	147		06.06	157	
Emergence		18.06	169	*0*	28.05	149	*0*	10.06	161	*0*
Fertilizer	P (SSP)	10.06	161		12.05	133				
	N (CAN)	10.07	191	*22*	16.06	168	*19*	04.07	185	*24*
	N (CAN)	29.07	210	*41*				26.07	207	*46*
Weeding		13.06	163		05.06	157	*8*	29.06	180	*19*
		10.07	191	*22*	10.07	192	*43*	23.07	204	*43*
Thinning out		10.07	191	*22*	17.06	169	*20*	25.06	176	*15*
Harvest	1st at thinning	08.07	189	*22*	16.06	168	*19*	25.06	176	*15*
	2nd at booting	03.09	246	*77*	15.07	197	*48*	22.07	203	*42*
	3rd at flowering		no		11.08	224	*74*		no	
	4th at maturity	15.10	288	*119*	08.09	262	*112*	27.09	270	*109*

Table 2.2   Positions of observations and sampling in Andropogon (A), Bauhinia (B), Control (C), or at 15 m from windbreak line in C only (C*) in 1993[1], 1992[2] and 1991[3]. H is the distance from the windbreak expressed in multiples of the WB height at the beginning of the season (2 m).

Parameter	Block	WB	Distance from windbreak line												
			1	2	3	5	7	10	15	22	24	25	26	26.5	m
			1					5		11		13			H
Wind speed[1]	3	B,C*	♦	♦			♦	♦							
Soil analysis (pH, N, P, K,...)[1,2,3]	1,2,3	A,B,C	♦	♦			♦								
Soil moisture[1,2,3]	1,2,3	A,B,C	♦	♦	♦	♦	♦	♦							
Soil temperature[1]	3	B	♦	♦	♦	♦	♦	♦	♦	♦	♦	♦	♦	♦	
Air temperature[1]	3	B,C*	♦	♦	♦	♦	♦	♦	♦	♦	♦	♦	♦	♦	
Rel. humidity[1]	3	B,C*			♦				♦						
Global radiation[1]	3	B	♦	♦	♦			♦							
Microclimate[2]	2	B	at 1, 4, 7, 10, 12, 14 and 20 m												
Yield & dry matter (DM)[1,2]	1,2,3	7 WBs,C	all rows												
Growth parameters & DVS[1]	1,2,3	B,C	♦		♦	♦		♦	♦						
Intermediate DM[1,2]	1,2,3	B,C	♦		♦	♦	♦	♦							

2.4   Measurements

2.4.1   Microclimate

Global weather data were collected at a central weather station at ISC, located approximately 1 km westward of the windbreak site. Microclimate modifications by the windbreak with respect to wind speed, air temperature and humidity were determined on the eastern (1992) and on the western side of a Bauhinia windbreak (1993). Measurements were confined to one Bauhinia -CR plot. In 1993, microclimate measurements were also performed in the middle of a neighboring control plot (Fig. 2.2). Light reduction was recorded adjacent to Bauhinia in 1993. The data were recorded every 30 seconds and averaged over 10-minute intervals using a data logger (21X, Campbell Scientific, Ltd., UK). Additionally, soil temperatures were measured manually on several occasions in 1993. All instruments were calibrated before and after the measurement period of each year.

Wind speed, air temperature and air humidity
Wind speed, air temperature and relative humidity were measured for two different configurations of instrumentation to monitor the microclimate changes from windbreaks in the

lee of normal winds (eastern side of WB) (configuration I, Fig. 2.3) and in the lee of storms (western side of WB) (configuration II, Fig. 2.2). Wind speed was measured with Vector cup anemometers (A100R, Vector Instruments, Ltd., UK). Psychrometers (H301, Vector Instruments, Ltd., UK) were used for readings of air temperature and relative humidity.

Configuration I consisted of seven stations at distances of 1, 4, 7, 10, 12, 14 and 20 m, on the eastern side of Bauhinia block 2 at a height of 1 m. The measurements were compared with those of a station on the windward (western) side of Bauhinia at a reference height of 4 m, which was above the shelter height (Fig. 2.3). These observations were performed over soil with short millet stalks to minimize crop influence in a 3 week period after the final harvest in 1992.

Configuration II was accompanied with observations of crop growth to gain insight in the overall effects of windbreaks, when functioning as shelter for storms. Hence, measurements were done at several locations to the west of Bauhinia (Table 2.2). Psychrometers were placed 50 cm above the crop continuously measuring air temperature and humidity at 3 and 15 m from Bauhinia and at the control at 15 m. Wind speed in all directions was measured at 1, 3, 10 and 15 m from Bauhinia and in the middle (15 m) of the control between July and August (DOY[1] 183 - DOY 236) in 1993. The instruments were installed ca. 30 - 60 cm above the crop, that was at approximately 1.0 - 1.9 m above the soil with increasing crop height. A further anemometer located in the middle of the control monitored wind velocities at a reference height of 3 m.

Radiation
Solar radiation transmitted through the Bauhinia canopy was measured with a set of 4 tube solarimeters (Delta T, Ltd, UK) arranged perpendicular to the line of the windbreak. The 0.6 m long tubes were placed with their centers at a distance of 1, 2, 3, and 10 m from the Bauhinia trees, and were installed 15 - 20 cm above the soil surface. Tubes in the field where not overshadowed by millet shoots so that the monitored radiation represents the radiation reduced by the windbreak only. An extra tube solarimeter was installed at 10 m above the soil for reference measurements. Bauhinia shade contours were traced throughout seven days (between DOY 287 and DOY 301) after the final harvest in October, 1992 in a plot (block 2) where only millet stubbles were left. The shade length was measured every 15 minutes between 8 and 18 h at 6 positions along both sides of the windbreak using a measuring tape. The six positions were distributed at the north, middle and south part of the 50 m long windbreak each with one

---

[1] DOY denotes day of year.

measurement opposite to the outer tree and a second opposite to the inner tree of the double row windbreak.

Soil and air temperature

Soil and air temperatures were measured along four transects (each used as a replication), laid out to the west of Bauhinia (-CR block 3) up to the east of *Acacia senegal* (Table 2.2). Temperatures were measured with a portable electronic thermometer (Technoterm 9400, Germany), every hour starting at 8 or 9 h and finishing at 15 or 16 h at 12 days spread over the growing season of 1993. The soil depths selected were 1 and 2 cm or 1 and 5 cm. For each distance, air temperature at a height of 1.9 m was measured directly after the soil temperature reading. The mean temperature value at distance x_i was determined as the average over the four replicates. For each distance x_i within a transect j, a relative temperature difference, $\Delta T_j(x_i)$, was calculated as the deviation of the temperature $T_j(x_i)$ from the average temperature along that transect:

$$\Delta T_j(x_i) = T_j(x_i) - \frac{1}{n}\sum_{i=1}^{n} T_j(x_i)$$

(2.1)

For each distance x_i the average temperature difference, $\Delta T(x_i)$, is found by averaging $\Delta T_j(x_i)$ over the four transects j:

$$\Delta T(x_i) = \frac{1}{4}\sum_{j=1}^{4} \Delta T_j(x_i)$$

(2.2)

For convenience, in the following the relative temperature difference will be noted as $(T_a - T_t)$, with T_a the actual $T_j(x_i)$ at position x_i and T_t the average temperature over the transect.

2.4.2 Soil

Water content and chemical properties were studied for soils in Bauhinia, Andropogon, and control -CR subplots of all three replicates (Fig. 2.2).

Soil water content

Soil water content was measured with a neutron probe throughout the season at various distances (1, 2, 3, 5, 7, and 10 m) from the windbreak line. At each distance measurements were carried out at depths between 0.10 and 1.90 m, with increments of 0.30 m once a week. The neutron probe in 1991 and 1992 was a Solo (Solo 25, Nardeux, France) and in 1993 a

Troxler (Type 3332). In 1992, technical problems with the Solo led to missing data in the period of 2.7 - 5.8 and 20.8 - 21.10.

Soil chemical properties
Soil samples were taken in May 1991 and 1993 before sowing and application of fertilizer. The sampling positions were 1, 3, and 10 m from the windbreak line at soil depths: 0 - 0.1, 0.1 - 0.2, 1.0 - 2.0 m. Each sample for analysis was a mixture of four field replicates. Prior to the analysis, samples were mixed, air-dried, and sieved (2 mm). The following soil chemical analysis were done: total N, organic carbon (Walkley and Black, 1934), pH (2M KCl), available phosphorus (Bray-1 procedure; Olsen and Sommer, 1982), exchangeable cations (K, Na, Ca, Mg, Al), total acidity. Exchangeable Al and total acidity were determined according to McLean (1982). Concentrations of Ca and Mg were measured by atomic adsorption, and Na and K by flame emission spectrophotometry, after extraction with 1 N ammonium acetate.

2.4.3   Millet

All reported results on plant production refer to the cropped area, not including the area occupied by windbreaks. Mean values of the replicates were calculated separately for each distance.

Yield
At physiological maturity, millet yields were determined for the crops in the shelter of seven windbreak species and in the control (each in three replicates) in 1992 and 1993 (Fig. 2.2). Millet straw and panicles were harvested by taking 20 pockets in sequence from each millet row parallel to the windbreaks. Additionally, the total number of pockets with millet plants was counted per row. Panicles were oven-dried at 60 °C and then threshed manually for grain yield determination. Straw biomass was left in the field and weighed after three weeks sun-drying. These raw data were adopted from Michels (1994) to quantify millet production as a function of distance from the windbreaks independently and dependently on WB species.

Growth and development
Crop growth and phenological development were observed throughout the season of 1993 in crop rows 1, 3, 5, 7, 10 and 15 of the -CR subplots of Bauhinia and control (Table 2.2). After emergence and after thinning the established number of plants per pocket was recorded. On 6 representative pockets of each of the selected crop rows phenology, plant height, and number of green and brown leaves were determined weekly. The number of leaves on the main culm was counted for the tallest plant of the pocket only. The tallest plant per pocket was identified in the

beginning of the season and called main plant. Plant height was measured as the distance from ground to tip of the newest leaf. Development stages (DVS) were determined according to Maiti and Bidinger (1981) and then transferred to the scala 0 - 2 (emergence to maturity), as suggested by Penning de Vries et al., (1989). The pockets studied in detail were harvested at physiological maturity shortly before final harvest.

Intermediate harvests were conducted at several rows per plot (Table 2.1 and 2.2) in 1992 and 1993: At thinning: 4 samples of 30 plants each, were taken at random from the total crop row. At booting: 4 representative pockets of each row were harvested. At flowering (only in 1992): 5 representative pockets per row were cut for dry matter determination. The remaining 20 pockets were harvested at maturity. The procedure from harvesting to dry matter determination was the same for booting, flowering and maturity. Prior to each harvest, the number of green and brown leaves, panicles and DVS of the plants were recorded. Plants were cut at ground level and separated into stems, leaves, and panicles. Leaf area of green leaves was measured using a portable leaf area meter (Licor Model Li-3000). Dry matter of plant organs was weighed after drying at 60 °C until the weight remained constant.

Model input characteristics

For determination of site- and cultivar-specific (CIVT) characteristics of millet under unshielded conditions, measurements were performed during the 1993 rainy season on the crop in the *Ziziphus mauritiana* plot, which was not in use for other studies. To exclude windbreak effects, plants beyond 10 m from the windbreak were selected for observing growth and development (phenological development, number of dead and living leaves), as performed in the Bauhinia and control plots. At intervals of 10 days measurements and subsequently harvests for dry matter production and allocation to plant organs were performed on 10 well developed plant pockets.

2.4.4   Bauhinia -windbreak

Height

The windbreaks were managed as hedge windbreaks, and so were pruned back to 2 m in April before the onset of each rainy season. After pruning, the height of the trees increased and, therefore, they were measured prior to pruning and at the end of the rainy season (using a tree measuring pole). In this thesis, reported heights of Bauhinia trees were calculated by averaging all trees and replicates per date.

Porosity

Porosity is defined as the ratio of pore space to the space occupied by leaves, twigs, branches and stem. Since this characteristic (aerodynamic porosity) is impossible to measure physically, optical porosity, defined as the ratio of perforated area to total area of a windbreak, was estimated (Loeffler et al., 1992). A series of black and white photographs was taken perpendicular to the windbreak at the onset, middle and end of the growing season in 1991-1993. Five photographs per windbreak were taken at a distance of 5 m and show a ca. 2 m long segment of the windbreak. A white sheet of 2*2 m was used as a background behind the windbreak to enhance contrasts. From the contrast in these photographs porosity was optically estimated.

Roots

To characterize the coarse root system of *Bauhinia rufescens* a border tree of block 2 (towards the road) was excavated at the end of the cropping season, November, 1992. Excavation was performed in a rather rough manner with shovels and small picks to keep labor time within a reasonable limit. The soil around the roots was removed vertically up to 3.7 m and horizontally up to about 8 m. The excavated coarse roots were left at the trunk, counted and measured in length, whereas fine roots (< 2 mm) were lost due to the rough method.

2.4.5   Statistical analysis

Means and standard errors (SE) were calculated for soil water content, soil temperature, soil nutrients, WB height and all field data on growth and development characteristics of millet. Furthermore, analyses of variance were performed using the General Linear Models (GLM) procedure of the SAS software (SAS Institute, 1988): Soil chemical properties and water contents were evaluated as Repeated-Measures over lateral distances from WB's and soil depths. Michels (1994) applied the GLM procedure on millet yields with Repeated-Measures over years, used F-tests, calculated contrasts of interests for interactions between treatments and the repeated factors, used Fisher's Protected LSD for comparisons among treatment means of Bauhinia, Andropogon and control, and applied Tucker's Honest Significant Difference for mean comparisons among all seven WB species, including the control when the ANOVA indicated significant treatment effects (Appendix A1).

3 RESULTS and DISCUSSION

3.1 Microclimate

3.1.1 Shading and radiation intensities

Diurnal course of radiation intensities in the west section of the Bauhinia windbreak are presented for days when the crop was vegetative (DOY 171 and 172) and for days shortly before flowering (DOY 232 and 234) in 1993 (Fig. 3.1). The data represent the radiation intensities 15 - 20 cm above soil reduced by interception of the windbreak only. Lowest radiation was measured at 1 m from the Bauhinia trees between 7 and 13 h.
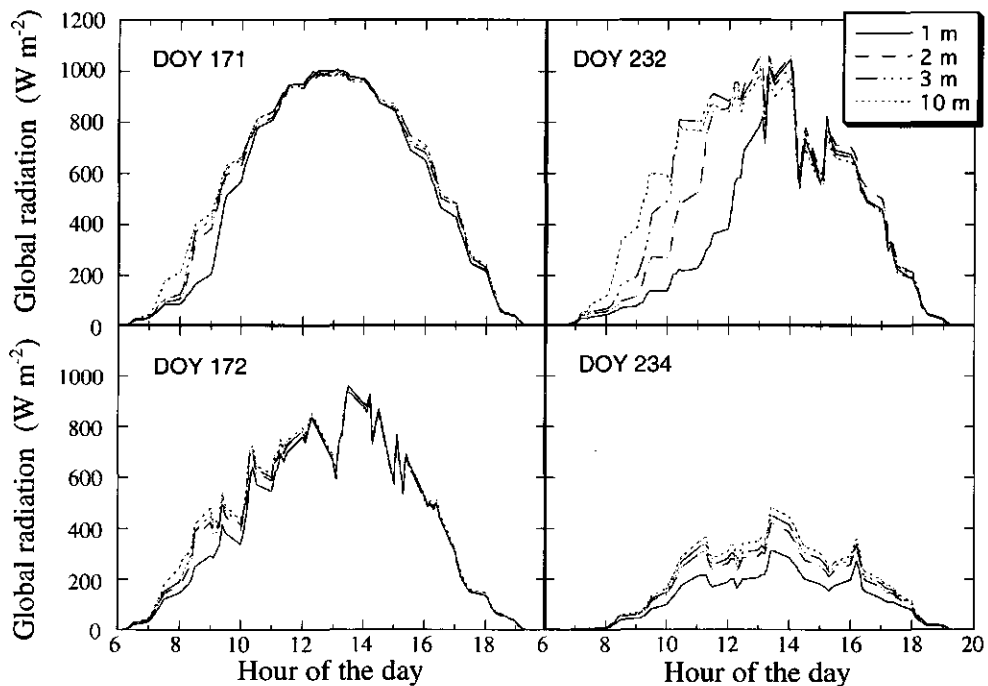
Figure 3.1   Diurnal course of global radiation at a distance of 1, 2, 3 and 10 m from the Bauhinia windbreak (-CR plot block 3) on days early (DOY 171, 172) and in the middle (DOY 232, 234) of the growing season of 1993 at ISC, Niger. DOY denotes day of year.

The occurrence of light reduction depends on the hour of day, the distance to the windbreak and also on the cloudiness of the sky. For instance, on DOY 234, when the sky was overcast during the whole day, radiation intensity was also reduced in the afternoon due to interception of diffuse radiation fluxes, originating always from all directions. The shading effect was much more pronounced in the late growing season when the WB trees were taller, i.e. projecting a longer shade. Substantial shading by the Bauhinia WB was restricted up to 3 m (ca. 1.5 H), considering that light intensities in the early and late hours of the day are low (Fig. 3.2).
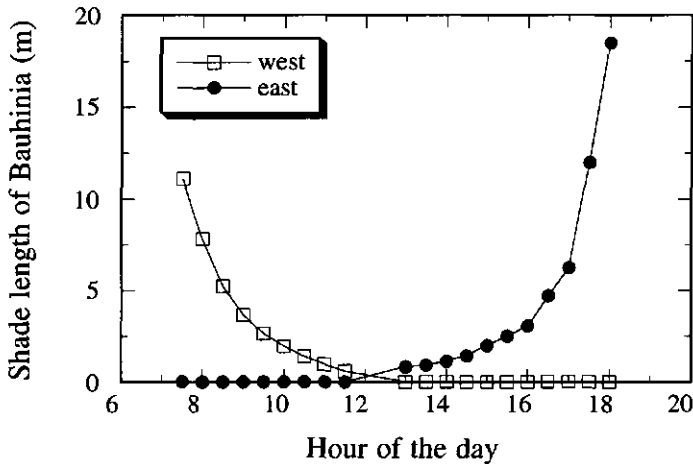
Figure 3.2   Diurnal course of shade extension at the west and east side of the Bauhinia windbreak (-CR plot, block 3) on DOY 294 in 1993 at ISC, Niger.

3.1.2   Wind speed

In 1993 velocities of mean winds (prevailing wind direction is west-southwest) were monitored above the crop from July till the end of August. During this period plant height increased from approximately 0.25 to about 1 m and, thus, the more than 2 m high windbreak was effective with respect to wind shelter for the crop. Close to the Bauhinia WB (B1 and B3) wind speed above the canopy was lower than further away at 15 m (B15) (Fig. 3.3). Wind speeds at B15 were approximately the same as in the middle of the control plots (C15: 1 m) when measured at the same height above the soil surface. On DOY 214, at B15 velocities were somewhat higher than at C15, because measurements were performed about 0.1 m higher (crop was taller). At low incident wind speeds (here: speeds at 3 m above the soil in the control = C15: 3 m) of about 2 to 3 m s^{-1} the reduction above the crop was 0.5 m s^{-1}, or velocities at B1 and B3 were about 80% of winds in the open field (B15 and C15). At incident speeds of approximately

5 m s^{-1} the reduction above the crop was about 1.5 m s^{-1}, that means velocities at B1 and B3 were about 70% of that in the open field.
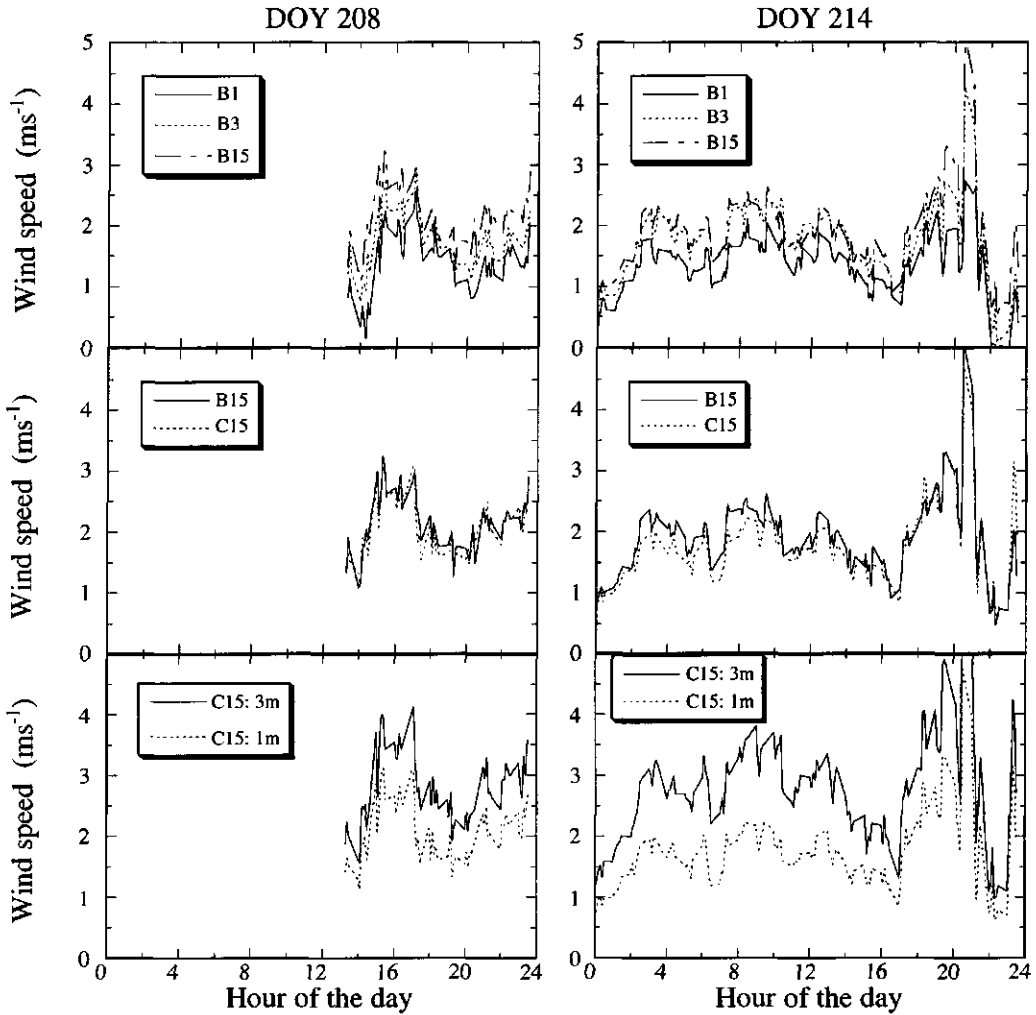
Figure 3.3   Diurnal course of wind speed above the crop at 1 (B1), 3 (B3) and 15 (B15) m from the Bauhinia windbreak and in the middle of the control at a height of 1 (C15: 1 m) and 3 (C15: 3 m) m for DOY 208 and 214 in 1993, ISC, Niger. On DOY 208 no wind speeds were recorded before 12:30 h.

Wind speed during storms was observed by Michels (1990) in all three Bauhinia and control plots of the windbreak site during a preliminary measurement period in 1990. Wind direction during storms was mainly easterly at the beginning of the rainy season. Later in the season,

storms from more northern and southern directions were also observed (Michels, 1990, see also Sterk, 1997), but this had no clear impact on the degree of wind speed reduction. In the control plots average speeds of storms where 5.59 and 6.87 m s^{-1} at heights of 0.3 and 0.7 m, respectively. Wind speed in the lee of Bauhinia was significantly reduced compared to the control (Appendix A1). The shelter effect of Bauhinia windbreaks reached at least up to 10 m (5 H; at a further distance no observations were done) and reduced the speed to 70 % and 66 % of that at the control plot at heights of 0.3 and 0.7 m, respectively. Results of 1990 and 1993 were used as input for the windbreak-crop simulation study of this thesis (Part B) to investigate, among others, the effect of wind speed reduction on evaporation (Subsection 6.3.3).

Studies on wind speed profiles including more measurement positions from the shelter showed a reduction in mean wind speeds in the lee up to 16 H (Banzhaf et al., 1992). They (1992) found behind natural bush savanna (on average 0.6 m high) at 0.3 m above a bare soil surface a wind speed reduction up to 80% of the control (Appendix A1). Furthermore, they found a linear decrease in speed from 2.8 m s^1 in the middle of a 90 m long windbreak to 2.1 m s^1 in the middle of a 6 m spaced windbreak during the millet cropping seasons. Brenner (1991) measured maximum shelter (i.e. minimum wind speed) at the start of the season at 6 H, which moved towards 3 H by the middle of the season, probably caused by the change in porosity of the windbreak.

3.1.3   Relative humidity and air temperature

In 1992, measurements were performed in the lee of prevailing winds, i.e. east of the Bauhinia. In 1993, readings were done at the opposite side, i.e. in the lee of storms at the positions of the crop growth studies (Table 2.2). In both years, the general impact of the windbreak on air temperature and humidity was negligible. Results of the west side of the windbreak are presented here.

There was no difference in relative humidity (RH) and air temperature between 1.5 H and 7 H leeward of the Bauhinia and in the middle of the control plot when ambient RH was above 50% (Figs. 3.4 and 3.5). Occasionally, when ambient RH was lower than 50% (rare during the rainy season), a slightly higher RH (ca. 3%) was recorded close to the windbreak than at 7 H or in the control, whereas air temperature was on average about 0.5 °C lower. The low effect on humidity and temperature is surprising, considering that wind speed reduction was monitored.
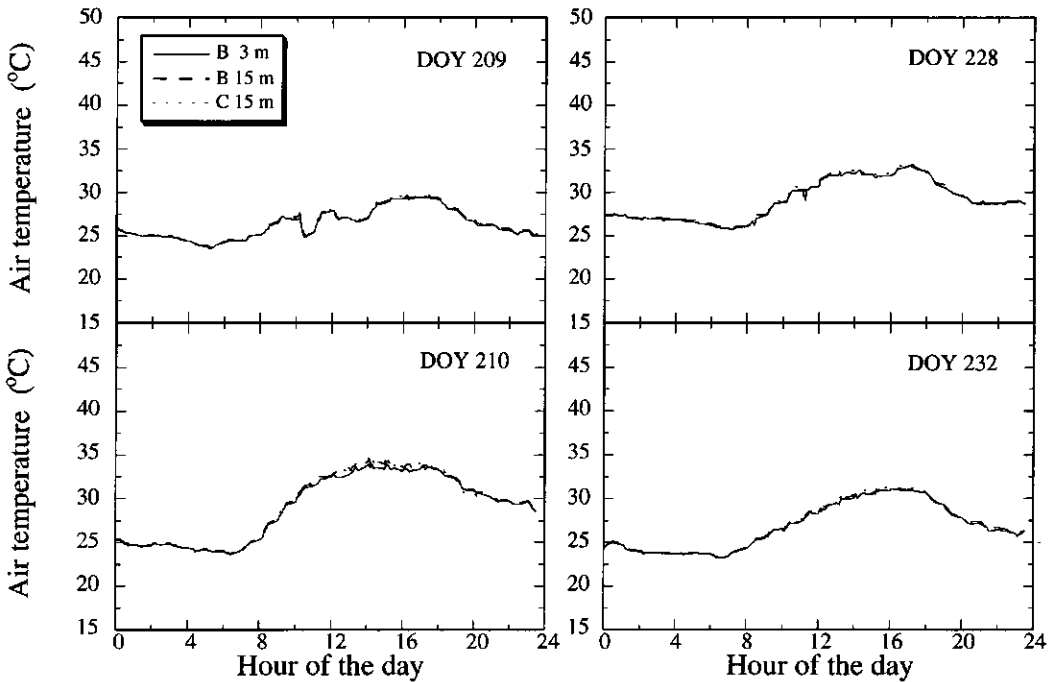
Figure 3.4   Diurnal course of air temperature above the canopy at a distance of 3 (B3) and
15 (B15) m from Bauhinia and in the middle of the control (C15) plot on four
days during the 1993 growing season, ISC, Niger.

Generally, by modifying wind speed and air flow turbulence, windbreaks can strongly reduce
the transport of heat and water vapour (McNaughton, 1988), however, the effects are opposite
for the quite and wake zones (Subsection 1.3; McNaughton 1988). Temperature within the
quiet zone should be higher during the day and lower at night compared to unsheltered fields
(often an increase of 3 °C at day and a decrease up to 1 °C at night have been reported for semi-
arid regions). Humidity is often found to be higher close to the shelter than in the open field. In
the wake zone, where next to reduction of wind velocities high turbulent downward
displacement of upper streamlines occurs, opposite effects than in the quiet zone are expected.
Modification of humidity and temperature by shelters was found in Sahelian agroforestry
projects (Brenner, 1991; Long and Persaud, 1988). Several reasons for the stability of the
above mentioned microclimate characteristics at our experimental site may be put forward,
mostly related to the special design of low height and narrowly spaced windbreaks:
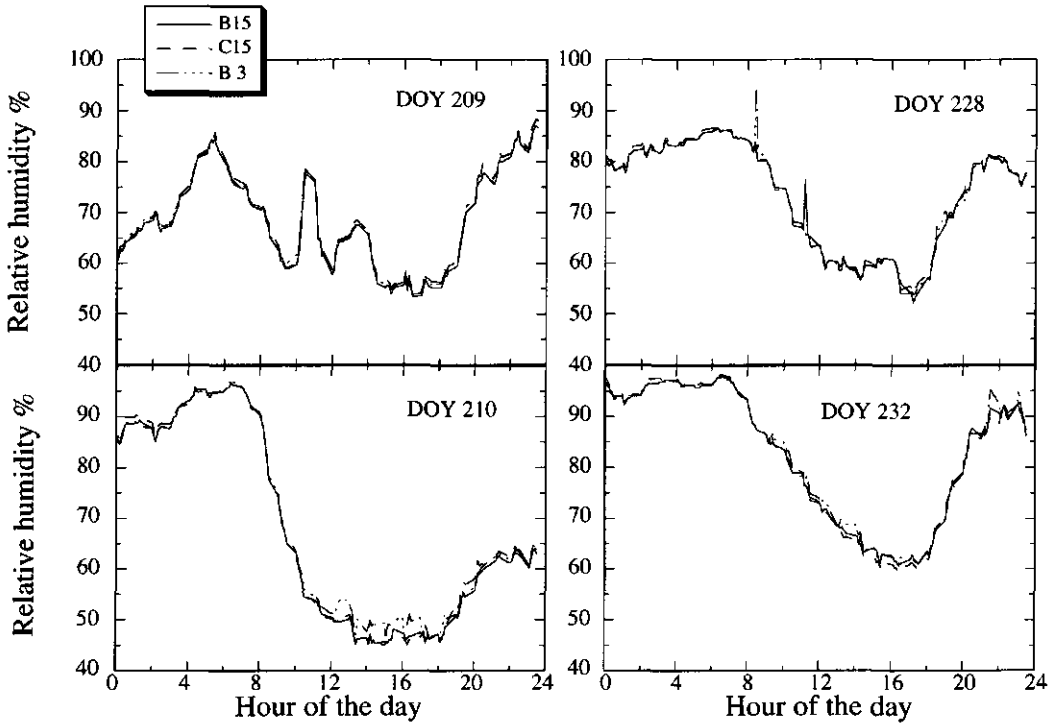
Figure 3.5   Diurnal course of relative humidity above the canopy at a distance of 3 (B3)
and 15 (B15) m from Bauhinia and in the middle of the control (C15) plot on
four days during the 1993 growing season, ISC, Niger.

- Positions of instruments were about 30 m north from the road, which formed a gap
  within the WB line (Fig. 2.2). Additionally, at a distance of about 30 m in the west-north
  direction a control (i.e. a second gap) was located. In front of gaps winds pass through
  with speeds exceeding the upwind scale (van Eimern et al., 1964). This, in combination
  with the narrow spacing between two windbreaks might have led to frequent changes in
  air flow pattern and therefore to frequent displacement of the quiet and wake zones, so
  that opposite effects were overlapping and faded (McNaughton, DSIR, and Jacobs,
  WAU, 1992 pers. comm.) or too low to be monitored. In this context it is important to
  note that the wind direction was somewhat varying (Sterk, 1993).
- For the quiet zone, another issue is that shade and/or enhanced crop transpiration
  (Brenner et al., 1995b) counteracted the rise in temperature due to lower wind speed and
  a subsequent reduced soil evaporation. Ong et al. (1991) found in a very narrowly spaced
  millet/groundnut intercrop (1:3 row arrangement) similar soil and leaf temperatures in

mono- and intercropped groundnut, largely because the reduction in radiation load owing to shading was presumably offset by the low wind speed in the intercrop.

- From approximately DOY 230 onwards, crop height reached almost the height of the windbreak, which then no longer predominated the microclimate of the crop.
- Microclimate modifications might have slipped through the spatial resolution, i.e. the small number of instruments across the transect. Probably, additional instruments, in particular installed at a distance of 1m from each of the plot bordering windbreaks (Bauhinia in the east, *Acacia senegal* in the west) might have shown microclimate modifications to some degree.

From this its follows, that the observed microclimate modifications are very specific for the present site and WB-design and, hence, can not be generalized.

3.1.4 Soil and air temperature - occasionally recorded

In agreement with the prevailing shading zone, soil temperatures up to 2 or 3 m from the Bauhinia and up to 2 m from the Acacia windbreaks were lower than those in the middle of the plot (Fig. 3.6). Depending on the hour of the day soil temperatures in the vicinity of the windbreaks were reduced through shading on average up to 10 °C, e.g.: On DOY 214 at 13 h the soil temperature was about 49 °C at 3, 10 and 22 m from Bauhinia, whereas in the WB interface zone 0 - 2 m the temperature was reduced to less than 38 °C. A similar reduction in soil temperature was found 2 m from the trunk of a scattered *Faidherbia albida* tree at ISC (Vandenbeldt and Williams, 1992). Consequently, on sunny days, in the most shaded zone (0 - 2 m = 0 - 1 H) soil temperature remained for a longer period ($\geq$ 2 hours) close to the optimum level for vegetative and reproductive growth of C4 - species (i.e. 28 - 33 °C) than in the unshaded or shortly shaded field zone. In our experiment soil temperatures often were above 37 °C for 3 to 6 h d^{-1}. Temperatures above 37 °C, even for only 3 to 4 h d^{-1} restrict both the rate of seedling emergence and the rate of leaf appearance of millet (Ong, 1983). At soil temperatures ranging from 45 to 47 °C germination is even completely prohibited (Ong and Monteith, 1985). Such high temperatures were found at the center of the plot shortly before (DOY 154) and after sowing (DOY 158). According to Vandenbeldt and Williams (1992) the duration of low soil temperatures after a rain is short, because of rapid soil drying, and so shading might be beneficial for emergence and early plant establishment. Nevertheless, in our experiment no difference in emergence between rows close to and far from the windbreak was found. Relative temperature difference (i.e. $T_a - T_t$, with T_a the actual temperature at position x_i and T_t the average temperature of the transect) was highest at 0.5 m from the windbreak between 11 and 14 h, when soil temperature reached its daily maximum. For a north-south oriented neem windbreak at ISC, highest soil and air temperatures were found at 6 and 3 H, respectively, lowest always at 1 H and intermediate at 10 H (Brenner et al., 1995b).

In our trial, air temperatures did not differ much with distance from the WB shelter, which corresponds to the continuous readings of psychrometers above the canopy (Fig. 3.7). During the morning hours, relative air temperature differences showed slightly (< 1.2 °C) lower values close to Bauhinia and up to 1.0 °C higher temperatures in the east of Acacia. The latter is probably due to additionally reflected radiation by the windbreak (Rosenberg, 1974). It is unclear why this effect did not occur during the afternoon at the west side of Bauhinia. In our experiment it was found that shading affected soil temperature more than air temperature, which is in agreement with findings of Corlett et al. (1992) and Dancette and Poulain (1969, cited by Vandenbeldt and Williams, 1992).
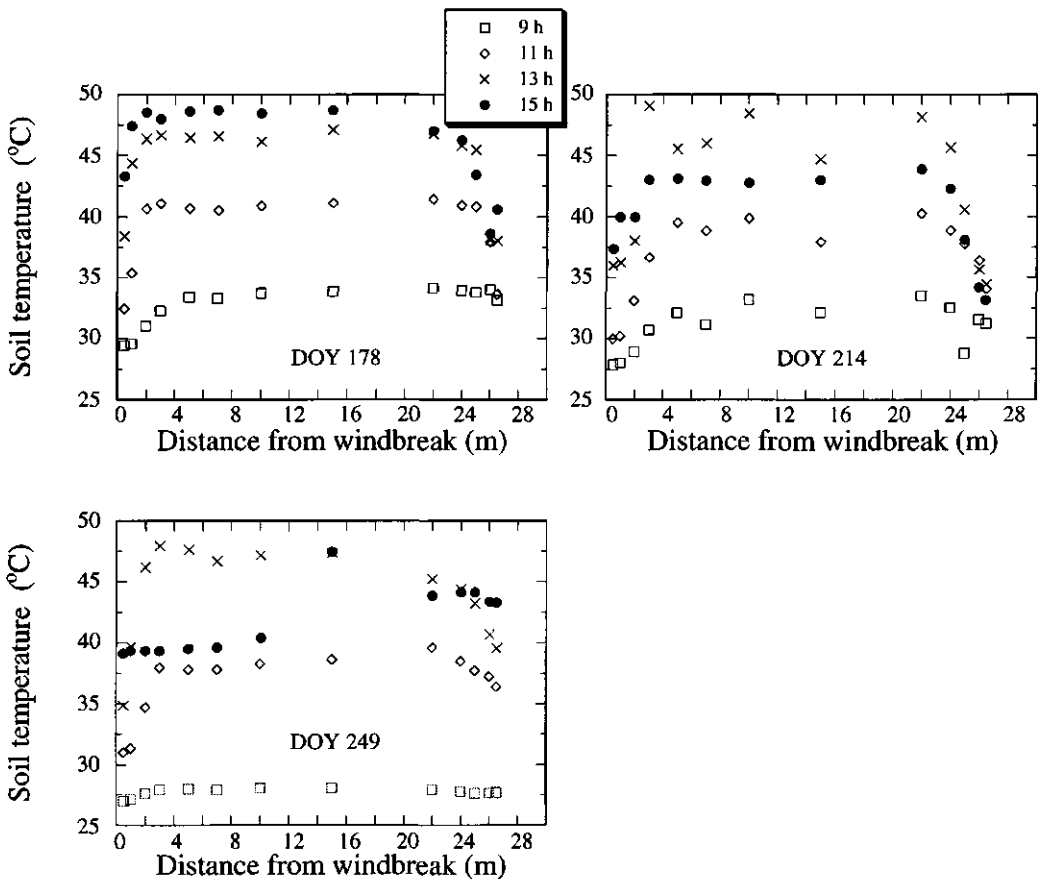
Figure 3.6   Soil temperatures at soil depth 0.01 m as a function of distance from the Bauhinia WB (0 m on x axis) towards the west shelter Acacia (30 m on x axis) on -CR plot block 1, on three days in 1993, ISC, Niger.
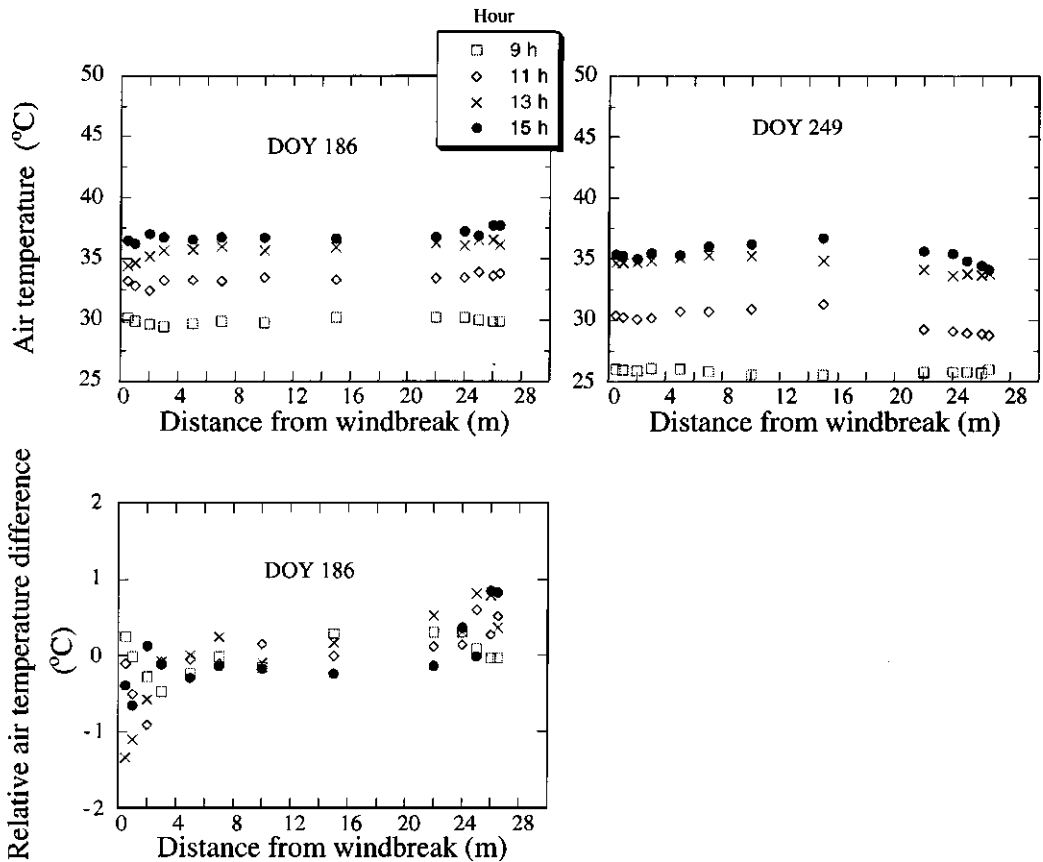
Figure 3.7   Relative air temperature difference and air temperature as a function of distance from the Bauhinia WB (0 m on x axis) towards the west shelter Acacia (30 m on x axis) on -CR plot block 1, during the cropping season 1993, ISC, Niger.

3.2   Soil

3.2.1   Rainfall and soil water content

Total annual rainfall and rainfall distribution for 1991 to 1993 - measured at ISC weather station - are presented in Figure 3.8. Brenner (1991) monitored rainfall within and outside a ca. 6 m high Neem-windbreak system. The difference between the two locations was small (< 26 mm y^{-1}). In our study, windbreaks were seasonally pruned back to 2 m height and fieldwards to

1 m, hence, rainfall interception by tree crowns can be neglected. Rainfall was distributed rather favourably in the three cropping seasons with only short periods of no or limited rain in 1993 (DOY 158 - 183 and DOY 195 - 210), but a long drought period during early plant growth in 1992 (DOY 158 - 200) and during the ripening phase of millet in 1991 (from about DOY 240 onwards).

During these drier periods, the volumetric moisture content close to Bauhinia was lower than at a distance of 10 m from the trees at all measured soil depths (0.4 to 1.9 m) (Fig. 3.8). In 1991 and 1993, the strongest effects of Bauhinia on soil water content were found at a depth of 1.9 m, e.g. the soil water content at 10 m was almost twice that at 1 m from the trees around DOY 220, 1991. This suggests either considerable tree root water uptake from soil depths below 0.4 m or extraction of more water from shallow layers, so that less water was penetrating more deeply. Contrary, during the early drought spell in 1992, soil water depletion was most distinct at 0.4 m soil depth. At the beginning of the rainy season, lower soil depths were not yet replenished (Garba and Renard, 1991) and this situation continued through the rather long drought spell from DOY 158 - DOY 200. Hence, water uptake must have been restricted to the upper layers and horizontal difference in subsoil moisture (at 1.0 m depth) remained small. Seasonal soil water contents were generally decreasing with depth below the soil surface.

In the Andropogon plots, the volumetric water contents did not vary much within the observed transects, similar to the control plots. Occasionally, in both plots soil moisture was slightly higher at a distance of 1 m than at 10 m, in particular at soil depths of 1 and 1.9 m. The reasons for this were that i) in both plots the first crop row showed rather poor growth and thus, water uptake by the crop was relatively low compared to that at greater distance from the windbreak line, ii) in the controls soil water loss due to evaporation from bare soil might have been lower than that due to crop transpiration as suggested by soil water simulations (Bley et al., 1991 and Subsection 6.3) and iii) for Andropogon it must be mentioned that this perennial grass was hardly growing in 1993.
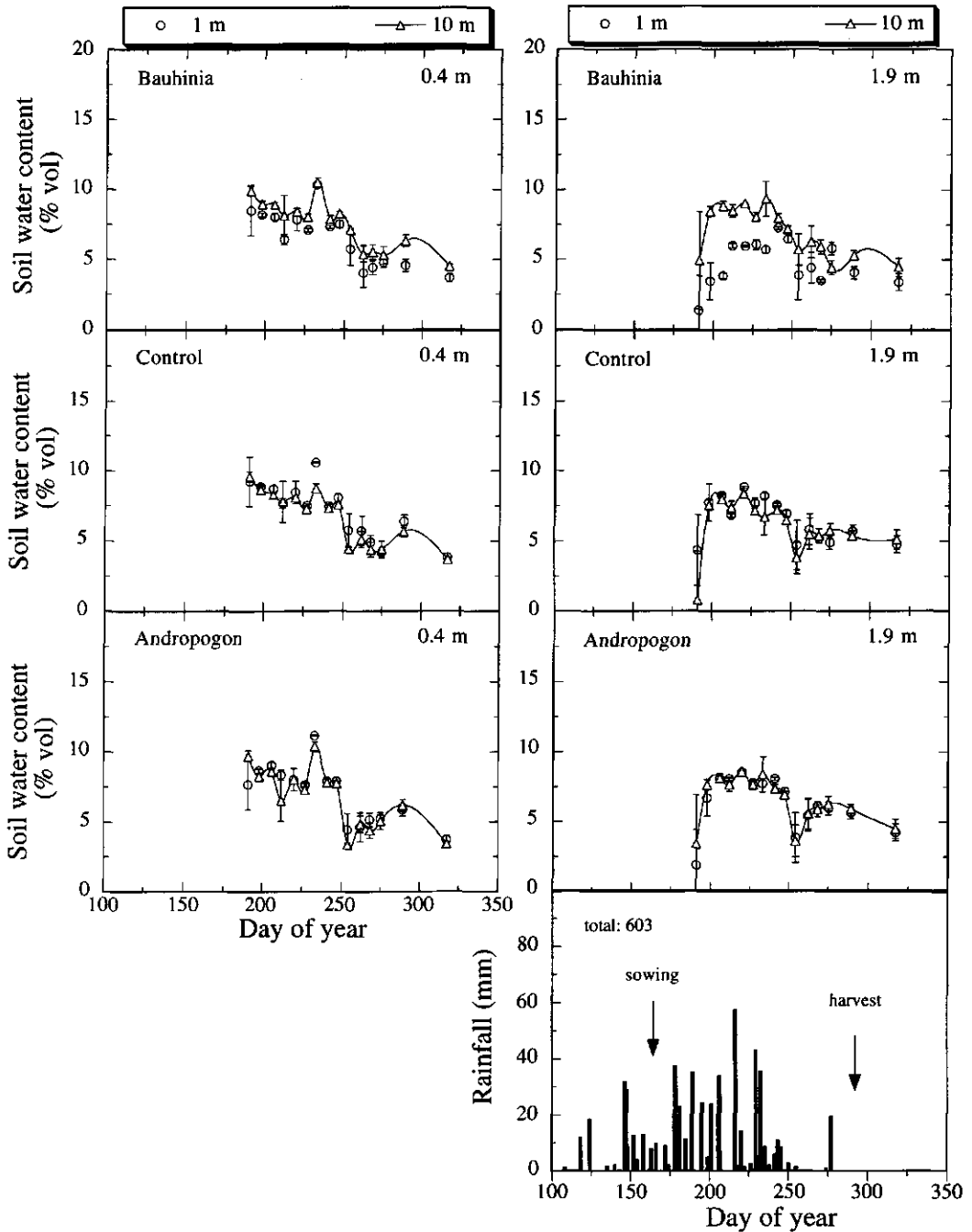
Figure 3.8a Soil water content for Bauhinia, Control and Andropogon plots without crop residues at 1 and 10 m from the windbreak at 0.4 and 1.9 m soil depth, and rainfall at ISC, Niger, 1991. Bars show SE of means.
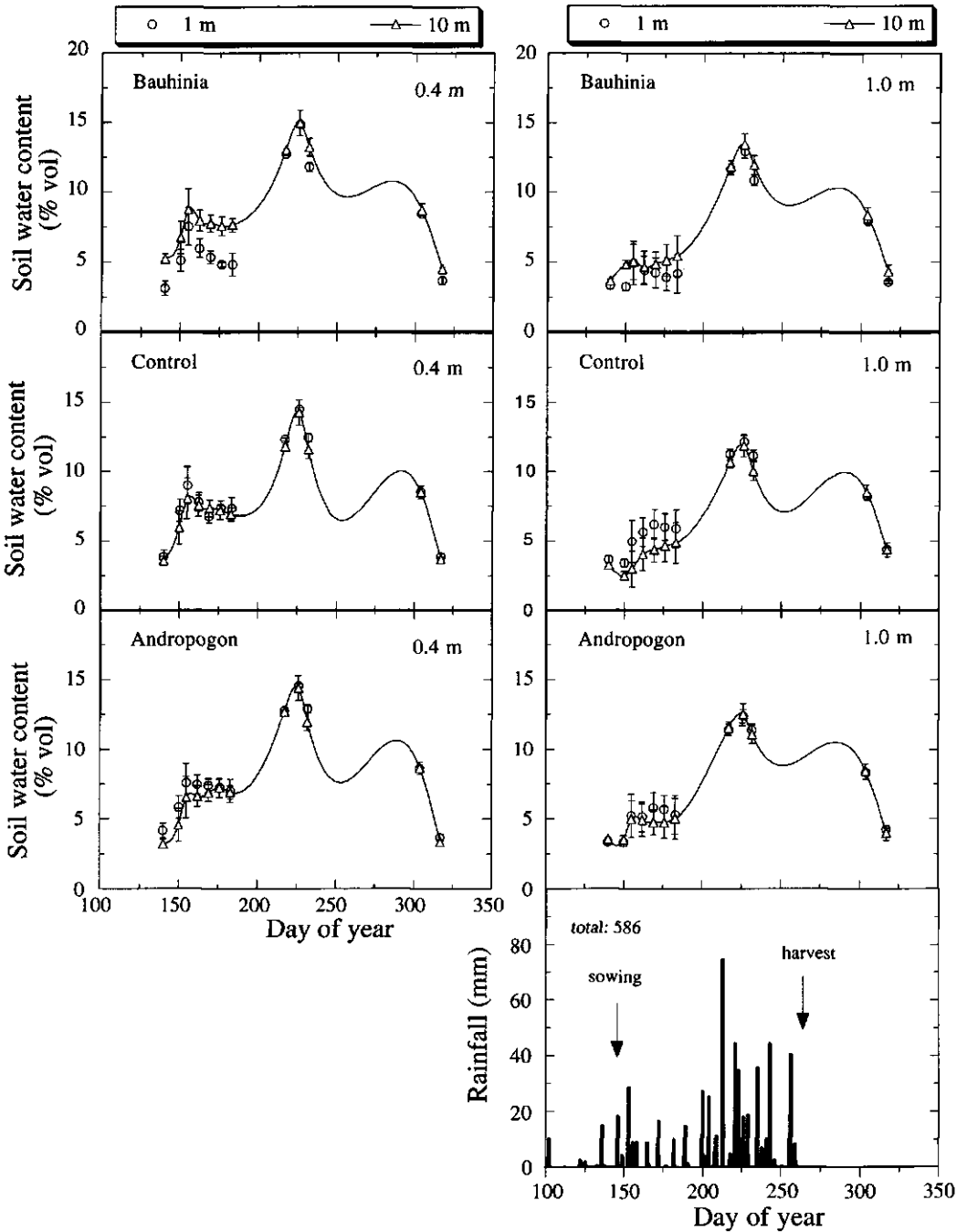
Figure 3.8b   Soil water content for Bauhinia, Control and Andropogon plots without crop
residues at 1 and 10 m from the windbreak at 0.4 and 1.0 m soil depth, and
rainfall at ISC, Niger, 1992. Bars show SE of means.
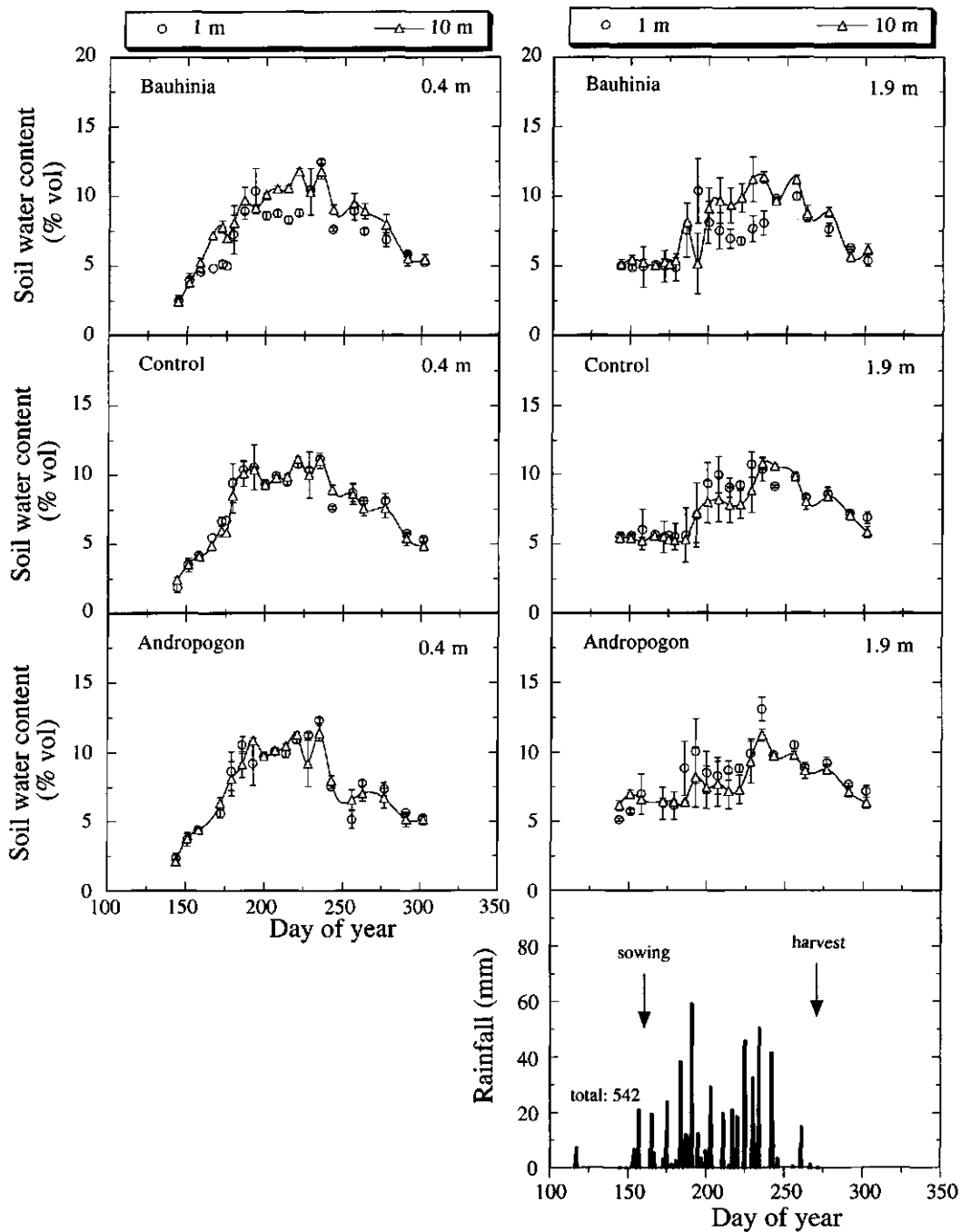
Figure 3.8c Soil water content for Bauhinia, Control and Andropogon plots without crop residues at 1 and 10 m from the windbreak at 0.4 and 1.9 m soil depth, and rainfall at ISC, Niger, 1993. Bars show SE of means.

The horizontal extent to which soil water content was influenced by the windbreak is shown in Figure 3.9 for the soil depth 0.4 m, an important depth with respect to water extraction by the crop. Soil water content was sometimes depleted up to 7 m from the windbreaks, but the strongest effects were observed at a distance of 1 and 2 m from the Bauhinia trees. At the same site during the dry year 1990 (375 mm rain during the cropping period) Bauhinia lowered soil moisture to depths of 0.7 m and deeper up to a distance of 7.5 m from the trees (Michels, 1990). In the Bauhinia plots horizontal gradients of soil moisture where often steepest at the lower depths (1.0, 1.6 and/or 1.9 m) for all 4 years (1990 - 1993 growing seasons). Whereas, at a depth of 0.40 m, Bauhinia's influence on soil moisture was only distinct during periods of severe drought (in 1990 on DAS 49 and in 1992 from DAS 13 - 33). Similarly Smith (1995) observed greater moisture depletion next to the windbreaks *Acacia holosericea and Acacia nilotica* at the 1.6 m than at the 0.4 m soil depth (Appendix B3).

Although in all years a depletion of soil moisture close to the Bauhinia was monitored for dry periods, over the seasons this effect was not significant (Appendix A1). Banzhaf et al. (1992) found also competition effects by windbreaks of natural bush savanna (< 1 m height; Appendix A1) to be restricted to drier periods. Smith's statistical analysis showed significant differences for the combined factor "species * distance" or/and "species * distance* depth", for some of the analysed dates. The influence of windbreaks on soil moisture in adjacent fields varied significantly among the tree species *Azadirachta indica, Acacia nilotica* and *Acacia holosericea* during dry periods in 1992 and 1993, especially in 1993 (Smith, 1995).

3.2.2   Soil nutrients

Chemical properties of the soil at the experimental site and their statistical analyses are reported by Michels (1994) and reproduced in Appendix A1. Important results with respect to crop growth behind the windbreak (line) were: Chemical soil analyses of 1991 and 1993 samples revealed that the nutrient status, in particular that of total N, and the organic carbon content of the soil was poor, and moreover, showed a high spatial variability. The chemical parameters did not differ significantly for Bauhinia and Andropogon windbreaks and distances, with the exception of, respectively , Na (1991) and P (1991), Mg (1991) and K (1991, 1993).

The overall effect of Bauhinia and even more of Andropogon on soil chemical characteristics was small, although there was a slight enrichment of some nutrients and organic carbon (C) behind Bauhinia and to a lesser extent behind Andropogon when results for each measurement point (distance*depth) were compared to corresponding control samples (Appendix A1). Significant effects were found only adjacent to Bauhinia windbreaks for total N, organic C and Mg in the top layer at 1 m, for Mg in the top layer at 3 m and for K in the 1 - 2 m soil layer at a

distance of 10 m from the windbreak (tree trunk). Litter fall might have caused the higher total N and organic C concentration at 1 m from the tree trunks. Soil fertility showed neither a trend towards the windbreak nor significant differences between the distances 1, 3 and 10 m in the Bauhinia, Andropogon and as expected, also not in the control plots.
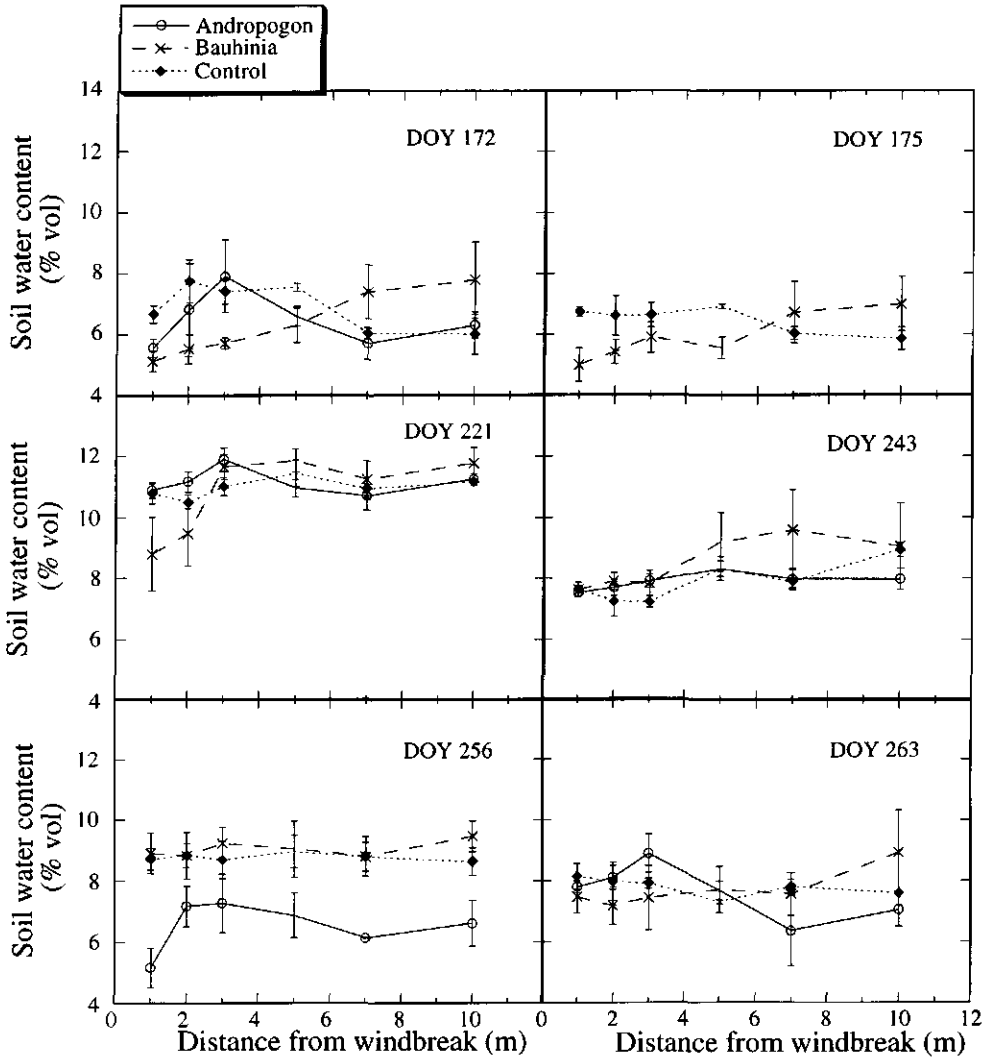
Figure 3.9   Volumetric water content at 0.4 m soil depth at several distances from the WB lines of Bauhinia, Andropogon and Control, for several days during drier periods in 1993. Bars show SE of means.

3.3   Millet

3.3.1   Yield

To show the spatial yield pattern between the windbreaks, results for each distance were averaged over all plots located between i) the first (0 m) and the second (30 m), ii) the second and the third (60 m) and iii) past the third windbreak line(s), respectively. The resulting yield pattern between two windbreaks was almost a concave curve (Fig. 3.10). At 30 m from the third windbreak line (90 m) there was no bordering windbreak and, hence, no yield reduction (with one exception). Obviously, the presence of the windbreak had a negative effect on crop growth in its vicinity.
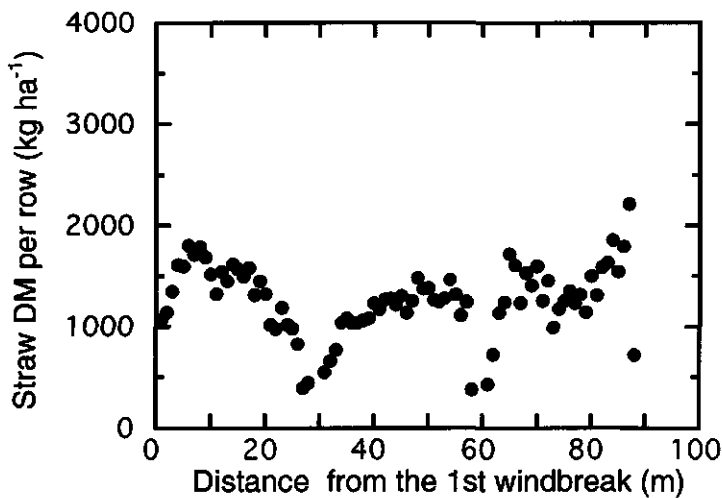
Figure 3.10   Millet straw dry matter as a function of distance from the most eastern windbreak line (0 m) at ISC, Niger in 1993. A second and third windbreak line are located 30 and 60 m from the first one. The dry matter values refer to averages over all plots with crop residues, except plots bordered by control plots.

The statistical analysis of Michels (1994) showed no significant effect of the WB species on straw dry matter and grain yield, but straw and grain production were always highest in plots of *Faidherbia albida*, a species that grows mainly during the dry season (Appendix A1). Plots with crop residues (+CR), had significantly higher production in both observation years. Millet

production averaged over all WB plots is presented for +CR and -CR plots in Figure 3.11. Between windbreaks the spatial yield pattern was similar for both treatments. Average straw dry matter initially increased quadratically with distance from the windbreak, reaching a maximum at about 6 m at the west of the trees, after which it slowly decreased. In 1993, this trend was followed by a slight increase at about 23 m, while in 1992 yield decreases continued up to about 5 to 7 m from the next windbreak line. In the adjacent zone a quadratic decrease was found in both years. Average grain yield as a function of distance seemed to be quadratic over the whole distance range between the windbreaks showing a maximum at about 3 m. In 1993, grain yield was very low due millet head caterpillar (*Heliocheilus* (=*Raghuva*) *albipunctuella*). It is unclear why the +CR plots showed lower yields than the -CR plots beyond approximately 25 m in 1992.
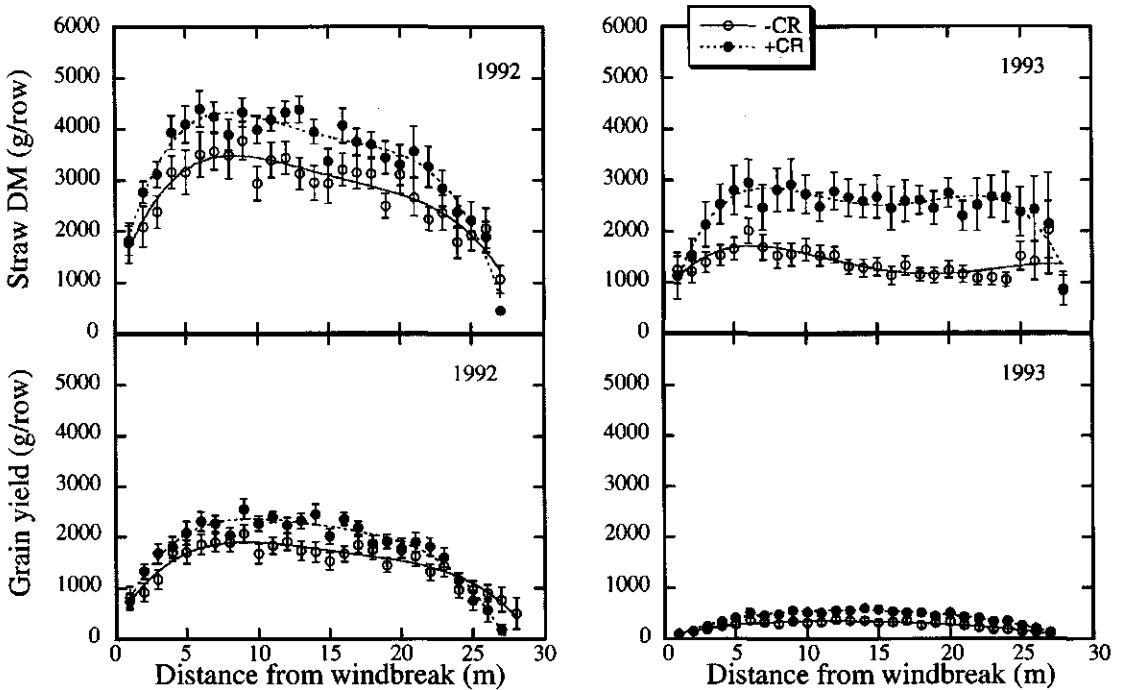
Figure 3.11   Millet straw dry matter and grain yield as a function of distance from the windbreak with (+CR) and without (-CR) crop residues, 1992-1993. One row consists of 20 pockets (ca. 0.002 ha). Bars represent SE of the mean.

Benefits from windbreaks can be established by yield comparisons of shielded and unshielded
sites, as in Figure 3.12, where we compare for each crop row straw dry matter production
averaged over all WB plots and all Bauhinia plots with the mean yields of the controls. The
effects of windbreaks on straw and grain yield in 1992 and on grain yield in 1993 were not
significant. In 1993, however, overall straw dry matter production in the WB plots was
significantly higher than in control plots (Michels, 1994), although no modifications in
microclimate that could have ameliorated millet growth have been measured in Bauhinia plots.
Growth conditions with respect to sand blasting, burial, total rainfall as well as diseases were
more unfavorable in 1993 than in 1992. In accordance, yields were lower in 1993, but the
difference between shielded and unshielded field was much larger than in the previous year,
which suggests that windbreaks compensated for or alleviated one or more growth constraints.
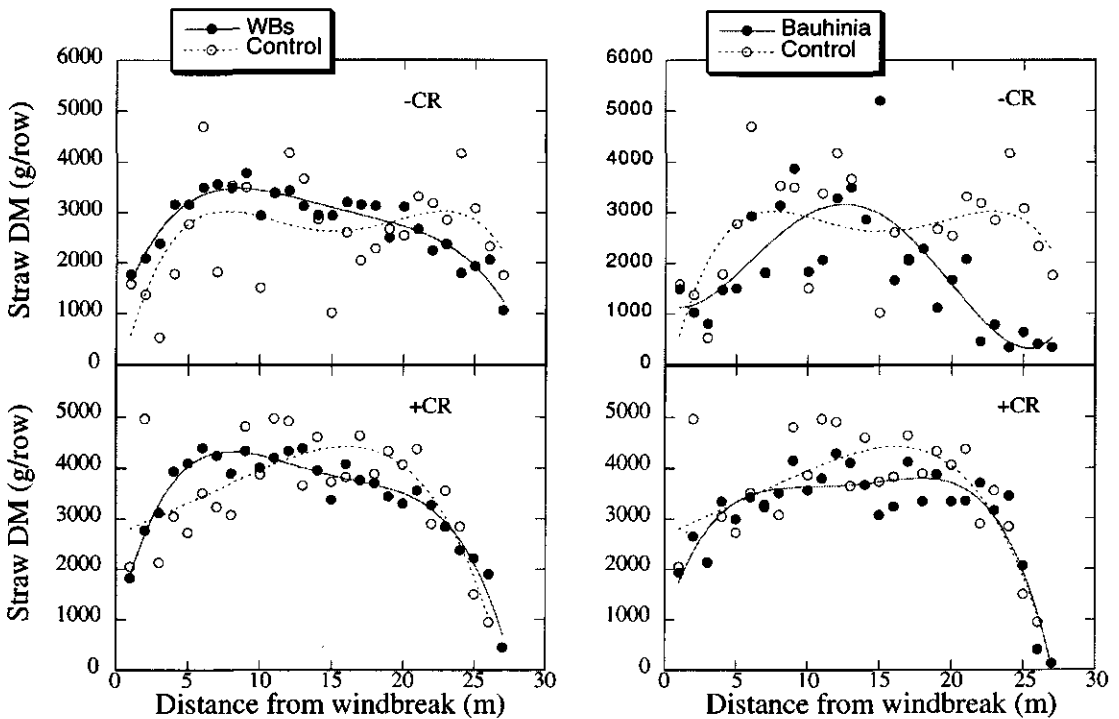
Figure 3.12a Millet straw dry matter as a function of distance from the windbreak line in
windbreak and control plots with (+CR) and without (-CR) crop residues, in
1992, ISC, Niger. One row consists of 20 pockets (ca. 0.002 ha).

For example, the higher production in WB plots could have resulted from protection against a heavy sand storm in 1993. This suggestion is supported by the following findings: Without crop residues yield differences between windbreak and control plots were largest within 10 m from the windbreak line. Within the same zone of Bauhinia -CR plots sand flux was significant (Michels, 1994) and covering of pockets with sand after a heavy storm in 1993 (not presented) was clearly reduced. In plots with crop residues, whose application also lowered sand flux (Michels, 1994), no distinct spatial variation in yield differences between windbreak and control plots was found. Bauhinia compared to control (Fig. 3.12) showed a much smaller effect (not significant) on grain yield than the average of all windbreaks. In general, high spatial micro variability in combination with a low number of repetitions made it impossible to establish growth differences between control and WB plots statistically significant in our experiments. Moreover, all control plots were located in the second or third WB line, thus, in the control plots, wind speed was probably lower than in "real" unshielded fields.
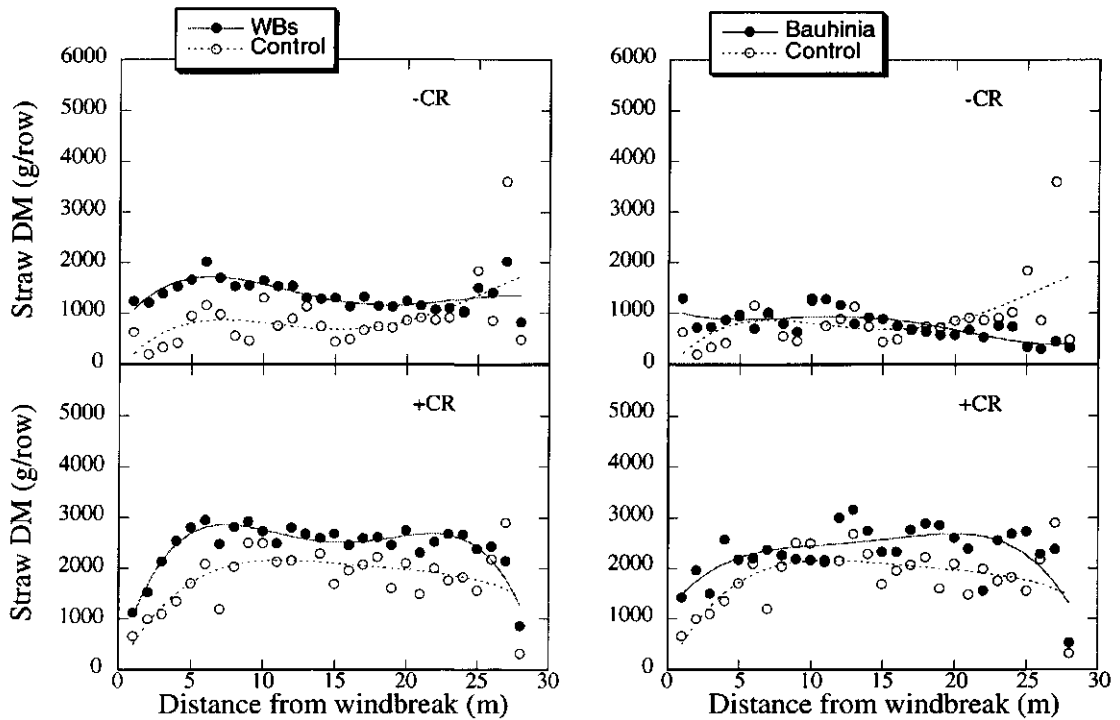
Figure 3.12b Millet straw dry matter as a function of distance from the windbreak line in windbreak and control plots with (+CR) and without (-CR) crop residues, in 1993, ISC, Niger. One row consists of 20 pockets (ca. 0.002 ha).

Consequently, the comparison of control with windbreak plots to establish microclimate modifications and related changes in crop production in WB plots was hampered (Subsection 3.1.2). This deficiency is partly compensated by the fact that yields and microclimate measures were also determined across transects at the tree-crop interface.

The growth reduction in the first 4 to 5 rows of the control plots is surprising, since competition can be excluded. In north-south direction, control plots were situated between two WB plots (Fig. 2.2). At the edges of those windbreaks with the vegetation-free zone (bare soil) of the control, turbulence and hence, increased evaporation may have occurred (McNaughton, 1988) and retarded plant growth. Higher temperatures in the bare soil zone could have played a role, too. Results presented in the following two subsections refer to the Bauhinia and control plots only.

3.3.2   Intermediate harvests

Dry matter production varied considerable among blocks, distances, and pockets (Fig. 3.13). Therefore, yield patterns behind Bauhinia WBs were less distinct than those averaged over all WB plots. Nevertheless, results of intermediate harvests in Bauhinia and control plots support the trends found for yields at maturity averaged over all windbreaks:

- growth reduction on both sides of the windbreak,
- maximum growth in the "open" field beyond 2.5 H,
- production in the open field was higher on plots with crop residues, but close to the trees it was equal for -CR and +CR plots.

Reduction in dry matter production occurred in the beginning of the season in 1992 and 1993, around flowering, and at the end of the growing period in 1992. In 1993, millet did not show much difference in dry matter production with distance from Bauhinia towards maturity. Except at booting (48 DAE in 1992, 42 DAE in 1993), total dry matter in the first row was higher than that in the second or third row westwards from Bauhinia, in particular in 1993. The curves of dry matter weight for stems and leaves followed that of the total plant and are, therefore, not presented here.
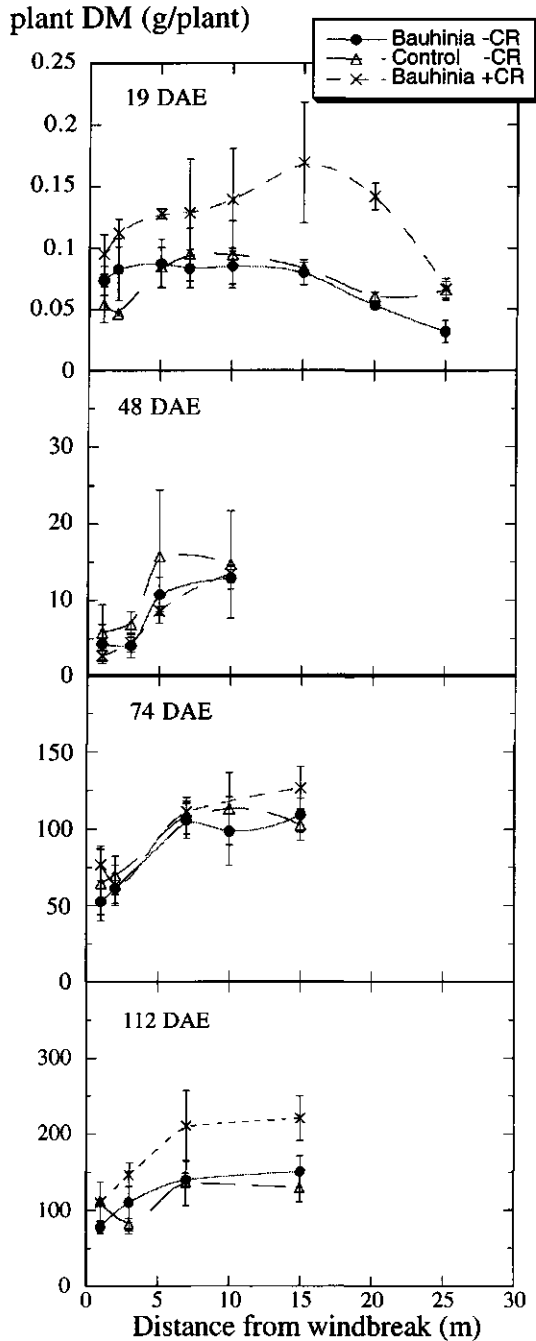
Figure 3.13a Millet straw dry matter in Bauhinia and control -CR plots and in Bauhinia +CR plots as a function of distance from the windbreak at several occasions in 1992, ISC, Niger. Bars show SE of means. DAE is days after emergence.

plant DM (g/plant): Bauhinia   plant DM (g/plant): Control
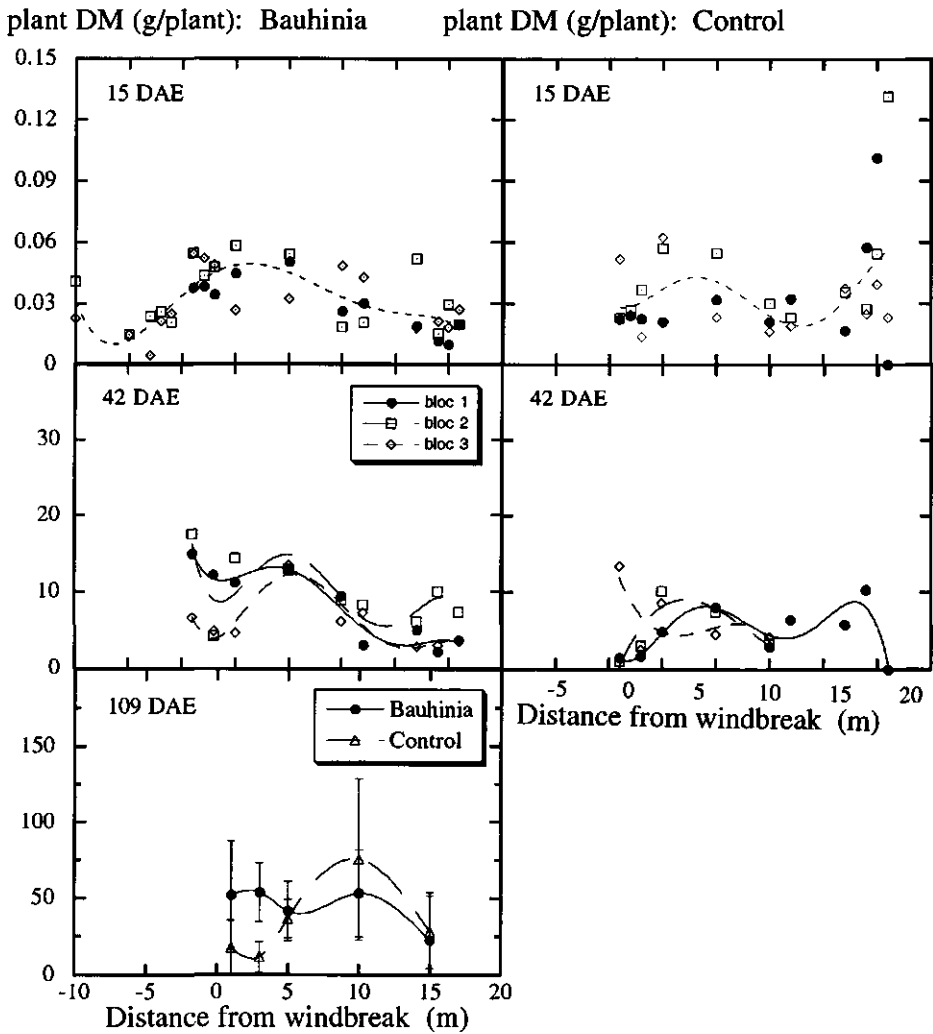
Figure 3.13b Millet straw dry matter in Bauhinia and control -CR plots as a function of
distance from the windbreak at two occasions in 1993, ISC, Niger. Bars show
SE of means. DAE is days after emergence.

3.3.3   Growth and development

In all plots the mean number of plants per pocket slowly decreased from 3 after thinning to 2.6 at the end of the growing season, due to stress factors like water or nutrient shortage, diseases, and pests. The Bauhinia windbreak had no impact on the number of plants per pocket, but the number of tillers and green leaves per plant, plant height and phenological development rate were higher for millet adjacent to Bauhinia than in the control plots (Table 3.2.), indicating that growth conditions for millet were more favourable behind Bauhinia than in unsheltered fields.

Table 3.2   Mean plot values of development stage (DVS), plant height, number of green leaves, and number of tillers, derived from the main plant of a pocket in -CR plots of Bauhinia and control in 1993, ISC; Niger. DAE is days after emergence.

DAE	Plot	DVS	Plant height (m)	Green leaves (# plant^{-1})	Tillers (# plant^{-1})
6	Bauhinia	0.18	0.7	1.8	-
	Control	0.18	0.6	1.8	-
64	Bauhinia	0.73	1.5	19.3	2.0
	Control	0.66	1.14	16.7	1.6
77	Bauhinia	1.00	1.65	13.4	1.8
	Control	0.95	1.26	11.2	1.4
103	Bauhinia	1.84	1.74	0.5	1.4
	Control	1.60	1.41	0.4	1.6

Millet, growing in the shelter of Bauhinia, developed faster than that in the control, from seven weeks after emergence onwards. Hence, 50% flowering was reached about 5 days earlier in Bauhinia plots (74 DAE) than in the control plots (79 DAE). This could be an advantage in years with a short growing season, e.g. when the rains start late or resowing is necessary. For both, Bauhinia and control plots, plants of the first row showed delayed development compared to the adjacent rows.

During the period from tillering to flowering the crop achieved its maximum photosynthetic area with approximately 20 and 16 leaves per plant in Bauhinia and control plots, respectively. The higher leaf number for plants behind the windbreak was due to a higher number of green leaves on the main culm and more tillers. In the early (< DOY 190) and late (> DOY 240) growing season there was neither a windbreak effect on tillering nor on the number of green leaves.
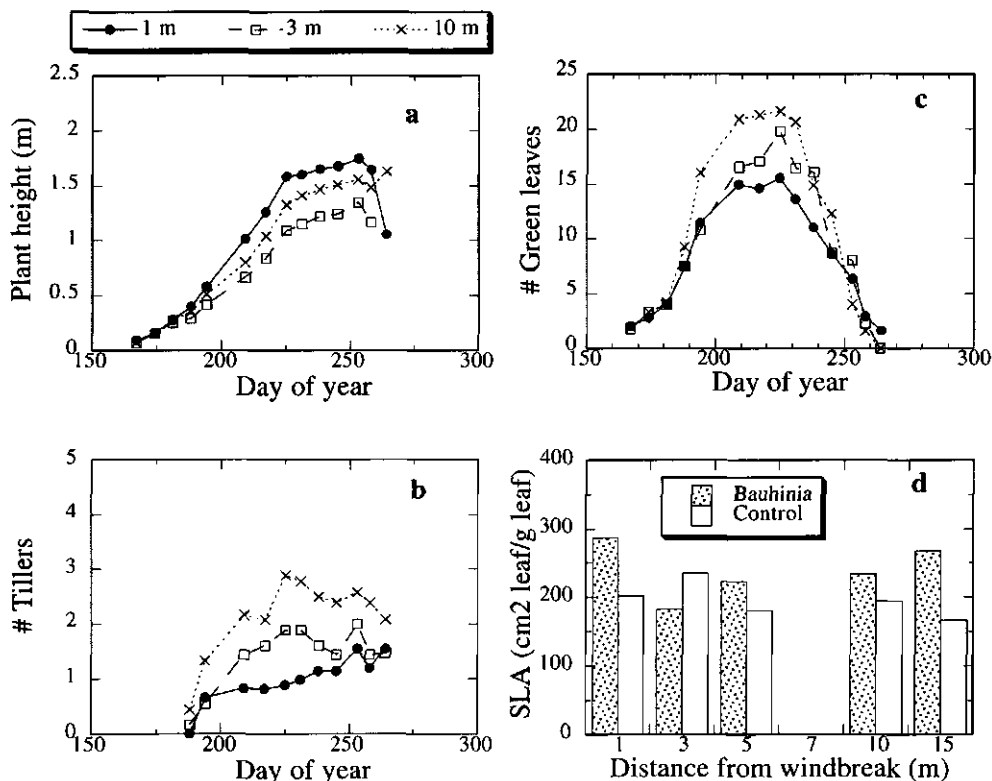
Figure 3.14 Plant height (a), number of tillers (b) and green leaves (c) of main millet plants per pocket in Bauhinia plots and specific leaf area (SLA) (d) all at several distances from the WB line during the growing season of 1993, ISC, Niger.

Specific leaf area (SLA, cm^2 leaf g^{-1} leaf) was generally higher for millet growing in the shelter of Bauhinia than for plants in the control. SLA was highest for plants growing more or less under the canopy of Bauhinia. Leaf area index (LAI) as well as the number of tillers and green leaves were much lower in the 3 m zone behind the windbreak (line) in both Bauhinia and control plots.

Plants reached their maximum height around 94 DAE (DOY 255). In the Bauhinia plots millet was 20 % taller (1.74 m) than in the control (1.41 m). Tallest plants were observed in the first row next to Bauhinia trees (2 m) (Fig. 3.14), while plants in the first row of the control were shortest (1.25 m).

3.3.4   Model input: parameters of unshielded millet

Millet parameters for unshielded conditions were derived from measurements during the 1993 growing season in Ziziphus plots (Tables 3.3 and 3.4). Here, crop growth was larger and development faster than in Bauhinia and control plots. Maximum number of green leaves per plant was similar to that of millet in Bauhinia plots and plant height was between the values found in Bauhinia and control plots. The reason for the somewhat better growth in Ziziphus plots is that only well developed plant pockets were selected at the onset of the season, whereas for each studied row in Bauhinia and control plots representative pockets had been selected for observation.

Table 3.3   Dry matter weight of plant organs of millet averaged over the main plants from the 10 selected pockets in -CR plots of Ziziphus in 1993, ISC, Niger. SE is given in brackets. DAE is days after emergence.

DAE	Total aerial DM	Green leaves	Dead leaves	Stem	Panicle + grain
			kg ha^{-1}		
21	14.3 (2.5)	14.3 (2.5)	0	0	0
32	62.9 (15.2)	47.3 (11.3)	0	15.7 (4.0)	0
50	714.4 (247.7)	356.9 (62.7)	27.8 (16.4)	329.7 (145.4)	0
61	1037.8 (407.2)	267.4 (85.4)	61.3 (25.7)	606.1 (222.2)	103.0 (38.3)
71	1908.1 (382.0)	388.6 (67.5)	122.8 (48.1)	1048.9 (190.4)	347.9 (85.6)
82	2229.6 (431.9)	275.7 (28.0)	277.7 (60.0)	1089.4 (200.1)	586.9 (112.8)
91	1618.4 (494.4)	79.5 (33.5)	262.8 (68.3)	725.2 (229.8)	550.9 (150.0)
103	1238.3 (263.9)	0	288.0 (48.3)	543.8 (126.1)	406.6 (102.1)
105	1608.4	0	334.4	755.0	519.1

Table 3.4   Development stage (DVS), plant height, number of green leaves, and leaf area index (LAI), averaged over the main plants from the 10 selected pockets in -CR plots of Ziziphus in 1993, ISC, Niger. SE is given in brackets. DAE is days after emergence.

DAE	DVS	Plant height (m)		Green leaves (# plant^{-1})		LAI (m^2 m^{-2})	
21	0.24		-	6.9	(0.43)	0.03	(0.005)
32	0.31	0.53	(0.05)	12.3	(2.28)	0.10	(0.030)
50	0.42	1.11	(0.14)	21.4	(2.39)	0.43	(0.062)
61	0.80	1.45	(0.08)	15.6	(3.37)	0.33	(0.075)
71	1.14	1.58	(0.13)	16.4	(2.66)	0.36	(0.075)
82	1.30	1.65	(0.14)	11.3	(0.73)	0.28	(0.023)
91	1.41	1.10	(0.14)	2.1	(0.89)	0.06	(0.027)
103	1.79	1.44	(0.09)	0		0	
105	2.0	1.47	(0.09)	0		0	

3.4   Windbreak-Bauhinia

3.4.1   Height
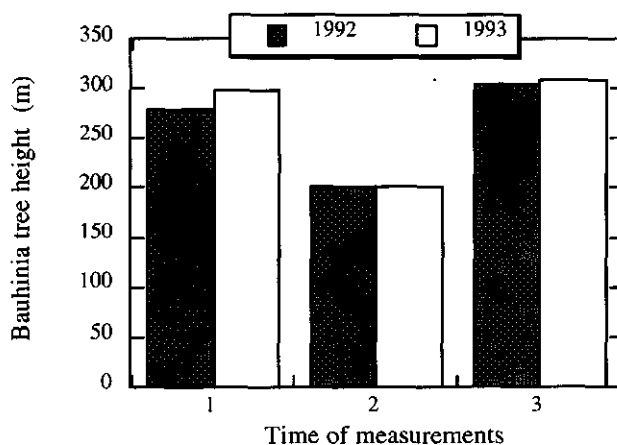
Figure 3.15   Mean height of the trees of *Bauhinia rufescens* prior to the rainy season before pruning (1), directly after pruning (2), and at the end of the rainy season (3) in 1992 and 1993, ISC, Niger.

Bauhinia was one of the more moderately growing trees of the six species used as windbreak in the trial. In 1992 and 1993, Bauhinia grew approximately 1 m in height and 0.5 m in width fieldwards. The heights prior to the rainy season in April, after pruning and at the end of the cropping season in November 1992 and August 1993 are presented in Figure 3.15.

3.4.2   Porosity

Estimates of optical porosity, based on contrast analysis of black and white photographs, varied between 60 and 90 % at the beginning of each season 1991 - 1993. At the end of the cropping seasons porosity values were in the range of 20 to 50 %. Porosity affects the degree of wind speed reduction and the length of the shelter zone as well as the turbulence level behind the windbreak (Heisler and Dewalle, 1988). Optimum porosity with respect to shelter extension and turbulence is usually considered to be 35 to 45%.

3.4.3   Roots

The excavated Bauhinia tree showed the following coarse root system: A total number of 16 roots with a diameter >> 0.01 m were dug out, including tap, shallow and sinker (downwards from lateral roots) roots. Three tap roots reached a depth of more than 3.7 m below soil surface. Their exact vertical extension is unknown, because (to save labor costs) digging was stopped at 3.7 m although one tap root was continuing. Most roots reached a depth of approximately 3 m. In horizontal direction a total extension of 8 m was found, with roots in 1 and 2 m depth close to the trunk and further away, respectively. Lateral roots were mainly concentrated in the upper 10 - 40 cm (see also Fig. 5.3).

3.5   Discussion and conclusions

3.5.1   Overall windbreak effects on millet

On the whole, millet production appeared to be positively affected by windbreaks in both years of experimentation, but only in 1993 differences between the windbreaks and the control were statistically significant for straw dry matter (Michels, 1994). Windbreak-millet studies with high *Azadirachta indica* (Long, 1989; Brenner, 1991) and low natural bush savanna (Banzhaf et al, 1992; Leihner et al., 1993) also showed statistically non-significant higher yields for the sheltered crop. For the windbreak species *Azadirachta indica* at ISC, positive influences have

been attributed to (i) a larger crop leaf area and (ii) a more efficient conversion of solar radiation into dry matter. Towards the middle of the cropping season, higher temperatures behind the shelter resulted in increased rates of leaf expansion and senescence compared to those in the unsheltered parts of the field. Higher radiation conversion efficiency is the result of higher vapour pressure of the air and, hence, lower vapour pressure deficits at leaf surface, which in turn increases stomatal conductances (Brenner et al., 1995b). In our study, the reasons for the slight tendency of yield increases are not obvious, since, with the exception of wind speed reduction, no microclimate modifications by Bauhinia have been observed.

In 1993, the beneficial WB effect could have been the result of protection against a rather heavy wind storm, that caused more sand flux in the control than the strongest storm in 1992 (Michels, 1994). Wind tunnel and field studies by Michels (1994) have shown that in particular burial of seedlings can cause severe damage to the crop. He observed that surviving plants from partially covered pockets were delayed in development and growth, resulting in reduced height and lower leaf number per plant. Although millet showed a high recovery capacity, grain yield from unaffected pockets was nearly twice that of the pockets that were partially covered (Michels, 1994). Protection against wind erosion, i.e. burial, could explain the observed faster development and taller plants with more tillers and leaves in Bauhinia than in control plots.

On the other hand, faster development is also associated with increased temperatures (Ong, 1983). Windbreaks are often reported to result in increased day temperatures and accelerated crop development. A rise in temperature may have a positive impact on crop growth and development, when it brings temperatures closer to optimum values as, e.g. reported by Brenner (1991) for millet during the period of vegetative growth and grain filling. However, stimulation of leaf expansion and early panicle formation need not necessarily result in higher grain yields, because leaf senescence is accelerated and the grain filling period shortened at the same time. In our fields, possibly small microclimate changes in temperature and humidity of the air might have occurred, but were not monitored because of the low spatial resolution of the instruments.

A more plausible explanation for the better growth in shielded fields is improved water availability. During the early cropping season when the crop canopy is still small, shade and reduction in wind speed will reduce the evaporation rate of the soil (Subsection 6.3.3), hence, more water is left for the crop. This could stimulate vegetative growth, accompanied by loss of water through transpiration. The latter could be detrimental when a dry spell follows a wet period. During the experimental years rather the opposite was the case and windbreaks might have had a positive impact with respect to water availability. In years with drought stress, Long (1989), Leihner et al. (1993) and Brenner (1991) found a substantial yield increase in windbreak fields in the Sahel, but contradictory results have been published also (Frank et al.

1974, Banzhaf et al., 1992), presumably due to different timing of drought occurrence. In both experimental years, overall, windbreaks increased straw dry matter more than grain yields, caused by a stronger reduction in grain yield than in straw biomass in the vicinity of the windbreak. According to Brenner (1991) shelters affect vegetative growth stronger than reproductive growth. He found that WB effects were always stronger in the early growth stages than during flowering and grain filling. This could not be confirmed in our experiment.

From the experimental results, it remains unclear whether the observed WB effects on straw and grain production in 1992 and on grain yield in 1993 were small due to the conditions of the specific windbreak-cropping system, the high micro variability of the soil and/or due to the deficient functioning of control plots to establish microclimate effects on crop growth (Subsection 3.3.1). However, it is evident that from half-way the cropping season (about flowering), when the crop reached almost the height of the windbreak, the impact of the windbreak through microclimate on production was negligible.

3.5.2   Competition

The growth reduction in the regions up to 4 to 5 m (2 to 2.5 H) on both sides of the Bauhinia is a strong indication of competition between WB trees and millet plants. Suppression of crop growth next to windbreaks caused by competition, especially for water, has often been reported (Lyles et al., 1984; Mellouli, 1989; Brenner et al., 1993; Onyewotu et al., 1994; Ong et al., 1996). Our measurements showed that in dry periods reduction in soil moisture was most severe at a distance of 1 and 2 m and could extend up to 7 m from Bauhinia trees. The maximum zone of water depletion agrees well with the observed lateral extension of coarse roots of Bauhinia (8 m). Generally, the degree of competition depends on the relative distribution of tree and crop root systems, but also on the depth of the water table. At the site, the water table was out of reach for both crop and trees; moreover, it was shown that windbreaks of *Azadirachta indica* , *Acacia nilotica* and *Acacia holosericea* extracted water from the same soil depths as the crop (Smith et al., 1996). Consequently, during periods of low rainfall, competition is likely to occur. Water consumption was probably lower for Andropogon than for Bauhinia, as no water depletion in the soil was observed adjacent to the perennial grass in 1992 and 1993. However, in seasons with severe drought stress Andropogon might also compete with millet as found by Renard and Vandenbeldt (1990) in a drier year (1987: 412 mm rain) at ISC.

Also among tree species water consumption can vary substantially and, forms one of the criteria for the selection of species for windbreaks. Smith (1995) suggested, based on higher soil water contents and lower transpiration, that *Azadirachta indica* is less competitive for water than either

Acacia holosericea or *Acacia nilotica* (Appendix B3). Nevertheless, crop yields behind the three species were lowest for *Azadirachta indica* (Appendix B3). Other factors than soil water must have been more growth limiting, e.g. light, since mean tree heights of *Azadirachta indica* were almost double those of the other two species towards the end of the cropping season (Smith, 1995). Competition for nitrogen or other nutrients is likely, since i) soil fertility is low and ii) nutrient uptake is related to water uptake. However, soil chemical analyses do not show significant differences with distance from the windbreak. Probably natural spatial variability in nutrients is even higher than depletion through extraction by trees. In addition, in the vicinity of trees, litter fall (Kessler, 1992) and reduced sand transport (Michels, 1994) might have compensated for N and nutrient uptake by trees, respectively.

In Bauhinia plots, above-ground competition, i.e. shading, was restricted to the morning due to their orientation towards the windbreak. During the major part of the morning, the shade extended only up to a region smaller than 1.5 H, because of the rather low height of the windbreaks. In the course of the season, the degree of light reduction above the crop canopy increased due to decreasing porosity. For the crop, however, this effect was partly counteracted by increasing crop height. In the first crop row, shade, that means a low ratio of red/far red radiation intensities (Ong et al., 1996) led to an increase in plant height and SLA, but resulted in a lower number of tillers and leaves per plant. Consequently, dry matter production of the first row was lower than of the adjacent rows. In addition, shading reduced soil temperatures in the first 3 m adjacent to the windbreak, to levels closer to optimum for millet growth. This may explain the relatively high growth rate at booting for millet in the row next to Bauhinia. During the major part of the growing season, however, millet growth appeared not improved across the shade gradient.

The results suggest that in view of competition, radiation intensities next to water availability was predominantly determining crop growth in the tree-crop interface. For a sound understanding of the processes involved in resource capture and use, the relative importance of each interaction should be quantified and they should all be integrated with the environment. From the experimental results it is not possible to isolate shade effects from water competition. In several agroforestry studies, below-ground interactions have been eliminated through vertical root barriers or by the use of artificial windbreaks, but the results obtained are often unsatisfactory. Roots may grow under or around the sides of the barriers or even through the barrier into the field. Artificial barriers do have the disadvantage that they exclude the interaction of living barriers with their environment, e.g. branches of tree WBs move with the wind and hence, they have a dynamic porosity. In this study, a simulation model is used to gain more insight in the competition effects through estimating radiation intensity and soil water content, CO_2 assimilation, transpiration and crop production in the tree-crop interface for various scenarios (Part B: Subsection 6.3.4).

3.5.3   Conclusions

For the investigated windbreak-cropping system, characterized by low WB heights and a 15 H space between shelters cropped by millet, it was found for two rather wet years that:

- There was a tendency for the overall aerial dry matter production to be enhanced by windbreaks. Growth reduction in the vicinity of the windbreak was more than compensated by increased production in the center of the plots when averaged over all WB plots. To a lesser extent this also held for the crop in Bauhinia plots.
- Yield reductions were observed up to 2.5 H at both sides of the windbreaks. Decreases of 30 % or more were confined to about 1.5 H, which corresponds with the zone of severe soil water depletion and shading.
- In dry periods, competition for soil water between windbreak trees and millet crops is likely at the interface region.
- The Bauhinia windbreak appeared to have no influence on relative humidity and air temperature beyond 1.5 H, although it clearly reduced wind speed. Therefore, the reason for yield increases in the middle of the field is presumably protection against wind erosion, i.e. reduction of lost seed pockets due to burial after one heavy storm and improved water availability.

Major factors determining straw and grain yield in WB sheltered plots were competition for soil water and light. In addition, wind speed reduction, yielding enhanced water availability and protection against wind erosion (especially in 1993) was likely to have an impact on crop growth, whereas microclimate modifications and competition for nutrients appeared to be negligible.

PART B - MODEL

Light and soil water effects of tree-crop interactions

"Things should be made as simple as possible, but no simpler."

Albert Einstein

Abstract

Windbreaks, can be beneficial for crops in various ways, in the Sahel for example through wind erosion control, soil conservation, and possible amelioration of the microclimate. However, they also compete with crops for resources, which may outweigh the potential benefits of windbreaks. Assessment of the competitive effects between crop and trees is complicated due to difficulties in determining below-ground competition and interference with other tree-crop interactions (Ong, 1996). Therefore, a model was developed for analyzing integrated and individual windbreak effects at the tree-crop interface, which were considered of major importance in the agroforestry experiment described in Part A of this thesis.

The model WIMISA simulates crop growth according to local soil moisture content and radiation intensity simultaneously for a number of rows parallel to a windbreak in daily time steps. Soil moisture content and radiation intensity are computed at process level with a high resolution in time and space. The crop routine is linked to a two-dimensional soil water module to account for horizontal gradients due to different water extraction patterns of trees and crop, and horizontally varying evapotranspiration. Competition for water is expressed by distributing available soil water between trees and crop in proportion to their uptake rates in a non-competitive situation. Water uptake is calculated on the basis of root length density distribution. Competition for light is incorporated as a reduction in instantaneous fluxes of direct and diffuse radiation at the top of the crop canopy due to interception by the windbreak. Windbreak growth is not simulated, but windbreak characteristics needed for the description of the agroforestry system are included exogenously either as constants or as a function of time. WIMISA was parameterised for a millet (*Pennisetum glaucum*) crop and the windbreak tree specie *Bauhinia rufescens*. Simulation results of the windbreak-cropping system were evaluated with data from Bauhinia plots of the wet years 1992 and 1993. WIMISA was run also for the dry year 1987, from which no windbreak-millet data are available.

Under windbreak shielded conditions, simulated straw and grain yield satisfactorily reproduced the spatial trend of the observations but not the yield levels. WIMISA overestimated straw dry matter, but underestimated grain yield. The latter is probably due to windbreak effects that are not included in the model. The reasons of discrepancy for straw dry matter are diseases, decomposition of dead plant material before final harvest in the field, and lack of a nitrogen module in WIMISA. Since simulated global radiation intensities and soil water content, as a function of time and distance from the windbreak, and percentage normalized yield reductions corresponded well with field observations, it can be assumed, that the processes of competition for water and light are simulated in their correct proportion. Hence, the model is appropriate to quantify the relative importance of competition for water and light in a windbreak-millet system, although some process descriptions needs further evaluation for application in other environments. In particular, the modelling of the tree-root water uptake requires more data for input and validation.

Simulations showed yield reductions up to 2 H from the windbreak. Surprisingly, this reduction was highest in the wettest year and intermediate in the driest year. In fields with no access to groundwater, competition for water between trees and crops is likely to occur in the beginning of the cropping season, when soil water availability is restricted to the upper horizons and transpiration of windbreak is higher than that of the crop. Under severe drought water remained the major factor (1992), otherwise light was of similar or major importance (1987 and 1993). For the Sahel, simulation results indicate that the extent of below- and above-ground competition does not only depend on rainfall amount and radiation intensities, but also depends on rainfall distribution and timing of shade.

4 DESCRIPTION OF THE MODEL WIMISA

4.1   Introduction

The explanatory model WIMISA (WIndbreak-MIllet-SAhel) has been developed to simulate growth of millet behind a windbreak in the Sahel. A windbreak-cropping system is very complex with many interrelated processes, which are to some extent reflected in the crop growth pattern with distance from the windbreak (Fig. 1.3). As described in Section 1.3, the yield pattern is related to the most growth determining factor(s). Whether that will be light, soil resources, wind erosion and/or other factors depends on the magnitude of the prevailing WB effects, varying with climate, soil type, WB-crop configuration and farming practices. Development of a model integrating all these relations is beyond the scope of this study, because it requires data from windbreak-cropping systems under various environmental and system conditions. The immediate objective of the present model is to provide a means for analyzing the effects of wind speed reduction and competition between crops and trees for soil water and radiation on millet growth. Those were identified as the major WB effects in an experimental study at the Sahelian Center of ICRISAT (Chapter 3). Thus, the present version of WIMISA incorporates effects operating at the tree-crop interface. However, to provide a basis for extended windbreak-cropping system simulation studies, WIMISA was designed such that other WB effects can easily be incorporated (Section 4.8).

The windbreak-millet cropping system of WIMISA consists of six subsystems: WEATHER, MICROCLIMATE, CROP, WINDBREAK, ROOTS and SOIL WATER (Fig. 4.1). For each subsystem a submodel simulates the dynamics of the subsystem's state variables. The rates of change simulated in each submodel may depend also on state variables of other subsystems, reflecting the main interactions in such an agroforestry system. Interactions in the WIMISA system are the following: WEATHER data define the overall conditions and constraints for many soil water, root and crop processes. Theoretically, all weather elements can be modified by the subsystem WINDBREAK (McNaughton, 1988). However, in WIMISA air and soil temperature, relative humidity and rainfall are assumed to remain unaffected. Hence, the WB only affects the MICROCLIMATE with respect to radiation and wind speed, both as a function of development (height, porosity) of and distance from the windbreak. Modified radiation and wind speed are inputs in the evapotranspiration equation and thus affect the subsystem SOIL WATER. Consequently, soil moisture content may vary with depth, but also with distance from the tree row(s). Differences in root water uptake between windbreak trees and millet crop may increase this horizontal variation in soil water content and influence the root water uptake

(ROOTS) under water shortage. Finally, local soil moisture content and radiation differentially affect the growth of millet in the various rows parallel to the windbreak (CROP). It must be emphasized that the above mentioned effects of the windbreak on millet growth are simulated for each row parallel to the windbreak simultaneously. In that way, the interrelations between adjacent crop rows are accounted for.
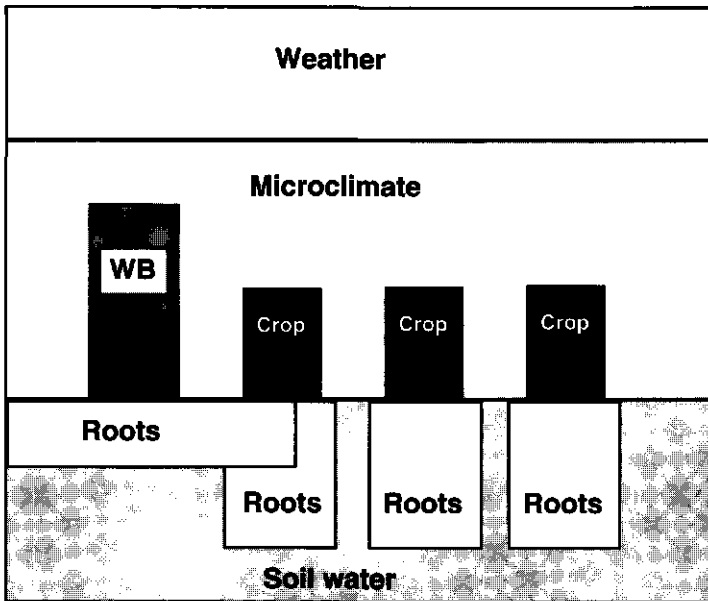
Figure 4.1   Subsystems (modules) of the model WIMISA

WIMISA has been developed by combining methods from several existing models with newly developed concepts (Section 4.8: Table 4.1):

- For simulation of the CROP subsystem the explanatory crop growth model CP-BKF3 (Verberne et al., 1995) was adopted and implemented in WIMISA (Section 4.3). The CP-BFK3 crop model was an appropriate choice, because it was developed, among others, for millet and accounts for the interaction of the crop with soil water, which facilitates incorporation of competition between windbreak and crop for soil water.
- The SOIL WATER subsystem is modelled using a semi-mechanistic approach. The one-dimensional water-flow approach of WEPS (Durar and Skidmore, 1995) and the two-dimensional water-flow model FUSSIM2 (Heinen and de Willigen, 1992) have been used

as starting points for the development of the two-dimensional water-flow simulation module of WIMISA (Section 4.6). Soil water flow is simulated in two dimensions to account for a possible horizontal gradient induced by horizontally varying evapotranspiration (Section 4.5) and different water extraction by WB trees and crop.

- Knowledge of WB characteristics and WB-related processes is limited. Consequently, competition effects and wind speed reduction had to be described using simple abstractions in order to restrict the number of assumptions and parameters. A large number of poorly estimated parameters would increase the model uncertainty, rather than the accuracy of the description of the system. For the same reason, WB growth is not simulated, but the necessary tree parameters are introduced either as fixed values or as time-dependent forcing functions. Competition for light is incorporated as light reduction through a barrier with increasing height and density (Section 4.4). For the description of the competition for soil water, tree root length densities in the soil profile are introduced as fixed values with time and depth (Section 4.7). Reduction of wind speed is incorporated by an empirical reduction factor for wind velocities in the first 5 H (ca. 10 m, with H the WB height) from the windbreak.

- For modelling spatial heterogeneity in windbreak-cropping systems, depending on the process, up to three dimensions are distinguished (Section 4.2). All processes, with the exception of overall weather, are simulated as function of the distance from the windbreak (i.e. x). Variations in the direction parallel to the windbreak (i.e. y) are assumed to be small compared to those in the x direction and the y-coordinate is therefore only used to keep soil water balance equations dimensionally correct. The vertical component of the system (i.e. z) is required for computation of local radiation intensities, millet root growth, root water uptake and other soil-water balance terms.

- For simulation of the dynamic behaviour of the system three time steps are distinguished. The overall time step of the model is one day in accordance with the interval of integration of dry matter growth (Penning de Vries and van Laar, 1982). Much smaller are the time steps for the processes of reduction in light intensity and the associated CO_2 assimilation and the soil water processes, which occur within the daily interval (Fig. 4.2). Time steps for radiation/assimilation can be selected within a reasonable range (e.g. 5 - 15 minutes). The SOIL WATER module uses a time step that is adjusted automatically to water flow rate and thickness or width of the soil cell, to keep the integration of the flow numerically stable without wasting computing time. Simulation of the water balance starts well in advance of sowing, so that realistic moisture contents are attained for germination and emergence.

The model requires input on crop, windbreak, soil and weather characteristics. Site independent parameters, such as millet crop physiological or sandy soil physical characteristics, were

derived from literature. Site-, year-, and cultivar-specific data for millet and windbreak, soil moisture and weather data were derived from a WB-millet system experiment, conducted during the 1992 and 1993 rainy seasons at the Sahelian Center of ICRISAT (ISC) in Niger (Part A). WB parameters refer to the local (Sahelian) tree species *Bauhinia rufescens* Lam., because most detailed studies were performed on Bauhinia-millet systems. Experimental results from 1993, derived from a separate plot outside the influence of the windbreak, were used for calibration, while those from 1992 and 1993 from the Bauhinia plots were used for evaluation of the model. The model was further evaluated with data from Bley (1990), collected at ISC. WIMISA-specific parameters are presented in Chapter 5. A list of all input parameters is given in Appendix B2. Simulation results are presented and discussed in Chapter 6.
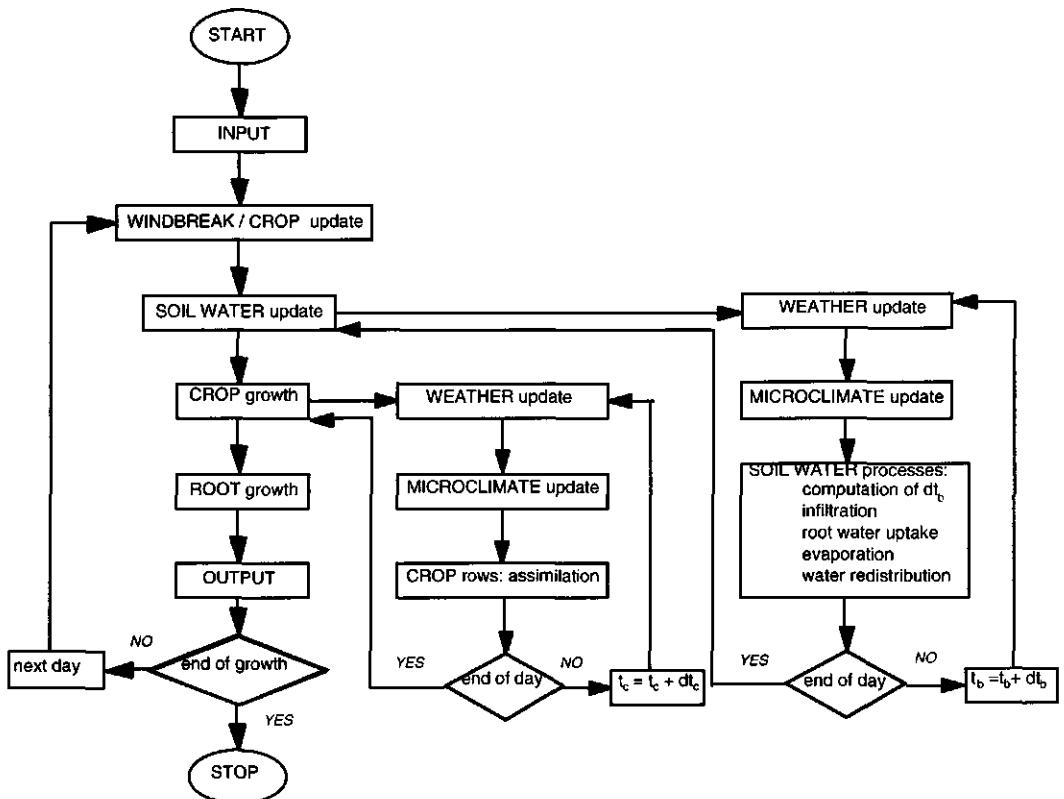
Figure 4.2   Task flow diagram of the model WIMISA including a) global task flow for one day, b) task flow for soil water balance in a loop of dt_b, and c) task flow for radiation/assimilation of crop rows simultaneously in a loop of dt_c.

4.2   Geometry of the windbreak-cropping system

WB effects vary with distance to the windbreak. As a result, crop growth may vary among rows planted at different distances parallel to the windbreak. For modelling spatial heterogeneity in the windbreak-cropping system a three-dimensional coordinate system is introduced: The x-coordinate is defined in horizontal direction perpendicular to the windbreak, the y-coordinate in horizontal direction parallel to the windbreak, and the z-coordinate in the vertical direction. WIMISA describes soil water balance, radiation and crop and root growth as function of the distance from the windbreak, but keeps simulations uniform in the y-direction. Variations in the direction parallel to the windbreak (i.e. y) are assumed to be small compared to those in the x-direction. Hence, gradients in the y-direction are neglected. A vertical component (z or h_m) is considered for computation of local radiation intensities, millet root growth, root water uptake and other soil-water balance terms. Space and time function dependencies are always included in the mathematical notations in this chapter with the exception of Section 4.3.
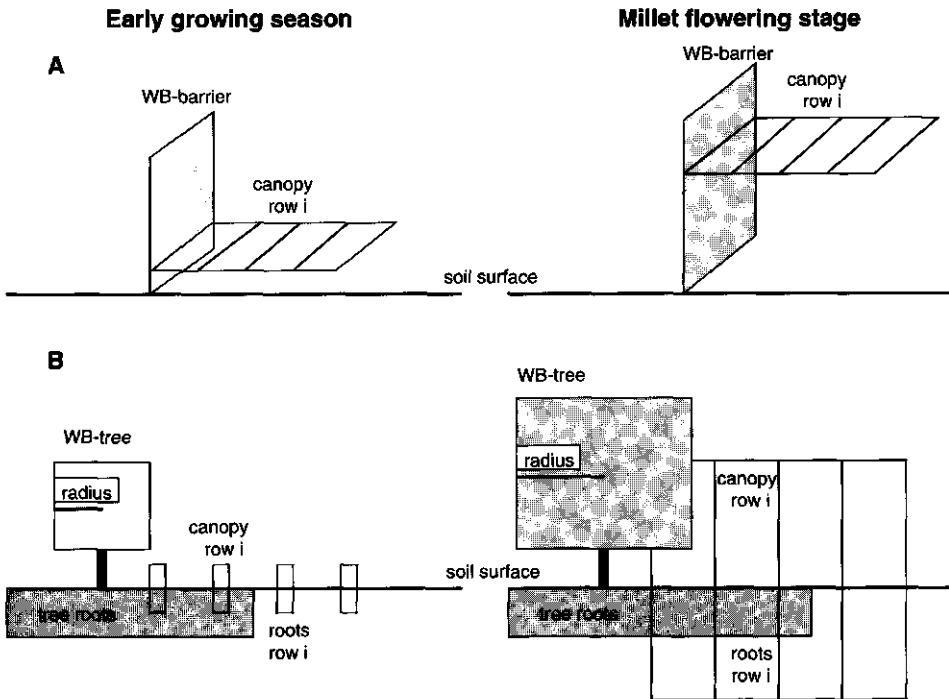
Figure 4.3   Schematic presentation of the spatial arrangement considered for computation of radiation (A) and soil-water balance (B) terms.

The geometry of the windbreak-cropping system plays an important role in the distance-dependent functions of wind speed, radiation and soil water. The spatial arrangement of windbreak, crop rows, and roots form the geometry of the model system. Figure 4.3 shows that the architecture of these components differs for the simulation of radiation and soil-water balance terms (evaporation, potential transpiration, and root water uptake) in agreement with the required input parameters of the implemented algorithms. This holds especially for the windbreak. In the calculation of light reduction, the windbreak is considered as a two-dimensional barrier of a certain height and porosity, located at the outer edge of the tree canopy next to the crop (Fig. 4.3A). On the other hand, computation of the soil water sink terms (Section 4.6) requires input on leaf area index, canopy radius and root distribution of the windbreak, resulting in a WB form as presented in Figure 4.3B. In the remainder of the text the first WB form is referred to as WB-barrier.

The position of the windbreak is chosen perpendicular to the erosive winds from the east and the prevailing winds from the west. The length of the windbreak is considered infinite so that edge effects can be excluded. Height and density of the windbreak increase in the course of the growing season to such an extent that their impact on radiation intensity and wind speed reaching the adjacent crop changes considerably. Consequently, the dynamics of those factors must be taken into account. Currently, wind velocity is not linked to dynamic WB characteristics, but an empirically determined mean reduction factor is applied. While the WB canopy (height and porosity) is regarded dynamic, its root mass is static. Time variance in "adult" tree roots is assumed to be of minor importance for the soil water balance and crop performance for one growing season in WIMISA (Groot, AB-DLO, pers. comm., 1996). Growth of the millet crop, with its first row planted at a certain distance from the tree trunk, is simulated for both above- and below-ground crop components.

Below-ground, two independent spatial arrangements are used for root distribution of millet and of trees, respectively (Fig. 4.13). The roots of millet are described by an exponential decrease in root density with depth inside a rectangular compartment, one for each crop row (Subsection 4.7.1). The root geometry of windbreak trees is fixed within a two-dimensional arrangement of compartments (Subsection 5.3.4). To account for horizontal variability in root length distribution, several zones are distinguished at both sides of the WB trunk. Vertically, each zone is subdivided in a number of soil compartments. For calculation of water uptake, the root densities of millet and windbreak from their compartment(s) are projected onto a grid of soil cells, which are needed for the numerical solution of equations in the SOIL WATER module (Fig. 4.11).

East ◄—   —► **West**

1.5 m

1 m

0   6   37.5   69 m

Model

3.5   7 m

row 1   row 2   row 10

bare soil

zone 1	zone 2	zone 3	zone 4	zone 5	zone 6	zone 7

0   1.5   3   4.5   6   7.5   9   10.5   16 m
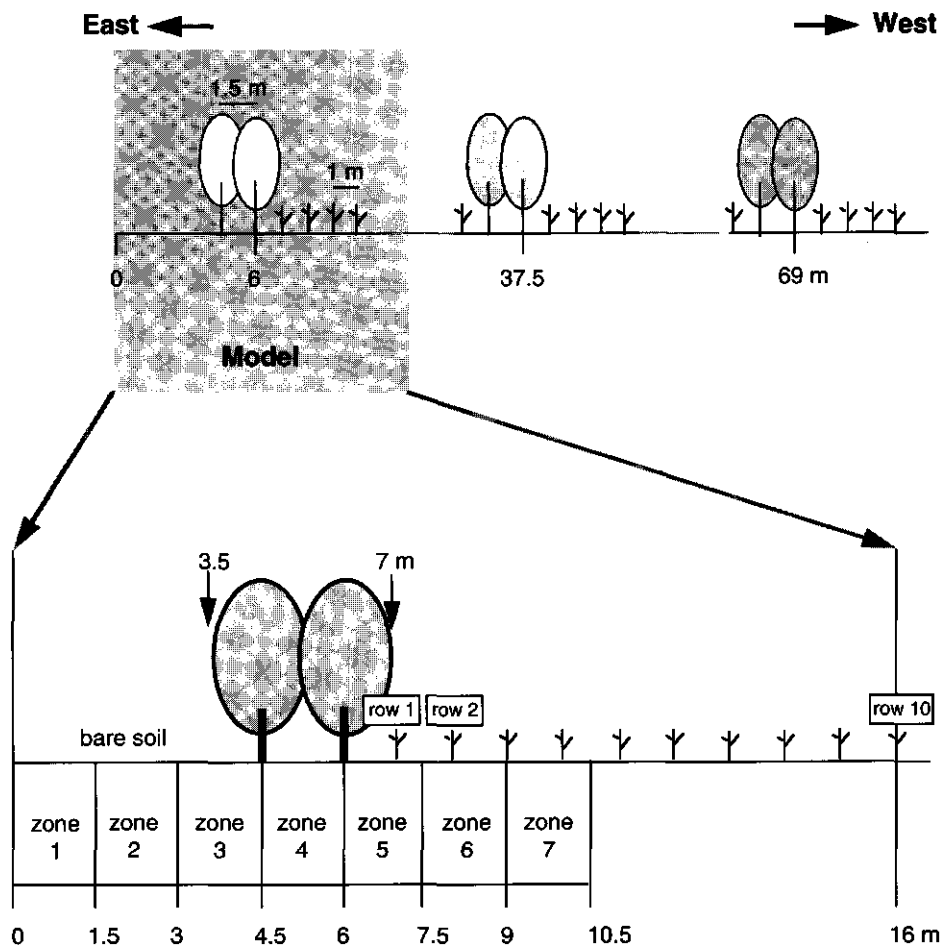
Figure 4.4   Schematic cross section through the experimental double-row windbreak-cropping system with a detailed cut of the model system. Positions of the system components are given relative to the left edge of the bare soil area.

Number and positioning of the individual system components are variable inputs. Hence, the system can be modified from a single windbreak with a long or short crop field length to a close alley-cropping system. In this thesis, simulations cover the following part of the experimental system (Fig. 4.4): one double row windbreak with on one side a bare soil and on the other side a crop. The crop field ranges from close to the tree trunk to a distance out of the influence of the windbreak. The bare soil region as far as rooted by the WB trees is taken into account in the soil water balance, because water flow in the vicinity of the tree rows is affected by different conditions on both sides of the windbreak despite a symmetric tree root system. The conditions differ with respect to water extraction (crop, bare soil), and evaporation (wind speed reduction

or not and shading in the morning or in the afternoon, for left and right side of the windbreak, respectively). The shading effect on the bare soil side has not yet been incorporated in the present version, but can be computed by separate simulation runs for each side of the windbreak. However, this will hardly affect the soil water balance of the crop field. In order to cover the entire experimental windbreak-cropping system, the model system described above has to be extended; mirroring is not possible due to the asymmetry of the system and its environmental conditions. In a follow-up study on optimum windbreak-cropping design the following factors should be considered: orientation, height, porosity, and spacing between windbreaks and crop and windbreak-species.

4.3   Crop growth

The concept of the CROP module in WIMISA is derived from the explanatory crop growth model CP-BKF3 (Cultures Pluviales-Burkina Faso, Verberne et al., 1995) and has been modified mainly with respect to the spatial and time computation interval of CO_2 assimilation. CP-BKF3, based on earlier models of van Kraalingen and van Keulen (1988), van Duivenbooden and Cissé (1989), Erenstein (1990) and Dijksterhuis and de Willigen (AB-DLO, pers. comm., 1995), simulates growth and yield of maize, sorghum and millet under varying weather and soil conditions in semi-arid regions. CP-BKF3 provides the option to describe three production levels: potential, water-limited and production limited by both water and nitrogen. In the current version of WIMISA, however, a nitrogen routine has not yet been introduced, so that crop growth is simulated under water-limited conditions (production level 2, see Section 6.1).

4.3.1   Crop growth as in CP-BKF3

Crop growth is driven by characteristics of the green leaf area, other crop properties and the abiotic factors irradiation, temperature, and soil water. Sowing can only take place after a minimum amount of rainfall and subsequent germination and plant establishment are strongly related to soil moisture content (Section 1.2). Simulation starts with the calculation of cumulative rainfall. When, within two days, cumulative rainfall exceeds a threshold value, sowing is assumed. Germination proceeds as long as the actual soil water content in the top soil compartments (where the seeds are) exceeds a critical value. When these conditions persist for a preset number of days, emergence takes place. If the top soil compartments dry out before emergence, the seedlings die and a new wave of germination starts after rewetting and

subsequent resowing. Optionally, emergence can be set to a fixed date, irrespective of soil moisture content.

After emergence, plant growth starts with predetermined initial values of leaf area index (LAI, m^2 leaf m^{-2} soil) and weights of plant organs. From emergence till physiological maturity the plant passes several growth and development phases. Phenological development of a growing plant is characterized by the order and rate of appearance of vegetative and reproductive plant organs (Fig. 4.5). In the model it is represented by the dimensionless state variable development stage (DVS). DVS ranges from 0 to 2, where 0 represents emergence, 1 50% flowering, and 2 physiological maturity (Penning de Vries at al., 1989). The rate of increase in DVS, the development rate, is defined as a function of temperature and day length (van Keulen and Seligman, 1987). As these two factors have different effects before and after flowering, two development rates have been defined: DVR1 for the phase from emergence to flowering (pre-anthesis phase) and DVR2 from flowering to maturity (post-anthesis phase). The effects of temperature and day length on DVR1 and the effect of temperature on DVR2 are described in tabulated functions (van Kraalingen and van Keulen, 1988). Many crop characteristics (e.g. death rates and distribution of assimilates) are related to the current DVS.
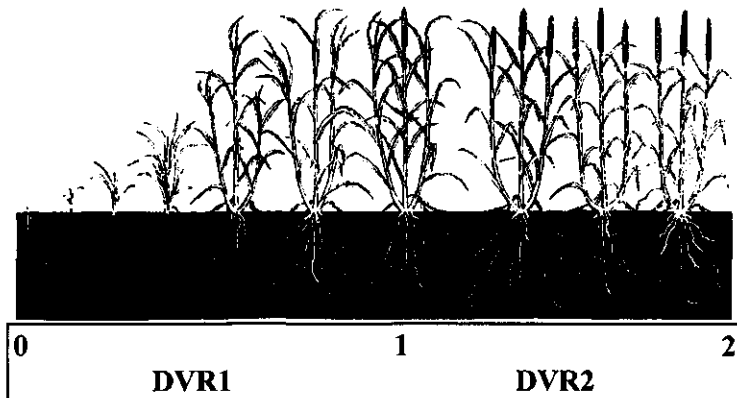
Figure 4.5   Schematic diagram of major development stages and rates of millet. DVS: 0 = emergence, 1 = 50% flowering (anthesis), 2 = maturity, and DVR1 = development rate for the pre-anthesis phase and DVR2 = development rate for the post-anthesis phase (after Maiti and Bidinger, 1981).

Daily gross CO_2 assimilation is based on the profile of absorbed photosynthetically active radiation (PAR) in the canopy and the photosynthesis light response curve of individual leaves. Absorbed PAR is a function of ambient light intensity, the amount and distribution of photosynthetic area within the canopy and the light extinction coefficient. Leaf area is calculated from leaf dry matter, using specific leaf area (m^2 leaf kg^{-1} leaf, SLA). SLA is introduced as a forcing function of DVS. Total photosynthetic area includes the stem area, calculated from stem dry matter and a constant specific stem area. The photosynthesis-light response curve is characterized by the initial light use efficiency (ε) and the light-saturated maximum assimilation rate (A_m), both influenced by air temperature. A_m is also dependent on the nitrogen content of leaves and leaf age, which develops as a function of DVS (van Keulen and Seligman, 1987).

CO_2 assimilation is computed at three selected depths within the canopy, to account for the attenuation of radiation with increasing LAI deeper in the canopy. For each depth interception of direct and/or diffuse PAR is computed for sunlit and shaded leaf areas, separately, as the diffuse and direct fluxes have different extinction coefficients. The sunlit and shaded leaf areas are related to leaf angle distribution. For millet, a spherical leaf angle distribution is assumed. Instantaneous canopy assimilation is approximated by integration over depth, using a three-point Gaussian integration method (Goudriaan, 1986). Finally, assimilation is integrated over the day to arrive at daily gross assimilation. Detailed descriptions of the calculation of absorption of radiation and instantaneous canopy assimilation are presented by Goudriaan (1977, 1982, 1986).

The assimilates fixed in the photosynthesis process are partially used in maintenance of existing plant structures. Maintenance requirements of a plant organ, r_{mx} (kg CH_2O ha^{-1} d^{-1}), depend on its weight, its chemical composition, and ambient temperature (Penning de Vries, 1975). For each of the organs a specific value per unit dry matter, c_{mx} (kg CH_2O kg^{-1} DM d^{-1}), at a maximum nitrogen concentration and a reference temperature of 25 °C is defined (Verberne et al., 1995). Each 10 °C increase in temperature doubles the carbohydrate requirement (Penning de Vries, 1982), which is accounted for by f_{mt}.

$$r_{mx} = c_{mx} \bullet DM_x \bullet f_{mt} \qquad (4.1)$$

with DM_x the dry matter of organ x in kg ha^{-1}.

The remaining carbohydrates are partitioned among leaf blades, 'stems' (including leaf sheaths and ear structures), roots, a reserve-pool of primary photosynthetic products and grains. Partitioning factors vary with DVS of the plant and may be modified by soil water status. Moisture stress in the plant leads to suboptimal growth rates for the aerial plant parts, which results in increased relative root growth rates and hence in a shift in the shoot/root ratio.

Transformation of carbohydrates into structural plant material requires energy (growth respiration). Its magnitude depends on the chemical composition (in this model on proteins and carbohydrates only) of the material being formed and thus varies among the various plant organs.

Growth of grains starts after flowering, when a rapidly increasing fraction of the daily assimilate production is allocated to grains (Appendix B2). If this does not satisfy the demand of the growing grains, reserves are translocated to supplement the assimilate supply. The demand, c_G in kg CH_2O ha^{-1} d^{-1}, is given by:

$$c_G = N_G \bullet P_G \bullet cv_G \qquad (4.2)$$

with N_G the number of grains per ha, P_G the potential growth rate of grains (kg DM grain^{-1} d^{-1}) and cv_G the factor for conversion of carbohydrates into grains (kg CH_2O kg^{-1} DM) (Verberne et al., 1995).

Millet reaches its maximum LAI at approximately 50 % flowering, when the majority of the tillers has expanded all its leaves (Maiti and Bidinger, 1981). Following flowering, there is a steady decline in leaf area as the older leaves begin to senesce. By the time of physiological maturity generally only 3 to 4 green leaves remain per tiller (Maiti and Bidinger, 1981). Senescence occurs when the leaves reach a certain age, expressed in thermal time (°C d) (Ong and Monteith, 1985), but leaves can also die before their physiological maturity, due to water stress or lack of light at high LAI (> 6). For the same reasons stems and roots can die. Their death rates are defined as a fraction of that of the leaves.

Moisture stress not only leads to death of plant parts, but also to a reduction in gross assimilation. Transpiration and CO_2 uptake both occur via stomata. If water is in short supply, transpiration requirements cannot be met by water uptake by roots, causing closure of the stomata with a proportional reduction in CO_2 uptake (van Keulen and Seligman, 1987). Thus, the actual rate of gross assimilation, G_a (kg CH_2O ha^{-1} d^{-1}), limited by soil moisture availability, is obtained by multiplying its potential value G_p by the ratio of actual transpiration and potential transpiration (T_a / T_p):

$$G_a = G_p \bullet \left(T_a / T_p \right) \qquad (4.3)$$

In addition drought affects 1) the dimensionless partitioning coefficients of shoot, F_{SH}, and roots, F_{RT}, 2) death rate of leaves, D_L (kg DM ha^{-1} d^{-1}), 3) root extension rate, RE (m d^{-1}), and 4) growth cessation. These effects are also described as a function of the ratio T_a / T_p (Verberne et al., 1995).

1)
$$F_{SH} = F_{SH}(DVS)\, f_{part}\big(T_a / T_p\big)$$
$$F_{RT} = F_{RT}(DVS) + F_{SH}(DVS)\big\{1 - f_{part}\big(T_a / T_p\big)\big\}$$
(4.4)

with f_{part} the reduction factor for allocation of assimilates to shoots due to water stress.

2)
$$D_L = DM_L \bullet RD_L \big\{1 - \big(T_a / T_p\big)\big\}$$
(4.5)

with DM_L is kg DM of leaves ha^{-1} and RD_L the maximum relative death rate of leaves due to water stress (d^{-1}).

3)
$$RE = RE_p \bullet \big(T_a / T_p\big), \quad \text{if } T_a / T_p \leq 0.75$$
(4.6)

where RE_p is the potential extension rate of roots (m d^{-1})·

4) Each successive day for which $T_a / T_p \leq 0.25$ is counted as a day of a severe drought period.

Simulation, normally, stops at physiological maturity (DVS = 2). Under water stress, the simulation can stop prematurely when a) the period of severe drought exceeds a certain number of days (21 days for millet in Niger) or b) when prior to flowering 90% of the total leaf mass is dead due to water stress. Furthermore, simulation ceases when the light saturated maximum assimilation becomes zero, which can happen when air temperature exceeds 50 °C or when leaves are very old.

4.3.2   Modifications of the crop growth part of CP-BKF3

In contrast to CP-BKF3, WIMISA describes the crop growth with a high resolution in time and space. CO_2 assimilation and all relevant growth processes are computed as a function of x, i.e. distance from the windbreak. WIMISA allows the simultaneous growth simulation of several crop rows and, thus, accounts for the interrelations between adjacent rows. As many crop rows can be modelled as the computer can store in its memory.

Computation of instantaneous CO_2 assimilation takes place at small time steps (e.g. 6 minutes) to account for a possible shading effect of the windbreak (Section 4.4). In CP-BKF3, this calculation was performed at three specified moments of the day, only. In both models, daily gross assimilation is obtained by integration of the instantaneous assimilation rates. In

WIMISA, integration is achieved by applying a simple rectangular and the three-point Gaussian method over time and LAI, respectively.

The strong correlation between nitrogen concentration of leaves and their photosynthetic performance is mimicked by changing A_m in dependence of the nitrogen content of leaves. However, since in WIMISA no nitrogen module is incorporated, the nitrogen content of leaves is always assumed maximum, so that simulations generally refer to conditions of optimum nitrogen supply. Whereas, CP-BKF3 simulates nitrogen conditions of leaves based on nitrogen conditions of the soil, as estimated from the model (fertilization, mineralization, decomposition of organic material).

In WIMISA, SLA is not a function of leaf age, but of DVS only, since the experimental data for computing SLA were determined without making a distinction between leaf age classes.

4.4   Microclimate: Radiation

Gross assimilation depends, among others, upon the quantity of absorbed photosynthetically active radiation (PAR in J m^{-2} soil s^{-1}). PAR is about 50 % of incoming global radiation, which varies with latitude, time of the year and atmospheric transmission. Furthermore, radiation intensity strongly varies over the day, following the sine of the solar angle with the horizon (sin β). For a windbreak-cropping system, also shading by the windbreak may have an impact on the diurnal PAR available for the crop, strongly varying over intervals much shorter than a day (following the position of the sun). Because of the non-linear response of photosynthesis to light intensity, spatial (distance to windbreak) and temporal variation, as well as composition of the incoming irradiance, in terms of its direct and diffuse fluxes, must be calculated accurately (Spitters et al., 1986). Because of the non-linearity, use of average values for light intensity would lead to erroneous estimates of assimilation (Spitters et al., 1986). WIMISA calculates instantaneous fluxes of direct and diffuse PAR for each crop row separately at intervals of minutes. The calculation procedure from daily total global radiation to these instantaneous fluxes of direct and diffuse PAR at the top of the millet canopy is presented schematically in Figure 4.6. All radiation terms are given in J m^{-2} soil s^{-1} if not indicated differently.

| Inputs: | Calculation of: | Module: |

Latitude of site
Day of year → **Day length**

Solar constant →

Incoming extraterrestrial radiation (I_0)

Measured incoming daily
global radiation I_g

Atmospheric transmission: at = I_g/ I_0

Time t of day

Instantaneous fraction diffuse radiation: $I_{dif}(t) / I_g(t)$

Instantaneous global fluxes of diffuse and direct radiation: $I_{dif}(t)$ and $I_{dir}(t)$

Distance x from windbreak
Windbreak characteristics
Crop height

Instantaneous fluxes of diffuse and direct radiation at the top of crop canopy: $I_{dif}(x,h_m,t$ and $I_{dir}(x,h_m,t)$

Fraction photosynthetically
active radiation: 0.5

Instantaneous fluxes of photosynthetically active diffuse and direct radiation at the top of crop canopy: $I_{par,dif}(x,h_m,t$ and $I_{par,dir}(x,h_m,t)$

WEATHER

MICRO
CLIMATE

Figure 4.6   Calculation procedure to derive instantaneous fluxes of direct and diffuse PAR
above the canopy from measured daily total global radiation (after Kropff and
van Laar, 1993).

4.4.1   Distribution of global radiation into direct and diffuse fluxes

Incident radiation at the earth's surface is partly direct, with angle of incidence equal to the angle of the sun, and partly diffuse, with incidence under various angles. The diffuse flux originates from scattering of the sun's rays in the atmosphere. Daily average atmospheric transmission (at) is defined as the ratio between measured daily global radiation incident upon the earth surface (I_g) and incoming radiation just outside the atmosphere (I_0) for the same latitude and day of the year: at = $I_{g,td}$ / $I_{0,td}$ (both in J m^{-2} soil d^{-1}). Atmospheric transmission is assumed constant over the day.

The proportion diffuse flux, $I_{dif}(t)$, is related to the transmission of global radiation, $I_g(t)$, through the atmosphere. When no measurements are available, the following equation can be used to estimate the instantaneous fraction diffuse radiation (after Goudriaan, 1982):

$$\frac{I_{dif}(t)}{I_g(t)} = 1.0 - \exp\left[-\frac{(0.18 - 0.08 \, at)}{\sin[\beta(t)]}\right] \qquad (4.7)$$

where $\beta(t)$ is solar elevation. The factor (0.18 - 0.08 at) in the exponent accounts for clear and overcast sky; it ranges from 0.1 for a very clear atmosphere (at = 1) to 0.18 for a rather humid and dusty one (at = 0). More details can be found in Ross (1981).

4.4.2   Shading by a windbreak

The presence of a windbreak reduces radiation intensity on the adjacent millet crop and eventually its assimilation. WIMISA estimates interception of radiation by a windbreak, considering the windbreak as a two-dimensional barrier with certain height (from ground level) and porosity (Figs. 4.3 and 4.7), derived from measured values for Bauhinia tree rows in the experiment (Section 3.4). This so-called WB-barrier is located at the distance that corresponds to the outer edge of the tree canopies next to the millet crop (Fig. 4.3). Hence, shading of millet from above is not considered; millet cover by overhanging tree branches played a minor role in the experimental design (only the first row adjacent to the windbreak was slightly overtoped by tree branches at the end of the growing season). The length of the WB-barrier is considered infinite, i.e. edge effects are neglected. Possible shading among crop rows is neglected, too.

Reflection, transmission and absorption by the tree canopy is implicitly accounted for in the fitted porosity factor, $\varepsilon_p(t)$ (Section 5.3). Hence, the intercepted fraction (I_t) from incident radiation (I_i) is defined as:

$$I_t(t) = \left\{1 - \varepsilon_p(t)\right\} I_i(t) \qquad (4.8)$$
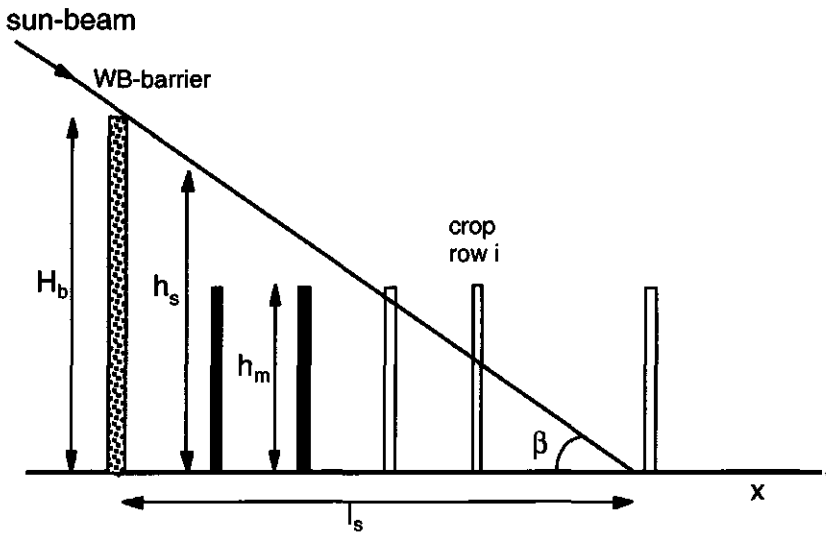
Figure 4.7   Shaded crop rows behind a WB-barrier of height H_b. Shade height and length
are denoted by h_s and ls, respectively; h_m is the crop row height, β the solar
elevation and x the distance from the WB-barrier.

The fraction interception from total I_g differs for direct and diffuse fluxes. Direct radiation (I_{dir})
comes from the direction of the sun, and can cast shade, contrary to diffuse radiation (I_{dif}),
coming from all directions. Consequently, the main effect of the WB-barrier on radiation is on
I_{dir}. Intercepted I_{dir}, the position and extension of the shade depend on solar elevation (β), the
angle of the sun beam (γ_b) with the line of the WB-barrier, and the WB-barrier height (H_b)
(Figs. 4.7 and 4.8). To compute the intensity of I_{dir} on the shaded part of the millet crop, the
position of the shadow is calculated first.
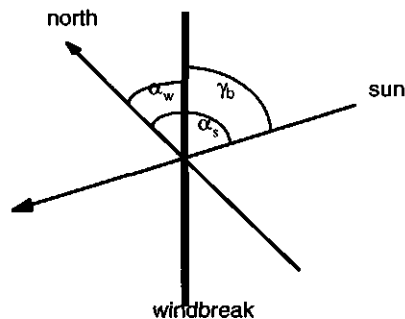
Figure 4.8   Angle of sun beam with the windbreak, γ_b, and with the north axis, α_s, and
angle of the windbreak with the north axis, α_w.

Form and position of the shadow change continuously with the position of the sun. At a certain
solar time the sine of the angle β of the sun with the horizontal is given by:

$$\sin[\beta(t)] = a + b\cos\left[\frac{2\pi}{24}(t_h - 12)\right]$$ (4.9)

with a $= \sin\lambda_a \sin\delta,$

  b $= \cos\lambda_a \cos\delta$

  λ_a $=$ latitude (rad)

  δ $=$ solar declination, varying with day of the year (t_d)

  t_h $=$ solar time

and

$$\sin[\delta] = -\sin\left[\frac{\pi}{180}23.45\right]\cos\left[\frac{2\pi}{365}(t_d + 10)\right]$$ (4.10)

Total length of the shadow, $l_s(t)$, and its height, $h_s(x,t)$, for each distance x are calculated as a function of time t (Fig. 4.7):

$$l_s(t) = \sin[\gamma_b(t)]\frac{1}{\tan[\beta(t)]}H_b(t)$$ (4.11)

$$h_s(x,t) = \{l_s(t) - x\}\frac{H_b(t)}{l_s(t)}$$ (4.12)

The instantaneous fraction of I_{dir} reaching the top of the canopy layer of crop row n depends on row height (h_m) and distance from the WB-barrier (x_n). If h_s exceeds h_m, the row is referred to as shaded and receives only the intensity of I_{dir} that penetrates through the porous area of the WB-barrier plus reflection from the windbreak. On the other hand, in situations of non-shading, the crop receives the full intensity of I_{dir}. Crop and WB-barrier height as well as porosity (ϵ_p) vary in the course of the cropping season. Their values are incorporated as linear functions of DVS and time, respectively (Appendix B2).

Subsequently, the incoming intensity of I_{dir} on top of each shaded and unshaded crop row at distance x_n is given as a function of time t:

$$I_{dir}(x_n, h_m, t) = \begin{cases} \epsilon_p(t)\, I_{dir}(t), & \text{if } h_s(x_n,t) > h_m(x_n,t) \\ \\ I_{dir}(t), & \text{if } h_s(x_n,t) \le h_m(x_n,t) \end{cases}$$ (4.13)

Analogic to I_{dir}, the WB-barrier intercepts part of I_{dif}. However, since diffuse radiation comes from all directions, any location close to the windbreak gets always a fraction ϵ_p plus a fraction

f_{dif}, coming from other directions than through the barrier. Directly adjacent to the WB-barrier the fraction $f_{dif}(0,t)$ is assigned a constant value a. The value of a has been estimated from fitting on experimental data (Section 5.3). For x > 0, $f_{dif}(x,t)$ increases linearly with x up to the value 1.0 at the end of the shaded region ($f_{dif}(l_s,t) = 1$):

$$f_{dif}(x,t) = a + \frac{1-a}{l_s(t)} x \qquad (4.14)$$

The intensity of I_{dif} at the top of a millet row is described by:

$$I_{dif}(x_n,h_m,t) = \begin{cases} \left\{1 - \varepsilon_p(t)\right\} + \left\{f_{dif}(t)I_{dif}(t)\right\} + \varepsilon_p(t)I_{dif}(t), & \text{if } h_s(x_n,t) > h_m(x_n,t) \\[2ex] I_{dif}(t), & \text{if } h_s(x_n,t) \le h_m(x_n,t) \end{cases}$$

$$(4.15)$$

These instantaneous fluxes of diffuse and direct global radiation multiplied by 0.5, represent the fraction PAR entering the top of the millet canopy and apply to the calculation of crop assimilation (Fig. 4.6). To compute the radiation term of the reference evapotranspiration equation (Subsection 4.5.1), the sum of $I_{dir}(x_n,h_m,t)$ and $I_{dif}(x_n,h_m,t)$ is used for the cropped zone of the system (this thesis: 7 - 16 m, see Fig. 4.4), while for the zone occupied by the windbreak and the bare soil (0 - 7 m) the sum of the unchanged radiation fluxes $I_{dir}(t)$ and $I_{dif}(t)$ is used.

4.5   Microclimate: Evapotranspiration

Evapotranspiration, the sum of soil evaporation and canopy transpiration, is practically the only loss of soil water in arid and semi-arid regions, where deep percolation can be neglected (van Keulen, 1975). Thus, its value is important for calculating to what degree the water requirements of the crop can be met.

4.5.1   Potential evapotranspiration

In WIMISA, potential evapotranspiration is calculated using the Penman (1948) method, which takes into account the radiation that provides energy for water vaporization in combination with the effect of turbulence in the air to transport the water from the evaporating surface. The

radiation and drying power terms are both a function of distance (x) from the windbreak, since radiation and wind speed vary with x.

$$E_o(x,t) = \frac{1}{\rho_{H2O}} \frac{1}{(s+\gamma)} \left\{ \frac{sR_n(x,t)}{\lambda} + \gamma\, f(u(x,t)\{e_s(t) - e_a(t)\} \right\} \qquad (4.16)$$

$$ET_o(x,t) = \frac{1}{\rho_{H2O}} \frac{1}{(s+\gamma)} \left\{ \frac{sR_n{}'(x,t)}{\lambda} + \gamma\, f'(u(x,t)\{e_s(t) - e_a(t)\} \right\} \qquad (4.17)$$

with (terms marked with * are further explained in Appendix B1):

E_o = evaporation rate from open water ($m^3\ H_2O\ m^{-2}$ soil s^{-1})

ET_o = evapotranspiration rate for a short grass canopy ($m^3\ H_2O\ m^{-2}$ soil s^{-1})

ρ_{H2O} = mass density of water ($kg\ m^{-3}$)

λ = latent heat of vaporization of water ($J\ kg^{-1}$)

γ = psychrometer constant ($kPa\ K^{-1}$)

$R_n{}^*, R_n{}'^*$ = net radiation for open water and a grass canopy, respectively according to Penman (1956) ($J\ m^{-2}\ s^{-1}$)

s *   = slope of the saturated vapour pressure-temperature curve at surface temperature ($kPa\ K^{-1}$)

$f(u)^*, f'(u)^*$ = wind function after Penman (1956) for open water and a grass canopy, respectively ($kg\ m^{-2}\ s^{-1}\ kPa^{-1}$).

$e_s{}^*, e_a$ = saturated vapor pressure according to Goudriaan (1977) and actual vapour pressure (kPa), respectively.

From the reference evapo(transpi)ration for open water (E_o) and a short grass canopy (ET_o), potential soil evaporation and potential crop transpiration, respectively, are calculated. Potential transpiration of the windbreak is estimated using a water use efficiency approach (Feddes and Koopmans, 1995). Potential rates of evaporation and transpiration (root water uptake) are adapted to actual rates on the basis of water availability and, for transpiration, also on root distributions of trees and millet plants (Sections 4.6 and 4.7).

4.5.2   Potential soil evaporation

$$E_p(x,t) = E_o(x,t)\, \exp\!\left[-k\, LAI\,(x,t)\right] \qquad (4.18)$$

The potential rate of evaporation, E_p ($m^3\ H_2O\ m^{-2}$ soil s^{-1}), from a partially covered soil depends on the evaporative demand at the soil surface. This demand is a function of the atmospheric demand and the degree of attenuation by the canopy cover, which can be described

as an exponential function of LAI characterized by the extinction factor k (-). The values of the proportionality factor k are different for trees and the millet crop due to differences in geometrical properties.

4.5.3   Potential transpiration

The potential rate of transpiration, $T_{p,C}$ (m^3 H_2O m^{-2} soil s^{-1}), for millet is derived from the reference evapotranspiration, ET_o, by multiplying with a crop coefficient, k_c (-) (FAO, 1984), and the fraction absorbed radiation (Verberne et al., 1995; Erenstein, 1990):

$$T_{p,C}(x,t) = k_c \ ET_o(x,t) \left\{ 1 - \exp\left[-0.75 \ K_{dif} \ LAI(x,t) \right] \right\} \tag{4.19}$$

with 0.75 K_{dif} = k, the extinction coefficient for total radiation and K_{dif} the extinction coefficient for diffuse visible light (-) (Feddes and Koopmans, 1995). The coefficient k_c is an empirically determined extinction factor that transforms potential evapotranspiration from a short grass cover into that for a specific crop species.

For calculating potential transpiration of the windbreak $T_{p,WB}$ (m^3 H_2O m^{-2} soil s^{-1}), the following water use efficiency approach (after Conijn, 1995) is used:

$$T_{p,WB}(t) = \frac{P_{WB}(t)}{E_W(t)} \tag{4.20}$$

where P_{WB} is the potential rate of dry matter production (kg DM ha^{-1} s^{-1}) and E_W is water use efficiency for dry matter production (kg DM ha^{-1} (m^3 H_2O m^{-2} soil$)^{-1}$). In the approach of Conijn (1995), P_{WB} is simulated as a function of absorbed radiation, whereas in the present model P_{WB} is introduced as derivative of the Bauhinia growth curve based on data of Lamers (1995; Subsection 5.3.3). E_W is given as a linear function of porosity of the windbreak.

4.6   Soil water

Soil water and its spatial distribution in the root zone is of crucial importance for emergence and plant growth (Section 4.3). Local water content is highly dynamic due to vertical and horizontal flow in response to hydraulic head gradients and due to sinks and sources. In the windbreak-cropping system, horizontal water flow may be induced by gradients in pressure head in horizontal direction, originating from shelter effects (i.e. radiation, wind speed) and the

difference in root water uptake between trees and crops. Although interception of rain by the tree canopy, stem flow and crown drip may add slightly to the horizontal gradient (Jetten, 1994; Conijn, 1995), they are not accounted for in WIMISA, because no data on these processes are available. However, stem flow is a small part of rainfall (Jetten, 1994) and the effect of crown drip and interception should be negligible for the present study where WB canopy width is small and tree branches were rarely hanging over the crop. Moreover, those processes are not considered for the crop either.

The model WIMISA simulates, in the absence of a water table, soil water dynamics in two dimensions for a soil profile that is homogeneous in horizontal direction and has a non-crusting surface. It is a finite soil system extending from the soil surface to a depth D_s, which is below the maximum rooting depth. W_s denotes the width and L_s the length of the soil system (Fig. 4.9).

The source of water for the soil system is infiltration of rain water, $I(t)$ (m^3 H_2O s^{-1}). The losses or sinks of water from the system are the total amount of water evaporated ($S_{ev}(t)$), transpired by the WB trees and millet crop through uptake by their roots ($S_{up}(t)$) and percolated into deeper soil zones ($S_{dp}(t)$). Laterally, there is no loss or sink, since at the lateral system boundaries inflow equals outflow. For a given time t the soil water balance becomes then:

$$\Delta SW(t) = I(t) - S_{ev}(t) - S_{up}(t) - S_{dp}(t) \tag{4.21}$$

with $\Delta SW(t)$ change in total soil water (m^3 H_2O s^{-1}).

4.6.1   Internal water flow in the soil system

For the description of the internal flow of water in the soil system xyz-coordinates are introduced (Fig. 4.9B). The x-coordinate is defined in horizontal direction perpendicular to the windbreak, the y-coordinate in horizontal direction parallel to the windbreak, and the z-coordinate in the vertical direction. The vertical coordinate z is considered negative downwards. WIMISA describes soil water, radiation and crop growth uniform in the y-direction. Consequently, gradients in the y-direction are neglected, but by taking L_s = 1 m the y-coordinate is conserved to keep the soil water balance equations dimensionally correct.

A

B
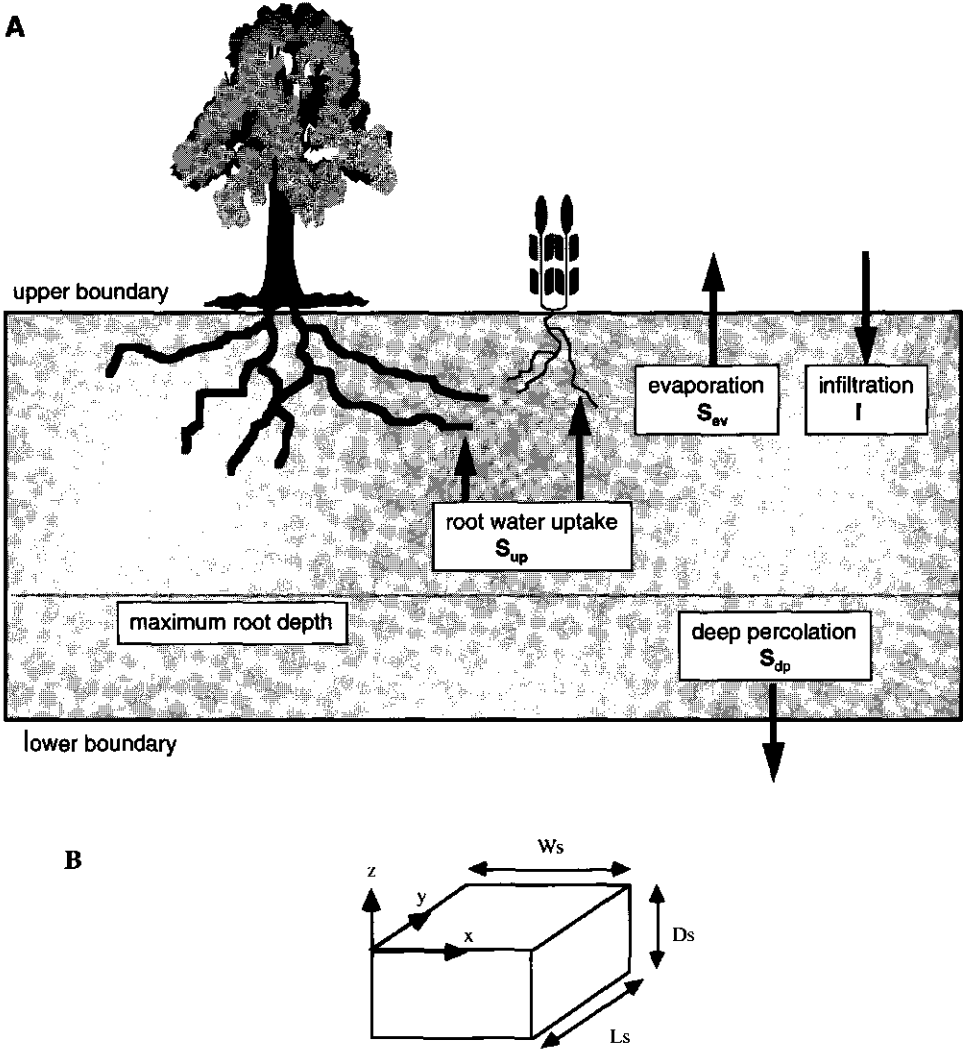
Figure 4.9   Soil system with processes of the soil water balance (A) and definition of xyz-coordinates, the length L_s, width W_s and the depth D_s of the soil system showing the system boundaries (B).

The volumetric soil water content at time t and position (x,y,z) in the soil profile is denoted by $\theta(x,y,z,t)$ with dimension m^3 H_2O m^{-3} soil. Its rate of change is given by the continuity equation (conservation of mass):

$$\frac{\partial\theta(x,y,z,t)}{\partial t} = -\nabla \bullet \mathbf{q}(x,y,z,t) + \frac{\partial \text{source}(x,y,z,t)}{\partial t} - \frac{\partial \text{sink}(x,y,z,t)}{\partial t} \qquad (4.22)$$

where $q(x,y,z,t)$ is the local rate of water flow (m[3] H$_2$O m^{-2} soil s[-1])[1,2]. Equation (4.22) expresses that the conservation of water mass must be satisfied at every point in the soil system including the boundaries. Local source (source(x,y,z,t)) and sink (sink (x,y,z,t)) terms (m[3] H$_2$O m^{-3} soil) are introduced in the continuity equation to account for the water that enters (infiltration) or leaves the soil system through evaporation and root water uptake. The processes by which water enters or leaves the soil system are mechanistically decoupled from the internal water flows. Thus, the sink and source terms are calculated independently of $q(x,y,z,t)$ and depend on the current water content, $\theta(x,y,z,t)$, only.

The rate of water flow $q(x,y,z,t)$ is calculated according to Darcy's law for water flow in porous media:

$$q(x,y,z,t) = -K(x,y,z,t)\nabla H(x,y,z,t) \qquad (4.23)$$

where $K(x,y,z,t)$ is the hydraulic conductivity (m s^{-1}), and $H(x,y,z,t)$ the hydraulic head (m), a measure for water potential. The y-component of q equals zero everywhere in the soil system, because of zero gradients of any variable in the y-direction.

The hydraulic head is given by:

$$H(x,y,z,t) = h(x,y,z,t) + z \qquad (4.24)$$

with $h(x,y,z,t)$ the soil water pressure head and z representing the gravitational head. The pressure head is related parametrically to volumetric soil water content by a power law (Campbell, 1974):

$$h(x,y,z,t) = h_{ae}(x,y,z)\left(\frac{\theta(x,y,z,t)}{\theta_{sat}(x,y,z)}\right)^{-C_b(x,y,z)} \qquad (4.25)$$

---

[1] Vectorial quantities are written in bold characters.

[2] The nabla operator is defined as $\nabla = \begin{pmatrix} \dfrac{\partial}{\partial x} \\[6pt] \dfrac{\partial}{\partial y} \\[6pt] \dfrac{\partial}{\partial z} \end{pmatrix}$ (m[-1])

where h_{ae} is the pressure head at air entry, C_b the so-called Campbell´s power (-) (Campbell, 1974) and θ_{sat} is water content at saturation. For readability, the functional dependency of h, H and K on θ is left out from the notation in this thesis.

C_b is the inverse of the pore size distribution parameter of the model developed by Brooks and Corey (1964) for the soil moisture retention curve. It describes the size distribution of the flow channels within the soil, which is a function of the microscopic geometry of the soil. The parameter h_{ae} is defined as the potential at which the largest water-filled pores start to drain and, hence, gas flow starts (Durar and Skidmore, 1995).

The hydraulic conductivity, K(x,y,z,t), is also parametrically related to the volumetric water content by a power law according to Campbell's method (Campbell, 1974):

$$K(x,y,z,t) = K_{sat}(x,y,z)\left(\frac{\theta(x,y,z,t)}{\theta_{sat}(x,y,z)}\right)^{C_k(x,y,z)} \tag{4.26}$$

where K_{sat} is the hydraulic conductivity at saturation (m s^{-1}). C_k (-) is the power value of this function and is calculated according to:

$$C_k = (2\,C_b) + 3 \tag{4.27}$$

The parameters h_{ae}, C_b, θ_{sat}, K_{sat} and C_k depend on soil type and thus may vary with the position in the soil profile (Section 5.4).

The reason for using the power law functions instead of tabulated θ-K and θ-h relations is that reliable measurements of unsaturated hydraulic conductivity as a function of θ are difficult to obtain. Campbell's method allows estimation of K from routinely measured soil texture and bulk density data or from Rawls et al.'s (1982) table of hydraulic properties per soil texture class (Section 5.4), as used in WEPS (Durar and Skidmore, 1995).

To start simulation of the soil water processes, initial conditions must be known. As h and K depend on volumetric water content, the initial state of the soil water profile is fully specified by the initial volumetric water content profile θ(x,y,z,0). The simulation starts at the end of the long dry season, so the initial soil water content of the soil system is set equal to the volumetric water content at air dry conditions. Additionally, the boundary conditions for H and ∇H must be specified to solve the differential equations.

4.6.2   Boundary conditions

The boundary conditions given below refer to the soil system as described in Figure 4.10.

upper boundary z = 0

side boundary
x = 0

side boundary
x = Ws

lower boundary z = Ds
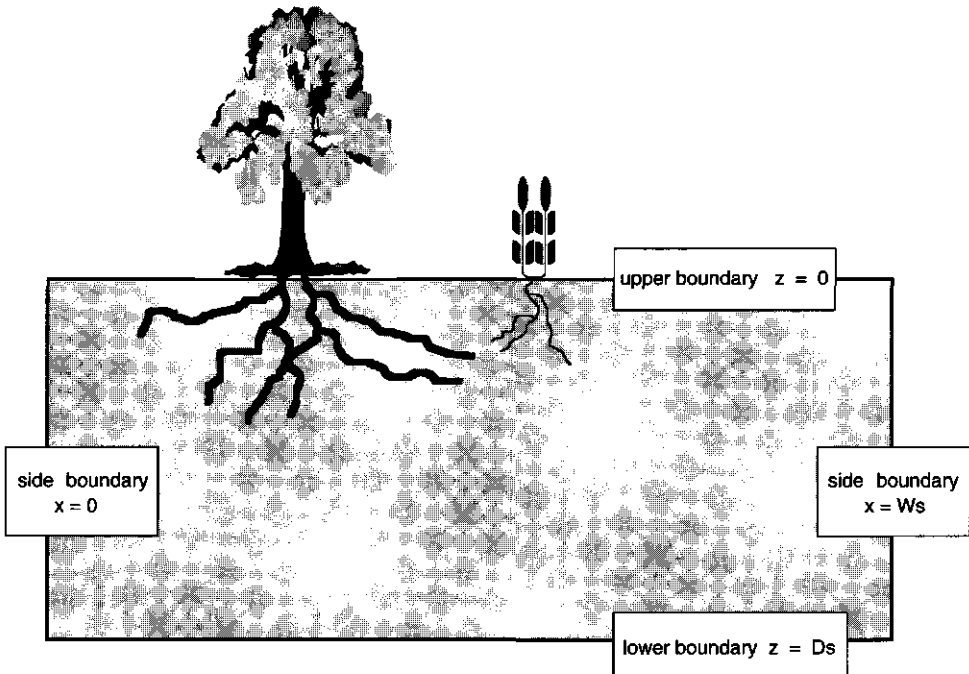
Figure 4.10   Boundaries of the soil system .

Upper boundaries
At the upper boundary, the soil-atmosphere interface, the net flow results from infiltration and evaporation. Both depend for their potential rates on external conditions (weather, soil surface properties) and for their actual rates on internal conditions (soil physical properties, current moisture status).

The source of water for the system, infiltration, is generally defined as the balance between precipitation, run-on and runoff (Stroosnijder, 1982). In a millet field in Niger, it was found that runoff and run-on can lead to substantial local redistribution of water at the soil surface (Gaze et al., 1997). However, when rainfall exceeds 200-350 mm most of the run-on is lost as drainage rather than adding to potential evapotranspiration. In years exceeding this rainfall threshold range (which is mostly the case at ISC), the effect of rainfall redistribution on the soil

water balance at field scale is negligible, because the extra drainage in run-on areas will be compensated by reduced drainage from runoff areas (Gaze et al., 1997). This, in combination with the fact that the experimental field was rather level, allows to ignore runoff and run-on processes in the soil water balance. Therefore, in the model infiltration is set equal to precipitation. Rainfall duration is estimated on the basis of rainfall amount according to an approach used by Verberne et al. (1995). The time of day during which rain falls and infiltration starts is determined randomly. As onset, duration and amount of rainfall are known infiltration per time step can be computed. For each time step, local infiltration is calculated by a cascade model (van Keulen, 1975). First, the uppermost soil compartment is filled up till field capacity. Any excess infiltration is added to the adjacent lower compartment with the same maximum storage restriction. This is repeated until total infiltration is dissipated within the soil system or any excess water is lost by deep percolation (sink term). Hence, the infiltration process occurs in vertical direction only through a series of source terms.

Evaporation is calculated on the basis of the reference evaporation of Penman (1948) and current local moisture content at the soil surface, $\theta(x,y,0,t)$ (Section 4.5). If potential evaporation can not be supplied by the soil compartments $(x,y,0)$, their available water content determines actual evaporation. Water for evaporation is extracted from the compartments directly below the soil surface (i.e. top layer $= (x,y,0)$) through a sink term.

An exact physical description of the flows of evaporation and infiltration is complicated, moreover, for a detailed system study as the present one it would cost an enormous computing time (Stroosnijder, 1982). To circumvent the problem, at the upper boundary gain and loss of water is taken into account through source and sink terms instead of by a boundary condition in terms of $h(x,y,z,t)$ or $\mathbf{q}$. This approach is similar to the sink term approach for root water uptake used in many models (e.g. Dierckx et al., 1986) and implies that at the upper boundary $(z = 0)$ the condition for the gradient in hydraulic head equals:

$$\frac{dH}{dz} = 0 \tag{4.28}$$

Lateral boundaries
At the left and right boundaries ($x = 0$ and $x = W_s$) it is assumed that:

$$\frac{dH}{dx} = 0 \tag{4.29}$$

and thus the horizontal flow at these boundaries equals zero. The position of the boundaries in the x-direction for the windbreak-cropping system have to be chosen such that it is reasonable to assume that a horizontal moisture gradient is negligible (Section 4.2).

Lower boundaries

At the lower boundary, the system remains unsaturated. Due to the deep water table level, groundwater (via capillary rise) has no influence on soil moisture dynamics in the root zone of Sahelian millet fields (Fechter, 1993). Therefore, at the lower boundary only deep percolation occurs. To ensure that this assumption is realistic, the soil system must be deep enough (here 7 m), so that $\theta(x,y,D_s,t)$ will be close to the water content at air dry conditions, θ_{ad}. In the case of free drainage, the gradient of the hydraulic head at $z = D_s$ becomes:

$$\frac{dH}{dz} = 1 \qquad\qquad (4.30)$$

Root water uptake

Root water uptake within the soil system is also accounted for by a sink term in the present model. Water extraction by roots of millet and windbreak trees depends, among others, on their root length density, available water content for plants and their potential transpiration, T_p. The latter (Subsection 4.7.3) defines the potential value for water uptake from the entire soil system, i.e. S_{up}.

With respect to the continuity equation (Eq. 4.22), at the upper and side boundaries the component of $q(x,y,z,t)$ perpendicular to the boundary surface disappears, by setting the corresponding gradient in water potential equal to zero. At the lower boundary, drainage is expressed in q. The magnitude of all sink or source terms depends on the position in the soil profile (Fig. 4.11). The numerical methods to quantify these rates are described in Subsection 4.6.4.

The use of a parametric model for the θ-K and θ-h relations and the infiltration process and the sink and source terms characterize the soil water approach as semi-mechanistic. The approach of compartment-based sink and source terms, moreover, is one of the reasons why the continuity equation (Eq. 4.22) and Darcy's law (Eq. 4.23) are not solved in the combined form of the Richards equation.

Early growing season   **Millet flowering stage**
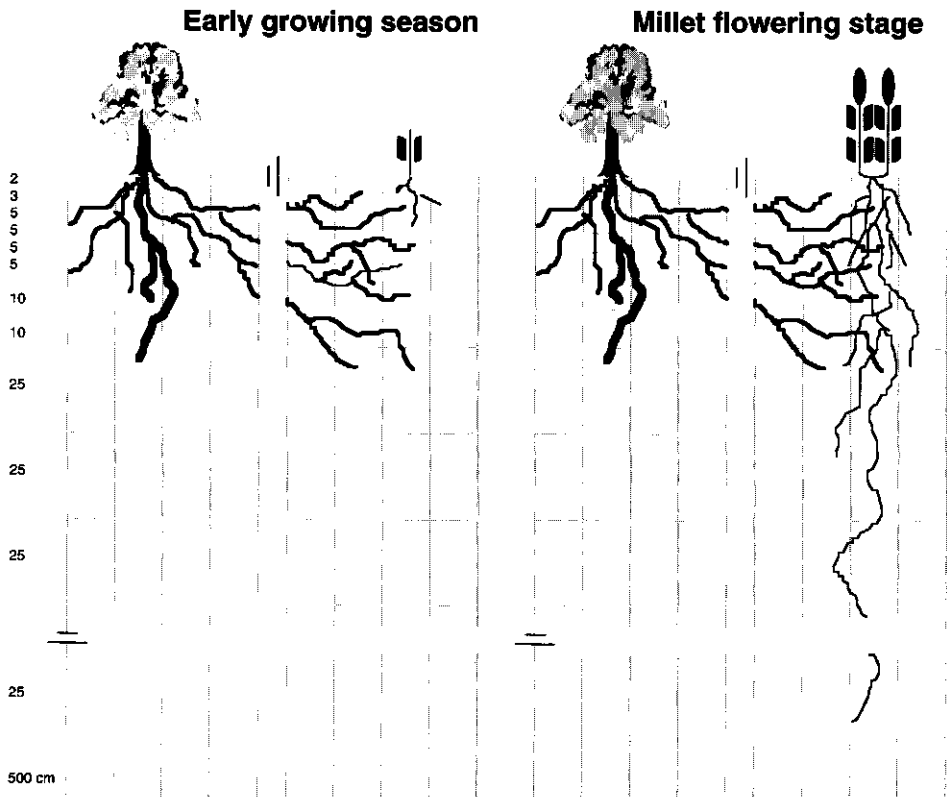
Figure 4.11   Root distribution of crop and windbreak over the soil cells, in which root water
uptake as sink is computed. In the present study, the uppermost soil cells are 2
cm and the deepest cells are 500 cm in vertical direction. Horizontal extension
of all cells is 100 cm. The root system of the trees is static while that of the
crop is dynamic. Because of symmetry of the tree root system, only one root
side adjacent to the windbreak is given.

4.6.3   The soil water balance

The total amount of water, SW(t), (m³ H₂O) within the soil system is obtained by integrating
over its volume (V):

$$SW(t) = \iiint\limits_{V} \theta(x, y, z, t) dxdydz \qquad (4.31)$$

Thus, in WIMISA the water balance for the total soil system can be formulated as:

$$SW(t) - SW(t_0) = \int\limits_{t'=t_0}^{t'=t} I(t')dt' - \int\limits_{t'=t_0}^{t'=t} S_{ev}(t')dt' - \int\limits_{t'=t_0}^{t'=t} S_{up}(t')dt' - \int\limits_{t'=t_0}^{t'=t} S_{dp}(t')dt' \qquad (4.32)$$

with t_0 the time at which the simulation starts.

The infiltration rate of the entire soil system at time t follows from:

$$I(t) = \iiint\limits_V \frac{\partial source(x,y,z,t)}{\partial t} dxdydz \qquad (4.33)$$

and, analogously, for the sink terms:

$$S_{ev}(t) = \iiint\limits_V \frac{\partial sink_{ev}(x,y,z,t)}{\partial t} dxdydz \qquad (4.34)$$

$$S_{up}(t) = \iiint\limits_V \frac{\partial sink_{up}(x,y,z,t)}{\partial t} dxdydz \qquad (4.35)$$

$$S_{dp}(t) = \iiint\limits_V \frac{\partial sink_{dp}(x,y,z,t)}{\partial t} dxdydz \qquad (4.36)$$

4.6.4   Numerical procedures

In this thesis, Darcy's law and the continuity equation are not solved in the combined form of the well known Richard's equation (Stroosnijder, 1982; Heinen, 1997). The latter, in our case, can not be formulated completely in terms of h or θ because in WIMISA there are no explicit analytical expressions for infiltration, evaporation, and root water uptake. For the same reason an analytical solution can not be obtained. A numerical solution is obtained by applying an (explicit) forward-time centered-space (FTCS) integration scheme (Press et al., 1990).

For discretisation of the computations it is sufficient to introduce a two-dimensional rectangular grid of node centered cells (also called control volumes) in the xz-plane (y $\equiv$ 0), because gradients in the state variables in the y-direction are neglected. The grid nodes (Fig. 4.12), denoted by the indices i and j, are equally spaced in the x-direction, but not necessarily in the z-direction. It is appropriate to use a narrow spacing in the z-direction near the soil surface, where

the gradients are steepest for infiltration and evaporation. It is assumed that, within each cell volume, soil water parameters (e.g. C_b) and the instantaneous values of the soil-water variables (e.g. θ, h) and sink and source terms are uniform, and that the soil water content remains in the range of θ_f and θ_{wilt}.

The rates of flow **q** at the boundaries of the cells are computed from Darcy's equation, approximating the gradient operator (∇) by finite central difference operations:

$$q_{i+\frac{1}{2},j}^{x}(t) = -\frac{1}{2}\left\{K_{i+1,j}(t) + K_{i,j}(t)\right\}\left\{\frac{H_{i+1,j}(t) - H_{i,j}(t)}{\frac{1}{2}\left\{\Delta x_{i+1,j} + \Delta x_{i,j}\right\}}\right\}$$

$$q_{i,j}^{y}(t) = 0$$

$$\text{(4.37)}$$

$$q_{i,j+\frac{1}{2}}^{z}(t) = -\frac{1}{2}\left\{K_{i,j+1}(t) + K_{i,j}(t)\right\}\left\{\frac{H_{i,j+1}(t) - H_{i,j}(t)}{\frac{1}{2}\left\{\Delta z_{i,j+1} + \Delta z_{i,j}\right\}}\right\}$$

where $\Delta x_{i,j}$ is the width and $\Delta z_{i,j}$ the thickness of the cell volume centered at grid node (i,j).

Integrating the continuity equation (Eq. 4.22) over the cell volume, $vol_{i,j}$, to obtain the change in soil water content gives:

$$\iiint\limits_{vol_{i,j}}\frac{\partial\theta(x,y,z,t)}{\partial t}dxdydz = \iiint\limits_{vol_{i,j}}-\nabla\bullet q(x,y,z,t)dxdydz + \iiint\limits_{vol_{i,j}}\frac{\partial source(x,y,z,t)}{\partial t}dxdydz -$$
$$\iiint\limits_{vol_{i,j}}\frac{\partial sink(x,y,z,t)}{\partial t}dxdydz$$

$$\text{(4.38)}$$

The first integral at the right hand side is computed using Gauss´s theorem, i.e.:

$$\iiint\limits_{V}\nabla\bullet v\,dV = \oiint\limits_{S}v\bullet n_S dS \qquad\qquad\text{(4.39)}$$

where **v** is an arbitrary but continuous vector field, S is the surface enclosing the volume V and n_S is a unit vector normal to the surface element, dS.

Applying a forward finite difference approximation for the time derivative of the soil water content in Eq. 4.38 and making use of Gauss´s theorem, it follows that:

$$\text{vol}_{i,j}\frac{\theta_{i,j}(t+\Delta t)-\theta_{i,j}(t)}{\Delta t}=\Phi_{i,j}^{\text{lower}}(t)-\Phi_{i,j}^{\text{upper}}(t)+\Phi_{i,j}^{\text{left}}(t)-\Phi_{i,j}^{\text{right}}(t)$$

$$+\text{vol}_{i,j}\frac{\partial\text{source}_{i,j}(t)}{\partial t}-\text{vol}_{i,j}\frac{\partial\text{sink}_{i,j}(t)}{\partial t} \qquad (4.40)$$

The fluxes across the cell surfaces, i.e. $\Phi^{\text{lower}}(t)$, $\Phi^{\text{upper}}(t)$, $\Phi^{\text{left}}(t)$ and $\Phi^{\text{right}}(t)$ (m^3 H_2O s^{-1}) for the boundaries in the x- and z-direction of the cell at grid point (i,j) are given by:

$$\Phi_{i,j}^{\text{lower}}(t)=\Delta x_{i,j}\Delta y\, q_{i,j-\frac{1}{2}}^{z}(t)$$

$$\Phi_{i,j}^{\text{upper}}(t)=\Delta x_{i,j}\Delta y\, q_{i,j+\frac{1}{2}}^{z}(t)$$

$$\Phi_{i,j}^{\text{left}}(t)=\Delta z_{i,j}\Delta y\, q_{i-\frac{1}{2},j}^{x}(t) \qquad (4.41)$$

$$\Phi_{i,j}^{\text{right}}(t)=\Delta z_{i,j}\Delta y\, q_{i+\frac{1}{2},j}^{x}(t)$$

where $\Delta y = 1$ m. We have assumed that $\mathbf{q}$ is uniform at the surface boundaries of the cell.
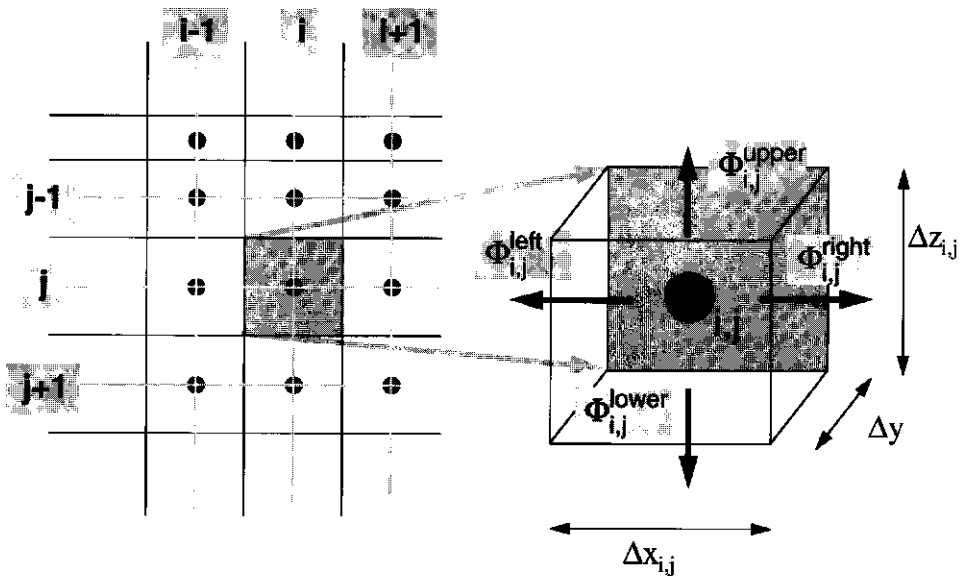
Figure 4.12 Example of a of grid with node centered cells and an enlarged cell volume including the notations for the node (i,j), fluxes (Φ) at the surface boundaries and the cell dimensions (Δ).

The local contribution to the evaporation sink term is derived from the potential rate of evaporation, $E_p(x,t)$, at the soil surface and available soil water contents. Within a time interval Δt only water in the cells of the top soil layer can evaporate. In dependence of local water availability $E_{i,0}^{max}(t)$, the maximum rate of evaporation (m^3 H_2O m^{-2} soil s^{-1}) from the upper soil cell (i,0), is computed as:

$$E_{i,0}^{max}(t) = \frac{\Delta z}{\Delta t}\left\{\theta_{i,0}(t) - \theta_{i,0}^{ad}\right\} \tag{4.42}$$

with $\theta_{i,0}^{ad}$ the volumetric soil water content at air dry. The evaporation sink term is then given by:

$$vol_{i,0}\frac{\partial sink_{i,0}^{ev}(t)}{\partial t} = \begin{cases} E_{i,0}^{p}(t)\Delta x_{i,0}\Delta y, & \text{if } E_{i,0}^{p}(t) \le E_{i,0}^{max}(t) \\[2mm] E_{i,0}^{max}(t)\Delta x_{i,0}\Delta y, & \text{if } E_{i,0}^{p}(t) > E_{i,0}^{max}(t) \end{cases} \tag{4.43}$$

The root water uptake sink term in cell (i,j) is computed from the actual rates of water extraction of millet rows ($U_{C(n)}$) and windbreak (U_{WB}) with roots inside cell (i,j). Let $U_{i,j}(t)$ (m^3 H_2O m^{-3} soil s^{-1}) denote the water uptake rate of all roots inside cell (i,j) (see Subsection 4.7.3), then:

$$vol_{i,j}\frac{\partial sink_{i,j}^{up}(t)}{\partial t} = U_{i,j}(t) \tag{4.44}$$

Following derivation of the expressions for the source and sink terms and the fluxes across the boundaries of the cells, the change in water content in a cell follows directly from Eq. 4.40.

The time step Δt is variable and calculated according to the Courant condition (Press et al., 1990; Feddes, 1982):

$$\Delta t = \zeta \min_{i,j}\left[\left|\frac{\frac{1}{2}\left\{\Delta x_{i,j} + \Delta x_{i+1,j}\right\}}{q_{i+\frac{1}{2},j}^{x}(t)}\right|, \left|\frac{\frac{1}{2}\left\{\Delta z_{i,j} + \Delta z_{i,j+1}\right\}}{q_{i,j+\frac{1}{2}}^{z}(t)}\right|\right] \tag{4.45}$$

where the factor $\zeta \le 1$; we have taken $\zeta = 0.3$. This condition ensures that the maximum displacement of water simulated within one period of integration corresponds with that of the real system. Within the determined time step infiltration, root water uptake, soil evaporation and water redistribution are calculated subsequently as shown in the task flow diagram (Fig. 4.2).

4.7   Roots and root water uptake

Root length distribution in the soil profile determines water uptake for trees and crops. In analogy to water flow, the distribution of root length and root water uptake are described in a two-dimensional framework (Fig. 4.13). The density of tree and millet roots varies with a) soil depth, b) distance from the windbreak, and c) distance from the millet stem. Root length growth of millet is simulated in daily intervals; root length of WB trees is fixed in time. In the situation of competition for water between millet and tree roots, available soil water is distributed between millet and the windbreak in proportion to their potential water uptake rates in the non-competitive situation.
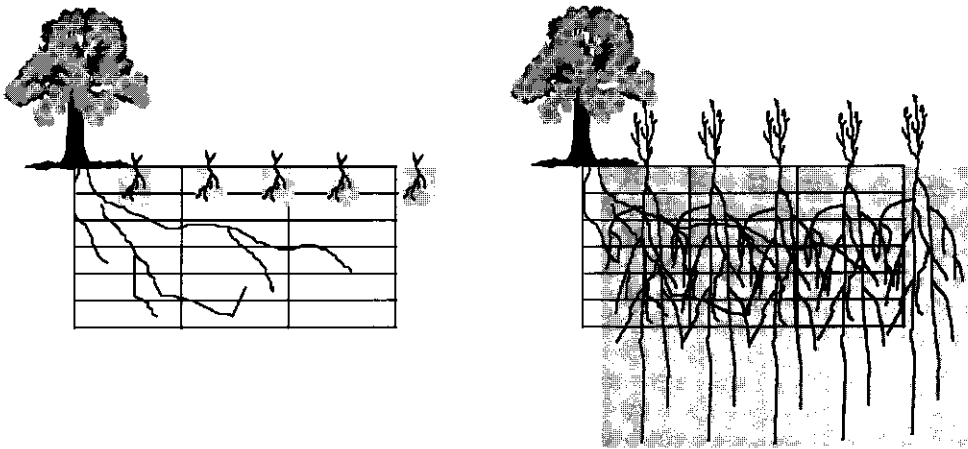
Figure 4.13   Root distribution of trees and crops within their compartments at the early growing season (A) and millet flowering (B) stage. Because of symmetry of the tree root system, only one root side adjacent to the windbreak is given.

4.7.1   Millet roots

Millet has a deep root system, but more than half of its root length is located in the upper 40 cm (Bley, 1990). In the model, the root profile starts at 0.5 cm (z_0) below sowing depth and may extend to a maximum depth, set at 2.20 m below soil surface (Azam-Ali et al., 1984). Within this profile, root length distribution is described for each crop row in a separate compartment, spanned by x (width) and z (depth) (Fig. 4.14). In daily intervals, WIMISA simulates root length density (i.e. root length per unit volume of soil) with a vertical exponential decay (Bley, 1990; Piro, 1993) inside the compartment.

Depth D(t) (m) and width W(t) (m) of the compartment increase with time. The increase in rooted depth follows from a constant rate of potential extension growth (RE_p, m d^{-1}, Eq. 4.6) multiplied by the water stress factor T_a / T_p. Horizontal root extension is derived from vertical root extension by multiplication with a constant factor. Maximum horizontal root extension is set to half the distance between crop rows (Piro, 1993), however, this can be adapted in the input file.
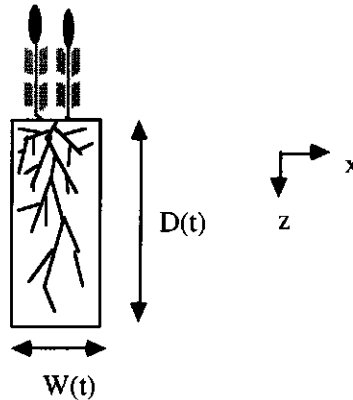
Figure 4.14   Root compartment of one crop row.

Root length, l_R (m), at a given position (x,z) in the root compartment is given by:

$$l_R(x,z,t) = l_{R,tot}(t)\,\Psi(x,z,t) \qquad (4.46)$$

where $l_{R,tot}(t)$ is total root length of the crop and $\psi(x,z,t)$ is distribution function for root length. The value of $l_{R,tot}(t)$ is derived from total root dry mass, $DM_R(t)$ (kg m^{-2}), soil and specific root length, $l_{R,spec}$ (m root kg^{-1} DM_R):

$$l_{R,tot}(t) = l_{R,spec}\,DM_R(t) \qquad (4.47)$$

Vertical root extension ceases under one of the following conditions: no assimilates are allocated to roots, soil moisture content in the soil compartment where the root tip is located is below θ_{wilt} (Salim et al., 1965), or maximum rooting depth of the crop is reached. Root mass, DM_R, depends on assimilate production and the fraction assimilates allocated to the roots (Subsection 4.3.1).

The distribution function for root length, $\psi(x,z,t)$, can be described by an exponential extinction with depth (after Verberne et al., 1995; Conijn ,1995):

$$\Psi(x,z,t) = \begin{cases} C\exp\left[-\dfrac{(z-z_0)}{p(t)}\right] & \text{for } x_0 - \dfrac{1}{2}W(t) \leq x \leq x_0 + \dfrac{1}{2}W(t), z_0 \leq z \leq z_0 + D(t) \\ \\ 0 & \text{for } x < x_0 - \dfrac{1}{2}W(t), x > x_0 + \dfrac{1}{2}W(t), z < z_0, z > z_0 + D(t) \end{cases}$$

(4.48)

with x_0 located at the plant stem or the middle of $W(t)$. The variable $p(t)$ is a proportionality factor that defines the specific root depth and is derived from fitting:

$$p(t) = aD(t) \tag{4.49}$$

with the coefficient a selected such that 60% of $l_{R,tot}(t)$ is located in the upper 40 cm of the soil.

C is a normalisation constant ensuring that ψ is a normalized function, i.e.:

$$\int\int \Psi(x,z,t)\,dxdz = 1 \tag{4.50}$$

Integration of Eq. 4.48 (see Appendix B1) yields:

$$\int_{z_0}^{z_0+D(t)} \int_{x_0-\frac{1}{2}W(t)}^{x_0+\frac{1}{2}W(t)} \Psi(x,z,t)\,dxdz = \frac{CW(t)}{p(t)}\left\{1 - \exp\left[-\frac{D(t)}{p(t)}\right]\right\} \tag{4.51}$$

And because of condition (4.50):

$$C = \frac{p(t)}{W(t)\left\{1 - \exp\left[-\dfrac{D(t)}{p(t)}\right]\right\}} \tag{4.52}$$

4.7.2   Windbreak trees: Bauhinia roots

The distribution of fine roots of WB trees, active in water uptake (Breman and Kessler, 1995), is given as input. To account for horizontal variability in root length density, at both sides of the WB trunk consecutive zones parallel to the WB are defined with a width related to tree canopy radius. Vertically, each zone is subdivided in a number of soil compartments. Within each compartment (Fig. 4.13) the root length density (m root m^{-3} soil) is fixed in time. The fixed root length distribution appears a realistic assumption during one cropping season for a full-grown windbreak (Groot, AB-DLO, pers. comm., 1996). Root data used in simulations are based on the measured tree root distribution of a Bauhinia-related species, *Acacia seyal* (Subsection 5.3.4).

4.7.3   Root water uptake and competition

Root water uptake from a given depth in the soil profile is affected by many factors (e.g. root density, soil hydraulic conductivity, water permeability of a root), which can not all be considered in a simple model approach. Atmospheric demand (potential transpiration), soil moisture content, and some root characteristics are often the minimum requirements for such a model. In principle, two approaches can be used to simulate the extraction of water by roots (Feddes and Koopmans, 1995).

The 'single root model' (Gardner, 1960) describes convergent radial flow of soil water toward a representative individual root. This approach assumes a constant flux to each unit length of a typical root, described by an infinitely long narrow cylinder of constant radius and absorbing properties. The flow equation is expressed in cylindrical coordinates and solved for the distribution of pressure heads, water contents and fluxes from the root outward (Hillel et al., 1975). The entire root system can be described as a set of individual roots, regularly spaced in the soil at distances which may vary with the soil profile (Feddes and Koopmans, 1995).

The alternative approach is called 'sink term' or 'root system model': the root system in its entirety is regarded as a diffuse sink that permeates the soil continuously, though not necessarily with a constant strength throughout the root zone (Hillel et al., 1975). The local strength of the sink term is related to the effective density of the roots in each layer. Various forms for the sink term, representing extraction by plant roots, have been applied. Some are similar to the Gardner (1960) expression, others describe the sink term as the product of maximum possible water uptake and a dimensionless function of soil water pressure head (Feddes et al., 1978). Maximum water extraction by roots is derived from the distribution of potential transpiration over the rooting zone or over the relative root length.

In WIMISA, a simplified 'single root model' and the 'sink term model' are applied for crop and windbreak, respectively. When actual soil moisture content falls below a critical value, root water uptake can not meet plant water requirements. In the model, this is accounted for by a dimensionless reduction factor for root water uptake for crop ($f_{up,C(n)}$) and windbreak ($f_{up,WB}$). If soil moisture content falls below wilting point, for which a value of -16000 cm for h (pF = 4.2) is often used, water extraction by plants becomes impossible. As described in Section 4.6 water extraction by roots is modelled as local uptake per soil cell and enters the soil water balance as a sink term. The sum of water uptake from all soil cells equals actual transpiration .

Millet

Extraction of soil water by millet roots is calculated similarly to the approach used in the model CP-BKF3 (Verberne et al., 1995). As in the single root model, the root is assumed to be a cylinder of uniform specific root surface, a_R (m² root m⁻¹ root), supporting a uniform water flux, q_R (m³ H_2O m⁻² root s⁻¹), into the roots. From the root length distribution, the maximum water uptake rate ($U_{max,C(n)}(x,z,t)$, m³ H_2O m⁻³ soil s⁻¹) of roots belonging to the crop in row n at position (x,z) becomes:

$$U_{max,C(n)}(x,z,t) = a_R \, q_R \, \frac{l_R(x,z,t)}{dx \, dy \, dz} \, f_{up \cdot C(n)}(x,z,t) \qquad (4.53)$$

with $l_R(x,z,t)$ the root length at position (x,z) and $l_R(x,z,t)$ / dx dy dz) the root length density (m root m⁻³ soil). The reduction factor for water uptake by millet, $f_{up,C(n)}(x,z,t)$ is introduced as a tabulated function of pF (Appendix B2). Each crop row (n) has its own root compartment (Fig. 4.13), but compartments may overlap in the course of time (not the case in the simulations of the thesis). I.e. roots of a certain crop row may reach into the soil below adjacent rows. Consequently, at a given position (x,z), water extraction can be the result of uptake by roots belonging to several crop rows: $\sum U_{C(n')}$.

Total maximum water uptake rate (m³ H_2O s⁻¹) of crop row n is found as:

$$U_{max,C(n)}(t) = dy \int \int U_{max,C(n)}(x,z,t)dxdz \qquad (4.54)$$

Potential crop transpiration, $T_{p,C(n)}$, sets the upper limit to water extraction of the crop in row n for the corresponding root compartment. Let $W_{C(n)}$ denote the width of crop row n, then the amount of water that can be potentially transpired is given by $T_{p,C(n)} \, W_{C(n)} \, \Delta y$. Thus, the actual local water uptake rate, $U_{C(n)}(x,z,t)$ in m³ H_2O m⁻³ soil s⁻¹, is given by :

$$U_{C(n)}(x,z,t) = \alpha U_{max,C(n)}(x,z,t) \qquad (4.55)$$

where the correction factor α is defined as:

$$\alpha = \begin{cases} 1 & ,\text{if } U_{max,C(n)}(t) \leq T_{p,C(n)}(t)W_{C(n)}(t)\Delta y \\[4mm] \dfrac{T_{p,C(n)}(t)W_{C(n)}(t)\Delta y}{U_{max,C(n)}(t) \bullet dxdydz} & ,\text{otherwise} \end{cases} \quad (4.56)$$

Windbreak trees : Bauhinia

To calculate water uptake by the windbreak, U_{WB} (m^3 H_2O m^{-3} soil s^{-1}), the 'Root System Model' (modified version of Conijn, 1995) is used :

$$U_{WB}(x,z,t) = T_{p,WB}(t)W_{wb}(t)\frac{l_R(x,z,t)}{\int l_R(x,z,t)dxdz} f_{up,WB}(x,z,t) \quad (4.57)$$

where W_{wb} is the width of the windbreak. $T_{p,WB}$ (m^3 H_2O m^{-2} soil s^{-1}) sets the upper limit to total tree water extraction of the windbreak from the soil profile. Hence, extraction of water from a certain position is proportional to relative root length, (l_R (x,z,t) / $\int l_R(x,z,t)$ dxdz), and to the reduction factor, $f_{up,WB}$, which is related to the pressure head. The shape of the reduction factor is described with the equation of van Genuchten (1987):

$$f_{up,WB}(x,z,t) = \frac{1}{1 + \left(\dfrac{h(x,z,t)}{h_{50}}\right)^m} \quad (4.58)$$

where h_{50} is the pressure head at which the extraction rate is reduced by 50%, for which a value of -3,200 cm is used (pF = 3.5). The parameter m is an empirical constant set to 1.5 (Jetten, 1994).

Competition

Competition for soil water at a certain position occurs when during a time interval Δt the sum of $U_{C(n)}$ and U_{WB} (total potential water uptake $U(x,z,t)$ exceeds the actual available soil water, $\theta(x,z,t)-\theta_{wilt}$. Hence, water uptake by millet and tree roots has to be adjusted when:

$$U(x,z,t) = U_{WB}(x,z,t) + \sum_{n'} U_{C(n')}(x,z,t) > \frac{\theta(x,z,t) - \theta_{wilt}}{\Delta t} \quad (4.59)$$

where n' is an index, that runs over all crop rows.

Available water is then distributed between trees and millet in proportion to their uptake rates in the non-competitive situation.

$$U_{C(n)}(x,z,t) := \frac{\theta(x,z,t) - \theta_{wilt}}{\Delta t} \; \frac{U_{C(n)}(x,z,t)}{\displaystyle\sum_{n'} U_{C(n')}(x,z,t) + U_{WB}(x,z,t)} \qquad (4.60)$$

$$U_{WB}(x,z,t) := \frac{\theta(x,z,t) - \theta_{wilt}}{\Delta t} \; \frac{U_{WB}(x,z,t)}{\displaystyle\sum_{n'} U_{C(n')}(x,z,t) + U_{WB}(x,z,t)} \qquad (4.61)$$

4.8   Model implementation

The simulation programme, especially its structure, has received ample attention during model development for two reasons: first to facilitate incorporation of the competition between windbreak and crops for light and water, i.e. to meet the requirements relating to spatial, structural and temporal heterogeneity of the system and secondly to allow easy extension of WIMISA with other important effects of a windbreak, i.e. air flow stream patterns and further microclimatic factors. Incorporation of all relevant WB effects is needed to provide a generally applicable, integrated and quantified assessment of the response of agricultural systems to windbreaks. In addition, a well designed model allows easy update for new understanding of system processes or new methods for describing them.

A key characteristic of the WIMISA programme is its modular structure. A set of modules is created (Fig. 4.15) with the CROP growth and SOIL WATER balance modules as the key part of the system. Within the programme, however, all modules are equivalent and completely independent, i.e. they do not use common blocks (global data areas). The modules communicate data to each other through a central control module, the DATA INTERFACE. This programme design allows easy modification, removal, addition, replacement or exchange of modules without disruption of the operational mode of the other parts of the programme.
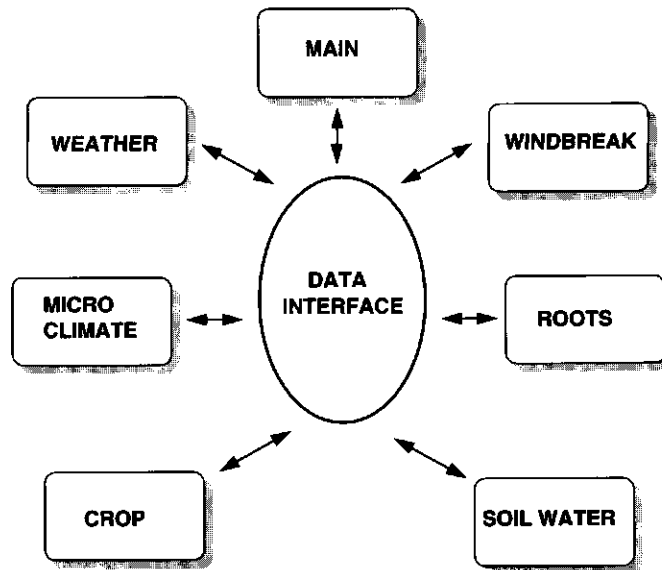
Figure 4.15   Modular structure of WIMISA.

Hence, (e.g. plant growth) modules are interchangeable, and more than one growth module can be connected simultaneously. In the present WIMISA version, CROP is based on an existing model (CP-BKF3, written in the programme language FORTRAN-77), which has an inline structure, i.e. a single subroutine contains a long consecutive stream of statements (all statements are in line) for performing different duties. This makes a computer programme difficult to read and especially difficult to maintain. Therefore, it was redesigned and recoded. The other modules consist of newly written source codes, partly originating from existing methods (algorithms) of one or more models, i.e. CP-BKF3, WEPS, RECAFS, FUSSIM2. Current modules and their origins are given in Table 4.1.

Techniques applied to support modularity, flexibility and readability of the programme are similar to those used in APSIM (The Agricultural Production Systems sIMulator, McCown et al., 1996):

- The programme is composed of modules each containing a set of small, highly independent, closed functions (comparable to subroutines). The modules are separate source files and can be compiled separately.
- Modules are limited in size, to facilitate independent development, readability, and testing.
- Functions are defined in such a way that each performs one limited task.
- Data interchange among modules occurs only through the module DATA INTERFACE.

- The necessary multi-dimensional variables, e.g. soil water content, are not declared with predefined dimensions but are allocated dynamically. Thus, the maximum size for the model system to be simulated is not limited by settings inside the programme, but by the memory accessible on the computer.
- The programme language is ANSI C, which facilitates readability and flexible programming (McCown et al., 1996).

The most important step with respect to modularity was the centralization of data communication through a separate module. This DATA INTERFACE module contains functions called by various WIMISA modules to access the (begin) address of variables that are allocated by modules other than the calling module. Moreover, DATA INTERFACE contains functions through which the various modules are initialized. The sequence of the actual system setup, initialisations and updating is controlled by the MAIN module. The input is organized in one file for each subsystem and a control input file with environmental and management parameters and output specifications (Appendix B2).

Table 4.1 List of current modules of WIMISA, their main functions and their origins. * with minor modifications

Module	Functionality	Derived from	Reference
CROP	sowing, emergence, development, assimilation*, respiration, conversion & partitioning of DM, LAI, dying of organs, water stress	CP-BKF3	Verberne et al. (1995)
SOIL WATER	infiltration, evaporation*, rain-intensity, (runoff: not used)	CP-BKF3	Verberne et al. (1995)
	redistribution	WEPS, FUSSIM2	Durar & Skidmore (1995), Heinen & de Willigen (1992)
ROOT	millet root length extension & distribution*	CP-BKF3	Verberne et al. (1995)
	root water uptake of millet		
	root water uptake of Bauhinia	RECAFS	Conijn (1995)
WEATHER	daily total radiation, air humidity & rainfall; maximum & minimum air temperature	CP-BKF3	Verberne et al. (1995)
MICROCLIMATE	evapotranspiration*		Penman (1948)
	temperature		Weihong (1996)
	radiation		de Wit et al. (1978)
	wind speed	Experiment	Chapter 3
WINDBREAK	forcing functions for: height, porosity and DM of Bauhinia	Experiment	Chapter 3
DATA INTERFACE	data interchange, modules initialisation		
MAIN	organisation & control		

5 PARAMETER DERIVATION

The model WIMISA requires general and specific input parameters for the description of its subsystems WEATHER, MICROCLIMATE, WINDBREAK, SOIL WATER, CROP, and ROOTS (Fig. 4.1). Generally applicable parameter values for the crop growth and soil water module have been derived from literature, and are thus independent of the experimental dataset used for testing of the model. This increases the general applicability of the model. Parameter values that are specific for site, year, crop cultivar, WB species, and soil, and weather data, are mainly based on experiments in a WB-millet or a sole millet system in 1990 to 1993 (Chapter 3; Michels, 1990; Lamers, 1995; Smith, 1995 and 1996a,b) and the experiments of Bley (1990). All these experiments were conducted at the Sahelian Center of ICRISAT (ISC), in Niger. This chapter describes the derivation of specific parameter values, which are used in the model. A complete list of parameters is given in Appendix B2.

5.1 Weather

Weather data consist of daily solar radiation, maximum and minimum air temperatures, vapour pressure, wind speed and precipitation. Simulation runs were conducted with data collected at the central weather station of ISC, located 1 km west of the experimental site. The wet year 1993 was used to calibrate the model. Relevant ISC weather data are available from 1985 onwards.

5.2 Microclimate

A windbreak changes the microclimate in the adjacent crop depending on its orientation, height and porosity. These characteristics are needed for calculation of the light intensity reaching the crop behind the WB-barrier (Section 4.4). Modification of wind speed, not yet related to the WB properties, is incorporated by a reduction factor of 0.7 for wind velocities exceeding 4 m s^{-1} in the first 5 H (ca. 10 m) in the lee of the shelter. For wind speeds equal to or lower than 4 m s^{-1} the reduction factor is set to 0.8 for the first 5 H. These values are based on observations in the lee of Bauhinia during storms (Michels, 1990) and normal winds (Subsection 3.1.2) at a height of 0.7 m and 1 m, respectively.

5.3   Windbreak: Bauhinia trees

In the WIMISA simulations the shelter is oriented north-south (i.e. $0°$ with the north direction) as in the WB-millet experiment. Most of the WINDBREAK input parameters have been derived from this agroforestry experiment (Section 3.4) and refer to the tree species *Bauhinia rufescens* Lam.. The influence of growth constraints (e.g. water stress) on tree height, tree DM production, leaf area development, and porosity were neglected, because these effects were neither studied experimentally nor found in literature for *Bauhinia rufescens*.

5.3.1   Height, crown radius and porosity

In the course of the growing season height, crown radius and density of the Bauhinia WBs increased (Table 5.1). Bauhinia's porosity (ε_p), as derived from black and white photography, was 80 % at the beginning and 20 % at the end of each growing season (Section 3.4). Following the approach for modelling light interception by the WB-barrier (Section 4.4), porosity of the windbreak determines the radiation intensity reaching the WB-shaded area. For parametrisation purposes the ε_p values have been adapted by fitting simulated and measured total global radiation on days early in the season and around flowering in 1993. This procedure was performed for measurements at 1, 2, 3, and 10 m from the WB tree trunk. At a distance of 10 m, the radiation was distributed almost symmetrically around 13 h, illustrating a negligible shading effect (Fig. 5.1). Simulated and observed global radiation agree well for the porosity as given in Table 5.1 with $f_{dif} = 0.5$ (f_{dif} is the fraction of diffuse fluxes, I_{dif}, coming from directions other than through the windbreak). The small underestimate of simulated daily maximum global radiation is due to the computation of instantaneous radiation fluxes from total daily global radiation, using a sinusoidal distribution over the day (Spitters et al., 1986). In this approach, changes of cloudiness within a day are not accounted for. Hence, on sunny days with cloudy periods reducing the daily total, the maximum of the simulated radiation sine curve is lower than the actually measured irradiation.

Radiation measured adjacent to the windbreak is the sum of fluxes transmitted through the porous area of the tree rows and fluxes reflected by their canopy. Theoretically, WIMISA does neither simulate reflection nor absorption of light by the WB canopy, but since ε_p has been fitted on the basis of radiation measurements, those processes are implicitly accounted for.
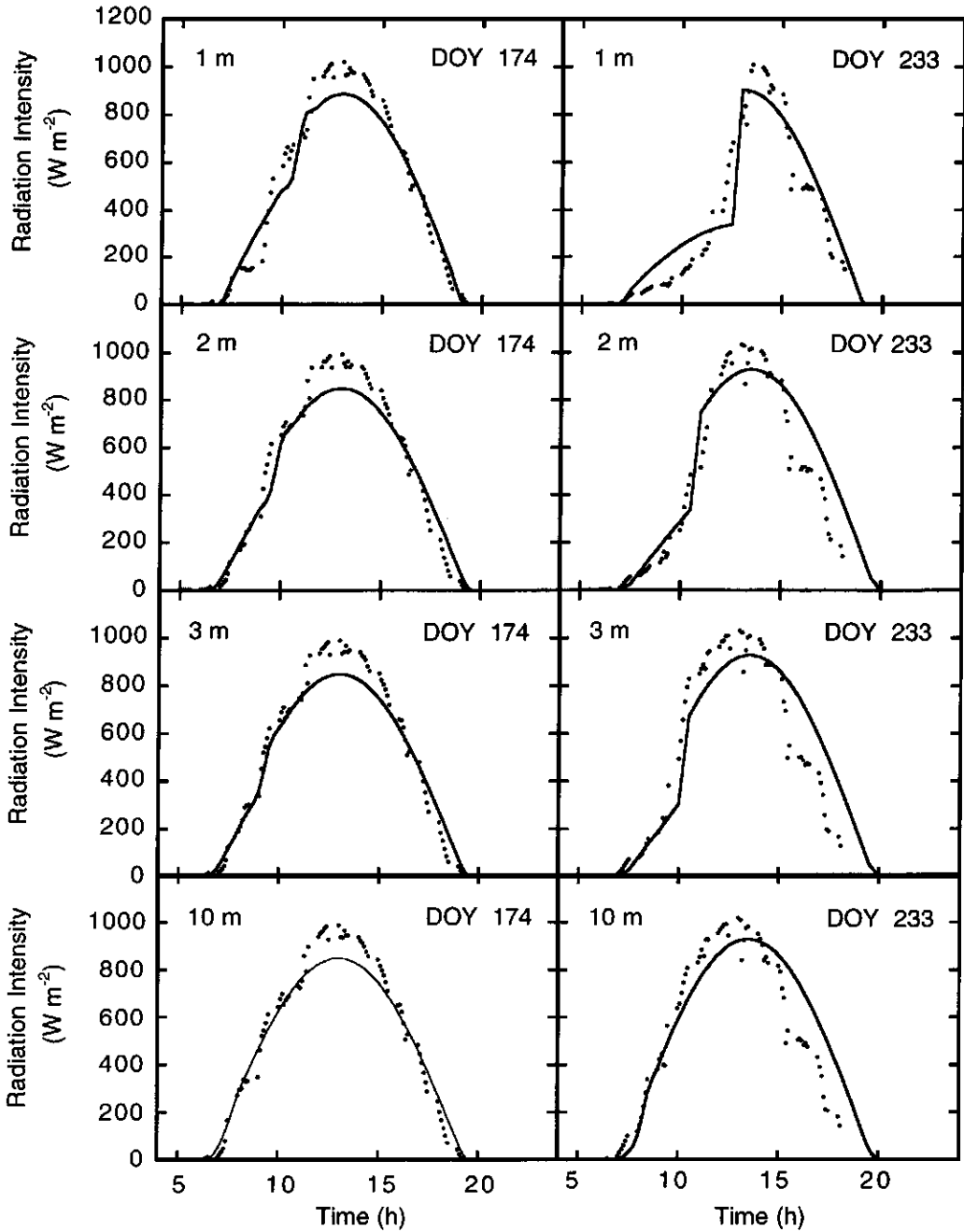
Figure 5.1   Diurnal course of simulated (solid line) and measured (dotted line) global radiation west of the north-south oriented windbreak, early (DOY 174) and late (DOY 233) in the growing season, ISC, Niger, 1993. DOY denotes day of the year.

5.3.2   LAI and k

Leaf area index (LAI) and radiation extinction coefficient (k) of the tree canopy are necessary to compute potential soil evaporation (Eq. 4.18). The coefficient k is estimated at 0.7 for leaves and branches of trees for photosynthetically active radiation (after Conijn, 1995). LAI as a function of time is estimated from observations by Smith (1995, 1996) and Lamers (1995) in an accompanying research programme in the same experimental WB-millet field.

Leaf area measurements of two Bauhinia trees yielded a mean LAI of 3.75 on DOY 282 in October 1992 (Smith, pers. comm., Institute of Hydrology, Wallingford, UK, 1996). For *Azadirachta indica*, LAI could be described empirically by a linear dependence on DOY with a slope of 0.0258 d^{-1} and an intercept of -2.02 (Smith et al., 1996); values were derived using multiple regression on data collected from leaf harvests in 1992 and 1993). Comparison of leaf production of both species (Lamers, 1995) showed that Bauhinia had a LAI growth rate similar to that of *Azadirachta indica*, assuming similar specific leaf weights (kg ha^{-1}). Using the relative LAI growth rate of 0.0258 d^{-1} and the measured value of 3.75 for LAI on DOY 282, LAI in the course of the growing season is described by:

$$LAI = -3.53 + 0.0258\ t_d \qquad (5.1)$$

with t_d = DOY. In 1993 the growing season started around DOY 157, which corresponds to an LAI of 0.52. This value is assumed to also hold for the period between the start of the simulation (e.g. DOY 100) and the onset of the growing season. LAI values for subsequent DOY's were computed also with Eq. 5.1 and used as time dependent input table in WIMISA.

5.3.3   Potential production rate and water use efficiency

For calculation of potential tree transpiration, $T_{p,WB}$, the potential rate of dry matter production, P_{WB}, and water use efficiency, E_W, are required (Eq. 4.20).

In Table 5.1, based on results of the WB experiment of Lamers (1995), the P_{WB} of Bauhinia has been derived exogeneously as a function of time. Lamers harvested total aerial production of Bauhinia in April (around DOY 110) and October (around DOY 275), 1992. Within that period the production was about 12 t ha^{-1}, which appeared the main part of the annual production and irrespective of the trimming regime (Lamers, 1995). Annual wood production of 12 t ha^{-1} in this region is very high compared to maximum annual production values in relation to rainfall reported by Breman and Kessler (1995) for woody plants in the Sudano-Sahelian zone: 3.7 and 12 t ha^{-1} for the southern Sahel and Sudan zone, respectively.

Table 5.1   Measured (bold) and estimated 'Bauhinia' parameters as a function of time, as derived from the WB-millet experiment at ISC with potential rate of DM production (P_{WB}) after Lamers (1995), and LAI after Smith (1995). Values for water use efficiency (E_W) result from fitting values calculated by Lövenstein et al. (1991) for *Acacia salicinia* and *Eucalyptus occidentalis* in the Negev Desert of Israel.

DOY	Height (H_b)	Crown radius	Porosity (ϵ_p)	P_{WB}	LAI	E_W
day of year	(m) measured	(m) measured	(-) fitted	(kg ha^{-1}d^{-1})	(-)	(kg ha^{-1}mm^{-1})
100	**2.0**	**1**	0.9	0	0.52	20
135						
157	2.0		0.9	91	0.52	20
161					0.62	
171			0.7			
182				106		
200			0.4		1.63	
230					2.40	
233		**1.5**	0.2			25
245				55		
265	**3.0**		0.2	24	3.31	
282					**3.75**	
300	3.5		0.2			

This high production on this experimental station may have been associated with the favourable growing conditions compared to 'normal tree sites' in the Sahel, as already mentioned by Lamers (1995): In 1992 annual precipitation (586 mm) was slightly above the local long-term average (562 mm), and moreover, through lateral roots trees may have had access to plant nutrients that were applied to the adjacent millet fields. In addition, regular weeding minimized competition with herbaceous plants. In comparison to on-farm results, it is also important to note that neither burning nor grazing disturbed the growth of the windbreak and that tree density was high. Thus, 12 t ha^{-1} obviously represents the maximum production possible under the conditions of the Sahel. Hence, this value may be used to derive the input parameter P_{WB} in WIMISA.

Assuming that the tree growth curve (DM$_{WB}$ versus time) can be characterized by a sigmoidal curve, the two data points of Lamers (160 and 12000 kg ha^{-1}) can be connected as presented in Figure 5.2 and described by:

$$DM_{WB} = 160 + (12000 - 160)\frac{1}{2}\left[1 + \sin\left(\frac{\pi}{2}\frac{t_d - 187.5}{87.5}\right)\right] \tag{5.2}$$

The P_{WB} (kg DM ha^{-1} d^{-1}) is the time derivative of the above equation (values in Table 5.1):

$$P_{WB} = \frac{dDM_{WB}}{dt} = 106.27\cos\left[0.017952(t_d - 187.5)\right] \tag{5.3}$$

These values represent potential growth rates under the environmental conditions of the Sahel.
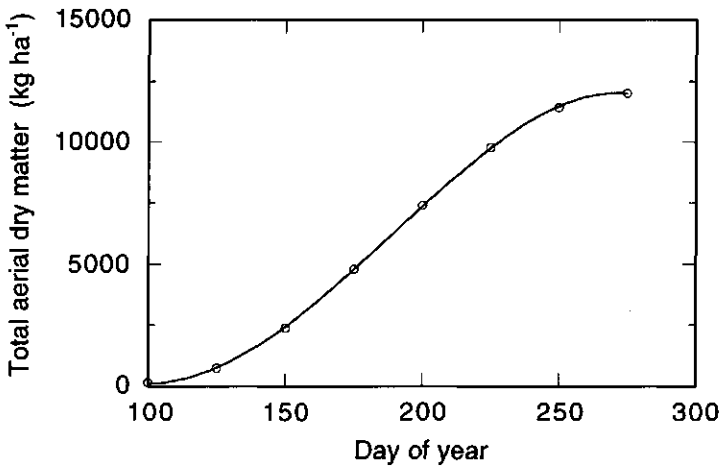
Figure 5.2   Estimated growth curve of aerial dry matter of Bauhinia from April till October 1992 at ISC (Source: Lamers, 1995).

Water use efficiency, E_W, here in kg ha^{-1} mm^{-1}, is given as a linear function of WB porosity. At high porosity (early millet growing season), E_W is assumed equal to that of a solitary tree, and at low porosity (end of millet growing season) it is set to the value for a closed canopy. These values were chosen, because similarly to a solitary tree, a tree with high porosity is more exposed to the drying power of the air (i.e. has a higher water demand per unit biomass production) than an individual tree in a dense forest and a tree with low porosity. Both E_W values (solitary tree and closed canopy) have been derived from Lövenstein et al. (1991).

5.3.4   Bauhinia roots

In WIMISA, the density distribution of fine root length of trees is needed in two dimensions for calculation of their water extraction and, hence, the competition for soil water between windbreak and millet (Section 4.7). Trees have coarse (primary) and fine (secondary) roots. While coarse roots function as support, fine roots are mainly important for root water uptake. However, the only available data on the root system of Bauhinia are those on coarse roots, derived from one excavated tree in the WB experiment (Subsection 3.4.3).

Literature reviews (Hellmers et al., 1955; Hairiah and van Noordwijk, 1986) suggest that tree roots can be classified on the basis of their primary root system. In semi-arid regions, both indigenous and exotic woody plants show either of two root systems: a) deep tap roots and many superficial branch roots (bimorphic) or b) shallow and extending roots, irrespective of soil depth (Breman and Kessler, 1995). The primary rooting pattern of the excavated Bauhinia tree is bimorphic and similar to that of *Acacia seyal* as shown in Figure 5.3. Soumaré et al. (1994) studied primary and secondary root systems of scattered *Acacia seyal* trees in the south Sahel (Niono, Mali) with climate (500 mm annual rainfall) and soil conditions (i.e. sandy soils with no access to soil water table) similar to those at the ISC site. As the fine roots particularly develop at the end of coarse roots (Breman and Kessler, 1995), it may be assumed that the fine rooting patterns of Bauhinia are also similar to those of *Acacia seyal*. Therefore, the required model input on distribution of fine roots of *Bauhinia rufescens Lam.* has been derived from measurements of *Acacia seyal* by Soumaré et al. (1994).

Soumaré et al. (1994) measured the weight of fine roots (diameter < 2 mm) at three distances from the tree trunk (one, two and three times the crown radius of *Acacia seyal* , i.e. r1, r2, r3), to a soil depth of 0.6 m. Vertically, the soil was subdivided into layers of 0.1 m. The lateral roots of *Acacia seyal* were concentrated in the upper 0.4 m of the soil. The density of fine roots was highest under the tree crown and decreased with distance from the trunk. The measured root densities of *Acacia seyal*, expressed in kg ha^{-1} (Table 5.2), were transformed into root length densities (m m^{-3}) by multiplying with the vertical component (depth of the layer) and the specific root length of trees, 0.5 m g^{-1}, as estimated by Conijn (1995).
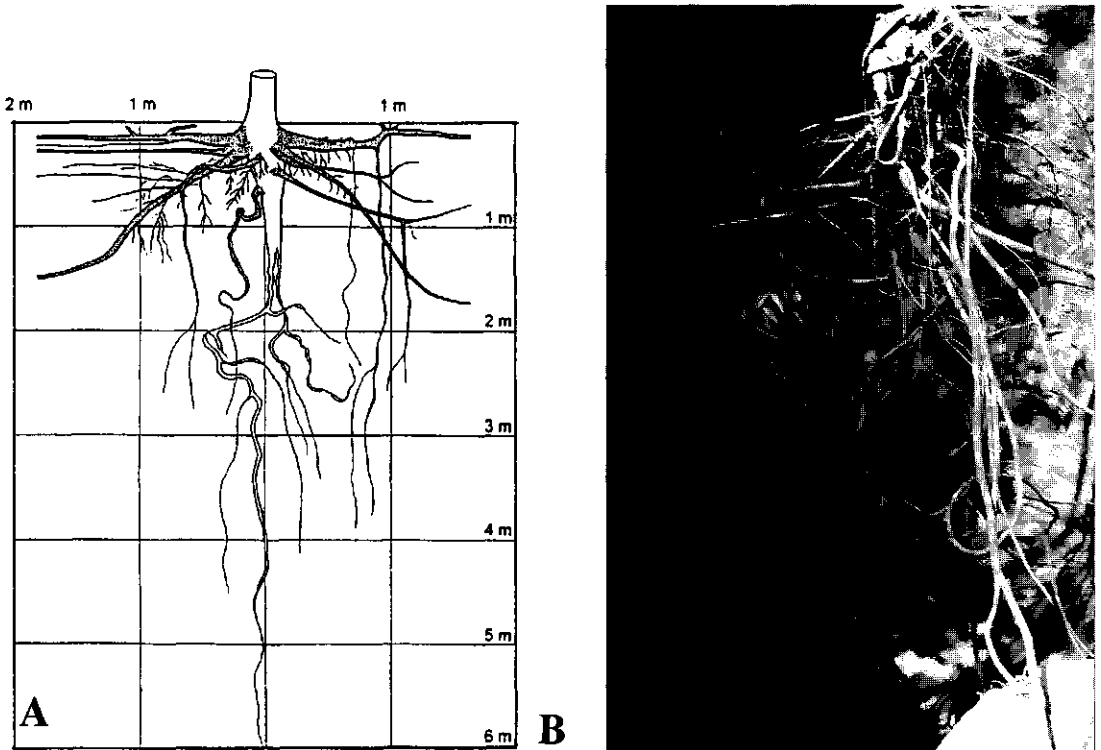
Figure 5.3   Distribution of coarse roots of *Acacia seyal* (A) at Niono, Mali (Source: Soumaré et al., 1994) and roots of an excavated*Bauhinia rufescens* tree (B) at ISC, Niger.

The resulting root length density distribution of *Acacia seyal* was transferred to a Bauhinia tree, using the vertical subdivision of Soumaré et al. (1994) and the crown radius of our Bauhinia trees for setting r1, r2 and r3. In the model, the tree root zone is partitioned into three subzones perpendicular to the windbreak: that under the tree crown (a1), that at the edge outside the tree crown (a2), and that in the open field far beyond the crown (a3) (Fig. 5.4). Root length densities within zone a_1, a_2, and a_3 are fixed at the transferred densities for distance r1, r2 and r3, respectively. Bauhinia's crown radius has been taken as width of each root subzone, because biomass of fine roots is reported to be "extra" high under the tree crown (Conijn, 1995, van Noordwijk et al., 1996). Bauhinia's crown radius was 1.5 m, which is about half that of *Acacia seyal*.

Table 5.2   Distribution of fine roots of a solitary *Acacia seyal* tree: DM_R = root weight per soil layer of 0.1 m depth at three distances (r1, r1 and r3; see text for explanation) from the trunk (Source: Soumaré et al., 1994).

Soil depth (m)	r1 DM_R (kg ha^{-1})	r2 DM_R (kg ha^{-1})	r3 DM_R (kg ha^{-1})
0.0 - 0.1	33.5	9.0	2.0
0.1 - 0.2	146.0	83.0	33.0
0.2 - 0.3	296.5	182.0	62.5
0.3 - 0.4	153.0	44.0	2.0
0.4 - 0.5	15.0	10.0	3.5
0.5 - 0.6	32.0	19.0	3.0

A further assumption had to be made on the relation root length density and woody plant density. The Bauhinia windbreak (1943 trees ha^{-1}) had a higher density than the Acacia parkland field with 400 trees ha^{-1} studied by Soumaré et al. (1994). It is difficult to predict the effect of tree density on rooting pattern. Studies from Australia on Eucalyptus show that with increasing tree density (from 304 to 2150 trees ha^{-1}) total root length ha^{-1} increases, but root length per tree decreases for 6% (Eastham and Rose, 1990). This is a rather small effect, and as the difference in tree density between the Acacia parkland and our Bauhinia WB is even less than in the Australian study, the root length density per Bauhinia tree within the windbreak was set equal to that estimated for a solitary Bauhinia tree. The distribution of root length densities at both sides of the windbreak is considered symmetric (Fig. 5.4).
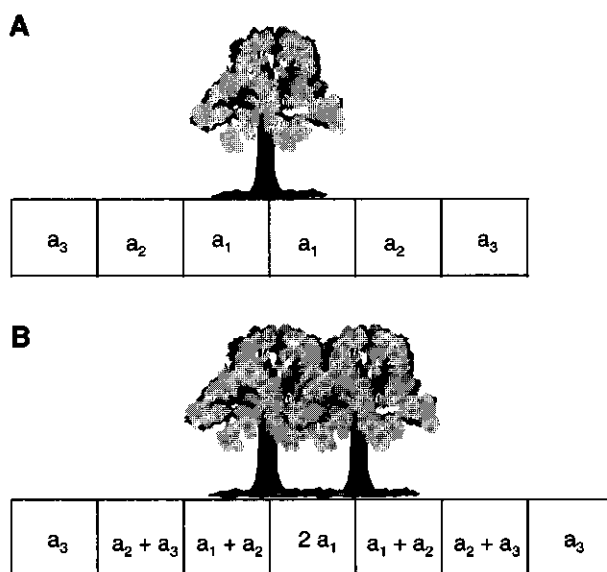
Figure 5.4   Horizontal root subzones (a_1, a_2, a_3) at each side of a single tree row (A) and overlapping root subzones ($2a_1$, $a_1 + a_2$, $a_2 + a_3$) of a double row WB (B). Scheme B is used for the present simulations.

In the experiment, the windbreak consisted of two tree rows at a distance of 1.5 m, so that their roots partly shared the same space. This is modelled by overlapping root subzone of row 1 and row 2, e.g. the zone between the two rows is exploited to the same degree by roots of each tree row and, hence, has a root length density of $2*a_1$. To account for possible horizontal soil water flow, WIMISA computes the soil water balance for the entire root region of the double row windbreak. Root length densities for each of the seven horizontal root subzones are given per layer in Appendix B2.

5.3.5   Remarks

The tree parameter values for water use efficiency, E_W, and root length distribution, $l_R(x,z)$, are rather uncertain estimates, because they have been derived from species and sites different (although comparable) than the experimental one. However, the accuracy of the simulated windbreak water use could be tested by comparing simulation results with data on daily transpiration and seasonal water use of *Azadirachta indica* and *Acacia holosericea* windbreaks of the same agroforestry field (Fig. 2.2) and growing seasons (Smith, 1995). By tuning E_W within the range given by Lövenstein (10-30 kg ha^{-1} mm^{-1} for root water uptake from the upper 3 m) simulated maximum transpiration rate and total seasonal transpiration of the windbreak

were calibrated closely to the values reported by Smith (Section 6.4; Appendix B3): For *Azadirachta indica* and *Acacia holosericea* daily transpiration fluctuated throughout the seasons of 1992 and 1993 between 1.5 and 6 mm d^{-1}. Highest total seasonal transpiration was found for *Acacia holosericea* with 320 mm during the growing period DOY 147 - DOY 259 in 1992, estimated on the basis of a modified Penman-Monteith equation (Jarvis and McNaughton, 1986, cited from Smith, 1995).

The Bauhinia windbreak characteristics porosity, P_{WB} and LAI are based on the experimental growth conditions in 1992 and 1993. The moment of onset of seasonal tree growth in relation to the day of sowing of the crop is important in view of competition. The start of windbreak growth is presumably related to the onset of the rainy season, which marks the moment of availability of water. In 1987, first rains started early in the season (21 mm before DOY 100), but were followed by a long period with poor rainfall till about DOY 183, when millet was sown at ISC (Bley, 1990). In this thesis, to account for the poor rainfall early in the season of 1987 compared to 1992 and 1993, WB growth curve and porosity time functions have been shifted by 5 days and the duration of LAI growth was prolonged by that period.

5.4   Soil

5.4.1   *Soil moisture retention curve and $\theta - K$ relation*

The soil moisture retention curve and the dependence of hydraulic conductivity on soil water content are required to solve Darcy's flow equation (Subsection 4.6.1), neither of which were determined during the experiments. Therefore, as in the hydrology submodel of WEPS (Durar and Skidmore, 1995), Campbell's (1974) method for calculating both characteristic curves, using parameter values from the literature has been applied.

The input parameters Campbell's power (C_b), pressure head at air entry (h_{ae}), hydraulic conductivity at saturation (K_{sat}), and water content at saturation (θ_{sat}) of Eqs. 4.25 and 4.26 are hydraulic characteristics of the soil, specific for a soil texture class. The current values of θ_{sat} = 0.395 m^3 m^{-3} and K_{sat} = 8.0*10^{-5} m s^{-1} have been derived from laboratory analyses of the soil of ISC, Niger (Bley, 1990). The values of C_b and h_{ae} (unknown for the soil at ISC) have been set equal to those for a sandy soil as estimated by Rawls et al. (1982) on the basis of soil hydraulic properties of many soils from the USA. Table 5.3 summarizes hydraulic properties for two soil texture classes, typical for ISC. Alternatively, values of C_b, h_{ae}, K_{sat}, can be

approximated with the mean of data on bulk density and soil texture according to Campbell (1985).

Table 5.3   Soil hydraulic properties for two soil texture classes (USDA) as reported by Rawls et al. (1982): pressure head at air entry (h_{ae}), water content at saturation (θ_{sat}), Campbell´s power (C_b) and hydraulic conductivity at saturation (K_{sat}).

Texture Class	h_{ae}	θ_{sat}	C_b	K_{sat}
	(m)	($m^3 m^{-3}$)	(-)	($m\ s^{-1}$)
Sand	0.163	0.437	1.441	$5.833 * 10^{-5}$
Loamy sand	0.256	0.437	1.808	$1.697 * 10^{-5}$

Applying the C_b and h_{ae} values recommended by Rawls (Table 5.3), and θ_{sat} found by Bley (1990), in Campbell's power law for the $\theta-h$ relation (Eq. 4.25), a reasonable fit is obtained with the experimental data of Bley (1990) (Fig. 5.5).
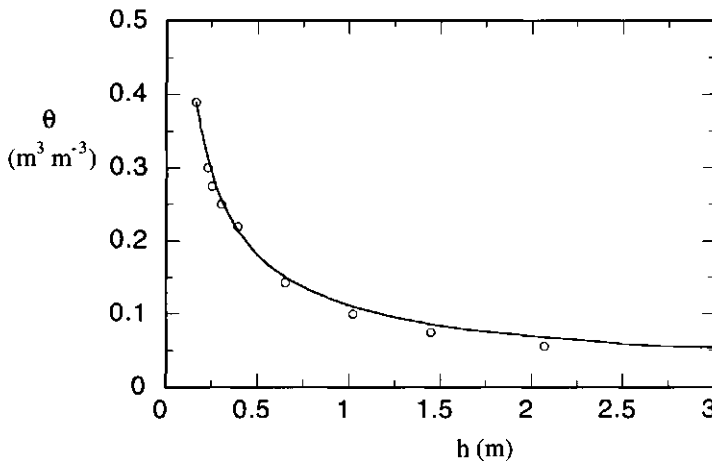
Figure 5.5   Soil moisture retention curve: comparison of the results of Campbell's method (1974) using h_{ae} = 0.163 m, C_b = 1.44, and θ_{sat} = 0.395 $m^3 m^{-3}$ (line) and Bley's (1990) experimental data for an ISC soil (dots). Bley determined the moisture retention curve by the field method of Hillel et al. (1972).

The relationship between conductivity K and θ as measured by Bley (1990) is fitted well by the power law (Eq. 4.26) using Bley's values for θ_{sat} and K_{sat} (Fig. 5.6). The latter is comparable to the K_{sat} value of $9.3*10^{-5}$ found by Payne et al. (1991a) and those of Rawls et al. (1982) (Table 5.3).

The good agreement between field observations and the results of calculation method for the soil moisture retention and the soil moisture conductivity curve suggests that Campbell's approach is suitable for sandy soils in the Sahel. Nevertheless, model performance should be most accurate using measured values (Payne et al., 1991b). However, determination of soil hydraulic characteristics as hydraulic conductivity is difficult under field conditions, because of spatial and temporal variability (Durar and Skidmore, 1995). Moreover, determination of such data is very laborious. Consequently, such data are scarce.
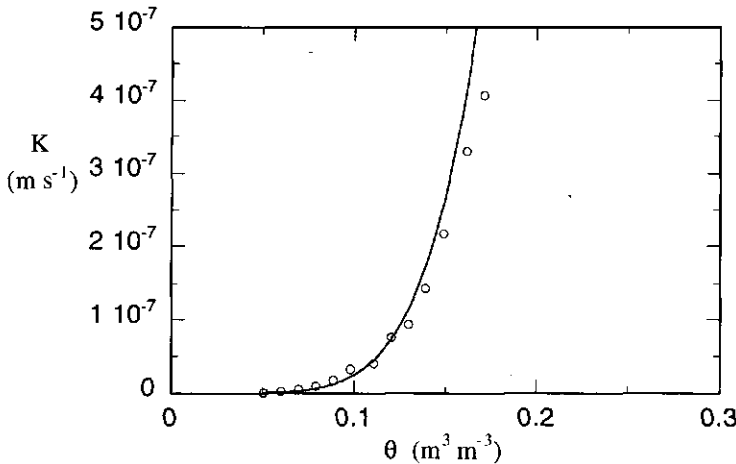
Figure 5.6   Soil moisture conductivity curve: comparison of the results of Campbell's method (1974) with $K_{sat} = 8 *10^{-5}$ m s^{-1}, $\theta_{sat} = 0.395$ m^3 m^{-3} (Bley, 1990) (line) and Bley's (1990) experimental data for an ISC soil (points). Bley determined the hydraulic conductivity by the field method of Hillel et al. (1972) and the calculation method of Jackson (1972).

The options to estimate soil hydraulic characteristics from more easily and routinely obtainable soil texture and bulk density data (Campbell, 1985) or even from a table for various soil texture classes (Rawls et al., 1982; Batjes, 1996; Bell and van Keulen, 1995), the so-called pedotransfer functions, enhances the applicability of a soil water module.

5.4.2   Characteristic soil water contents

Additionally to the θ-h and θ–K relations, θ_{sat} and volumetric water contents at field capacity, θ_f, at wilting point, θ_{wilt}, and at the start of the simulation are required. Their values have been derived from experimental data reported for sandy soils in Niger (Table 5.4), on the basis of the following considerations:

- The parameter θ_{sat} is used in Eqs. 4.25 and 4.26, which are based on the theory that pore size distribution of a soil is an important factor with respect to θ–K and θ-h relations (Green and Ampt, 1911). Similarly the laboratory method for determining θ_{sat} yields the pore volume of a soil, whereas values derived from field measurements are generally lower. Therefore, the θ_{sat} found by Bley (1990), using the laboratory method, was applied.
- Plant available soil water is held between θ_f and θ_{wilt}. A pressure head of -15000 hPa has traditionally been associated with permanent wilting point (Veihmeyer and Hendrickson, 1950). The pressure head associated with θ_f is somewhat arbitrary and has been defined differentially by different authors (Table 5.4, de Ridder et al., 1991), due to a strong gradient in the h-θ relation of sandy soils (Fig. 5.5). A value of h of -100 hPa, often used for sandy soils, even underestimates field capacity (Payne et al., 1990); they therefore suggest a field capacity of about 0.12 to 0.16 m^3 m^{-3}, corresponding to a pressure head of about -50 hPa. Bley (1990) defined θ_f and θ_{wilt} as water content at -62 hPa (pF 1.8) and -15543 hPa (pF 4.2), respectively. Available volumetric water content was approximately 0.09 m^3 m^{-3}. This fraction was used as a norm for θ_f - θ_{wilt}, because accurate estimation of available water is a prerequisite for accurate simulation of water extraction by plants and possible growth reduction due to water shortage. Most values reported were obtained with the field method giving approximately 0.12 and 0.03 m^3 m^{-3} for θ_f and θ_{wilt}, respectively (Table 5.4). As these values are close to the experimental data (Subsection 3.2.1), they were used as input in the soil water module. In the WB-millet experiment the maximum values for θ were 0.12 (1993) and 0.15 (1992); the minimum values for θ were about 0.02 and 0.03 m^3 m^{-3}.
- Theoretically, initial soil water content of the top soil should be set equal to at air dry conditions, θ_{ad}, if the simulation starts before the onset of the rainy season when the soil is still dry. As a rule of thumb, θ_{ad} may be set to 1/3 of θ_{wilt} (van Keulen, 1975).

For each soil texture class the before mentioned soil characteristics (θ's, h_{ae}, K_{sat}, C_b) have to be specified. The Sadoré soil, classified as a sandy "Psammentic Paleustalf" of the Labucheri series in the USDA taxonomy (West et al., 1984), consists of 2 texture classes: sand in the upper 20 cm and loamy sand continuing to a depth exceeding 2 m. However, Bley (1990)

found for the retention curve only small differences with soil depth. Hence, in the model only one texture class, i.e. sandy soil, is considered for the complete soil profile.

Table 5.4   Volumetric water contents (m^3 m^{-3}) at saturation (θ_{sat}), field capacity (θ_f) and wilting point (θ_{wilt}) as measured for sandy soils in Niger and as reported for sandy-loamy sand soils in the USA by Rawls et al. (1982)

Author	Location, method	Saturation θ_{sat}	hPa	Field capacity θ_f	hPa	Wilting point θ_{wilt}	hPa
	Niger,						
Bley, 1990	ISC, laboratory	0.398	0	0.18	62	0.03-0.04	15543
	ISC, field	0.310	0	0.10	62	0.01	15543
Payne et al., 1990	3 sites, field	0.280	0	0.12-0.16	50		
Fechter, 1993	Tara, laboratory	0.350	0	0.18	100	0.06	15000
	USA,						
Rawls et al., 1982	sand-loamy sand	0.437		0.091-0.125		0.033-0.055	

5.5   Millet

Most crop characteristics needed as model input, e.g. all assimilation and respiration characteristics, the distribution of assimilates, the temperature and day length dependence of crop development and root characteristics were adopted from CP-BKF3 (Verberne et al., 1995), a model developed and calibrated for millet in the Sahel. Its crop parameter set has been derived from experimental data of different millet cultivars and different regions in the Sahel (mainly Mali: Jansen and Gosseye, 1986; van Heemst, 1988; van Duivenbooden and Cissé, 1989, Erenstein, 1990).

For determination of site- and cultivar (CIVT)- specific characteristics, an experiment was conducted during the 1993 rainy season in the Ziziphus plot of the agroforestry field (Subsection 3.3.4). In intervals of 10 days measurements were performed on 10 preselected plant pockets, which were harvested. All these pockets were assumed to be located outside the influence of the windbreak, so that the observed data were suitable for calibration of a millet system (unsheltered millet field), i.e. established number of plants per pocket, phenological development, dry matter production allocated to plant organs, leaf area, number of dead and living leaves.

5.5.1   Initial biomass

Initial dry matter (DM_0) defines the starting point for the growth simulation. According to Carberry et al. (1985) initial shoot dry matter for millet is 1 g plant[-1]. In the experiments, plant density after thinning was 30.000 plants ha^{-1}. Using Carberry's estimate results in an DM_0 of 30 kg ha^{-1} or 27 kg ha^{-1}, taking into account a correction for reduced plant numbers due to several storms in 1993.

5.5.2   Development rates

From experimental data on development stage (DVS), development rates (DVR) can be calculated as the inverse of the period between successive phenological events. In the Ziziphus plot, millet required on average a period of 70 and 34 days for the pre-anthesis and post-anthesis phase, respectively (Subsection 3.3.4). Dates of 50% flowering and physiological maturity varied among the plants by about 1-2 days.

The rate of phenological development can be affected by temperature and day length. In WIMISA, DVR is corrected by a temperature and/or day length dependent factor, as reported by Verberne et al. (1995). Such correction factors should be applied to DVR values, which are obtained under reference (controlled) temperature and day length conditions. In our experiments, however, the development of millet cultivar CIVT was observed in the field. On the other hand, the experimental and reference conditions must have been similar, because: Firstly, the critical day length for reduction of development rate in the pre-anthesis phase (DVR1) (> 13.6 h) was never achieved at the experimental site, since at ISC station photoperiodical day length varies between 12.1 and 13.6 hours during the rainy season (Sadoré: Fechter, 1993). Secondly, for the temperature, simulations not taking into account its effect on DVR resulted in a negligible acceleration of development. Consequently, our measurements could be treated as if obtained under reference conditions. The development rates computed from the experimentally determined development stages result in DVR1 = 0.0143 d^{-1} and DVR2 = 0.0294 d^{-1}. Slight adjustment of these values, i.e. DVR1 = 0.0141 and DVR2 = 0.0305, gave better agreement between simulated and measured aerial dry matter production and still a good fit for DVS (Fig. 5.7). These rates are of the order of magnitude of those reported by Fechter (1993: 0.015 and 0.033), Erenstein (1990: 0.014 and 0.025), and Verberne et al. (1995: 0.0143 and 0.0250).
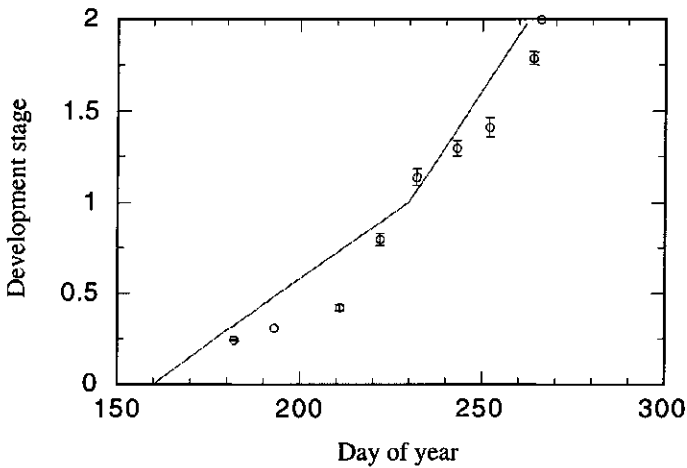
Figure 5.7   Phenological development of millet as simulated (line) with DVR1 = 0.0141 and DVR2 = 0.0305 and measured (dots) at ISC (1993). Bars show SE of means.

5.5.3   Assimilate partitioning

Assimilate partitioning among roots, leaves, stem, comb (panicle), reserves and grain changes with development stage. Partitioning coefficients to the various organs in dependence of DVS as reported in CP-BKF3 (Verberne et al., 1995; see Appendix B2)) were applied in WIMISA, because data from the Ziziphus plot showed a poor correlation between the fractional distribution of dry matter to the various organs and DVS. The latter is due to a high variability in growth and development of millet. It is commonly stated that the distribution of assimilates is, among others, cultivar-specific, i.e. it differs between short and long millet cycle cultivars. It is not known to which cultivar the partitioning coefficients reported by Verberne et al. (1995) refer, but simulation with these coefficients resulted in a fractional distribution of aerial dry matter that agrees reasonable well with observed values of the millet cultivar CIVT having a cycle of 90 - 120 days (Fig. 5.8). Consequently, they were applied as model input.
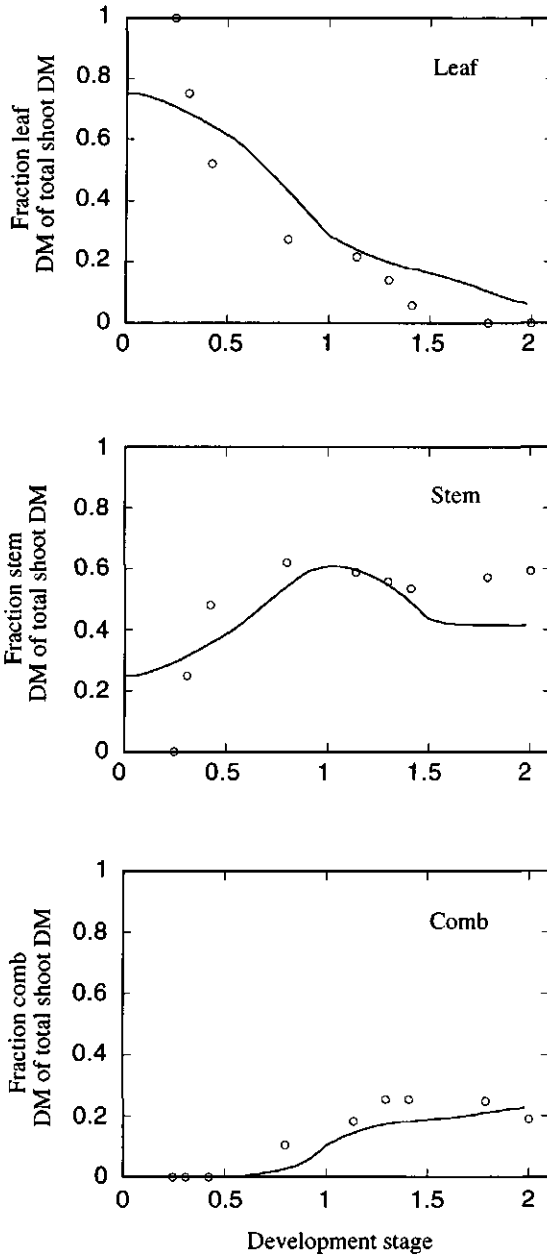
Figure 5.8   Simulated (line) and measured (dots) fractional distribution of aerial dry matter as a function of DVS. The reserves are assumed to be located in the stem.

5.5.4   Specific leaf area

Specific leaf area (SLA) is a very important crop parameter, as it determines the photosynthetically active leaf surface and thus directly affects assimilate production. The input parameter SLA (ha leaf kg^{-1} leaf) in dependence of DVS has been derived from a polynomial fit through the observed mean data of SLA (n = 10) as a function of mean DVS. With increasing development stage, specific leaf area decreased from 0.0022 at the beginning of the growing season to 0.0010 at the end (Appendix B2). These values are close to those (0.0024 - 0.0013) reported by Fechter (1993) for millet with a final total aerial dry matter of 5 to 6 t ha^{-1}. Erenstein (1990) also reported a decrease in SLA, but with higher absolute values (0.0035 - 0.0018). Furthermore, SLA is known to increase with decreasing light intensities (Terry et al., 1983) as leaf area is mainly determined by temperature: higher light intensities lead to more dry matter and hence to thicker leaves (Ong and Monteith, 1985, van Keulen, AB-DLO, pers. comm., 1997). This may be the reason for the slight tendency of highest SLA directly adjacent to Bauhinia (Subsection 3.3.3). However, the experimental data showed much variability, so that no clear distance effect on SLA could be established for incorporation in WIMISA.

5.5.5   Leaf longevity

Leaf age is defined in terms of a temperature sum of the daily mean temperature above a base temperature (10 °C). Leaf longevity (SPAN, °C d) sets the threshold value for leaf senescence of millet. During the experimental period of 1993 leaf life ranged from 20 to 49 days or in temperature sum 607 to 1022 °C d. Most frequently observed values were between approximately 800 - 855 °C d, and 800 °C d was used in WIMISA. In the model of Erenstein (1990) a SPAN of 890 °C d is applied for a short and long type millet, while in CP-BKF3 SPAN varies from 900 (short cycle millet: 90 days), and 1000 (cycle of 115 days) to 1100 °C d (long cycle millet: 140 days).

5.5.6   Roots

Potential root extension rate (RE_p) is important for simulation of root water uptake, because it determines the actual instantaneous rooted depth D. Since no root growth measurements were carried out, a RE_p of 4.5 cm d^{-1} and a maximum rooting depth of 220 cm were used, as reported by Bley (1990) and Azam-Ali et al. (1984), respectively. The value of 4.5 cm d^{-1} seems reasonable for RE_p, considering the values observed by other authors: 2 - 4 cm d^{-1} (Jansen and Gosseye, 1986 and ODA, 1987, cited by van Duivenbooden and Cissé, 1993), and 5 cm d^{-1} (Erenstein, 1990). Squire et al. (1987) found an average RE_p of 4.5 cm d^{-1} in the first

30 days of the growing season and a maximum extension rate of 7 cm d^{-1} as did Azam-Ali et al. (1984). The maximum rooting depth, although fixing the limit for vertical root extension, hardly affects simulated water uptake and production of millet, because root length is modelled to be concentrated in the upper 40 cm of the soil.

5.5.7   Millet height

Plant or more precisely crop row height (h_m, see Fig. 4.7) is only required for simulations including the windbreak effect shading. The height of each crop row determines, among others, whether it is shaded (Section 4.4). Light intensity, in turn, influences h_m. Therefore, input data were not derived from the Ziziphus plot, but from measurements at various distances from the Bauhinia windbreak in 1993 (Subsection 3.3.3). These values for h_m, incorporated as DVS-dependent variables, implicitly account for the shade by the experimental windbreak under the environmental conditions of the 1993 growing season. For general application, shading and drought (and lack of nitrogen) should be introduced as separate reduction factors for h_m. However, from the observed values, these factors could not be derived.

6 SIMULATION RESULTS and DISCUSSION

WIMISA was first calibrated for an unshielded millet field in Niger (Sections 6.1 and 6.2), and subsequently the selected parameter set has been applied to simulate and analyze the growth of millet growing behind a specific windbreak, i.e. characterized by orientation, height, porosity and root distribution (Section 6.3). Crop growth and soil water balance modules were tested versus the datasets of the WB-millet experiment of the cropping seasons 1992 and/or 1993 (Chapter 3), both wet years. Furthermore, the model was run for the dry year 1987. Model performance was examined in more detail by varying crop input parameters pivotal for plant growth (sensitivity analysis, Section 6.4). Performance of the model, possible improvements, application examples and the effects of windbreaks on competition for light and soil water as well as the effects induced by wind speed reduction are discussed in Section 6.5.

6.1   Calibration of the CROP module

Accurate prediction of growth characteristics of unshielded millet is a crucial requirement for a model intended to describe and analyze the response of that crop to WB effects. Therefore, CROP, the crop growth module of WIMISA, was calibrated for millet under the environmental conditions of ISC, Niger. Calibration was performed in two steps. First the available input values for site and cultivar specific parameters according to Chapter 5 were applied. However, the simulation results were overestimating the field observations (Fig. 6.2) and therefore, recalibration was necessary. Three problematic issues can be identified.

The main reason for WIMISA's overprediction in Figure 6.2 is that the present model simulates crop production under consideration of water limitation only, while under the experimental conditions nitrogen was obviously limiting, too. WIMISA does not (yet) relate assimilation and dying rate of plant organs to the actual nitrogen status of the crop, but the nitrogen concentration of the organs is fixed to their maximum values (Appendix B1). Hence, WIMISA does not simulate the effect of nitrogen limitation on crop growth.

The second point is a general problem of crop growth models. An enormous number of crop parameters, which depend on environmental and/or genetic characteristics, is needed to describe the (complex organization of) processes determining plant growth (van Keulen and Seligman, 1987). Ideally, all parameters should be introduced in the model as function of their

environmental/genetic response, either empirically or mechanisticly based. In practice, there is never enough data to achieve this (van Keulen and Seligman, 1987; Spitters, 1990) and so in WIMISA, water and nitrogen influences on parameter values are not always considered. This explains part of the poor simulation results presented in Figure 6.2.

A third issue is the high spatial variability in the experimental and in Sahelian fields in general (Brouwer and Bouma, 1997), which made it difficult to derive representative values for model parameters, and thus may also have contributed to the discrepancy between simulation and field data, but since that is difficult to assess, this last point was not further considered for recalibration of WIMISA.

To improve the accuracy of WIMISA simulations, the lack of a nitrogen module and the second issue are compensated through recalibration of direct and indirect responsible parameters. Their values, although sensitive to environmental factors, were not available for millet as function of environmental conditions in Niger. Therefore, these parameters were specified for three characteristic (production) conditions, which refer to the classification system for different production situations from de Wit and Penning de Vries (1982). Thus, for each of the three production levels a parameter value set is defined (Table 6.1):

- Potential production conditions of the Sahel (production level 1 = L1); The parameter set L1, derived from literature, was used to test general model performance (Subsection 6.1.2).
- Water limitation (production level 2 = L2) is the level for which the model was designed. WIMISA calibrated with data from the site (first calibration, Chapter 5) should reasonably simulate crop growth under water limitation (Subsection 6.1.3). The experimental dataset is refereed to as L2.
- Water and nitrogen limitation (production level 3 = L3) represent the conditions of the experimental site. Therefore, L3 parameter set was needed for accurate calibration (Subsection 6.1.4) and testing of simulation results of the windbreak-millet system (Subsection 6.3.1).

6.1.1   Potential production conditions of the Sahel

According to de Wit's classification (de Wit and Penning de Vries, 1982) potential production, or production level 1, is attained under optimum growth conditions with respect to water and nutrient availability, and in the absence of diseases and pests. Crop yield is then only determined by the type of crop, the level of irradiance, and the temperature regime (de Wit,

1986). Production level 1 (L1) for the Sahel is defined here as production under conditions of moderately to high fertilizer application and relatively high rainfall.

Table 6.1   Suggested sets of parameter values for simulation of production levels 1, 2 and 3: initial biomass (DM_0), maximum relative death rate of leaves (PERDL), leaf longevity (SPAN), specific leaf area (SLA) and initial light use efficiency (LUE).

Production level	Input parameter				
	DM_0	PERDL	SPAN	SLA	LUE
	kg ha^{-1}	d^{-1}	^oC d^{-1}	m^2 kg^{-1}	kg CO_2 ha^{-1} h^{-1}/J m^{-2} s^{-1}
L1-F[1]	30	0.03	1000	0.0024 - 0.0013	0.40
L1-E[2]	30	0.03	1000	0.0035 - 0.0018	0.40
L2	30	0.05	800	0.0022 - 0.0010	0.38
L3	16	0.05	800	0.0022 - 0.0010	0.38

[1] SLA values reported by Fechter (1993) for CIVT in Tara, Niger. [2] SLA values found by Erenstein (1990) for short and long cycle millet in the 5th region of Mali.

In the Sahel, under such conditions, maximum total aerial dry matter production for millet is reported to range from 6 t ha^{-1} under moderate fertilization (Fechter, 1993: Tara, 604 mm in 1990; Bley, 1990: Sadoré, 692 mm in 1988) to 12 t ha^{-1} under high fertilization (van Duivenbooden and Cissé, 1989: Nioro du Rip, 917 mm in 1988). In the windbreak-millet and Ziziphus field experiment, the production conditions were below potential, as indicated by the realized total yields of approximately 2 ton ha^{-1} (Section 3.3), well below the above mentioned maximum production. Consequently, the experimentally determined values for input parameters were obtained under water and/or nitrogen-limited conditions and, hence, not appropriate for calculation of potential production in case that they are sensitive to water and/or nitrogen deficiency.

Nitrogen and water limitations may lead to reduced leaf area and, under more severe stress, leaves die earlier than under adequate supply of these resources (van Keulen and Seligman, 1987). Hence, we found experimentally a leaf longevity (SPAN) of 800 ^oC d instead of 1000 ^oC d as applied in CP-BKF3 for a medium duration millet cycle of about 115 days (Verberne et al., 1995) (Table 6.1). Some authors (Aase, 1978; Spiertz and Sibma, 1982, cited in van Keulen and Seligman, 1987) reported that the specific leaf area (SLA) is rather invariant. However, when water and nitrogen shortage via reduction in transpiration leads to loss of turgor, not only leaf weight, but probably also SLA decreases due to thicker leaves (Spitters,

1982). That this could be true is indicated by the somewhat higher SLA found by Fechter (1993) for the same cultivar (CIVT) under presumably better growth conditions than in our experiment (higher final yields) (Table 6.1). Erenstein (1990) and van Duivenbooden and Cissé (1989) found even higher SLA values (for different cultivars) than Fechter. Furthermore, Fechter (1993) reported for the initial light use efficiency (LUE) a value of 0.40 instead of 0.38 kg CO_2 ha^{-1} h^{-1}/ J m^{-2} s^{-1} as applied by Verberne et al. (1995).
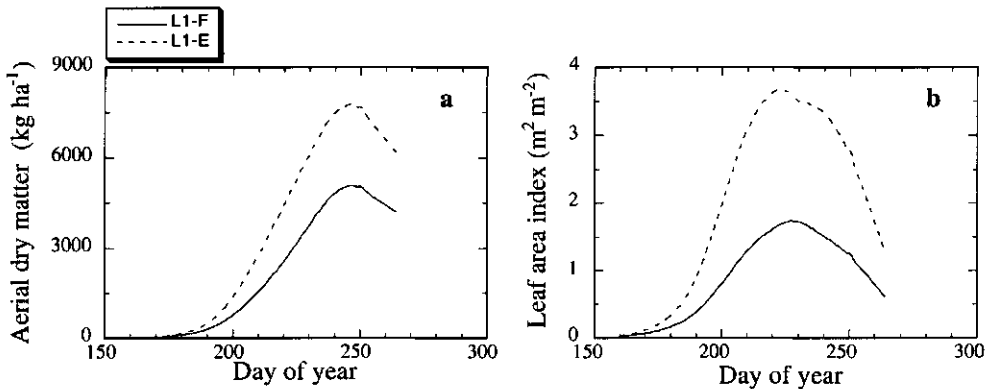
Figure 6.1   Simulated potential millet production in the Sahel, L1-F and L1-E for the cropping season of 1993, ISC, Niger: a) total aerial dry matter and b) LAI.

These higher values for LUE, SLA and SPAN in combination with an initial biomass (DM$_0$) of 30 kg ha^{-1} and the weather data of 1993 with high (542 mm) and well distributed rainfall were used in the WIMISA simulations to approximate potential millet production, L1. The parameter set including SLA values found by Fechter is noted as L1-F and the set with SLA values derived from Erenstein is noted as L1-E (Table 6.1). Using L1-F in WIMISA, the results (Fig. 6.1) were close to those from SWASUC (Fechter, 1993) and CERES-Millet (Godwin et al. 1984, Jones et al. 1986) for moderate fertilizer and soil tillage: Simulated total aerial millet production was 5.7/ 6 and 5.8/ 7.6 t ha^{-1} for SWASUC/ CERES for 1989 and 1990, respectively in Tara, Niger. Corresponding simulated LAI (leaf area index) values were 2.2 / 1.8 and 2.1 / 2.6, respectively. Plant density in the Fechter experimental and simulation study (33,333 plants ha^{-1}) was a bit higher, explaining the higher yields and LAI he found. For several highly fertilized locations in Mali, simulation with the Erenstein millet model (SUCROS-like) for a short cycle millet type and 550 mm rainfall yielded 8 - 9 t ha^{-1} total aerial production (Erenstein, 1990) which is close to the simulation result of L1-E .

6.1.2   Water limited production

WIMISA, designed to simulate millet growth at production level 2, was calibrated using data of the Ziziphus-CR plot experiment in 1993 (Section 5.5) with respect to crop development, SLA, leaf longevity (SPAN, PERDL), initial biomass (Table 6.1: L2), and grain number. The model calibrated in this way, substantially overpredicted total aerial production and LAI (Fig. 6.2). This is not surprising, since there is evidence that the crop in the Ziziphus-CR plot, as in all other experimental plots without crop residues (-CR), suffered from nutrient stress (Chapter 3): plots with crop residues (+CR) showed a 32 % higher production of aerial dry matter compared to plots without crop residues (Michels, 1994). Obviously, the applied crop residues alleviated (some of) the constraints for growth. For example, applying crop residues will increase the availability of nutrients, reduce soil evaporation and soil temperatures (Unger et al., 1991) and protect the crop against sand storms (abrasion, covering by sand). Under the environmental conditions during the two experimental years, it is likely that the main advantage of crop residues was that of improved soil fertility, as supported by results of Bley (1990). He found similar millet production for trials with fertilizer and without crop residues (-F+CR) and vice versa (+F-CR) for the dry year 1987 and the wet year 1988.
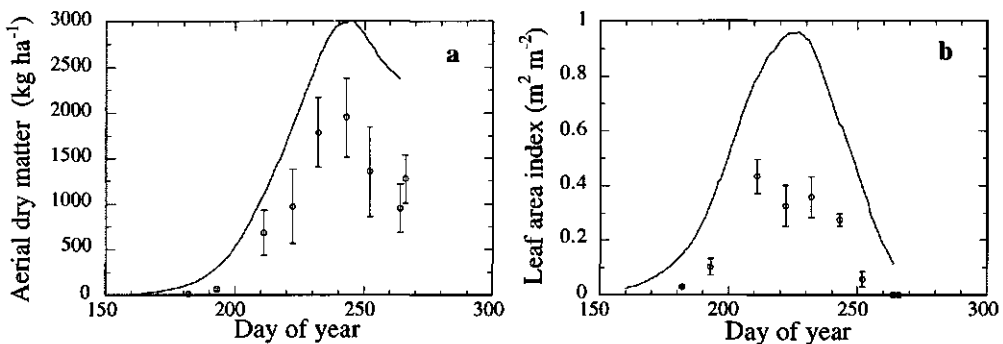
Figure 6.2   Simulated (line) and measured (Ziziphus plot, dots) total aerial dry matter (a) and LAI (b) for the cropping season of 1993, ISC, Niger. Simulation for water limited growth conditions (L2). Bars show standard error of means.

In the simulation, total aerial biomass was overestimated by about 35%, i.e. comparable to the earlier mentioned difference between -CR and +CR plots in the WB-millet experiment by Michels (1994). This suggests that WIMISA using L2 is suitable to estimate millet growth under conditions of water limitation at ISC in 1993.

6.1.3 Water and nitrogen limited production

To account for nitrogen deficiency without incorporating nitrogen processes in soil and plant, the input value for initial biomass was systematically decreased till simulated and observed data corresponded for the growing season of 1993. An initial biomass (DM_0) of 16 instead of 30 kg ha^{-1} showed good agreement (Fig. 6.3). This approach does not explain the effect of the growth limiting factor on the processes determining gross assimilation, e.g. initial light use efficiency, assimilation rate, assimilate distribution and leaf senescence, but results in a realistic reduction in growth rate and final production. In the field, growth constraints during the early growing season such as nitrogen shortage reduce the initial growth rate of plants, which in turn decrease the development of biomass and LAI. Slower development of LAI delays the onset of maximum growth rate and assimilation per m^2 soil resulting in a decrease in production at final harvest when the duration of the growing season is not extended to a similar degree. The latter rarely is the case in the Sahel where the growing season is generally short (Chapter 1). Hence, in the model, growth and yield reduction due to nitrogen deficiency (that means a reduction in growth rate) can be approximated by decreasing the DM_0 to a certain degree. This type of correlation is revealed in studies on the effect of plant densities (corresponding to a certain DM_0) on growth pattern with time (Spitters, 1982). Note, that if DM_0 would have been derived from measurements (instead of from observed plant density under optimum conditions), the value probably would have been lower than 30 kg ha^{-1}.

Results of simulation with $DM_0 = 16$, reproducing the actual crop growth in the Ziziphus plot in 1993, are shown in Figure 6.3 together with the field observations under water and nutrient deficient conditions of 1993 (Table 6.1: L3). The correspondence between field observations and simulation was good, considering the generally high spatial variability of millet production, typically for poor sandy soils in the Sahel. Generally, living and not total dry matter is presented in Figure 6.3, because measured values of living biomass were more accurate than those of total biomass, since dead plant material once fallen from the plant was quickly decomposed on the hot sand. For the Ziziphus plot grain yield was not measured by mistake. However, as the harvest index (HI) computed from simulation results was close to the HI given by Ong and Monteith (1985) for the rainy season of the Sahel, and to HI values found in other trials at ISC (Fechter, 1993; Bley,1990), grain yield appeared to be reasonably well estimated by WIMISA .

Simulated aerial dry matter agreed well with the field measurements with the exception of the early season and final harvest (Fig. 6.3a). The simulated maximum value of 1997 kg living DM ha^{-1} (2302 kg total DM ha^{-1}) was close to the measured 1952 kg living DM ha^{-1} (2230 kg total DM ha^{-1}) in the Ziziphus plot. The agreement between simulated and measured stem weight,

including reserve dry matter, was excellent from DOY (day of year) 210 onwards (Fig. 6.3b), when compared with simulated total stem weight and living stem weight for the middle and late growing season, respectively. In the field measurements, no distinction has been made between dead and living stem material during the intermediate harvests. Therefore, for the mid-growing season, when part of the stem was already dead but still on the plant, the simulation results must be compared with simulated total stem dry matter. Comparison of simulated and measured leaf weight shows that the simulated results were generally overestimated but the maximum value was within the error range of the observations (Fig. 6.3d).

Table 6.2 Simulated and observed harvest indices (HI). L1-E, L2, L3 give the parameter set used for simulation with WIMISA (Table 6.1). L2* and L3* denote experiments with high and low fertilized fields, respectively.

Source	Aerial dry matter (kg ha⁻¹)	Grain yield (kg ha⁻¹)	HI
Simulated			
WIMISA L1-E (1993)	8330	1761	0.21
WIMISA L2 (1993)	3521	751	0.21
WIMISA L3 (1993)	2300	521	0.23
Observed			
Bley (ISC, 1987) L2*	3953	777	0.20
Bley (ISC, 1987) L3*	1647	369	0.22
Bley (ISC, 1988) L2*	6018	883	0.15
Bley (ISC, 1988) L3*	2958	448	0.15
Fechter (Tara, 1989) L2*	4390	1241	0.28
Fechter (Tara, 1990) L2*	5988	1535	0.25

The pattern of LAI development was simulated well, but the absolute value was overestimated for most of the time (Fig. 6.3c). Similarly, dry matter weights of leaves, stems and shoot were overestimated in the early growing season. However, from DOY 210 onwards stem and total aerial dry matter were simulated satisfactorily and leaf biomass was simulated reasonably accurately. Thus, the overestimation of LAI is not always reflected in higher dry matter production, probably due to simultaneous parameterisation of compensating processes (e.g. a low LUE in combination with other factors that enhance SLA). This is an example of the consequences of poor understanding of the sensitivity of certain parameters to environmental factors. After DOY 250 the simulated values of LAI were higher than measured, partly due to the initially slightly underestimated dying rate of leaves after flowering (ca. DOY 230). Another

reason is the underestimation of living green area in the field: small green parts of mainly brown leaves could not be measured for technical reasons.
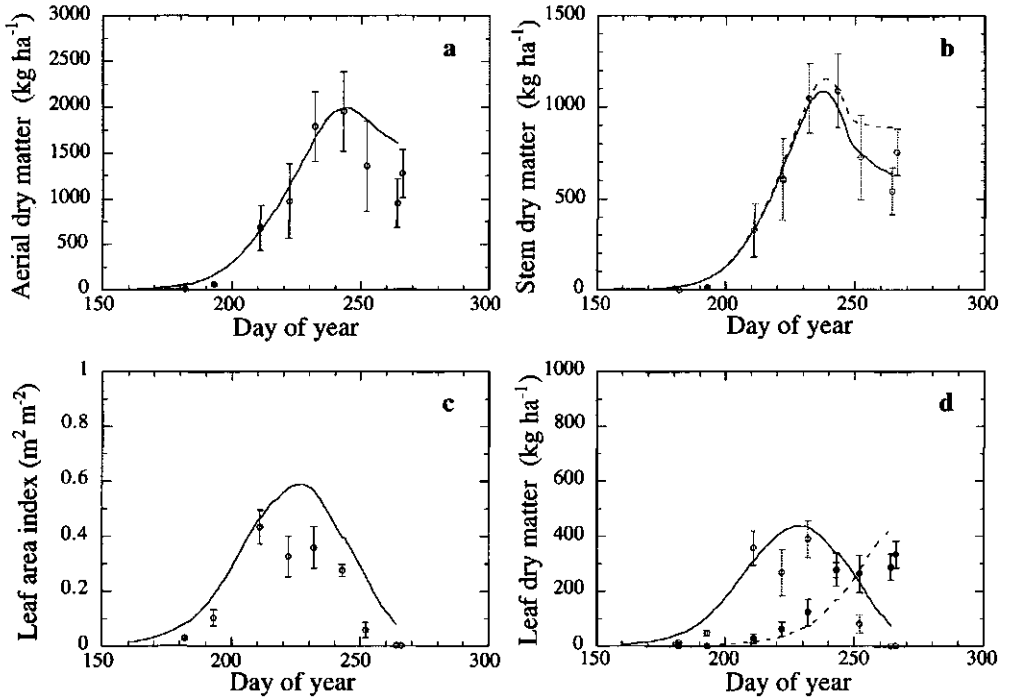
Figure 6.3   Simulated and measured (Ziziphus plot) living aerial dry matter (a), living stem dry matter (solid line) and total stem dry matter (dotted line) (b), LAI (c), and green leaf weight (solid line) and dead green weight (dotted line) (d) for the cropping season of 1993, ISC, Niger. Simulation for water and nutrient limited growth conditions (L3). Bars show standard error of means.

Various approaches to simulate LAI of cereals exist (Meinke, 1996). Most of them poorly simulate LAI (Fechter, 1993) and/or have poor general applicability (Meinke, 1996), among others because their sensitivity to environmental conditions is insufficiently understood or unknown. A method that avoids sensitive feedback, by using conservative parameters (Meinke, 1996), improved the prediction of leaf area of wheat and could be successful for many other cereals including millet. Accurate simulation of low LAI, is in particular problematic. Goudriaan (1977) as well as Kropff and van Laar (1993) developed an approach that improved the simulation for LAI < 1 (see Section 6.5). A simple correction for such cases was applied by van Duivenbooden and Cissé (1989).

Despite poor prediction of LAI, WIMISA using the L3 parameter set was suitable to estimate the unshielded millet production under the experimental conditions of the Ziziphus plot in 1993. Thus, the calibrated crop module appeared to be suitable for application in a windbreak-millet system model.

6.2   Calibration of the SOIL WATER module

The soil water module was calibrated using values for soil water parameters (θ_i, θ_f, and θ_{wilt}, K_{sat}) characteristic for the soil at ISC as given in Section 5.4. Simulated seasonal water content of the soil followed the course and level of the data measured at a distance of 10 m from the windbreak in 1993 (Fig. 6.4). In some periods the model slightly underestimated volumetric soil water content (θ_v) at depths of 0.4, 0.7 and 1.0 m. Overestimation of LAI contributed to a lower simulated θ_v. The differences in simulated and field data appear to be too small to affect the simulation of crop growth. The discrepancies in θ_v at a depth of 1.9 m were also unimportant for the results of crop growth simulation, since root water uptake is concentrated in the first 0.4 m below the soil surface. At 1.9 m depth, θ_v was underestimated by approximately 0.01- 0.02 m^3 m^{-3} until DOY 235. Thus, after the dry season soil moisture at 1.9 m depth was replenished in the field faster than estimated by WIMISA. The reason is that, in the model, redistribution of water in the lower layers is delayed by large soil cell thickness (Subsection 4.6.4).

Redistribution of water within the soil profile is highly dependent on conductivity at saturation (K_{sat}), which moreover, determines the water content of the entire rooting zone. This is illustrated by comparison of simulation with a low (adopted from Bley, 1990) and a high value for K_{sat} (Figs. 6.4 and 6.5): Simulation with $K_{sat} = 1.7*10^{-4}$ m s^{-1} instead of $K_{sat} = 8.0*10^{-5}$ m s^{-1} resulted in a somewhat higher transport to the top soil, increasing soil evaporation, as well as higher flow downwards, possible increasing deep percolation. Hence, a high K_{sat} reduced total water content for the soil profile. The process of redistribution was simulated more accurately with the semi-deterministic WIMISA than with the parametric CP-BKF3 soil water module, as illustrated in Figure 6.6. Fechter et al. (1991) also found better results from the deterministic module SWATRER (Dierxks et al. 1986) than from the parametric model CERES-Millet (Godwin et al. 1984, Jones et al. 1986).
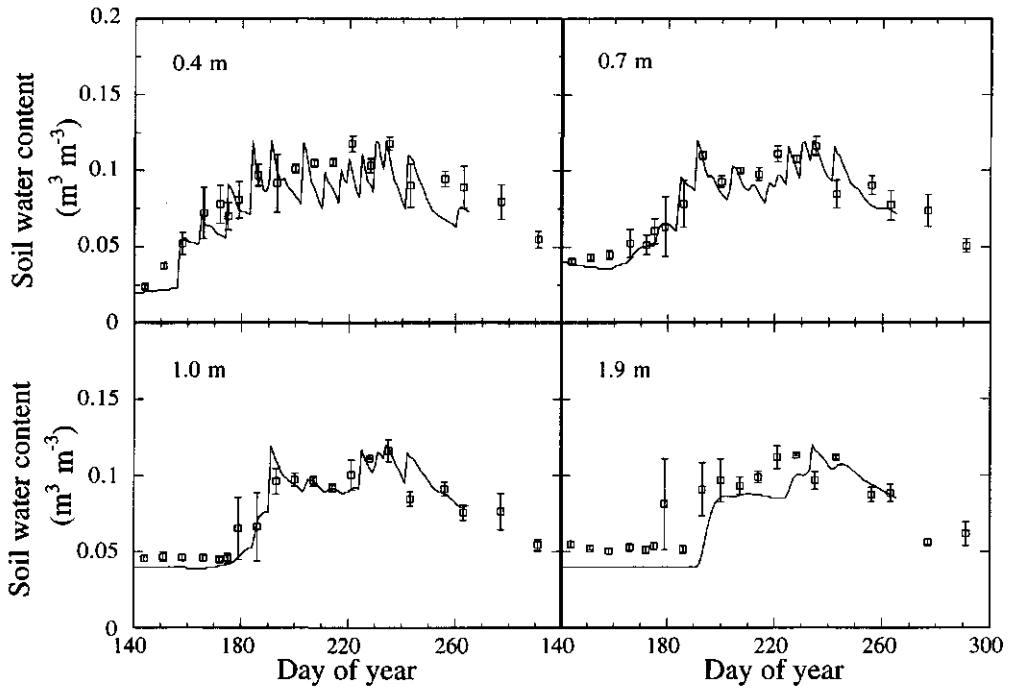
Figure 6.4   Simulated (line) and measured (dots) volumetric soil water content (θ_v) at 0.4, 0.7, 1.0 and 1.9 m soil depth for $K_{sat} = 8.0*10^{-5}$ m s^{-1} at ISC, Niger, 1993. Measurements refer to a distance of 10 m from the windbreak. Bars show standard error of means.
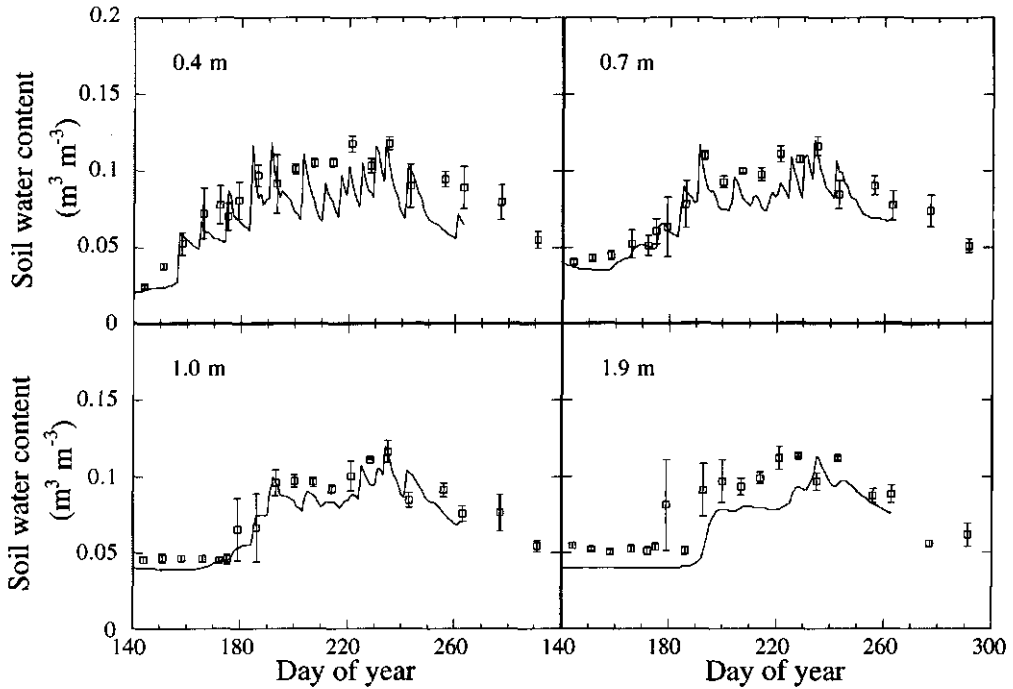
Figure 6.5 Simulated (line) and measured (dots) volumetric soil water content (θ_v) at 0.4, 0.7, 1.0 and 1.9 m soil depth for $K_{sat} = 1.7*10^{-4}$ m s^{-1} at ISC, Niger, 1933. Measurements refer to a distance of 10 m from the windbreak. Bars show standard error of means.
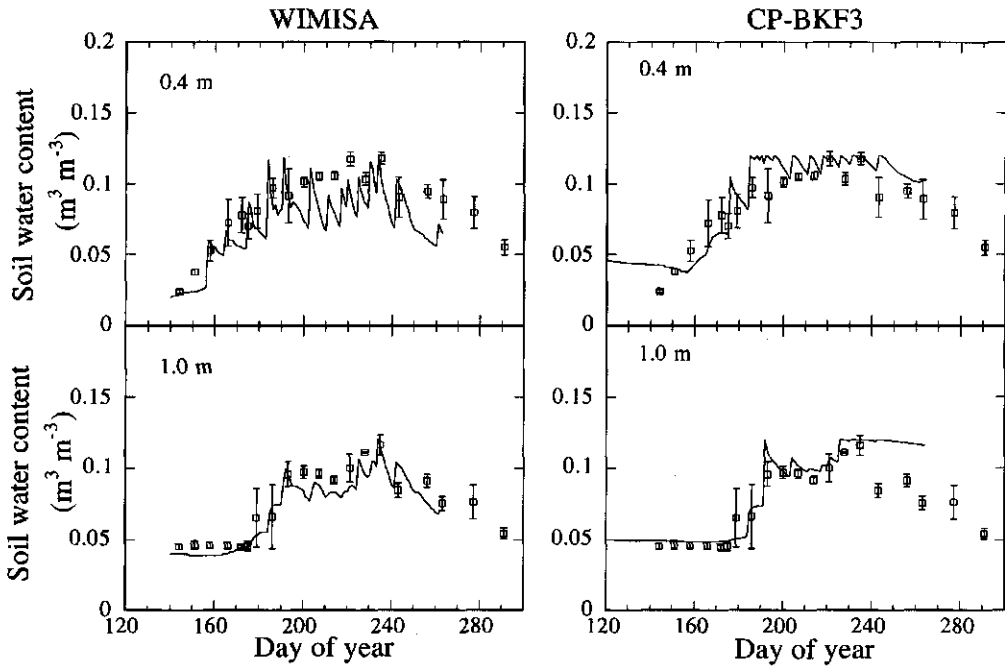
Figure 6.6   Volumetric soil water content measured (dots) and simulated (line) with
WIMISA and CP-BKF3, a parametric model with daily time steps, at ISC,
Niger, 1993. Measurements refer to a distance of 10 m from the windbreak.
Bars show standard error of means.

WIMISA results of seasonal water balance components for the Sadoré soil in 1993 are
compared to simulation results from SWATRER for soils in Sadoré (Bley, 1990) and Tara
(Niger, Fechter, et al., 1991) (Table 6.3), since field data on those components of the present
experiment are lacking. SWATRER was calibrated and evaluated on the basis of studies on soil
hydraulic conductivity, soil moisture retention, actual soil evaporation, stomatal conductances
and computed actual transpiration (Penman-Monteith). For both sites SWATRER accurately
simulates the dynamics of soil water content (Bley,1990; Fechter et al., 1991).

The soil water partitioning of WIMISA showed that about 52 % of the seasonal rainfall (=
infiltration) leaves the system through evapotranspiration, which is in the range of 30 - 65 %
reported for the Sahel (Bley et al., 1991; Payne et al., 1991c, Wallace, 1991, Rockström et al.,
1997). As expected, at low crop LAI (< 1) and hence, low soil cover the main part is lost by
evaporation from the soil surface (E_a), whereas at high LAI transpiration (T_a) is the major part
of total evapotranspiration. Further losses from the soil system occurred through deep

percolation (D). WIMISA results on cumulative E_a, T_a and D in relation to LAI and rainfall were assumed to be reasonable since they are similar to results of SWATRER, which were tested against field data (Bley, 1990).

Table 6.3   Soil water balance simulated with WIMISA and SWATRER for millet fields in the Sahel during the rainy season. Results from SWATRER were derived from Bley (1990) and Fechter et al. (1991). The soil profile in WIMISA comprises 7 m while that in SWATRER had a depth of 2 m. DOY is day of year and DAS is days after sowing.

Model, Year, Production level	Rainfall (mm)	E_a[1] cumulative (mm)	T_a[2] cumulative (mm)	T_p[3] cumulative (mm)	LAI max	D[4] cumulative (mm)	Change soil water (mm)
WIMISA (Sadoré		DOY 140 -	DOY 265)				
1993: L 3	532.2	234.4	45.5	45.9	0.59	8.1	252
L2	532.2	194.2	71.8	72.1	0.96	9.7	257
L1-F	532.2	135.8	122.3	123.7	1.73	11.4	262
L1-E	532.2	76.0	205.96	212.5	3.67	9.7	239
SWATRER (Sadoré		DAS 1 -	DAS 98)				
1986:L 3	535.9	180	72.9	72.9	0.69	170.7	146.1
L 2	535.9	177.1	137.2	137.2	0.84	132.7	93.2
1987: L3	411.8	143.9	94.1	105.2	0.68	110.5	84.5
L 2	411.8	136.3	178.1	210.7	1.45	65.1	49.7
1988: L3	613.2	169.8	92.9	92.9	0.83	251.8	153.3
L2	613.2	132.1	227.7	227.7	2.45	156.8	132.9
SWATRER (Tara		DOY 176 -	DOY 285)				
1989: L2	493	168	151	165	2.2	94	80

[1]Actual evaporation, [2]Actual transpiration, [3]Potential transpiration and [4] Deep drainage below 2 m and 7 m, for SWATRER and WIMISA, respectively.

Early in the growing season when LAI was almost zero and the soil had been recently wetted by rain, WIMISA estimated a maximum E_a of 7 mm d^{-1}, which then falls off towards the end of the cropping season till approximately 1.0 mm d^{-1} (Appendix B3). An E_a of 7 mm d^{-1} is high compared to the highest actual evaporation rates reported by Bley (1990) and Wallace et al. (1993) of about 2.5 mm d^{-1}. In both cases, rainfall occurred the night before the evaporation measurements, hence, water that evaporated between the time of rainfall and measurements was lost and not included. Others found higher values too, e.g. Fechter (1993) found 4.2 mm d^{-1}

and Hall and Dancette (1978) measured for soils in Senegal a maximum evaporation rate of 5 mm d^{-1}. Stroosnijder and Hoogmoed (1984) reported for the Sahel that the average daily evaporation over the growing season decreases from 2.5 mm d^{-1} for a bare soil to 1.5 mm d^{-1} for a soil with a vegetation cover characterized by LAI = 1. Overall, WIMISA evaporation rates appear to be realistic.

In agreement with Bley's data, daily T_a increased with production level, i.e. with LAI from about 1.2 to almost 4 mm d^{-1} in a wet year (Appendix B3). On a seasonal scale, WIMISA simulated a ratio of T_a/ LAI which is lower than that from SWATRER-Sadoré, but similar to results from SWATRER-Tara (Table 6.3). T_a was about 8 and 13 % of infiltrated water for L3 and L2, respectively, which agrees with estimates from the model SOIL (Alvenäs and Jansson, 1997) for non-fertilised and fertilised millet in the Sahel, Niger (Rockström et al., 1997). In years with high rainfall (> 500 mm) all simulations predicted a T_a that was equal or close to T_p. This suggests little water stress for unshielded millet. It must be noted that under conservative water scarcity T_a /T_p becomes 1 because of the feedback between LAI and T_p.

WIMISA simulates drainage at a depth of 7 m below the soil surface, whereas SWATRER models it a depth of 2 m. Consequently, WIMISA results for D are much lower than those of SWATRER (Table 6.3). When WIMISA computations are confined to the upper 2 m of the soil profile, seasonal changes in soil water content were in the order of increasing production level 85 (L3), 82 (L2), 77 (L1-F), and 70 (L1-E) mm. These values represent root zone water storage and approach simulations from SWATRER. For a given annual rainfall, moisture storage in the rooted profile decreases with increasing LAI as a consequence of higher transpiration per soil unit area. WIMISA and SWATRER results on seasonal D just below the root zone show that drainage is substantial (supported by Rockström et al., 1997) and not negligible as sometimes reported for Sahelian soils in a dry year or when runoff occurs (Stroosnijder and Hoogmoed, 1984: they had runoff in millet fields with topsoil susceptible to crust formation) supporting the idea that seasonal soil water is not the growth limiting factor in the Sahel when rainfall exceeds 500 mm (Bley et al., 1991; Fechter et al., 1991). Unfavourable rainfall distribution over time explains why a crop used such a small proportion of seasonal available water and why deep percolation was high. This is nicely illustrated by the SWATRER estimates of water partitioning (D, T_a) and LAI for the unfavourable cropping season of 1986 and the more favourable (although drier) year 1987 in terms of rainfall distribution.

The correspondence of measured and calculated θ_v, and the reasonable agreement between simulated fractional soil water distribution of the WIMISA soil water balance and simulation results from SWATRER, indicate the ability of WIMISA to describe adequately the soil water dynamics of a millet field for the conditions in southwest Niger.

6.3   Windbreak-millet system

In this section simulation results on tree-crop interactions are presented. First the overall effect of these interactions (i.e. local conditions of radiation, soil water and wind speed) on crop yields are shown (Subsection 6.3.1). Then WB effects on soil water (Subsection 6.3.2) and microclimate (Subsection 6.3.3) are discussed in detail. Finally, the reasoning for competition between trees and crops is analyzed for two wet and one dry year (Subsection 6.3.4). For simulations, the geometric arrangement of the windbreak-millet model system mimics the experimental windbreak-cropping design (Fig. 4.4), i.e. the crop was growing westwards to the north-south oriented windbreak, having a height of 2 to 3 m and a porosity of 0.9 and 0.2 at the beginning and end of the rainy season, respectively. The distance between and within crop rows was 1 m, which was also the distance between the first crop row and the outer tree trunk of the windbreak. Thus, distance from windbreak expressed in m equals crop row number. Both notations are used in the following text. As in Part A (crop) rows refer to crop lines parallel and transects refer to lines perpendicular to the windbreaks. The tree-crop interface enclose a region of 10 m (5 H) from the windbreak.

6.3.1   Crop yields

The model was evaluated with data from +CR and -CR plots of Bauhinia using simulation runs of production level 2 and 3, respectively, both for the 1992 and the 1993 growing season. Simulated straw and grain yield showed an asymptotic course with distance from the windbreak in 1992 (Fig. 6.8) and 1993 (Fig. 6.7). Directly adjacent to the shelter, i.e. at 1 m, the production is much lower than at 10 m, where competition is supposed to be virtually absent. In the field, biomass production varied along the transect perpendicular to the Bauhinia windbreak, nevertheless there was a clear tendency of an increase in yield with distance from the windbreak, with the exception of millet straw in -CR plots in 1993.

Measurements and simulation
For the 1993 growing season the simulated straw production was substantially overpredicted. Measured values for straw dry matter were about 50 % lower than simulated values (Fig. 6.7a, c). Two reasons have to be mentioned for this discrepancy. First, as mentioned in Section 6.1, plant material that had died long before maturity, especially leaves, was already decomposed by the time of the final harvest. From measurements it appeared that about 30 % of dead leaves were decomposed by the time of final harvest. When simulated values of straw dry matter were reduced by the amount of decomposed dead leaf biomass (Fig. 6.7a: L2 corrected) the agreement between simulation and measurements became somewhat better. Secondly, the crop had been attacked by stem-boring caterpillar (*Coniesta ignefusalis*) and millet head caterpillar (or

millet head-miner moth *Heliocheilus* (=*Raghuva*) *albipunctuella*). The latter reduced grain yield, therefore, potential values of grain yield, estimated on the basis of cob/grain ratio of the un-affected panicles are given in Figures 6.7b and d. Simulation of grain yield was reasonable for the zone of 4 ~ 10 m from the windbreak for both production levels.

For the 1992 growing season the agreement between simulated and field data was much better, but still somewhat overestimated for the straw dry matter even after correction for decomposed leaves. (Figs. 6.8a, c). Grain yield was simulated well for the first three m from the windbreak, but beyond crop row 3 WIMISA underestimated grain yield (Figs. 6.8b, d).
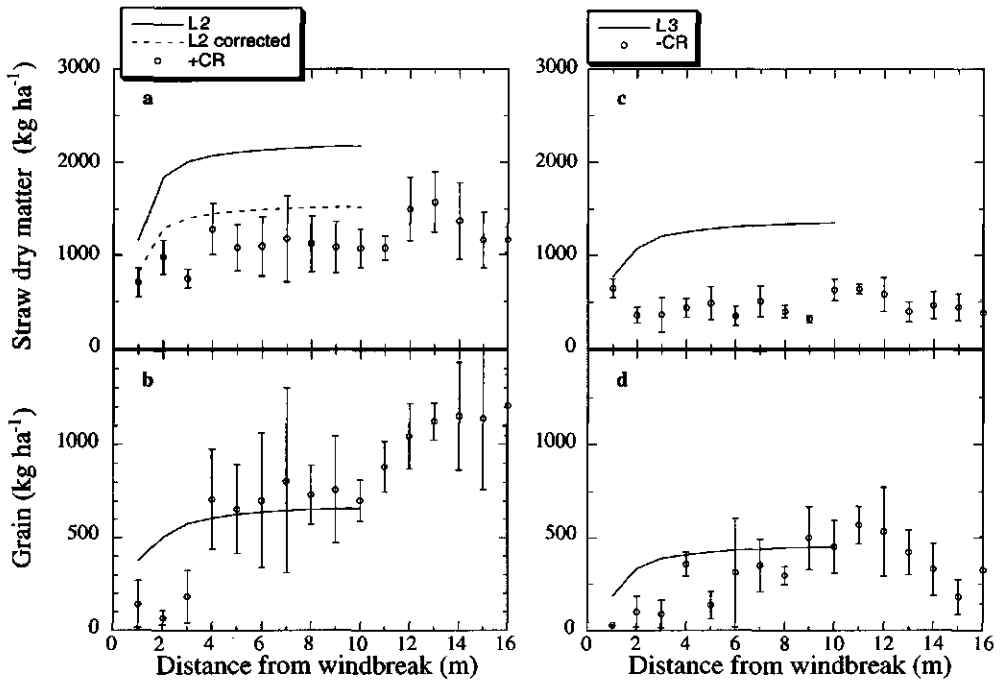
Figure 6.7   Simulated (line) and measured yield (dots) at two production levels (where L2 ≈ +CR and L3 ≈ -CR) as a function of distance from the windbreak in 1993, ISC, Niger: (a, c) straw yield and (b, d) grain yield. Bars show SE of means.
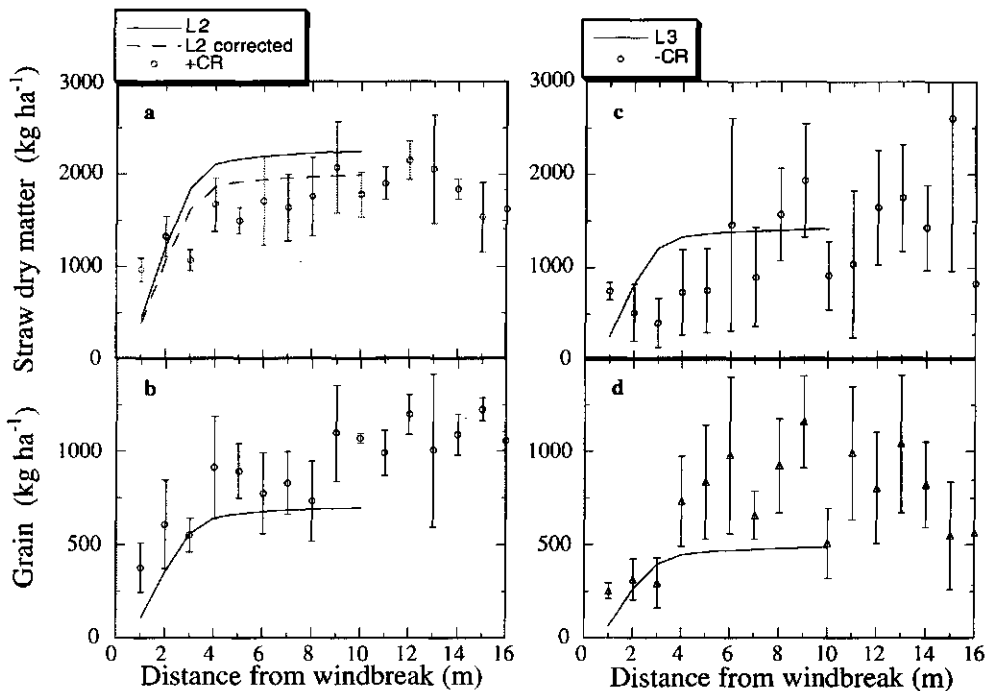
Figure 6.8   Simulated (line) and measured yield (dots) at two production levels (where L2 ≈ +CR and L3 ≈ -CR) as a function of distance from the windbreak in 1992, ISC, Niger: (a, c) straw yield and (b, d) grain yield. Bars show SE of means.

It is surprising that WIMISA overestimated straw dry matter but underestimated grain yield, since the model showed reasonable HI values for unshielded millet (Table 6.2). To check the reasoning behind this discrepancy and to test the estimation of grain yields adjacent to windbreaks the following was done: 1) The best fit between simulated and measured datasets was selected for straw dry matter (since the model was not calibrated for grain yield) (Fig. 6.9). Simulation results of production level L3 (should be comparable with -CR) corresponded best to straw dry matter averaged per row over all Bauhinia plots (+CR and -CR, i.e. all) and Bauhinia +CR plots for 1992 and 1993, respectively. 2) These combinations were then compared for simulated and measured grain yields: Figure 6.10 shows a good agreement between simulation and observations for the first three crop rows but underprediction beyond crop row 3. Assuming that HI is simulated accurately, we can now draw the conclusion that WB effects other than competition, which are not modelled, were influencing grain yield beyond 4 m from the WB barrier. In 1992, straw seemed also to benefit from the windbreak at a further distance (9, 10 m). Obviously, beyond 3 m the windbreak ameliorated the growth of

grain but to a lesser extent and beyond a further distance the vegetative production in 1992. Whether this windbreak benefit may outweigh yield reduction from competition or even results in an overall increase in grain production in relation to unshielded fields and whether vegetative or generative crop growth is influenced mainly by the shelter are discussed in Chapter 3.
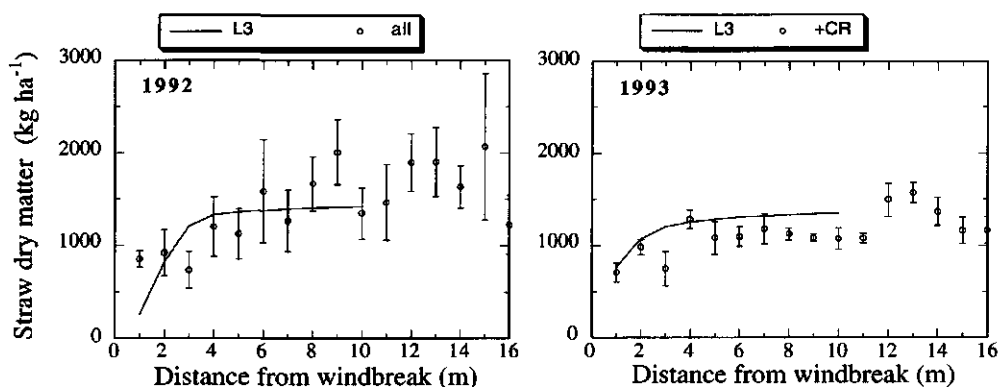
Figure 6.9   Best fit of simulated (line) and measured straw (dots) dry matter adjacent to the windbreak for the growing season of 1992 and 1993, ISC, Niger. Bars show SE of means.
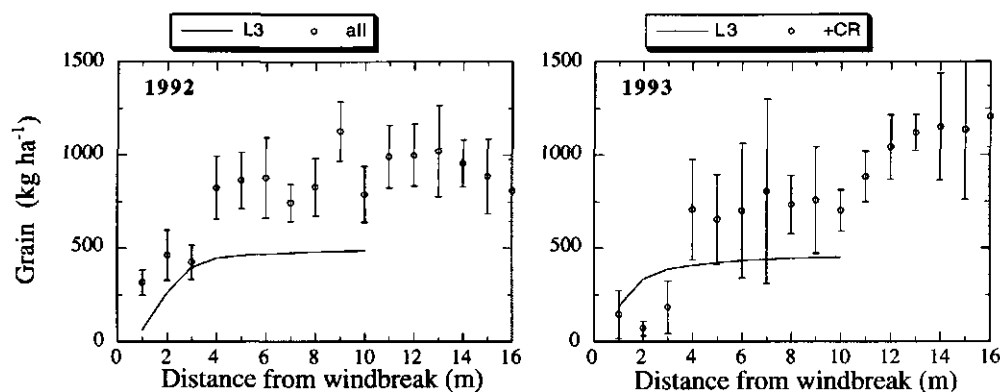
Figure 6.10   Grain yield as a function of distance from the windbreak: Comparison of simulated results of production level L3 (line) with row averages of all Bauhinia plots and Bauhinia +CR plots for 1992 and 1993 (dots), respectively, ISC, Niger. Bars show SE of means.

Yields in the tree-crop interface

WB effects on millet production in the tree-crop interface are correlated in this chapter with respect to yields at 10 m from the windbreak. At this distance (10 m equals 5 and 3.3 H for the beginning and end of the growing season, respectively) competition effects generally are negligible (Kort, 1988; Brenner et al., 1993); and yield decreases due to sudden enhanced turbulence and evaporation are reported to occur beyond 5 H (McNaughton, 1988; Brenner, 1995a, Onyewotu et al., 1994). Furthermore, in our experiment yield increases (probably due to beneficial microclimatic conditions) occurred at a lower or further distance than 10 m (Section 3.3).

In the first crop row of the tree-crop interface, millet production was considerably reduced compared to 10 m from the windbreak (Figs. 6.7 and 6.8), varying from 28 to almost 90% for WIMISA results in both seasons. Simulated yield reduction differed more between years than between production levels, suggesting that radiation intensity or rainfall distribution, rather than total amount of available water and nitrogen were limiting growth. Simulated yield reductions in the first 2 m were much higher in 1992 (ca. 65%) than in 1993 (23 - 42%), although the total seasonal rainfall and nutrient status of the soil in both years were comparable. Measurements showed also a higher straw reduction for the first 2 m in 1992 (ca 44%) than in 1993 (ca 27%), but the opposite was the case for the observed grain yields.

Yield reductions were always most severe in the zone 1 - 3 m from the windbreak and they were higher there for grains than for straw, in particular in the first crop row. Simulated reductions showed a steady decline with distance, whereas in the field the second or third row showed sometimes higher reductions than the first or second one, due to high spatial variability in physical and chemical soil properties possibly in combination with WB effects that might, although not visible, have influenced crop growth. Hence, it is misleading to quantify observed yield reductions per row. Yield reductions in the field were more consistent when averaged over the zone 1 - 3 and 4 - 9 m from the windbreak and normalized with respect to the average yields of row 10 to 12 m. These normalized experimental yield reductions are compared with simulated yield reduction averaged over the same distances and normalized to 10 m from the windbreak for data of the 1992 growing season, which showed best simulation results. For the two zones the normalized yields were similar for measured and simulated data, with the exception of grain in the zone 4 - 9 m of -CR plots (Fig. 6.11b). In the latter region, several observed crop rows showed higher grain yields than at the reference distance. With the exception of straw in the 1 - 3 m zone of +CR plots (Fig. 6.11a) measured yield reductions were slightly higher than estimations from WIMISA, suggesting that shade and competition for water alone were not responsible for the substantial yield loss in the vicinity of the windbreak.
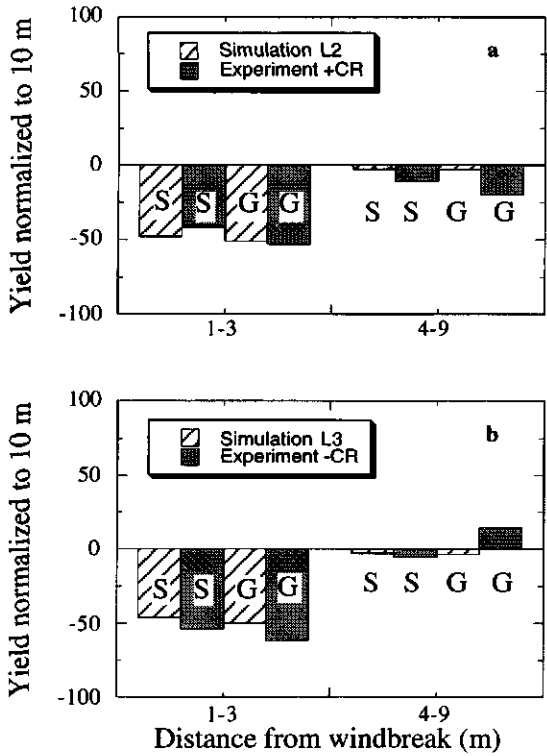
Figure 6.11   Percentage yield reduction averaged over the zone of 1-3 m and 4-9 m adjacent
to the windbreak normalized with respect to 1) yield at 10 m (simulation) and
2) the average yield between 10 and 12 m from the windbreak (measurements)
at two production levels (a) L2,+CR and (b) L3, -CR in 1992, ISC Niger: (S)
straw dry matter and (G) grain yield.

Above mentioned extent of yield reductions are comparable to observations from Brenner et al.
(1993). They found reductions of 45% in grain and 27% in straw yields over a distance of 0.5-
1.7 H at ISC in 1989 with somewhat lower rainfall during the cropping season (404 mm) than
in 1992 (586 mm). In general, millet yield reductions near windbreaks reported for agroforestry
systems in semi-arid regions showed a wide range varying with year (weather), but also with
windbreak specie, height, design, management (pruned or unpruned) and the presence of a
water table (Kort, 1988; Long and Persaud, 1988; Kessler, 1992; Brenner et al., 1993;
Onyewotu et al., 1994). Reported yield reductions occurred in the range of 0 to 2 H and
sometimes even up to 3 H (Kort, 1988). On the other hand, when competition can be excluded,

yields might be enhanced, for instance under *Faidherbia albida* canopies, a species growing in the contra season, millet and sorghum production were higher than in the open due to an improved soil fertility.

6.3.2   *Soil water*
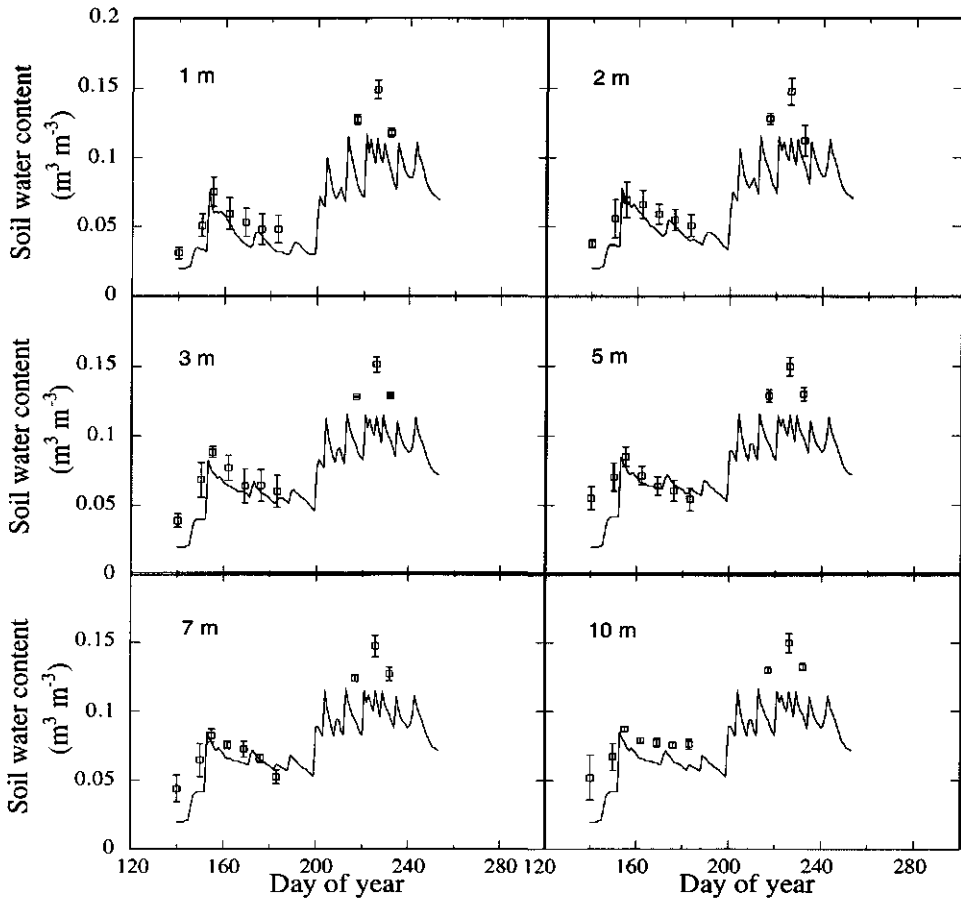
Figure 6.12   Simulated (line) and measured (dots) volumetric soil water content (θ_v) in 0.4 m depth at a distance of 1, 2, 3, 5, 7, and 10 m from the trunk of the WB trees, 1992 growing season at ISC, Niger. Bars show standard error of means.
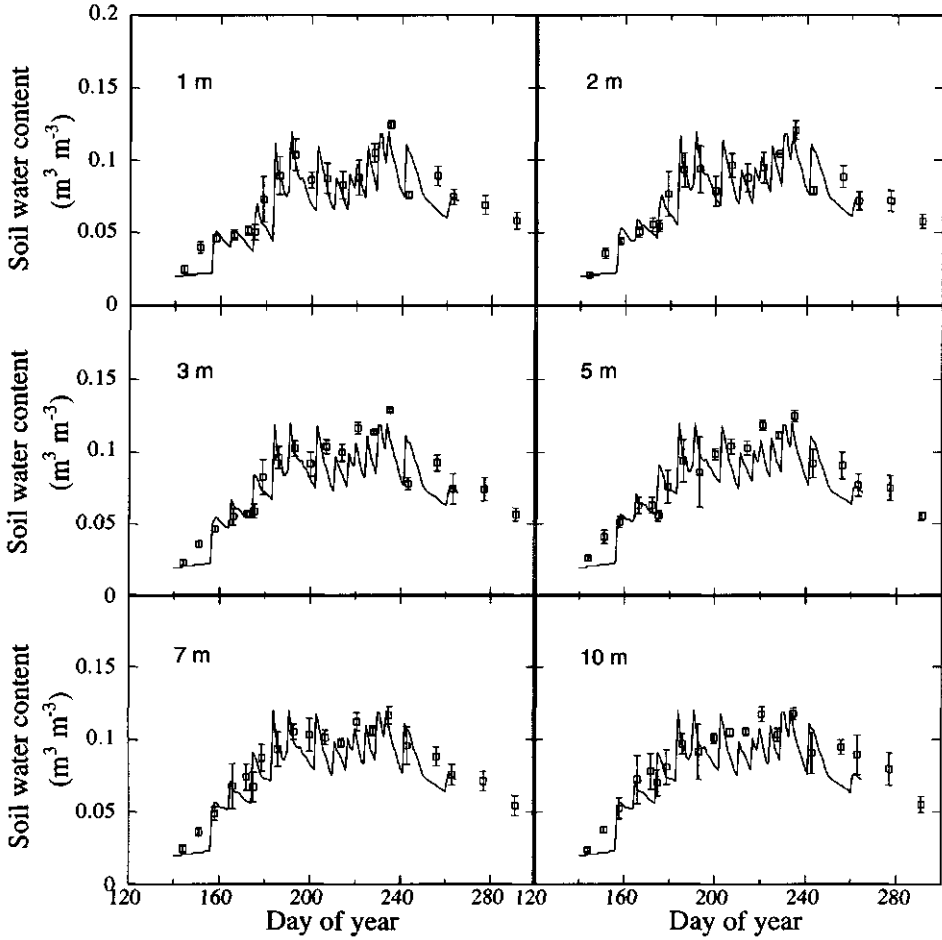
Figure 6.13 Simulated (line) and measured (dots) volumetric soil water content (θ_v) in 0.4 m depth at a distance of 1, 2, 3, 5, 7, and 10 m from the trunk of the WB trees, 1993 growing season at ISC, Niger. Bars show standard error of means.

Measurements and simulation

Comparable to the simulations of an unshielded millet system, the time course of volumetric soil water contents (θ_v's) was simulated well for all distances at soil depth 0.4 m for the 1992 and 1993 growing seasons (Figs. 6.12 and 6.13). At other depths simulation and field data also

showed good agreement (Appendix B3). However, in 1992, observed maximum θ_v's were not achieved with the model, since they exceeded the input value for model parameter θ_f ($\theta_f = \theta_v$ at field capacity), which sets the upper value for θ_v. The distribution of soil moisture with depth showed a decrease from the top (0.4 m) to the bottom of the soil profile (1.9 m), with the exception of the onset and end of the rainy season (Fig. 6.14). The water content per depth differed between the various distances from the windbreak (only 1 and 10 m are shown); for instance low soil depths (> 1.0 m) were replenished sooner further away from the windbreak, indicating that the proximity of the windbreak affected θ_v.
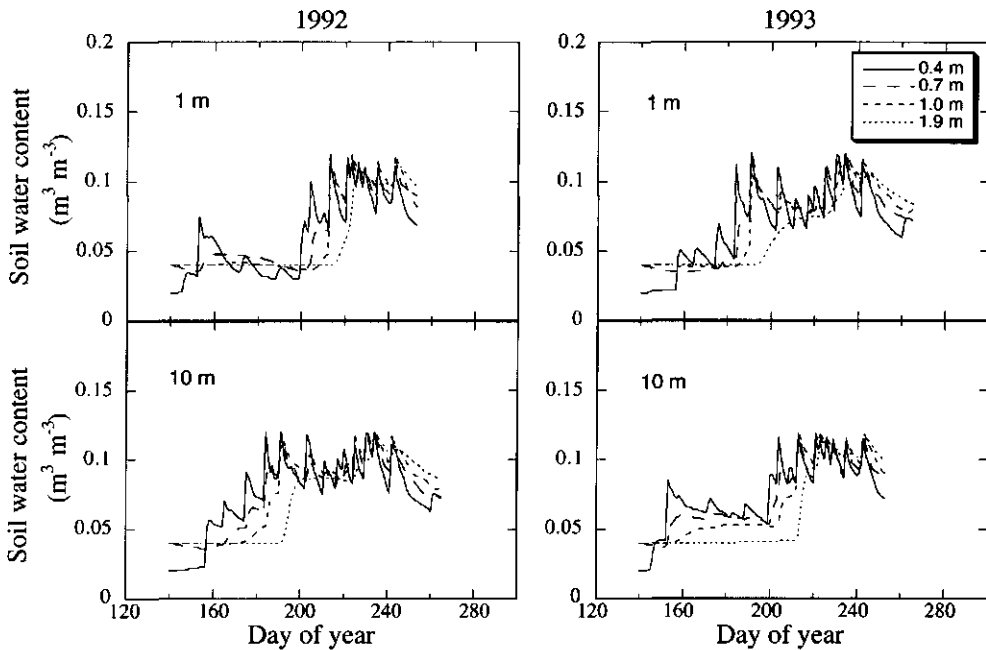
Figure 6.14   Simulated volumetric soil water content (θ_v) in 0.4, 0.7, 1.0 and 1.9 m depth at a distance of 1 and 10 m from the trunk of the WB trees at ISC, Niger, in 1992 and 1993.

Extraction of soil water by windbreak trees

Simulated potential transpiration ($T_{p,WB}$) of Bauhinia WB trees as a function of time was similar for 1992 and 1993 with the exception of the beginning of the season and shortly before flowering (each time ca. 0.5 mm difference) (Fig. 6.15). The similarity can be explained by the fact that Bauhinia's growth curve was assumed to be the same for both years (Subsection 5.3.5), and consequently, $T_{p,WB}$ was exclusively determined by weather. The actual daily amount of transpiration ($T_{a,WB}$) of windbreak trees followed the pattern of rainfall and drought

periods and achieved potential values only at the end of the cropping season when $T_{p,WB}$ declined but rainfall was still high. In 1992, actual water use was lower than in 1993, due to a poorer distribution of rainfall. Total seasonal water use of Bauhinia trees was estimated by WIMISA with 299 and 345 mm for 1992 and 1993, respectively.
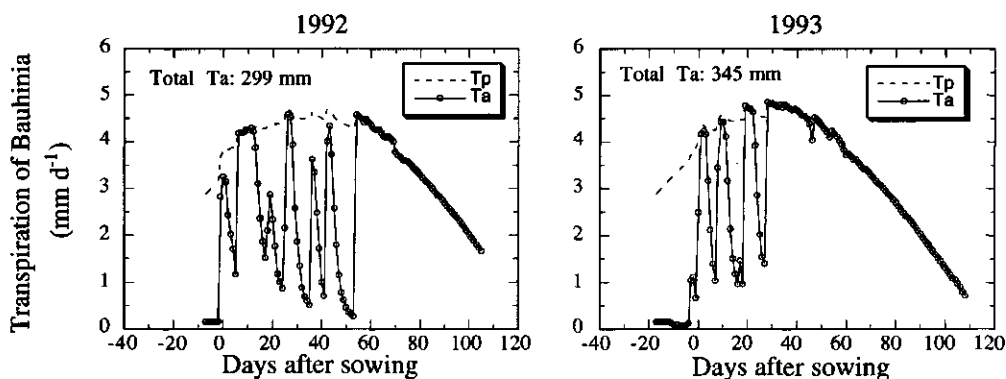
Figure 6.15   Simulated daily potential ($T_{p,WB}$) and actual ($T_{a,WB}$) transpiration rates of the Bauhinia windbreak in 1992 and 1993 at ISC, Niger.

The degree to which Bauhinia's water extraction affected θ_v in the vicinity of the trees at various soil depths is shown for a selection of days from the cropping seasons of 1992 and 1993 (Figs. 6.16 and 6.17). To facilitate comparison of simulated θ_v between the two years in relation to crop growth stage, time is now expressed in days before (DBS) and after sowing (DAS) of millet. Before sowing (DBS 7), when LAI of the windbreak is still low (< 0.5), there is no horizontal gradient in soil moisture, according to WIMISA simulations. Obviously, transpiration, and thus, extraction of soil water by windbreak trees was still negligible with respect to θ_v. Later, simulated θ_v was increasing with distance up to 3 to 4 m from the windbreak, but this holds only for the days that θ_v was equal or lower than 0.1 m^3 m^{-3}. In the vicinity of the windbreak water depletion by trees was almost confined to the upper 0.4 to 0.7 m of the soil, whereas at a depth of 1.9 m soil water was rarely depleted. The reason for this being that, in the model, water uptake by tree roots is restricted up to 0.6 m below the soil surface. This assumption is based on a study on the sources of water for tree transpiration at the same experimental site by Smith et al. (1996a). He found that windbreak trees and millet used water from the top soil profile when it was wet (< 1 m depth) and from the top 3 m of the soil during dry spells, with a large portion from the top 0.5 m. Nevertheless, on two presented days soil water gradients occurred also in 1.9 m soil depth: On DAS 75 in 1992, the upper 1.0 m soil was almost at field capacity due to 44 mm rainfall the day before, whereas at 1.9 m depth θ_v was much lower. Apparently not enough rain water had yet penetrated to replenish the low

depths in the soil profile, after the dry week preceding the rainfall on DAS 74. Especially in the vicinity of the windbreak θ_V was depleted at 1.9 m depth. Here water flowed upwards as a response to a gradient in water potential (pressure head) which had built up during the last dry period through evapotranspiration. Generally, one day after rain (DAS 75 in 1992 and DAS 35, 78 in 1993) soils were still at field capacity and consequently there was almost no horizontal gradient in θ_V up to at least 1 m below the soil surface. On DAS 65, 1993 millet had a maximum LAI and roots reaching up to 1.40 m soil depth. There must have been a strong competition for water in the upper 0.6 m of the soil, where tree roots must have extracted a considerable amount of water, so that water from the lower depths was forced to flow upwards.
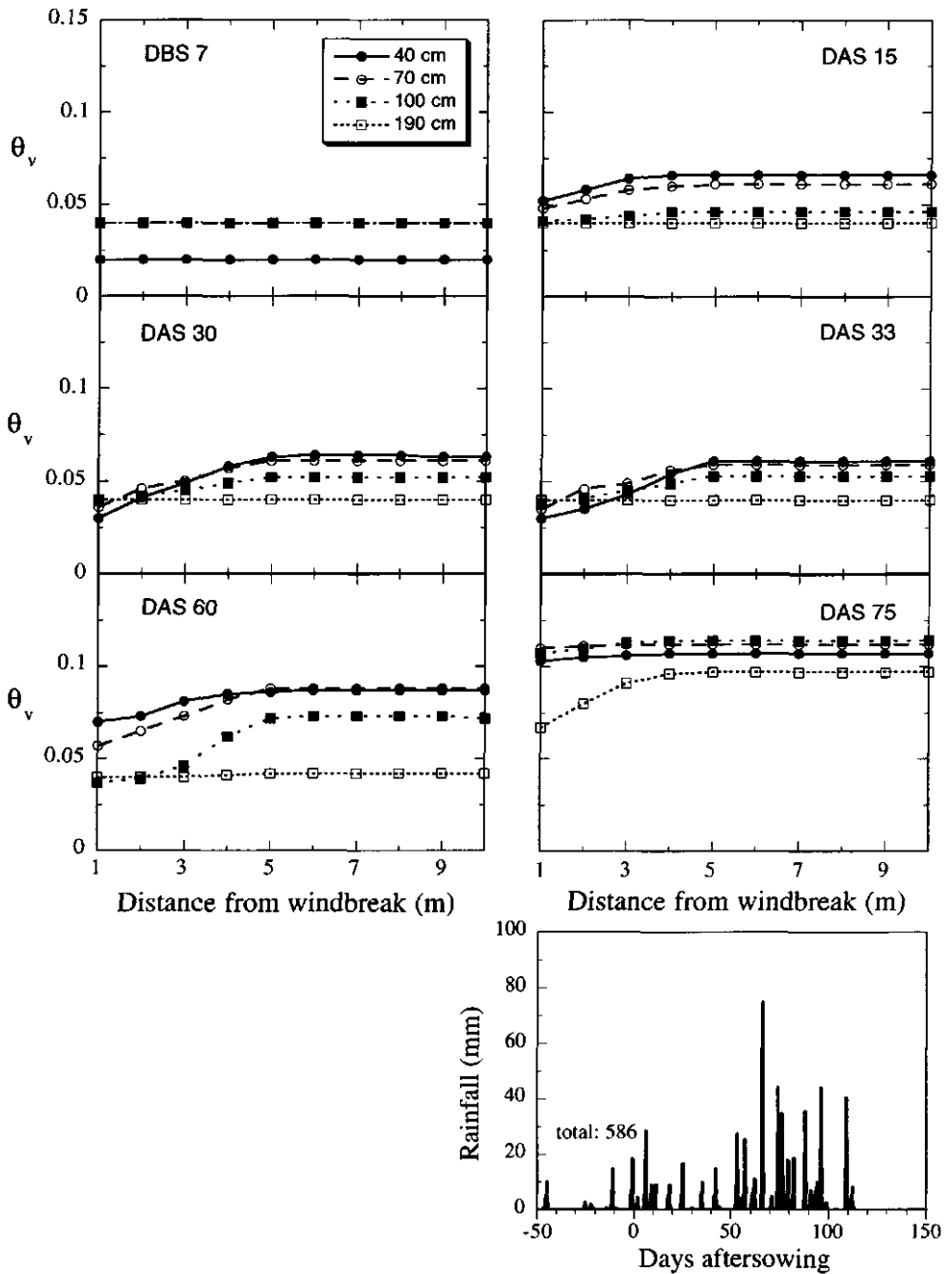
Figure 6.16 Simulated volumetric water content (θ_v) in 0.4, 0.7, 1.0 and 1.9 m soil depth at several distances from the trunks of Bauhinia windbreak and rainfall in 1992 at ISC, Niger .
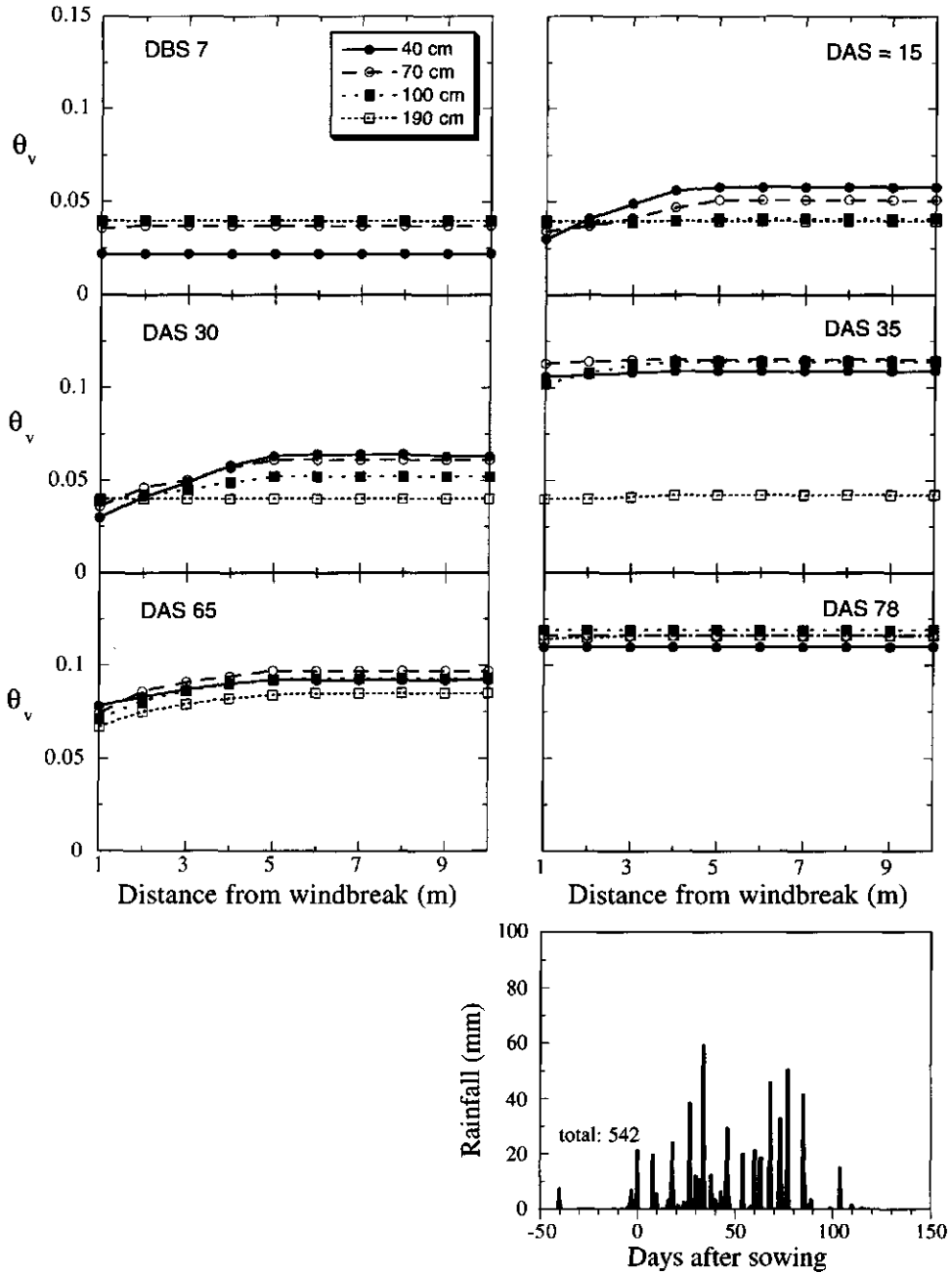
Figure 6.17 Simulated volumetric water content (θ_v) in 0.4, 0.7, 1.0 and 1.9 m soil depth at several distances from the trunks of Bauhinia windbreak and rainfall in 1993 at ISC, Niger .

Simulated differences in θ_v between the first 1 - 4 m from Bauhinia trees were confirmed by field observations (Fig. 6.18, Subsection 3.2.1). In periods of continuous drought the θ_v close to the trees was considerably lower compared to the θ_v at 10 m from the windbreak. According to the field measurements, however, water depletion occasionally reached further into the field (up to 5 or 7 m) than was found from WIMISA. Moreover, in the field at low depths (1.9 m < z > 1m) horizontal gradients in θ_v occurred more frequently and higher than predicted by WIMISA (Subsection 3.2.1). Probably, the model underestimates the extension of water extraction by the tree windbreak in horizontal and vertical direction. Model inputs on tree root distribution are restricted to 1.5 m field length (x) and 0.6 m soil depth (z), because information on root data beyond these borders were lacking.

These results illustrate that in both years, tree water use reduced adjacent θ_v. During the major parts of the growing seasons, there was sufficient rainfall to keep the soil moist at most depths, with the exception of the early growing season in 1992. At this time millet roots were not penetrating far into the soil, so that the low water content in the upper 0.4 m might have caused water stress for the crop. The question arises if tree water use had any effect on the availability of water to the crop and crop growth during the seasons of 1992 and 1993. The latter will be analyzed in Subsection 6.3.4.

Horizontal water flow

Under the given conditions water extraction by trees built up a horizontal gradient in pressure head resulting in horizontal flow in 1992 and 1993 up to 4 m from the tree trunk. Accumulated over the growing season this flow was net positive in the direction towards the windbreak and was approximately 10 % of the water flux in vertical direction, i.e. $q(x) = 0.1 * q(z)$ (Appendix B3). Horizontal movement was highest in the upper soil, but even there $q(x)$ was by far too small to compensate for the water extracted by the trees. Simulation tests showed that $q(x)$ contributed only to a very small degree to the availability of water for the crop, e.g. for the 1992 growing season simulations with $q(x) = 0$ led to 1 % yield decrease in the first crop row. In years with more distinct drought spells, as simulated with a fiction weather dataset (1992 weather, but eliminating rainfall on DOY 200 (30 mm) and on DOY 204 (25 mm)), $q(x)$ was not large either. Consequently, $q(x)$ appears not to be important for the simulation of water uptake by the crop and crop production adjacent to the present windbreak system on sandy soils in the Sahel.
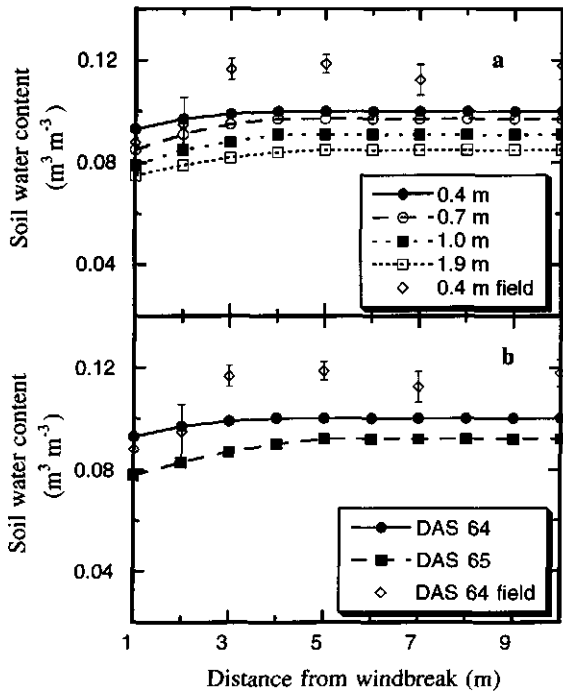
Figure   6.18   Simulated volumetric water content at soil depths of 0.4, 0.7, 1.0 and 1.9 m at several distances from the Bauhinia windbreak on DAS 64 (a,b) and DAS 65 (b) and measured water content (field) at a depth of 0.4 m on DAS 64 (a,b) at ISC, in 1993. On DAS 63, there was 18 mm rain. DAS denotes days after sowing. Bars show standard error of means.

6.3.3 Microclimate in dry and wet years

WIMISA accounts for modifications of wind speed and radiation as a function of distance from the windbreak. Both factors influence the evaporation and thus indirectly the availability of water for the crop. Radiation in addition determines crop assimilation directly (Subsection 6.3.4).

Radiation on top of the canopy

As we have seen from experiments (Fig. 3.1), the 2 - 3 m high Bauhinia windbreak shaded the crop mainly up to 1.5 H. In particular, on top of the first crop row (1 m) the global radiation was considerably reduced (Figs. 3.2 and 6.19). Over the whole cropping season, simulations showed a reduction of 27, 19, and 21 % of incident global radiation on top of the first row for 1987, 1992, and 1993, respectively. Beyond row 4 the total seasonal reduction was negligible with respect to assimilation (see also Fig. 6.23, 1993). The radiation intensity on top of the canopy varied not only with distance from the windbreak and year, but also with increasing density of the barrier, reflected by the more pronounced light reduction later in the season when the LAI of Bauhinia was high and it's porosity low (Figs. 3.1 and 6.20). Simulation results demonstrate that shading became considerable around DAS 10. From then onwards relative light reduction at row 1 compared to row 10 increased almost linearly towards the end of the growing season up to 40% and 20% for direct and diffuse radiation flux, respectively. In 1987, maximum light reduction was achieved shortly around flowering (DOY 60), whereas in 1992 the crop was almost mature by the time that maximum light reduction occurred. Competition for light may vary from year to year due to varying periods between the seasonal onset of the windbreak LAI development and the sowing of the crop. In 1987, first rains started early in the season (21 mm before DOY 100), but were followed by a long period with poor rainfall approximately till DOY 183. The latter delayed sowing of millet so that the windbreak probably had already developed a considerable tree canopy by the time that the crop was emerging.
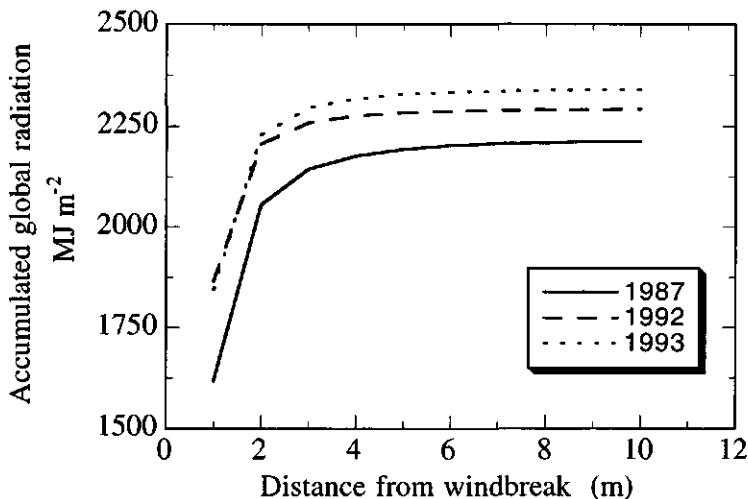
Figure 6.19   Simulated global radiation on top of the crop canopy accumulated over the growing season of 1987, 1992 and 1993 as function of the distance from the windbreak.

Since simulated global radiation data have been well calibrated with measurements at various distances from Bauhinia (Fig. 5.1), we can assume that they are realistic for the present windbreak-cropping system in 1992 and 1993. The results of the 1987 season have to be treated with care, because dynamic WB characteristics were adapted for the 1987 season using rough estimates (Subsection 5.3.5). Whether the applied method for light interception by windbreaks is suitable for other environments and designs, has still to be investigated.
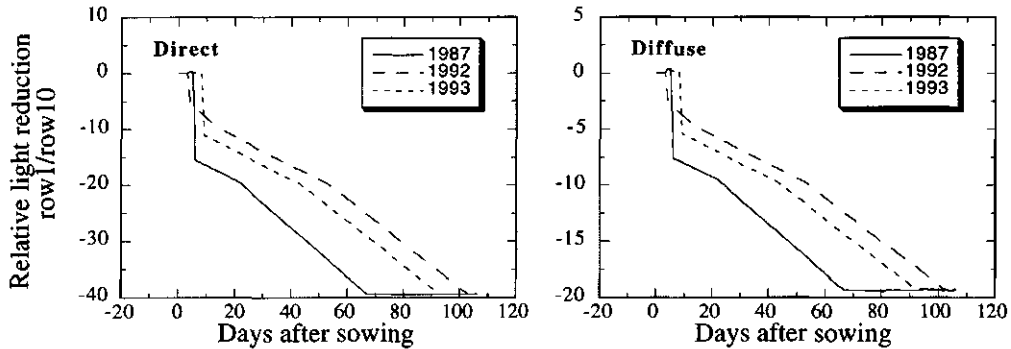
Figure 6.20   Simulated reductions of daily direct and diffuse flux of global radiation at 1 m when compared to 10 m from the windbreak.

Evaporation

The results of the soil water balance indicate that tree root water uptake impeded the moisture content towards the tree trunk. However, the windbreak had also a positive effect on soil moisture: Total actual evaporation (E_a) was decreased in the adjacent 5 m from the windbreak, and the total actual transpiration of crops ($T_{a,C}$) was lower in the first 3 m adjacent to the windbreak (Fig. 6.21). The reduction of E_a was most severe at the first crop row, supposing that incident radiation was of major importance, since wind speed reduction was kept constant up to 5 H. The impact of wind has to be taken cautiously, since the approach of wind speed reduction is derived from a rough empirical relation. A comparison of evaporation from three simulation scenarios: 1. no WB trees are present, 2. WB trees without considering wind speed reduction (only shade), and 3. WB trees reducing light and wind speed, confirms that shade was primary reducing E_0 and E_a (Fig. 6.22). Only in 1992 shade was not alone responsible for local E_a. At 1 m from the windbreak E_0 and E_a were decreased by approximately 32 and 35%, respectively.
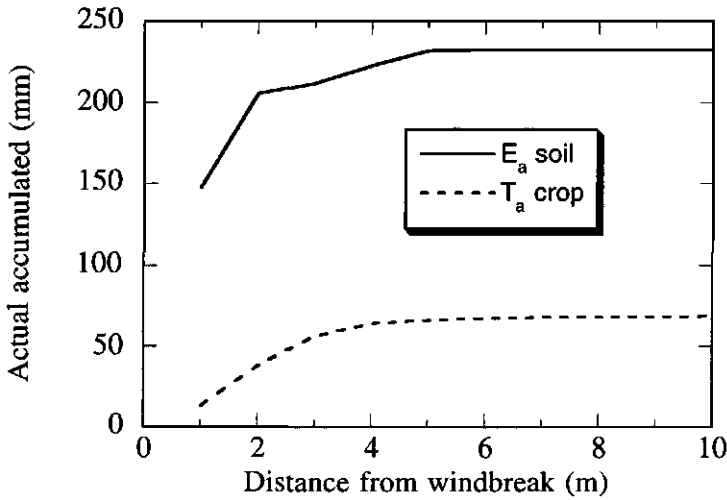
Figure 6.21 Simulated actual soil evaporation (E_a) and potential crop transpiration ($T_{a,C}$) accumulated over the cropping season of 1992 with distance from the windbreak.
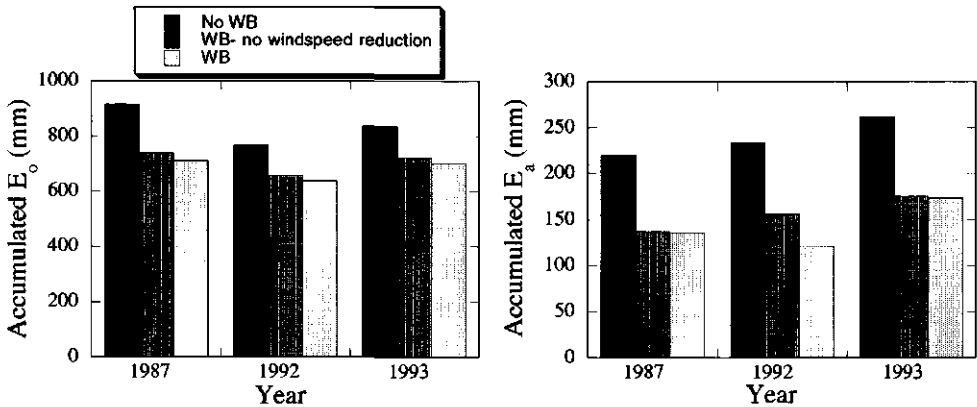
Figure 6.22 Simulated potential (E_0) actual evaporation (E_a) accumulated for the seasons of 1987, 1992, 1993 at 1 m from the windbreak (WB) for three scenarios: no WB, WB without considering wind speed reduction (only shade) and WB reducing wind speed and light.

6.3.4   Competition in dry and wet years

Crop yield reduction near windbreaks, as shown in Figure 6.9, often results from a combination of above- and below-ground competition. The degree of reduction varies naturally with years, i.e. with weather conditions, that determine the extent to which light and water resources are limiting dry matter production of the crop. Various simulation scenarios to identify the causes of competition are presented here for dry and wet years at ISC. Since the experimental years 1992 and 1993 were both rather wet, WIMISA was run also for the dry year 1987 (412 mm). WIMISA results for unshielded millet in 1987 were tested against data of Bley (1990) (Appendix B3).

Dry matter production

To "separate" competition for light and for soil water, three scenarios were compared for 1987, 1992 and 1993 at ISC (Fig. 6.23):

1. millet growth with no WB trees present (unshielded millet);
2. millet growth adjacent to WB trees, but with shading effect turned off by setting the WB porosity constant to 1 (trees compete for water only);
3. millet growth adjacent to WB trees, with trees competing for both light and water.

Below-ground competition for soil water was defined as the reduction in crop yield in the vicinity of the windbreak when shade was excluded (Scenario 2). Above-ground competition behind a windbreak was defined as the difference in yields between shaded (Scenario 3) and non-shaded crops (Scenario 2). Scenario 1 was used as a reference. Presented yields refer to straw dry matter.

In 1987 and 1993, yield reductions were almost equally attributable to above- and below-ground competition in a zone of 1 - 3 m adjacent to the trees (at row 1: 31 and 30 % for 1987 and 24 and 21% for 1993). At a larger distance (3 - 4 m) yields were reduced by light competition alone. The results of 1987 have to be interpreted with caution, because two dynamic WB characteristics were adapted for the 1987 season using rough estimates. On the other hand, yields of 1987 showed the same trend as in 1993, a year with a comparable favourable rainfall distribution. In 1992, yield reduction was primarily caused by competition for water (78% at row 1), and the inclusion of shade only slightly reduced yields further (2 % at row 1 and about 3 - 4% at row 4). The response of potential tree transpiration ($T_{p,WB}$ = P_{WB}/E_W) to actual tree transpiration is not included in WIMISA. This feedback would to some degree reduce water uptake by trees under conditions of water shortage (Eq. 4.58). But, since P_{WB} was derived from LAI observations of 1992 (Subsection 5.3.3) a possible overestimate of tree water uptake must have been small in that year.
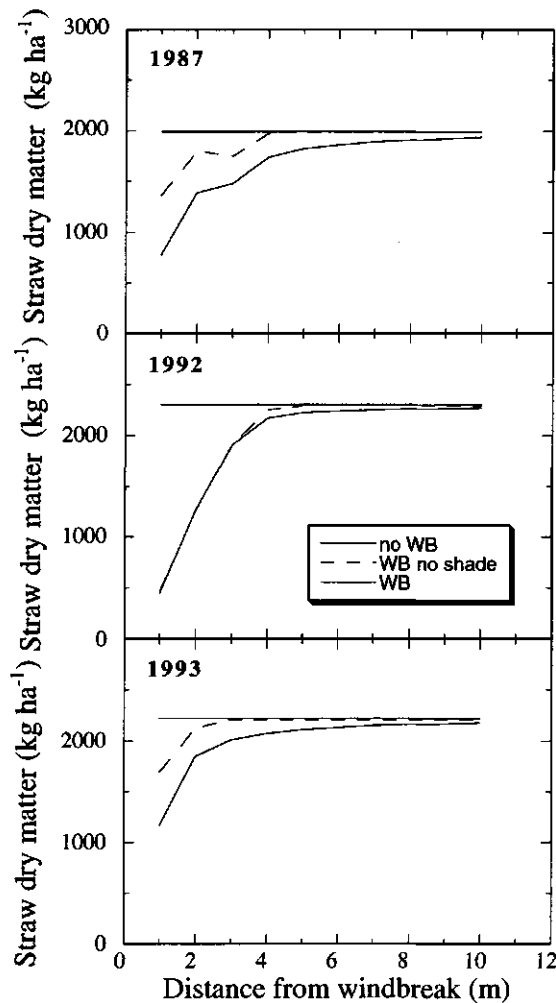
Figure 6.23   Simulated straw dry matter for unshielded millet (no WB), millet adjacent to
WB trees compete with crops for water (WB no shade), and millet adjacent to
WB trees compete with crops for water and light (WB) for the 1987, 1992,
and 1993 growing seasons at ISC, Niger. All simulations were run with
dataset L2.

The scenarios illustrate the relative importance of the individual effects of light and water
competition for crop production in the tree-cop interface, but do not explore the absolute
contribution of each of the two growth factors to production in Scenario 3. The effects of light
and soil water interact and are, hence, not additive. Excluding shade may enhance crop growth

which in turn could increase water uptake. Conversely, when water stress is reduced by exclusion of tree root water uptake, crop assimilation may be enhanced directly (stomatal opening) and modified indirectly through a greater photosynthetically active leaf area (changes in the distribution of assimilates between roots and shoot, slower rate of leaf aging and dying (Subsection 4.3.1)).

Assimilation

To elucidate the contribution of the individual (light and water) competition effects involved in dry matter production, we need to turn off one of the two effects, but retain the feedback between them. In WIMISA, this is done most easily for the exclusion of water competition. The influence of water stress on assimilation is incorporated by multiplying daily gross assimilation with the reduction factor T_a/T_p at the end of each day (Eq. 4.3). Daily output prior to this multiplication gives daily CH_2O assimilation of millet, competing with trees for both light and water, but excluding the water effect (which mimics the effect of stomatal closure) of that day on assimilation. Following this approach, we present daily CH_2O assimilation per unit of leaf area for two scenarios (Fig. 6.24):

1. millet adjacent to WB trees, competing for both light and water, as corrected for water stress (simulates combined effect of shade and stomatal closure);
2. millet adjacent to WB trees, competing for both light and water, not corrected for water stress, i.e. before multiplication with T_a/T_p (simulates shade effect only).

Note, that the presentation of assimilation per unit LAI disregards the effects of light and water on the development of photosynthetically active leaf area and the correlated total assimilate production. Taking the assimilation of crop row 10 as reference, it follows from comparison of Scenario 1 with Scenario 2: In 1987 and 1993, both water and light almost sequentially decreased assimilation per LAI. In the beginning of those cropping seasons, water played a major role. Then from approximately DAS 35 (1987) and 30 (1993) onwards, only shade reduced assimilation (Fig. 6.24), with the exception of several days between DAS 70 and 80 in 1987, when water and light were simultaneously limiting. At the end of 1993, assimilation/LAI was higher at row 1 than at row 10 (Scenario 1, 2), because a somewhat slower crop development delayed ageing of photosynthetically active leaves in the vicinity of the windbreak.

Scenario 1: shade and water

g CH$_2$O m^{-2} leaf day^{-1}

Scenario 2: shade only

g CH$_2$O m^{-2} leaf day^{-1}
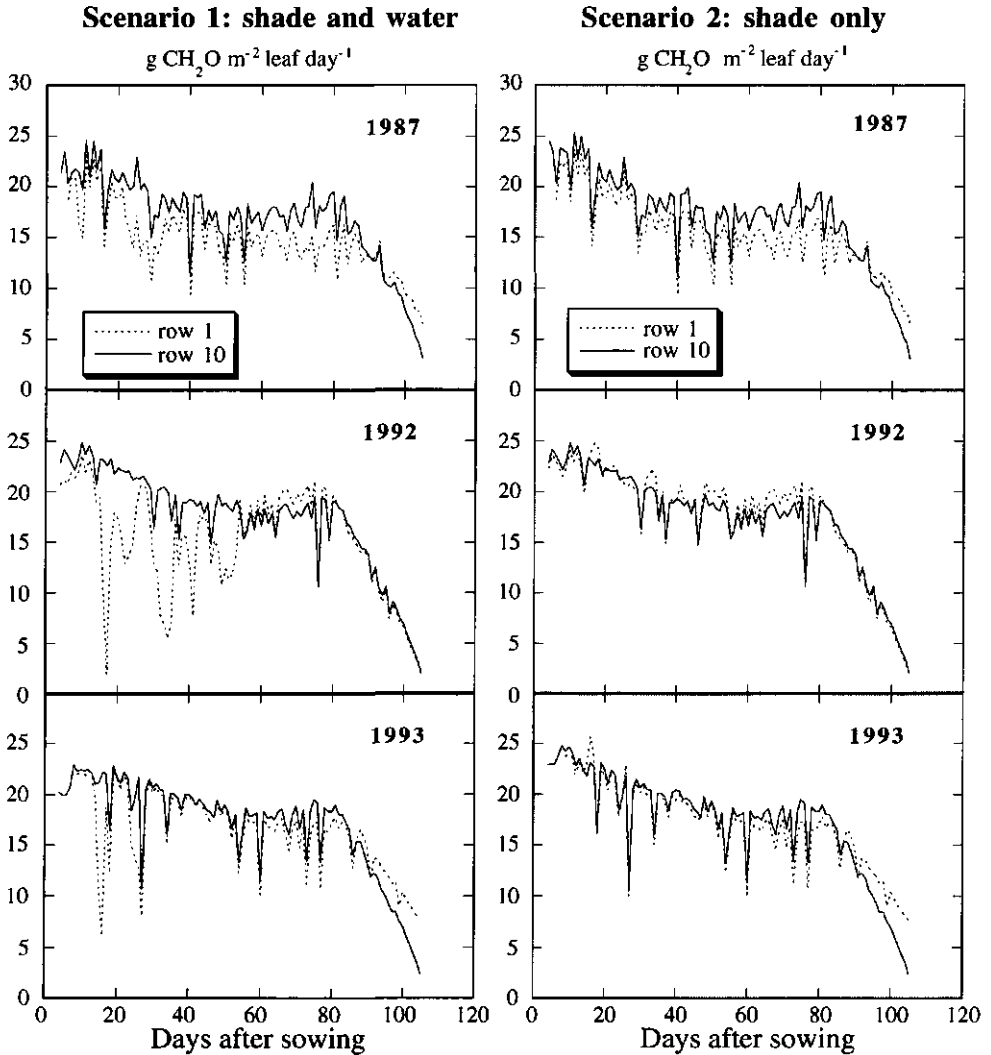
Figure 6.24 Daily gross CH$_2$O assimilation at 1 and 10 m from the windbreak for the 1987, 1992, and 1993 growing seasons at ISC, Niger. a) Scenario 1: shade and water competition and b) Scenario 2: only shade (see text for explanation).

In 1992, the strong reduction in straw dry matter was due to reduced assimilation at the onset of the growing season caused by water stress (Scenario 1), whereas light on average was not limiting (Scenario 2). On the contrary, shade even had a positive effect on assimilation/LAI

when water competition was turned off (Table 6.4). Apparently, incoming radiation at row 1 was used more efficiently for photosynthesis than estimated for the open field. The reason is a combination of a rather high seasonal radiation intensity (Fig. 6.19) and a low light reduction by the windbreak (compared to the other two years, Fig. 6.18), thus the radiation intensity at the top of the canopy must have been close to the level of saturation (A_m) of the non-linear assimilation-light response of leaf photosynthesis. In addition, due to a higher LAI at row 10 light extinction was stronger there. Consequently, under the ambient light intensities in 1992, assimilation per unit LAI averaged over the entire canopy depth was higher at row 1 than at row 10. Similarly, the assimilation in Scenario 1 was higher at row 1 than at row 10 in the period from about DAS 55 to DAS 80, when obviously neither light nor water was limiting. The causes of strong water stress can be examined by comparing the time course of rainfall, soil moisture and Ta/Tp.

Table 6.4   Contribution of individual competition effects to total seasonal gross CH_2O assimilation per unit LAI of millet, competing with trees for water and light at ISC.

Year	% reduction in CH_2O/ LAI in row 1 compared to row 10 due to		
	Water	Light	Total
1987	2.9	11.1	14.0
1992	13.7	-1.7	12.0
1993	2.4	7.4	9.8

Table 6.5   Total seasonal reduction in gross CH_2O assimilation (per unit soil area) of millet, competing with trees for water and light at ISC.

Year	reduction in total CH_2O (%) in row 1 compared to row 10 due to	
	Water	Total
1987	1.07	61.03
1992	3.41	77.85
1993	0.35	46.55

Water stress for the crop

During all years, rainfall was rather adequate to meet crop demand for water and, hence, T_a/T_p was close or equal to 1 almost during the entire cropping season at a distance of 10 m from the windbreak (Figs. 6.25 and 6.26). The situation was different in the vicinity of the windbreak, where water extraction of trees caused occasionally that T_a/T_p was lower than 1, especially in 1992 as expected from the simulated assimilation data. Transpiration data (Appendix B3, Fig. 6.15) indicate that competition from the windbreak was stronger than that exerted by an adjacent area of millet, in particular at the beginning of the season when all water had to be taken up from the surface horizon (Garba and Renard, 1991). Brenner et al. (1993) found that $T_{a,WB}$ was much higher than $T_{a,C}$ at the beginning of the season, but this was reversed by the middle of the season, when the crop had an LAI of approximately 2.0. In our simulation study crop LAI was at its maximum 0.52 for crop row 1.

Close to the windbreak (row 1) we see: Despite higher seasonal precipitation in 1992 compared to 1987 and 1993, availability of water for the crop was lower during 1992 than during the other two seasons, due to a less favourable distribution of rainfall, particularly in the first 50 DAS. In 1992, water stress continued from DAS 5 to about 55 (Fig. 6.25) and led to reduction in assimilation per unit LAI (Table 6.4) and per unit soil area (Table 6.5). In the beginning of the 1987 and 1993 growing seasons, there were also dry periods but shorter or interrupted by small showers, thus, less severe. This is reflected in the water stress factor T_a/T_p, which was less often and less strongly reduced in 1987 and 1993 in the zone 1-4 m adjacent to the windbreak. Due to feedback between LAI and $T_{p,C}$ as well as between T_a/T_p and LAI, only sudden severe water shortage for the crop will strongly reduce T_a/T_p. The deviation between the percentage reduction in assimilation/LAI and assimilation/unit soil area illustrate the strong influence of light and especially water on leaf area growth. LAI simulation results are presented for the three years in Appendix B3.
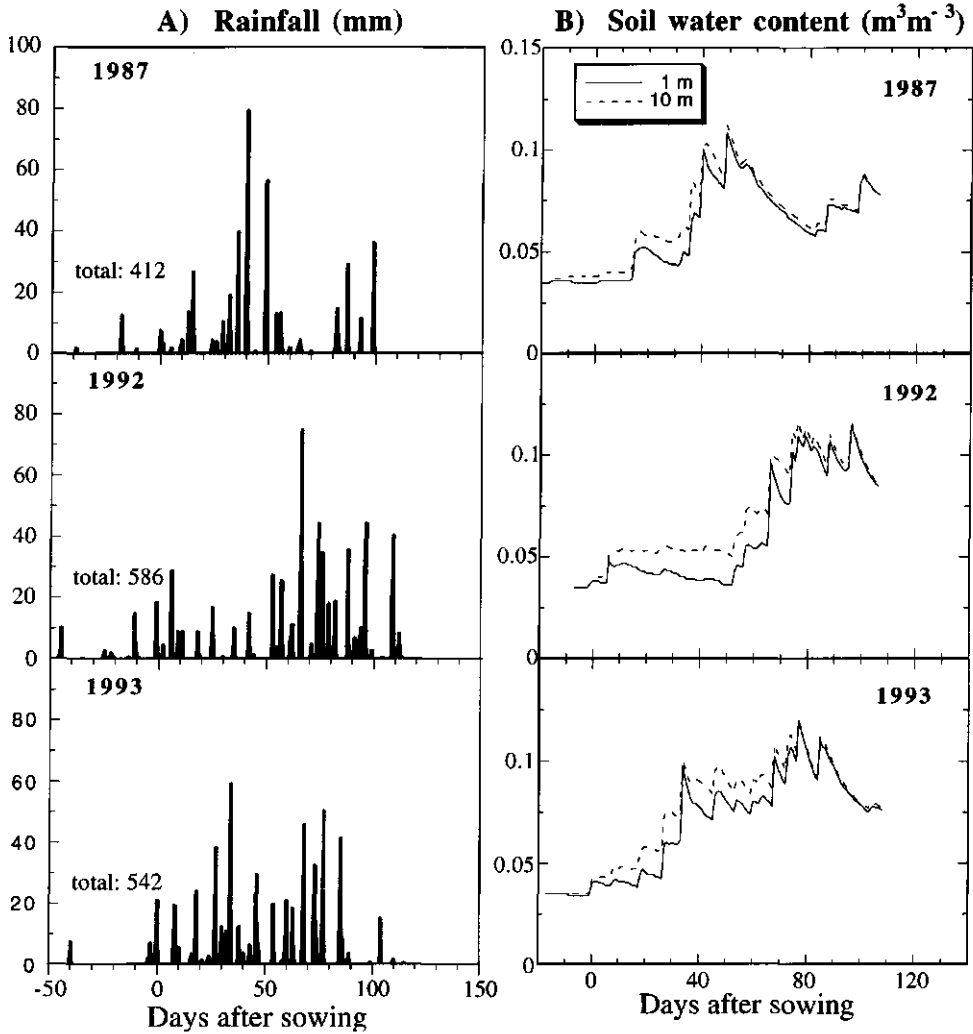
Figure 6.25 Seasonal distribution of rainfall (A) and soil water content averaged over the simulated root zone at distances of 1 and 10 m from the windbreak (B) in 1987, 1992 and 1993 at ISC, Niger. All simulations were run with dataset L2.
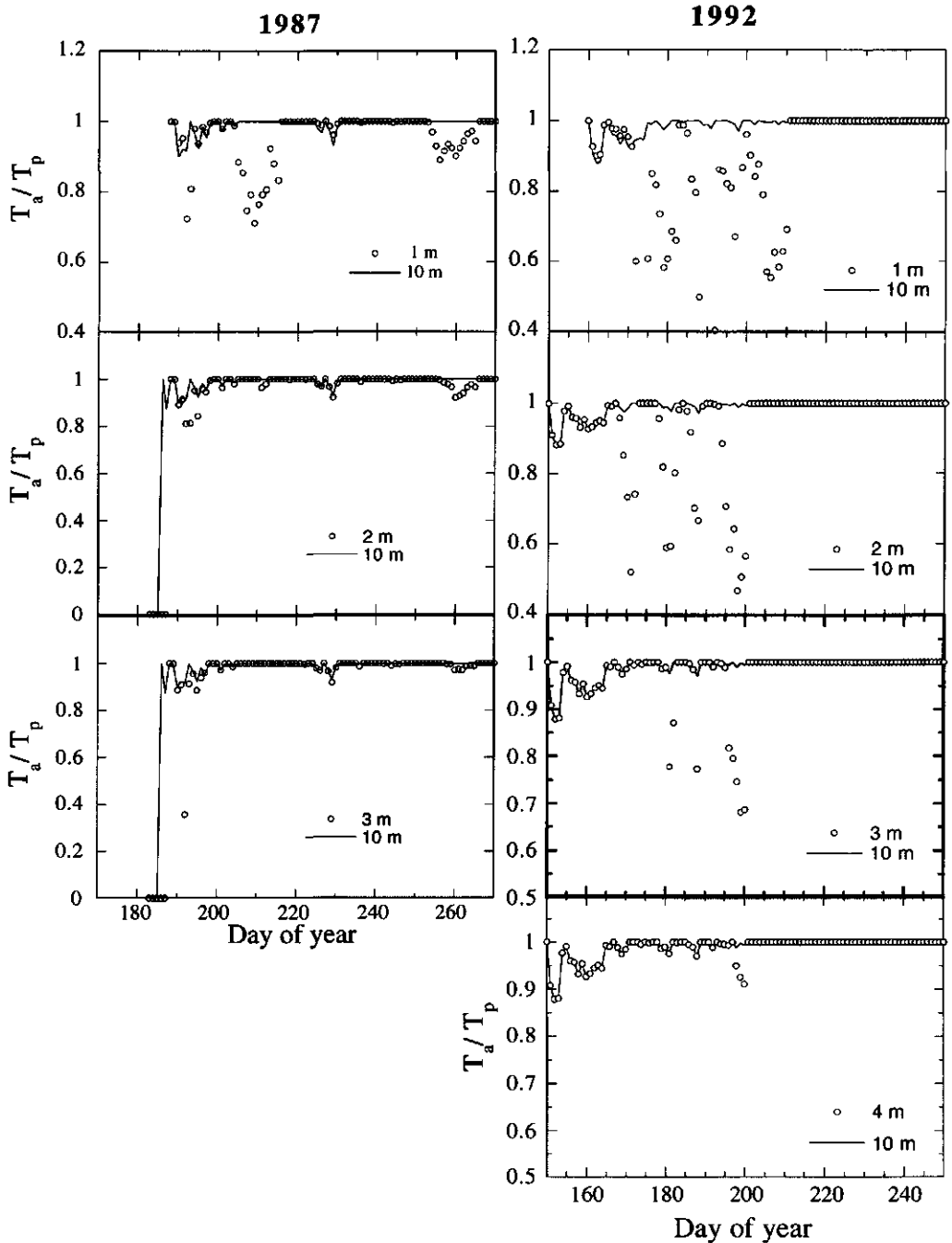
Figure 6.26 Simulated water stress factor T_a/T_p at 1, 2, 3 and 4 (1992 only) m distance from the Bauhinia windbreak compared to that at 10 m distance in 1987, 1992 and 1993. All simulations were run with dataset L2 for millet, competing with trees for water and light at ISC, Niger.
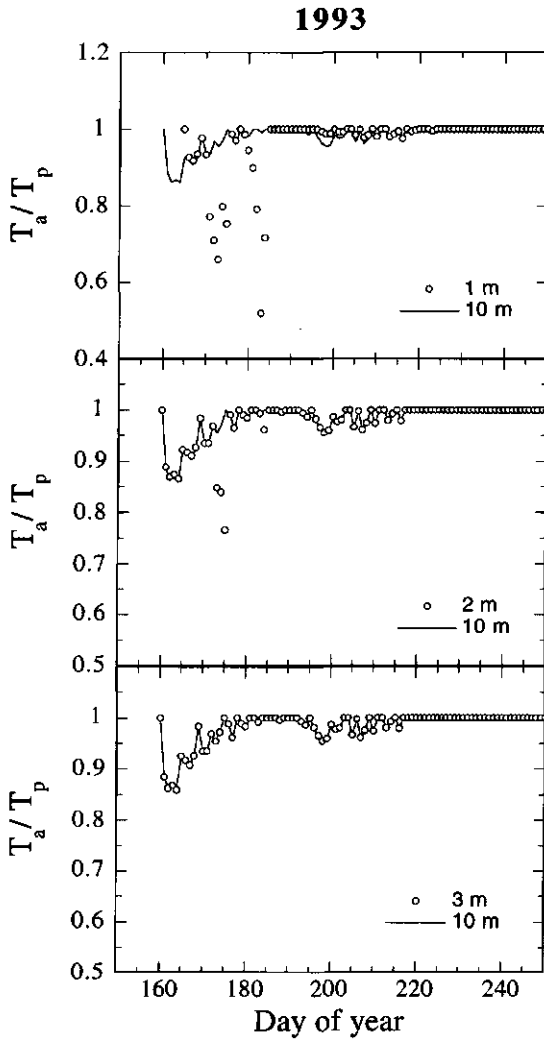
Figure 6.26   (Continued).

Discussion

Surprisingly, water and total competition was strongest in the wet year 1992, intermediate in the dry year 1987 and lowest in 1993. This demonstrates that rainfall pattern is more important than absolute rainfall amounts. According to Sivakumar and Wallace (1991), shortage of water in the semi-arid tropics is not a consequence of low annual rainfall, the problem is the seasonal distribution of rainfall and the rate at which water is lost by soil evaporation (Monteith, 1991).

In all three years, crop yields were reduced by tree water use at the onset of the season, when available water, as well as crop roots were restricted to the upper soil and when rainfall was low. Brenner et al. (1993) reported that competition for water between trees and crops was likely at the start of the season, but becoming less important towards the middle of the season, when transpiration of the crop exceeded that of the windbreak on a ground area basis.

C_4 cereals such as millet rarely become light saturated, consequently their photosynthesis will be reduced in the shade. Light was growth-limiting mainly in 1987 and the shading effect was negligible in 1992, as expected from the ambient radiation intensities of those years (Subsection 6.3.3). In 1987, incoming light intensities were lowest while light reduction was strongest, because of the early start of windbreak growth in comparison with the time of crop sowing (Subsection 6.3.3). The results of the various scenarios illustrate that the shading effect on assimilation/LAI is important only when water shortage is not too severe (Table 6.4), because high water stress coincides with decrease in photosynthetic leaf area, which in turn reduces light competition (lower LAI results in reduced extinction of light and, hence, higher assimilation averaged over the depth of the canopy). According to Corlett et al. (1992), millet yield was reduced proportionally to the degree of shading as long as water was not limiting. Brenner et al. (1993) found that the magnitude of above-ground competition (expressed as reduction in straw dry matter) corresponded to the reduction in photosynthetic quantum flux density caused by a neem windbreak at ISC. Similar effects of shade were found in other agroforestry system studies (Long and Persaud, 1988; Onyewotu et al., 1994; Kessler, 1982).

Averaged over the zone 0.5 - 2.0 H, straw dry matter reduction due to light was 18 % in 1987 and 11 % in 1993, which agrees reasonably well with straw dry matter reduction reported by Brenner et al. (1993) for a somewhat smaller zone (0.5 - 1.7 H) adjacent to a neem windbreak (13% compared to average yield between 1.7 - 3.1 H, in 1989 with 467.5 mm rain). Long and Persaud (1988) measured reductions of 20 % in straw dry matter, over a distance of 0.5 to 2.0 H when compared to yields at 2 H, behind a neem windbreak in the Maggia valley. There, competition for water did not play a role, since the trees had access to groundwater. In the model (as in the experiments), the windbreak was short with tree branches not much hanging over the crop. Often windbreaks are more than 5 m high and extend much further into the cropped field (larger crown size). Such shelters cause naturally more shade. Nevertheless,

neither Brenner et al. (1993) nor Long and Persaud (1988) observed remarkably more yield loss due to shade by a 6 and 10 m high neem windbreak, respectively. The relatively small reduction difference between the low Bauhinia and high neem windbreak may be explained by the fact that a possible positive effect of shade on crop SLA was not included in WIMISA. This needs further investigations. Further possible reasons are differences in a) characteristics of the two tree species with respect to height, porosity and water use and b) period between start of seasonal growth of crop and tree.

All simulations refer to a crop which is shaded between 7 - 12 h (crop was westwards of the windbreak). Shade in the afternoon would be expected to reduce assimilation slightly less, because leaf extension is highest in the morning (Fechter, 1993). Since the effect is small, and additionally other microclimatic factors (temperature and wind speed) may differ at the west and east side of the windbreak, it is doubtful that this would influence final yields; e.g. Kessler (1992) found no clear relation between sorghum yields and cardinal direction from the trunk of scattered trees.

6.4   Sensitivity analysis

Modifications of model parameter values are used to perform a sensitivity analysis. The dataset of production level L3 was chosen as reference, since the model was calibrated for this production level. The standard values of the parameters, both for unshielded and shielded millet simulations are those defined in the input files (Appendix B2), e.g. $DM_0 = 18$, PERDL = 0.05, SPAN = 800, specific leaf stem 0.0004, $K_{sat} = 0.8$, Ew = 20 - 25. Depending on the type of parameter, its value was changed to a certain percentage or given a range of values that refer to their "natural" variability. Since this analysis is very (computing) time consuming, in particular for the windbreak shielded crop, we made a selection of:

- parameters that are of main importance in terms of LAI development and dry matter production, which are either uncertain (difficult to derive) or expected to be very sensitive to environmental conditions (Subsection 6.4.1),
- parameters that are of importance in terms of soil water dynamics, crop available water and thus possible affect millet growth (Subsection 6.4.2),
- parameters that are of importance in terms of tree root water uptake and thus may influence competition (Subsection 6.4.3),
- time steps for assimilation/radiation and soil water terms (Subsection 6.4.4).

6.4.1 Crop parameters

The sensitivity of most crop parameters, which were adopted from CP-BKF3, have been tested by Verberne et al. (1995). Those tests showed that parameters that charcaterise maximum photosynthesis and SLA, are rather sensitive, and therefore, should be selected from site specific values. For WIMISA, crop growth parameters, which had been recalibrated (Table 6.1), were varied to reveal the response of the model on variation in these parameters in terms of living aerial dry matter and LAI. In addition specific root length and K_{dif} were tested.

In Figure 6.27 absolute responses of the millet growth model to the changes in parameter values are shown. The initial biomass (DM_0) has a strong impact on the growth curve, due to its exponential character. Simulation run tests with DM_0 values between 15 to 50 show an increasing dry matter production and LAI increase. Obviously, $DM_0 = 50$ corresponds to a plant density at which intraspecific competition is still outweighed by higher yields of more plants. Initial light use efficiencies, reported for millet are in the range of 0.38 (Erenstein, 1991) and 0.4 (Fechter, 1993). Similar to DM_0 this parameter has to be chosen with care and preferentially be based on cultivar specific data. To a lesser extent, but still sensitive are the parameters leaf longevity, specific stem area and K_{dif}, all having an impact on the computation of assimilation. This is not the case for the parameters relative mortality and specific root length which are rather stable with respect to aerial dry matter and LAI.
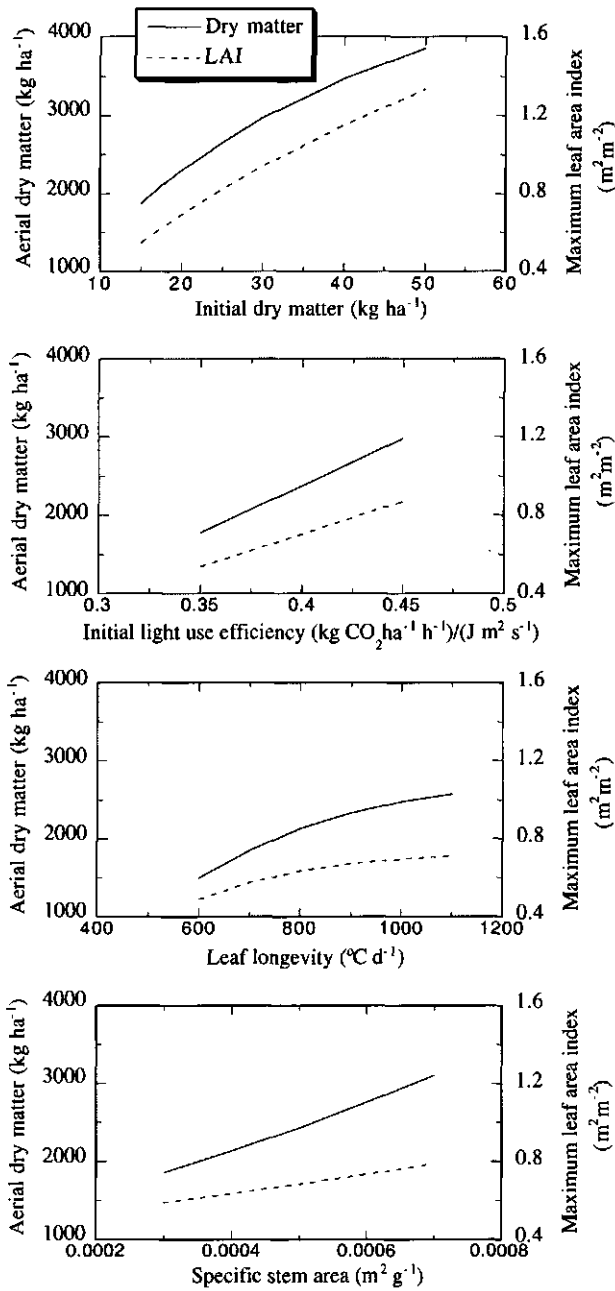
Figure 6.27 Sensitivity of crucial crop parameter values with respect to aerial dry matter and maximum leaf area as simulated by WIMISA for 1993 growing seasons, at ISC, Niger.
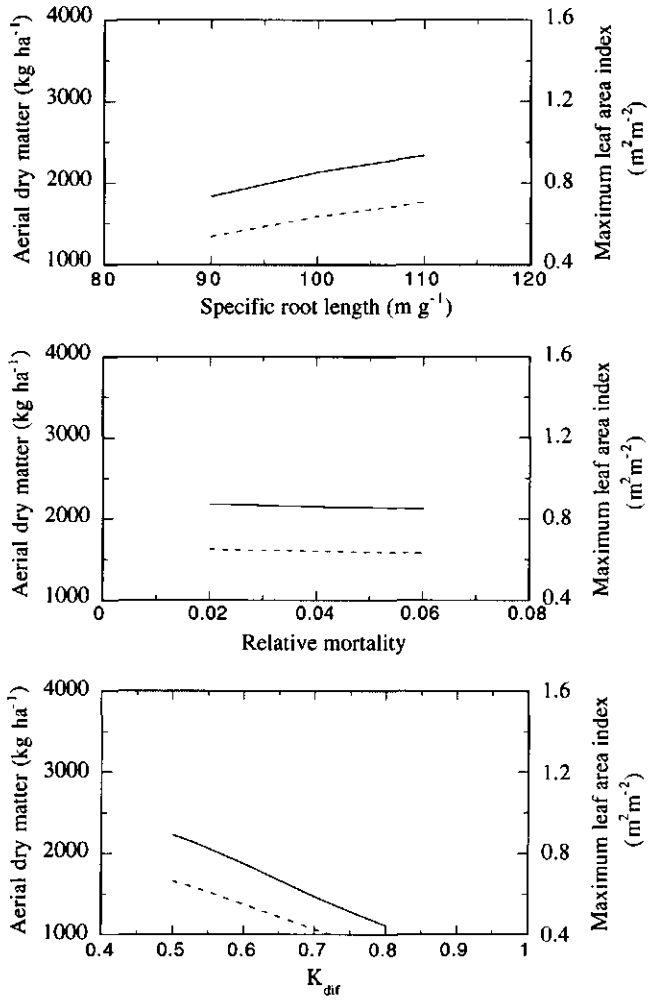
Figure 6.27 (Continued).

6.4.2   Soil parameters

The sensitivity of the model to parameter K_{sat} (conductivity at saturation) was important with respect to water distribution within the soil profile (Figs. 6.4 and 6.5) and final crop dry matter, but negligible for tree water use (Table 6.6). Fortunately, the available data on K_{sat} allow a reliable estimate of this input parameter (Section 5.4). Further tests revealed that the simulations are rather insensitive to θ_i. In 1992, θ_f in the field was slightly higher than the model input value, resulting in somewhat underestimation of θ_v. However, those underestimation hardly affected the accuracy of simulated crop yields, since those high values of θ_f occurred when soils moisture was sufficient for plant growth for most of the time (Subsection 6.3.2).

Table 6.6   Effect of conductivity at saturation (K_{sat}) on aerial dry matter of millet and windbreak transpiration ($T_{a,WB}$).

Parameter	Aerial DM (kg ha^{-1})	$T_{a,WB}$ (mm)	
K_{sat} (m s^{-1})	crop row 1	potential d^{-1}	seasonal
0.8 e-4	814	5	356
0.9 e-4	800	5	356
1.7 e-4	697	5	347
2.4 e-4	600	5	354

6.4.3   Windbreak parameters

Parameterisation for the Bauhinia windbreak could not be completed due to lack of quantitative data. Therefore, estimates were made on the basis of Bauhinia related tree species. Most uncertain parameters are E_W (water use efficiency) and $l_R(x,z)$ (root length distribution) (Section 5.3). Some confidence in those values was achieved by comparing simulation results against available data on daily transpiration and water use of *Azadirachta indica* and *Acacia holosericea* trees (Smith, 1996). By tuning E_W within the range given by Lövenstein et al. (1991: 10 - 30 kg ha^{-1} mm^{-1} for root water uptake from the upper 3 m) simulated daily transpiration and total seasonal transpiration of the windbreak were calibrated closely to the values reported by Smith (Appendix B3). The degree of yield reductions due to water extraction by trees depends on the value of E_W (Table 6.7).

Table 6.7   Effect of the value for water use efficiency (E_W) on aerial dry matter of millet, crop transpiration ($T_{a,C}$) and windbreak transpiration ($T_{a,WB}$).

Parameter E_W	Aerial DM ($kg\ ha^{-1}$) row 1	row 10	seasonal $T_{a,C}$ (mm) row 1	row 10	$T_{a,WB}$ (mm) maximum d^{-1}	seasonal
10-15	483	1830	8	33	9	-
10-20	661	1912	14	44	8.1	525
10-30	771	1914	15.9	44.1	7.5	391
15-25	665	1921	13.7	44.1	5.7	377
20-25	695	1921	14.2	44.1	4.9	347

6.4.4   Time steps

Time steps lower or equal to 0.25 h do not influence crop production (Table 6.8). For the computation of assimilation, larger time steps than 15 minutes result in enhanced aerial DM and LAI, because of (i) averaging the radiation intensities over a steeper traject of the leaf light response curve and (ii) the method used for integration (trapezium). Larger intervals for calculation of soil water balance terms, on the contrary, result in a lower production due to increased evaporation, deep percolation and, thus, a lower water availability in the root zone. The effect of time step on soil water content has been shown also in the comparison of WIMISA and CP-BKF3 (Section 6.2). Since errors in the computation of both, radiation and water redistribution will increase with time steps > 1 h, those tests were left out here.

Table 6.8   Effect of time step of computation of assimilation and soil water balance terms on aerial dry matter and leaf area index (LAI) of unshielded millet, using DM_0 = 18.

Assimilation time step (h)	Aerial DM ($kg\ ha^{-1}$)	LAI ($m^2\ m^{-2}$)	Soil water time step (h)	Dry matter ($kg\ ha^{-1}$)	LAI ($m^2\ m^{-2}$)
0.01	2133	0.635	0.01	2132	0.634
0.05	2133	0.635	0.05	2132	0.634
0.10	2133	0.635	0.10	2132	0.634
0.20	2133	0.635	0.20	2132	0.634
0.25	2133	0.635	0.25	2133	0.635
0.50	2155	0.642	0.50	2124	0.632
1.00	2191	0.659	1.00	2104	0.625

6.5   Discussion and conclusions of part B

The present model integrates the effects of competition between WB trees and crops for soil water and radiation on millet growth. Crop growth, incoming radiation intensities and soil water dynamics are incorporated at process level, whereas light interception by the windbreak and tree water use are modelled using a simple description of the windbreak component. The limited information available on (Bauhinia) tree characteristics made it necessary to confine those descriptions to the most important parameters. Calculations of root water uptake (ROOTS) and radiation (MICROCLIMATE) as a function of distance from the windbreak are used as input for the CROP and SOIL WATER module. Inaccuracies in these inputs, originating from the necessary simplifications, are assumed to be smaller than variations due to temporal and spatial heterogeneity within the system. Both, time and space are considered with high resolution. Further improvements of model concepts and the accuracy of parameters as well as additional data for model validation are needed to increase confidence in model analyses and predictions for windbreak-cropping systems under various environmental conditions and system designs.

6.5.1   Evaluation of the model

The performance of a model as a representation of reality depends on the accuracy of the process-based approach and the certainty of parameters (Meinke, 1996; Poethke et al., 1994). Agroecosystem models contain substantial elements of empiricism and hence uncertainty, which has to be considered in the evaluation of model output (Monteith, 1997). Experimental data used for development of the crop and, especially, the soil water module were largely independent from the data used for calibration and evaluation. This assures a minimum degree of predictive value of simulation results, which is required for a proper understanding of the system modelled (van Keulen, 1976). WIMISA incorporates 85 parameters, including those for environmental and management settings (11). The major part refers to crop characteristics (41 shoot + 8 root parameters) from which many were derived from a large set of literature data and, hence, have a rather general validity in terms of cultivar and site. The soil parameters (12) are very reliable for homogeneous sandy soils in the Sahel. Windbreak characteristics (13) used in quantifying shading effects are easy to obtain, but those applied in the water uptake equations are difficult to obtain and assumptions had to be made. Most critical and uncertain parameters are those describing tree root length distribution (Section 5.3). The numerical values of these parameters rather than the applied algorithms form the major constraint on the accuracy of the model. Weak and strong points of important process approaches are discussed below.

Growth of unshielded millet

The calibrated model yielded acceptable estimates of (unshielded) straw dry matter for production level L3 (water and nitrogen limited conditions), although the nitrogen module is not yet included. This is not surprising, since the model output was fitted by modifying values of crucial crop characteristics. This recalibration comprised introduction of parameter values (Table 6.1) derived from literature for comparable growth conditions. For adaptation from L2 to L3, the value of DM_0 was reduced to 59%, only somewhat lower than the ratio of aerial dry matter in +CR plots (N limitation) and -CR plots (no N limitation) (68%) (Subsection 6.1.2). In addition, we tested the input datasets for production levels L3 and L2 (Table 6.1) against millet field data from nutrient-poor and more fertile soils at ISC, respectively (Appendix B3): WIMISA results reasonably agreed with those field data.

Introduction of nutrient modules could replace the second calibration procedure. That would increase realism, precision and generality of the model. Most nutrient models, at the present stage, account only for nitrogen availability. Whether incorporation of a pure nitrogen (N) module is sufficient for accurate simulation of millet growth in farmers' fields in the Sahel is questionable, since next to N, phosphorus (P) is often growth limiting (Bationo et al., 1990; Payne et al., 1991a). In reality millet does not respond to N fertilizer until the P demand is met (Rebafka, 1993). Methods for N limitation could be derived (translated, adapted or linked) from existing models for instance from CP-BKF3, WaNuLCAS or HyPAR (Mobbs et al., 1997). The HyPAR and WaNuLCAS approaches have the advantage that they consider spatial heterogeneity as required for agroforestry systems. The module CROP already contains the option to consider various levels of N concentration in leaves and their impact on assimilation and respiration. Therefore, the present version can mimic a predetermined N limitation by input of corresponding N concentrations in leaves.

A further weak point of WIMISA is the estimation of LAI. The applied equation is not appropriate for simulating LAI before canopy closure, i.e. LAI = 1, while maximum LAI for millet was 0.5 during the cropping season of 1993. In WIMISA, leaf area was calculated from leaf dry matter using Specific Leaf Area (SLA, m^2 leaf kg^{-1} leaf). Hence, simulated results are extremely sensitive to SLA, physiological parameters characterizing CO_2 assimilation, and assimilate partitioning coefficients for the leaves. In the field, before canopy closure, leaf area development is usually restricted by the potential rates of cell division and expansion, which depend on temperature rather than on the supply of photosynthates (Horie et al., 1979). Therefore, Kropff (1993) applied for the computation of LAI during the early growth period (until LAI = 1) a temperature dependent relative leaf area growth rate:

$$LAI_{ts} = N\ LAI_0\ \exp(RL_{ts}) \qquad\qquad (6.1)$$

where is LAI_{ts} the leaf area index (m^2 leaf m^{-2} surface) at a specific temperature sum after emergence (ts, ^oC d), N is the plant density (plants m^{-2}), LAI_0 the initial area per plant at seedling emergence (m^2 plant^{-1}), and RL_{ts} the relative leaf area growth rate at a specific temperature sum (^oC d).

For millet it is shown that soil temperature affects initiation and appearance of leaves. Optimum temperature for millet leaf appearance rate is 28 - 33 ^oC and temperatures above 37 ^oC, even for short periods (3 - 4 h d^{-1}), restrict this rate (Ong, 1982) and, hence, the relative leaf area growth rate. Soil temperatures above 37 ^oC frequently occurred for several hours a day ($\geq$ 3 h d^{-1}) (Subsection 3.1.4). Consequently, including these temperature effects would yield a lower LAI than the current approach, presumably closer to values found in the field.

Despite the poor estimation of LAI, the model accurately simulates the use and conversion of incident light in terms of assimilates, as indicated by the correspondence of simulated and measured total aerial dry matter. This would suggest that errors in LAI prediction either have been calibrated in the original model by adjusting parameter values or mitigated by compensating errors elsewhere. Thus, if LAI prediction, and light interception are improved, modifications will be required in the description of biomass accumulation, too. At this stage, the equation for leaf area development was not adapted or replaced by Eq. 6.1, because of lack of data (e.g. not enough LAI or SLA data as a function of time, no value of RL_{ts}). Since LAI is the driving force for assimilation, its computation should be improved before considering any further model development.

Estimated grain yield was tested by comparing simulated HI with HI observations from several millet growth studies in the Sahel. Although the HI of millet is rather stable over a range of environmental conditions and biomass productions (Ong and Monteith, 1985), WIMISA, calibrated directly for grain yield would increase the confidence in its simulation. This is important for investigating the impact of windbreaks on grain yield.

Windbreak shielded millet growth
WIMISA gave reasonable estimates of straw and grain yields for millet westward of a windbreak, considering the high spatial variability and the fact that nutrient limitations are not yet included. These simulation results, however, showed less agreement with measurements than those of the unshielded millet-system. The reasons are: (i) the model was calibrated for the unshielded system, (ii) yields of sole crops were derived from preselected well established pockets, whereas in the WB study pockets representative for the plot were harvested, moreover (iii) the Bauhinia plot was severely infested with diseases. It should be noted, that millet production generally shows a high spatial variability in Sahelian fields, which complicates parameterisation as well as evaluation of the model (van Keulen and Seligman, 1989). The

overprediction of straw dry matter is not hampering the present analysis of competition between trees and crops, because the magnitude of simulated yield reductions corresponded with that of the field data. Moreover, competition for nutrients appeared to be negligible in the field (Chapter 3).

Soil water dynamics
Soil water contents were simulated satisfactorily in time and space. Simulations of transpiration (crops and trees) and evaporation need further evaluation, since no data from the experimental year were available for comparison. Some confidence in the model results may be derived from the fact that SWATRER simulated similar values when related to rainfall and LAI. Once transpiration data for model testing are available it would be interesting to apply additionally the Penman-Monteith approach (1965), that generally gives more accurate predictions, for a detailed analysis of the effect of rainfall pattern on crop transpiration and water stress. In the present model the Penman approach was chosen, because of data limitations (aerodynamic resistance and single leaf or canopy resistance).

Roots
Knowledge of the spatial and temporal distribution of tree and crop root systems and soil-root processes of water and nutrient uptake is required to quantify competition for water and nutrients in agroforestry systems. The current understanding of tree root architecture is still fragmentary, and field research is required to produce experimental data to test and develop concepts of soil resource uptake (Lively et al., 1997). This is particularly true for the Bauhinia-millet system for which input data on WB roots were derived from another tree species, which was familiar in terms of root structure.

The uncertainty on estimates of root length distribution and, hence, water use by the windbreak does not allow quantification of the magnitude of competition for water. However, comparison of scenarios for years with different rainfall amounts and patterns allows examination of the importance of water competition in dry and wet years. The results may be considered realistic, because of the following background information: First, several studies in the Sahel have shown the approximate tree root distribution to be realistic, since the major part of tree roots is mostly confined to the upper 0.4 - 0.6 m of the soil. Besides, at the site, trees had no access to groundwater. Secondly, total seasonal transpiration as well as maximum transpiration rates are of the same order of magnitude as found for other tree species at the site and season. Furthermore, the correspondence between simulated and observed normalized yield reductions in the vicinity of the windbreak in 1992, when water was the primary competition factor, indicates that simulated water stress duration and degree are realistic.

Radiation

Numerous physically-based light interception models for agroforestry systems exist, but in WIMISA a simple approach was applied to restrict the number of estimates. Time course and pattern of shade are modelled mechanisticaly for a windbreak component, that is defined as a two-dimensional barrier and whose absorption, reflection and transmission of light are computed implicitly. In contrast to many light-interception models, this approach has the advantage of feasible transfer to other windbreak-cropping systems, since only four easy to obtain parameters are required.

In 1993, for the given system, the reduction in global radiation was estimated well, as shown by the good agreement between simulated and observed radiation intensities at various distances from the WB-barrier. The conversion from global to photosynthetically active radiation (PAR) using a factor 0.5 is appropriate when the ratio PAR/global radiation for light transmitted through the windbreak remains unchanged. This is a rough approximation, since leaves preferentially absorb PAR. Time course measurements of PAR as a function of distance from the windbreak would give a more accurate description of crop available PAR. Unfortunately, the ratio PAR/global radiation transmitted is unknown for a range of windbreak densities and also unknown for the separate fluxes of direct and diffuse radiation. In the current model, the accuracy of local radiation intensities is derived from the explicit computation of direct and diffuse fluxes in small intervals as a function of WB porosity .

General

The dataset was not adequate to derive all parameter values needed in WIMISA, thus, several approximations and assumptions have been made to perform the calculations; e.g. those for the computation of tree water use. Introduction of empirical relations and assumptions is a general problem of agroecosystem models. The possibilities to test biophysical relations rigorously in the field are very limited (time and costs) compared to their demand. Modelling networks for experimental datasets, models and other software (such as GCTE metadata (1997) and CAMASE (Plentinger and Penning de Vries, 1995)) may help to some extent. But, to turn modelling into an accurate, effective and efficient research tool supplementary methods that deal with uncertainty have to be provided. One option is to replace explicit descriptions of processes by simplified more generally valid relations/rules (Meinke, 1996). This requires more basic understanding of most processes than currently available. An alternative is to account quantitatively for the uncertainty in model predictions that are inevitable consequences of uncertain inputs (Monteith, 1997). Analysis of uncertainty (e.g. Sensitivity analysis, Least-Squares estimation, Kalman filter and Monte Carlo approaches) is an important issue when dealing with predictability (Keesman, 1998). Certainly, such analyses do not work for complex systems, but individual crucial subsystems can be tested.

Although the model contains assumptions that require better quantification and evaluation with field data, the processes of competition for water and light are presumably simulated in the correct proportion for the current system, as suggested by the following: simulated global radiation intensities and soil water contents, as a function of time and distance from the windbreak, and percentage of yield reductions normalized to 10 m corresponded well with field observations.

6.5.2   Tree-crop interactions

According to Cannell et al. (1996) there will only be yield benefits from agroforestry systems when trees acquire water, light and nutrients that the crop cannot. In the present windbreak-millet system, species utilized the resources competitively rather than complementary, resulting in yield reductions in the vicinity of the trees. In the three years, yield reductions were found up to about 2 H, similar to results reported for windbreak-cropping systems that are comparable in terms of environment and design (Brenner et al.,1993; Long and Persaud, 1988). The contribution of light and water to the yield reduction varied in the course of the season. At the onset of the season, always water competition existed. Later, the contribution of each of the two factors was strongly dependent on water availability. Under severe drought water remained the major factor (1992), otherwise light was of similar or major importance (1987 and 1993). This sequence of growth-limiting factors can be explained by the fact that shade was becoming intense only later in the season when the tree crown was developed, while in the beginning water availability is always confined to the upper soil where crop and tree roots compete and soil evaporation is still high due to low soil cover and few shade by trees (Keulen and Seligman, 1992).

In the Sahel, water deficiency is one of the prime constraints to crop production. Therefore, at first glance, it seems surprising that in 1992, the year with the highest seasonal rainfall, competition was strongest and even more that it was due to competition for water. This result supports that rainfall pattern is more important than actual amount of rain in these regions.

Windbreaks are often reported to have a positive effect on crop water availability. In our study, sheltering trees reduced evaporation mainly by shade and somewhat by wind speed reduction, to an extent, however, that could not compensate tree water use. Horizontal flow was also far too small to compensate for water uptake by trees. Hence, the crop adjacent to trees suffered from water stress. Horizontal flow (q_x) and vertical flow (q_z) are both driven by the gradient in H. However, for q_x, the gravitational head in H does not play a role. Therefore, in a homogeneous soil with no disturbance (such as at the site) q_z is much larger than q_x.

Obviously, the horizontal gradient in θ created by tree moisture extraction was not sufficient to cause high q_x. Under conditions of spatial heterogeneity in texture and/or infiltration capacity, q_x could become more important for the soil water balance.

In addition to the reduction in evaporation, the model accounts for the facilitative mechanism of light reflection by the windbreak, which is implicitly accounted for in the radiation module. Of minor importance for the present system and, therefore, neglected in this thesis was the impact of the windbreak on air temperature, relative humidity of the air and infiltration of rainwater. It was assumed that all rainwater infiltrates, since at ISC soils are characterized by a very high hydraulic conductivity at saturation (West et al., 1984) and the field was rather level and free of crusts, thus, runoff was negligible. In the experiment, temperature and relative humidity apparently did not vary with distance from the windbreak.

In Mediterranean regions shade is found to have a positive affect on canopy temperature and transpiration, increasing crop production (Dupraz, INRA-LEPSE, pers. comm., 1998). Similar benefits were found for maize under shade nets (25 % shade) in semi-arid Kenya (Lott et al., 1997). The situation was different for the present system where assimilation and yields were severely reduced of the hardly light saturated millet crop grown under shade. At crop row 1, the reduction of the direct radiation flux was increasing from about 10 % to almost 40 % during the cropping season. Shade decreased soil temperatures up to 3 m from the trunks, but hardly affected air temperature. Presumably due to reduced evaporation and transpiration (both processes lower air temperature) this effect vanished. In the field, only directly in or under the trees air temperatures were significantly lower, but this affected the first crop row only (Chapter 3).

No positive impact of the windbreak on millet production was observed nor estimated by the model up to 5 H. Beyond 5 H, grain yield and straw dry matter showed a slight increase, thus, although not visibly, some facilitative effects must have occurred. Further field studies are needed to investigate effects of windbreaks that might improve (grain) yield.

The relative importance of each individual effect depends, apart from the weather, on type of agroforestry system and location (Ong, 1996), and, therefore, there is still much work to be done in the field and in the computer room (Monteith, 1997).

6.5.3   Applications of WIMISA

WIMISA has the potential for a wide range of applications due to its high resolution in time and space and the flexible structure of the model system. Several of these applications have been presented already in the previous sections:

(i)   Prediction of yield potential under potential growth conditions and conditions of water and nitrogen limitation for an unshielded and shielded millet crop.

(ii)   Analysis of soil water balance components, including horizontal flow.

(iii)   Detailed analysis of competition for soil water and light between windbreak trees and crops.

Possible further applications include:

(iv)   Simulation of modifications of instantaneous radiation and wind speed through windbreaks with different characteristics (height, width, porosity), which mimics various tree species, WB-designs and management practices.

(v)   Estimation of the effect of spatial variation in infiltration capacity on the soil water balance and millet yield. In that situation, the runoff and run-on functions, which were switched off for simulations in this thesis, have to be used.

When a nutrient module and capillary rise of soil moisture from the groundwater table are incorporated, the model can be used as a tool to predict yield potential under various environments and for:

(vi)   Estimation of the effect of spatial variability in soil fertility on millet yield potential. This can be tested through induced horizontal variation in nitrogen availability from the soil.

Once the module MICROCLIMATE is completed, such that it considers all essential microclimate changes associated with a windbreak and feedbacks between trees and crop, the model can be used for:

(vii)   Estimation of effects of microclimate changes by windbreaks on millet yield potential in the Sahel.

The present model version can only evaluate effects of WB-design on competition for light and water, which is insufficient for determination of boundary conditions under which windbreaks may be beneficial for sustainable agriculture in the Sahel. An established simple erosion model would be easy to implement in WIMISA and then (additionally to the above mentioned incoproration) the following final target of a windbreak-cropping system model can be achieved:

(viii) Optimization of windbreak-cropping systems in terms of number of tree rows per windbreak, spacing between windbreak lines, WB height and porosity, species and management strategies such as pruning.

6.5.4   Conclusions

Reasonable agreement between simulated and measured dry matter production was obtained for a windbreak-millet cropping system under the conditions in Niger. Since simulated global radiation intensities and soil water content, as a function of time and distance from the windbreak, and yield reductions normalized to 10 m corresponded well with field observations, it can be assumed that the processes of competition for water and light are simulated in the correct proportion.

Thus, the model is appropriate to quantify the relative importance of competition for water and for light in a tree-crop interface, although some process descriptions need further evaluation for application in other environments. In particular the modelling of water uptake by trees requires more data for input and validation to allow quantitative analysis and prediction for windbreak-cropping systems under various environmental conditions. For general applicability a nutrient module has to be incorporated, the static tree root system should be replaced by a dynamic description, and as well as the crop height and SLA be related to environmental conditions. Such modifications as well as incorporation of further windbreak effects can easily be implemented in WIMISA, due to its spatial and temporal flexibility, and the centralization of data communication through a separate module.

In the present windbreak-millet system competition for water and for light outweighed positive effects of lower evaporation, so that yields were reduced in the zone 1 - 4 m (0.5 - 2 H) adjacent to the windbreak.

In fields with no access to groundwater, competition for water between trees and crops is likely to occur at the beginning of the rainy season, when soil water availability is restricted to the upper horizons and transpiration of the windbreak is higher than that of the crop. Horizontal soil water flux $q(x)$ was not important and did not reduce competition for water in the vicinity of the WB line.

Combining our simulation results with data from similar windbreak studies, it becomes evident that not only water but also light can be an important growth limiting factor in windbreak-cropping systems in the semi-arid zone, especially under moderate water stress. This has to be considered when WB-designs and management practices are to be determined. Strong water stress reduces the photosynthetically active leaf area and hence the effect of low light intensities on assimilation per unit leaf area.

Water and light limitation may simultaneously reduce crop assimilation. Consequently, competition models should account for all growth-limiting resources instead of considering only the most growth-liming factor as many of the current models do.

For the Sahel, simulation results indicate that the extent of below- and above-ground competition does not only depend on rainfall amount and radiation intensities, but also depends on rainfall distribution and the period between the seasonal onset of tree and crop growth.

Although it requires further refinement and verification, the WIMISA model is potentially a useful tool for understanding and analysing the complex interactions between species in windbreak-cropping systems. After incorporation of nutrient, complete microclimate and erosion effects the model allows to quantify overall WB effects and screen different WB-designs.

7 GENERAL DISCUSSION AND CONCLUSIONS

The question whether windbreak-cropping systems are beneficial to farmers in the Sahel is not to be answered simply by a yes or a no. Due to the complex interactions of external factors and internal system components, which are not yet completely understood, it is still impossible to provide generally applicable rules for yield predictions from sheltered crops. Moreover, trees can be of multiple use and we must not forget that the answer should be related to farmers' aims and needs in the short- and long-term, which vary from one region to another (Lamers, 1995).

In this context it should be noted, that the present study does not consider direct tree benefits such as supply of wood and livestock fodder, but only indirect WB effects, both positive and negative in terms of crop growth. Therefore, this research might give a rather one-sided and much too negative picture from the possible output of such systems. This is particularly true for the simulation study, since restricted to the competition zone. Prior to evaluation of the implementation of windbreaks in current land-use systems all direct and indirect positive and negative aspects should be integrated and quantified in terms of social and agronomic feasibility and economic profitability, but this is beyond the scope of this study. Economic analyses for each of our seven WB species have been performed to some extent by Lamers (1995). His cost-benefit analysis of grain and straw production showed that the increase in gross margins varied between - 2% for *Andropogon gayanus* and + 35% for *Faidherbia albida*, when yields and costs were not adjusted for land taken out of the production by the windbreaks.

Thus, considering crop yields the present experimental results, in agreement with several other studies in the Sahel, suggest that introduction of windbreaks is of low profitability for farmers-at least in the short-term. Amelioration of the microclimate is not consistent, but sensitive to macroclimate and characteristics of system components (e.g. WB height, spacing, species). For instance in this experiment, with rather low and narrow spaced windbreaks, temperature changes brought by wind speed reduction and shade were opposite and have apparently vanished. Brenner et al. (1995b) found a positive temperature effect on yields towards the middle of the growing season and a negative influence at the onset of the season for 2 - 3 times higher neem windbreaks spaced at 200 m apart. In the future more studies on optimum windbreak designs are needed.

Conservation of soil water is often reported as one of the advantages of windbreaks in semi-arid regions, but experiments illustrate that this is very doubtful to occur in the Sahel. The gain in soil water as result of reduced soil evaporation is shifted simultaneously to crop transpiration

rather than conserved for a later dry spell (Brenner et al., 1995b, Smith et al., 1996b). Nevertheless, water shifting has a somewhat positive impact on crop water use and this may partly explain the yield increases in the centre of the WB plots, where competition was absent but shading and wind speed reduction occured. Simulation results from WIMISA illustrated that shading and wind speed reduction led to reduction in soil evaporation of up to 5 m (2.5 H). Consequently, in the zone 1.5- 2.5 H with (almost) no tree water use this "saved" water became available to the crop. Up to about 1 H severe competition for water occurred during drought periods and reduced yields (experiment and model). However, WIMISA underestimated especially the vertical extension of water competition. Apparently, the assumptions on tree root distribution were not sufficiently accurate. There is generally a lack of knowledge on tree roots and water use. Further study is required to quantify the effects of tree transpiration on the water budgets of WB systems in the Sahel (Smith et al., 1996b).

The experimental results suggest that water competition alone was not responsible for the yield losses, since production was lower adjacent to *Azadirachta indica* WBs, than adjacent to two species that used more water, i.e. *Acacia holosericea* and *Acacia nilotica*. (Smith, 1995). *Azadirachta indica* , which was twice as high as the other two species, might have been more competitive for light. This conclusion was supported by the simulation study, illustrating that shade can be as growth-limiting as water, when water stress is not too strong. Consequently, both the capture of water and light are criteria for the choice of tree/crop species and pruning regimes. Negative effects of competition for water, nutrient, and light can be kept small by pruning (van Noordwijk et al., 1996). However, canopy pruning will also decrease its function as a windbreak. Besides shelter efficiency and competive strength, tree species for the Sahel(ian windbreaks) have to be selected following criteria such as fast establishment and production of feed for livestock and firewood. A survey showed that farmers prefer trees with multiple use (Lamers et al., 1994). Another approach to deal with competition is planting close to the trees a strip of a crop species that is less sensitive to shade or water competition for instance the cash crop cowpea (Lott et al., 1997). Of course, it will never be possible to explore all possible benefits of tree implementation, therefore optimum systems in terms of species, design and management practices have to be chosen towards regional needs and site conditions.

Erosion control probably contributed to the enhanced crop production in the centre of the sheltered fields at ISC, but as mentioned above, overall crop yield increases were not large. Besides, rather low WB spacings (protection up to ca. 7 H) are required to ensure protection of the crop (Banzhaf, 1988; Michels, 1994). This in combination with high investments for WB establishment and maintenance and the low acceptance of farmers (Lamers, 1995) caused that currently parklands and the regeneration of natural woody vegetation get more attention for research and application. On the other hand, none of the windbreak studies covered a sufficient

number of seasons to show the long-term effect of windbreaks on erosion control and protection. Michels (1994) and Sterk (1997) found that wind erosion decreased the amounts of fine soil particles and organic matter remaining in the field, which may have significant negative effects on long-term soil productivity. Before the long-term impact of windbreaks and alternatives such as e.g. parklands on land sustainability are investigated and compared, windbreak-cropping systems remain an option. Especially for the northern Sahel, which is more arid and prone to wind erosion than the region around Niamey.

Covering the soil with crop residues can reduce wind erosion too (Michels, 1994; Sterk 1997), besides mulch benefit with respect to soil fertility, soil organic matter, reduced evaporation, rehabilitation of crusted soils and infiltration (Buerkert et al., 1995; Mando, 1997). Nevertheless, crop residue will not be a panacea for erosion control since the amount needed to achieve sufficient protection is about 1500 kg ha^{-1} (Sterk, 1997), which cannot be provided in most parts of the Sahel, where general biomass production is low and the alternative use of straw high.

The final target to assess the agronomic feasibility and economic profitability of agroforestry systems can most efficiently and effectively be performed by means of models, once crucial gaps in knowledge are filled. A model approach is particularly desirable for such systems since they are complex and require long-term consideration. WIMISA is a first step to achieve a tool for optimising windbreak-cropping designs, including management practices in the Sahel. Despite the uncertainty on tree root distribution the model satisfactorily estimated normalised percentage yield reductions in the 1 - 3 m zone. The model is appropriate to quantify the relative importance of competition for water and for light in the tree-crop interface, although some process descriptions need further evaluation for application in other environments. Improvement can be achieved by linking, replacing and incorporating modules from other existing models such as WaNuLCAS and HyPAR and comparing their simulation results. Incorporation of the WB effect on soil erosion control is difficult due to the lack of understanding of a regional mass budget; the locations of erosion and deposition are hard to determine (Hermann, et al., 1996; Hermann and Sterk, 1996).

To summarise it can be concluded that the introduction of trees in Sahelian agricultural systems is an appropriate option for land use since it appears to be a realistic way to meet three major problems of the Sahel at the same time, i.e. land degradation, and the increasing demand for (fire)wood and livestock fodder. The choice of tree/crop combinations and their arrangement are still issues to be investigated on a regional scale. However, with the current progression in experimental knowledge and model development some answers can be expected in the near future. High priority for further research should be given to:

- below-ground interactions of species, their root architecture, dynamics and functioning, to fill the gap of resources utilisation - one of the major issues in agroforestry systems and modelling,
- long-term effects of wind erosion control on soil fertility and sustainability of agricultural fields to gain a better insight in the effectiveness of the primary function of windbreaks
- improving and testing existing agroforestry models by means of uncertainty modelling and comparison with additional field data,
- integration of social, economic and biophysical driving forces that bring changes in land use for which windbreak-cropping systems is only one option.

SUMMARY

In the Sahelian zone, future food supply is insecure due to increasing land degradation. Wind erosion contributes significantly to impoverishment of the sandy soils, which are often loose and sparsely covered by vegetation for most of the year. At the onset of the growing season (May - July), strong winds often precede rains and may cause damage to the young seedlings by abrasion and burial. A possible control measure is the implementation of windbreaks (WBs) that reduce the wind velocity near the soil surface, thus protecting soil and crops. Moreover, the change in air flow may lead to a more favourable crop microclimate. Higher crop yields and increases in the long-term sustainability of crop production may be the result of effective windbreaks integrated in crops. However, windbreaks also compete with crops for limited resources, which may outweigh their potential benefits.

Windbreak experiments, reported in literature, illustrate various benefits as well as negative impacts of windbreaks on crop growth (Chapter 1). In addition to a more favourable microclimate and reduced wind erosion, increased soil fertility, and complementary use of resources by trees and crops are possible agroforestry benefits. On the other hand, competition and allelopathic interactions between species, as well as attraction of pests and diseases by trees may reduce crop production. Whether the overall windbreak effect results in yield increases or losses depends on many interacting factors, e.g. climate, soil properties, crop species and WB-design. The few studies performed in semi-arid regions give insufficient insights to formulate generally applicable rules that allow extrapolation of experimental results to other locations or from one WB-design to another. Understanding of the tree-crop interactions is required for the design of optimum windbreak-cropping systems that can provide an option for sustainable land use in the Sahel.

This research aimed at enhancing the understanding of positive and negative influences of windbreaks on crop production by i) collecting field data (Part A) and ii) analyzing crucial tree-crop interactions in terms of dynamic and spatial occurrence by means of a model (Part B).

Between 1991 - 1993, experiments were performed at the ICRISAT Sahelian Center (ISC), Niger, to study the effects of low, narrowly spaced windbreaks on microclimate, light, water and nutrient resources at the windbreak-crop interface, and the growth of pearl millet (*Pennisetum glaucum*). Millet, a C_4 tropical cereal, is the principal food crop in Niger, since it is particularly adapted to conditions of high temperatures, nutrient-poor soils and low rainfall. The windbreaks were north-south oriented, i.e. perpendicular to storms and prevailing winds

and, hence, protecting crops sown on their west side. The agroforestry system under study consisted of various shelter species and plots without windbreaks as control. Measurements were performed along transects across the tree-crop interface. Radiation, wind speed, relative humidity, and air temperatures were measured continuously and soil temperatures occasionally measured in *Bauhinia rufescens* plots. Bauhinia windbreaks were 2 and 3 m high and had a porosity of 0.9 and 0.2 at the onset and the end of the growing season, respectively.

Crop yields adjacent to seven windbreak species and in control plots were determined. In two rather wet years of experiments it was found that the overall yield in windbreak plots was slightly (mostly not significant) higher than in the control plots. Up to a distance of 2.5 H (with H the windbreak height) from windbreaks lower yields were measured than in the middle of the plots.

Growth reduction in the vicinity of the windbreak was more than compensated by increased production in the center of the plots when averaged over all plots. The magnitude of yield increases varied among the tree species, e.g. in Bauhina sheltered crops this positive effect was rather small. From the experiments the causes for yield increases remained unclear, since no amelioration in the microclimate was observed. Air temperature and relative humidity (at the top of the sheltered crop) were constant with distance from the Bauhinia windbreak, although the shelter reduced wind velocity up to a minimum of 5 H. Generally, the influence of shade and wind speed on temperature and relative humidity are opposite and, presumably, negated in the present system. Shade, however, lowered soil temperatures, but this had no measurable impact on crop emergence and yields. Protection against wind erosion, enhanced water availability and/or small microclimate modifications (too small to be recorded) may have caused higher yields.

The zone of severe yield reduction (0.5 - 1.5 H) corresponded to that of the strongest reduction in radiation and soil moisture, indicating competition effects. To assess competition between crops and windbreaks, soil water and nutrient status were observed in the windbreak-crop interface and in control plots. Nutrient status did not vary significantly across the tree-crop interface or between windbreak and control plots, whereas soil moisture was strongly reduced in the vicinity of trees during dry periods. Then, trees were likely to compete with crops for water since they had no access to groundwater. Competition for water apparently occurred although total rainfall was rather high in the experimental years. From these results it was concluded that in dry years competition for water would be much stronger. That this is not necessarily the case, was shown by a simulation study covering a dry and two wet years (Part B).

Competition for water and light, and wind speed reduction within the 0 - 5 H tree-crop zone were considered to be of major importance in the agroforestry experiment, as described in Part A of this thesis. Consequently, to assess the agronomic feasibility of windbreaks in the Sahel, those effects have to be quantified.

Assessment of the competitive effects between trees and crop is complicated, due to difficulties in determining below-ground competition and interference with other tree-crop interactions. A model approach is helpful to quantify and integrate individual effects of tree-crop interactions. When starting this study, no windbreak-cropping system model was available. Existing crop models lacked spatial heterogeneity, and temporal detail as required for the description of agroforestry systems. Therefore, a model, WIMISA (WIndbreak MIllet SAhel), has been developed by combining methods from existing models with newly developed concepts, with special attention to resolution in time and space.

WIMISA simulates crop growth as influenced by local soil moisture and radiation intensity simultaneously for a number of rows parallel to a windbreak in daily time steps. Soil moisture content and incoming radiation intensities are computed at process level in smaller time steps. Windbreak growth is not simulated, but windbreak characteristics are introduced either as fixed values or as time dependent forcing functions. As knowledge of the WB characteristics is limited, competition for light, tree water uptake, and wind speed reduction are described using a simple model of the windbreak component to restrict the number of assumptions. Reduction in wind speed is incorporated through an empirical factor for wind velocities in the first 5 H from the windbreak.

Competition for light is incorporated as light interception by a two-dimensional WB-barrier, as a function of its height and density (both increasing during the cropping season). WIMISA calculates instantaneous fluxes of direct and diffuse radiation for each crop row separately at intervals of 6 minutes. The interval for the computation of CO_2 assimilation was set in accordance with the radiation calculations. Soil water flow is simulated in two dimensions to account for horizontal gradients due to different water extraction by trees and crop, and horizontally varying evapotranspiration. Spatial detail in vertical and horizontal direction is introduced through an arrangement of compartments. The soil water module uses a time step that is adjusted automatically to water flow rate and thickness of the soil compartment. Competition for water is expressed by distributing available soil water between trees and crop in proportion to their uptake rates in a non-competitive situation. Water uptake is calculated on the basis of root length density distribution.

WIMISA was parameterised for millet, the tree species *Bauhinia rufescens* and soil characteristics of ISC. Specific crop parameters of the model for a sole millet system were

determined throughout the growing season in a separate plot outside the influence of a windbreak. Simulations were confined to the competition zone (i.e. 5 H).

Simulation results of the windbreak-cropping system were evaluated with data from Bauhinia plots of the 1992 and 1993 growing seasons. WIMISA gave reasonable estimates of straw and grain yields for millet westward of a windbreak, considering the generally high spatial variability and the fact that nutrient limitations are not included. Grain yield beyond 3 m was underestimated, probably due to windbreak effects not included in the model. This suggests that in addition to light other microclimate factors might have been somewhat modified by the windbreak, although not observed. Since simulated global radiation intensities and soil water contents, as a function of time and distance from the windbreak, and percentage yield reductions normalized to 10 m corresponded well with field observations, it can be assumed, that the processes of competition for water and light are simulated in the correct proportion.

In the present agroforestry system, species utilized the resources competitively rather than complementary, resulting in (ca. 20 - 30 %) yield reductions in the 0.5 - 2 H zone adjacent to the windbreak. This extent of competition zone and magnitude of yield losses correspond to field data and results reported for other windbreak-cropping systems in the Sahel.

Three scenarios where competition effects for water and for light were separated by turning off one of the effects during simulations, were compared for the 1987, 1992 and 1993 growing seasons. Surprisingly, water and total competition were highest in the wet year 1992, intermediate in the dry year 1987 and lowest in the wet year 1993. In fields with no access to groundwater, competition for water between trees and crops is likely to occur at the beginning of the rainy season, when available soil water is restricted to the upper horizons and transpiration of the windbreak is higher than that of the crop. Neither horizontal water flow nor reduced soil evaporation as a result of shade could compensate for tree water use. Under severe drought, water remained the major factor (1992), otherwise light was of similar or major importance (1987 and 1993). Simulation results indicate that the degree of light and water competition also depends on rainfall distribution and the time laps between the seasonal onset of tree and crop growth.

The model is appropriate to quantify the relative importance of competition for water and light in a windbreak-millet system, although some process descriptions need further refinement (i.e. LAI development) and evaluation for application in other environments. In particular, modelling of tree-root water uptake requires more data for input and validation. Once, nutrient, complete microclimate and erosion modules have been incorporated in WIMISA, the model allows quantification of the overall WB effects and screening of different windbreak-cropping systems.

RÉSUMÉ

Dans la zone sahélienne, l'approvisionnement en nourriture dans l'avenir est incertain à cause de la dégradation progressive des terres. L'érosion éolienne contribue de façon significative à l'appauvrissement des sols sablonneux qui sont souvent meubles et très peu recouverts d'une végétation pendant la majeure partie de l'année. Au début de la saison des cultures (mai-juillet), des vents forts précèdent souvent les pluies et peuvent causer des dégâts aux jeunes semis par l'abrasion et l'ensablement. Une mesure de contrôle possible est l'implantation de brise-vents qui réduisent la vélocité du vent au ras du sol, protégeant alors le sol et les cultures. De plus, le changement du courant d'air peut créer un microclimat plus favorable pour les cultures. Des rendements de cultures plus élevés et l'augmentation à long terme d'une production agricole durable peuvent être le résultat effectif des brise-vents intégrés aux cultures. Cependant, les brise-vents rivalisent aussi avec les cultures pour les ressources limitées, ce qui peut diminuer leurs bénéfices potentiels.

Selon la littérature, les expériences sur les brise-vents, présentent aussi bien des résultats bénéfiques que des impacts négatifs des brise-vents sur la croissance des cultures (Chapitre 1). En plus de la création d'un microclimat plus favorable, de la réduction de l'érosion éolienne, de l'augmentation de la fertilité du sol, l'utilisation complémentaire des ressources par les arbres et les cultures sont des avantages possibles pour l'agroforesterie. D'autre part, la compétition et les inter-actions alléopathiques entre les espèces, ainsi que l'attraction des pestes et des maladies par les arbres, peuvent réduire la production agricole. Que l'effet général du brise-vent résulte en une augmentation de la production ou en pertes dépend de plusieurs facteurs inter-actifs tels que le climat, les propriétés du sol, les espèces de cultures et la disposition des brise-vents. Les quelques études réalisées dans les régions semi-arides donnent un aperçu insuffisant pour formuler des règles généralement applicables qui permettent l'extrapolation des résultats expérimentaux à d'autres localités ou d'une disposition de brise-vents à une autre. La compréhension des inter-actions entre arbres et cultures est nécessaire pour la disposition des systèmes optimum de cultures-brise-vents qui peuvent fournir une option pour l'utilisation durable des terres au Sahel.

Cette recherche a pour but de renforcer la compréhension des influences négatives et positives des brises-vents sur la production agricole par i) la collecte des données de terrain (partie A) et ii) l'analyse des inter-actions crutiales arbres-cultures en termes d'existence dynamique et spaciale au moyen d'un modèle (Partie B).

Entre 1991 - 1993, des expériences ont été menées au Centre Sahélien (ISC) de l'ICRISAT, au Niger pour étudier les effets des brise-vents à espacement moyen et étroit sur le microclimat, la lumière, les ressources en eau et en nutriments à l'interface culture-brise-vent, et la croissance du petit mil (*Pennisetum glaucum*). Le mil, un céréale tropical C_4, est la principale culture vivrière au Niger, puisqu'il est particulièrement adapté aux conditions de températures élevées, des sols pauvres en nutriments et de faible pluviométrie. Les brise-vents étaient orientés nord-sud, c'est-à-dire perpendiculaires aux tempêtes et aux vents dominants, protégeant ainsi les cultures semées du côté ouest. Le système de l'agroforesterie en étude consistait en diverses espèces protégées et de parcelles sans brise-vents comme moyen de contrôle. Des mesures étaient effectuées le long des transects à travers l'interface arbre-culture. La radiation, la vitesse du vent, l'humidité relative, et les températures de l'air étaient continuellement et celles du sol occasionnellement mesurées dans les parcelless de *Bauhinia rufescens*. Les brise-vents de *Bauhinia rufescens* avaient une hauteur de 2 à 3 m et avaient une porosité de 0.9 et 0.2 respectivement au début et à la fin de la saison des cultures.

Les rendements des cultures adjacentes à 7 espèces de brise-vent et dans les parcelles témoins, étaient déterminés. En deux années plutôt humides d'expérimentation il a été établi que le rendement global dans les parcelles à brise-vents était légèrement (beaucoup moins significatif) plus élevé que dans les parcelles témoins. Jusqu'à une distance de 2.5 H (avec H la hauteur du brise-vent) des brise-vents, on a mesuré des rendements plus faibles qu'au milieu des parcelles.

La réduction de la performance à proximité du brise-vent était plus que compensée par une production accrue dans le centre des parcelles quand on établi la moyenne de toutes les parcelles. L'ampleur des augmentations du rendement variait entre les espèces d'arbres, par exemple, à l'intérieur des cultures protégées par les Bauhina, cet effet positif était plutôt moindre. A partir de ces expériences on ne peut pas établir clairement les causes des augmentations de rendement, car aucune amélioration n'a été observée au niveau du microclimat. La température de l'air et l'humidité relative (au sommet des cultures protégées) étaient constantes avec la distance du brise-vent de Bauhinia, quoique la protection ait réduit la vélocité du vent jusqu'à un minimum de 5 H. Généralement, les influences de l'ombre et de la vitesse du vent sur la température et sur l'humidité relative, sont opposées et, vraissemblablement, annulées dans le système actuel. L'ombre cependant, réduit les températures du sol, mais cela n'avait aucun impact mesurable sur l'émergence des cultures et les rendements. La protection contre l'érosion éolienne a renforcé la disponibilité de l'eau et/ou les petites modifications du microclimat (très faibles pour être enregistrées) peuvent avoir entrainé des rendements plus élevés.

La zone où le rendement a considérablement baissé (0.5 - 1.5 H) correspondait à la plus forte réduction de radiation et d'humidité du sol, indicant les effets compétitifs. Pour évaluer la compétition entre cultures et brise-vents, l'eau du sol et l'état nutritif étaient observés dans l'interface brise vent-cultures et dans les parcelles témoins, tandis que l'humidité du sol était fortement réduite à proximité des arbres durant les périodes sèches. Ensuite, il y avait de fortes chances que les arbres et les cultures se concurrencent pour l'eau puisqu'ils ne peuvent pas atteindre la nappe d'eau. La compétition pour l'eau a vraissemblablement eu lieu quoique la pluviométrie était plutôt élevée pendant les années expérimentales. A partir de ces résultats il a été conclu que pendant des années sèches la compétition pour l'eau serait beaucoup plus forte. Pour montrer que cela n'est pas nécessairement le cas, une étude de simulation couvrant une année sèche et deux années humides a été effectuée(Partie B).

La compétition pour l'eau et la lumière, et la réduction de la vitesse du vent de 0 - 5 H à l'intérieur de la zone culture-arbre étaient considérées être d'une importance majeure dans l'expérimentation agroforestière, comme cela a été décrite dans la Partie A de cette thèse. Par conséquent, pour évaluer la faisabilité agronomique de brise-vents dans le Sahel, les effets compétitifs doivent être quantifiés.

L'évaluation des effets compétitifs entre arbres et cultures est compliquée à cause des difficultés à déterminer la compétition sous sol et l'interférence avec d'autres interactions arbre-culture. Un modèle d'approche est utile pour quantifier et intégrer les effets individuels des interactions arbre-culture. Au début de cette étude, aucun modèle de système de culture avec brise-vent n'était disponible. Les modèles existants sur les cultures manquaient d'hétérogénéité spatiale, et de détail temporel comme requis pour la description des systèmes d'agroforesterie. Par conséquent, un modèle WIMISA (WIndbreak MIllet SAhel), a été développé en combinant des méthodes des modèles existants avec des concepts nouvèllement développés, en accordant une attention toute particulière à la résolution dans le temps et dans l'espace.

WIMISA simule la croissance de la culture comme étant influencée simultanément par l'humidité du sol et l'intensité de radiation pour un certain nombre de lignes parallèles à un brise-vent pendant différentes étapes de la journée. Le taux d'humidité du sol et les intensités de radiation qui arrivent sont calculés au niveau de l'opération en petits intervalles de temps. La croissance de brise-vent n'a pas été simulée, mais les caracteristiques du brise-vent sont introduites soit comme des valeurs déterminées soit comme des fonctions dépendantes du temps. Comme la connaissance des caractéristiques du brise-vents est limitée, la compétition pour la lumière, le prélèvement d'eau par l'arbre et la réduction de la vitesse du vent sont décrites en utilisant un modèle simple du composant de brise-vent pour limiter le nombre des

hypothèses. La réduction de la vitesse du vent est incorporée à travers un facteur empirique pour les vélocités du vent dans les premiers 5 H à partir du brise-vent.

La compétition pour la lumière est incorporée comme l'interception de la lumière par une barrière brise-vent à double dimension, en tant qu'une fonction de sa hauteur et de sa densité (les deux croissants au cours de la saison des cultures). WIMISA calcule les flux instantanés de la radiation directe et diffuse pour chaque ligne de cultures séparément par intervalles de 6 minutes. L'intervalle de calcul de l'assimilation CO_2 était établi en conformité avec les calculs de radiation. Le mouvement de l'eau du sol est simulé en deux dimensions pour prendre en compte les inclinaisons horizontales dûes aux différents prélèvements d'eau par les arbres et les cultures, et l'évapotranspiration qui varie horizontalement. Le détail spatial selon une direction verticale et horizontale est introduit grâce à un arrangement des compartiments. Le module d'eau du sol utilise un intervalle de temps qui est automatiquement ajusté au mouvement de l'eau et à l'épaisseur du compartiment du sol. La compétition pour l'eau est exprimée en distribuant l'eau du sol disponible entre arbres et cultures proportionnellement à leur taux d'absorption dans une situation non compétitive. L'absorption d'eau est calculée sur la base de la distribution de la densité et de la longueur de la racine.

WIMISA était paramètré pour le mil, l'espèce *Bauhinia rufescens* et les caractéristiques du sol de ISC. Des critères spécifiques de culture du modèle étaient déterminés pour un seul système de mil durant toute la saison de croissance dans une parcelle séparée en dehors de l'influence de brise-vent. Les simulations étaient limitées à la zone de compétition (c'est-à-dire 5 H).

Les résultats de simulation du système de culture avec brise-vent étaient évalués avec les données des parcelles de Bauhinia des saisons de croissance de 1992 et 1993. WIMISA a donné des estimations raisonnables de production de paille et de grains pour le mil situé côté ouest du brise-vent, en tenant compte de la forte variabilité spatiale et du fait que les limitations des nutriments ne sont pas inclus. La production de grains au delà de 3 m était sous-estimée, probablement à cause des effets du brise-vent qui ne sont pas inclus dans le modèle. Ce qui veut dire que le microclimat a dû plus ou moins être modifié par le brise-vent, quoique cela n'ait pas été observé. Puisque la simulation des intensités de radiation globale et des taux d'humidité du sol, comme une fonction de temps et de distance par rapport au brise-vent, et que le pourcentage de baisses de rendements normalisé à 10 m correspondaient bien avec les observations de terrain, on peut conclure que les procédés de compétition pour l'eau et la lumière ont été correctement estimés.

Dans le système présent d'agroforesterie, les espèces, au lieu d'utiliser les ressources d'une manière complémentaire, elles les utilisaient d'une manière compétitive, ce qui résulte en (ca. 20

- 30%) des baisses de rendement dans la zone de 0.5 - 2 H adjacente au brise-vent. Cette surperficie de la zone de compétition et l'ampleur des pertes de production correspondent aux données de terrain et aux résultats mentionnés pour d'autres systèmes de culture avec brise-vent au Sahel.

Trois scénarios étaient comparés pour les saisons de croissance 1987, 1992 et 1993. Pendant les simulations, les effets de compétition pour l'eau et pour la lumière étaient séparés en arrêtant un des effets. Etrangement, l'eau et la compétition totale étaient plus élevées pendant l'année de bonnes pluies 1992, moyens pendant l'année de sècheresse, et le plus bas pendant l'année de bonnes pluies 1993. N'ayant pas accès à la nappe phréatique dans les champs, les arbres et les cultures compétissent vraissemblablement pour l'eau au dédut de la saison des pluies, quand l'eau disponible du sol est limitée aux horizons de surface et que la transpiration du brise-vent est suppérieure à celle de la culture. Ni le mouvement horizontal de l'eau, ni la réduction de l'évaporation du sol dûe à l'ombre ne peuvent compenser l'utilisation d'eau par l'arbre. En période de grave sècheresse, l'eau demeurait le facteur principal (1992), autrement la lumière était d'une importance similaire ou capitale (1987 et 1993). Les résultats des simulations indiquent que le degré de compétition pour l'eau et pour la lumière depend aussi de la répartition des pluies et de l'intervalle de temps entre le début de la saison de croissance de l'arbre et de la culture.

SAMENVATTING

De toekomstige voedselvoorziening in de Sahel zone is onzeker vanwege de voortschrijdende landdegradatie. Winderosie is medeverantwoordelijk voor de verschraling van de gronden, die vaak zandig, los en schaars met vegetatie bedekt zijn. In het begin van het groeiseizoen (mei-juli) treden, voorafgaand aan de regen, vaak stormen op. Deze stormen kunnen veel winderosie veroorzaken en kiemplanten beschadigen of bedekken. Een mogelijke beheersmaatregel om de windsnelheden aan de grond te reduceren en zo de bodem en het gewas te beschermen is het aanbrengen van windhagen. Tevens kunnen windhagen de luchtstroming beïnvloeden, zodat een gunstiger microklimaat ontstaat voor het gewas. Integratie van effectieve windhagen in het gewas kan op de langere termijn een duurzaam hogere gewasproductie tot stand brengen. Echter, windhagen concurreren met het gewas om de natuurlijke hulpbronnen zoals water en licht. Dit kan de potentiële voordelen van windhagen te niet doen.

In de literatuur zijn verschillende experimenten met windhagen beschreven die zowel de gunstige als de negatieve effecten van windhagen op het gewas illustreren (Hoofdstuk 1). Benevens een gunstiger microklimaat en reductie van winderosie kunnen windhagen nog andere voordelen brengen zoals een verhoogde bodemvruchtbaarheid en complementair gebruik van natuurlijke hulpbronnen. Aan de andere kant kunnen windhagen een lagere gewasproductie veroorzaken in geval van allelopathie of door het aantrekken van ziekten en plagen. Of windhagen uiteindelijk tot hogere gewasopbrengsten leiden hangt van vele factoren af, bijvoorbeeld bodemeigenschappen, gewassoort en het ontwerp van de windhagen. De studies die in semi-aride gebieden zijn gedaan hebben onvoldoende inzicht opgeleverd om algemeen geldende regels te formuleren die het mogelijk maken om experimentele kennis van de ene locatie of windhaagontwerp naar andere situaties te extrapoleren. Een vereiste voor het ontwikkelen van een optimaal windhaag-gewassysteem dat bijdraagt aan meer duurzaam landgebruik in de Sahel is een grondige kennis van de boom-gewas interacties.

Het doel van dit onderzoek is het inzicht in de positieve en negatieve invloeden van windhagen op de productie van gierst te verhogen. Het onderzoek omvat i) het verzamelen van veldgegevens (deel A) en ii) het analyseren van de optredende effecten van windhagen op het gewas in ruimte en tijd door middel van een model (deel B).

De experimenten zijn bij het ICRISAT Sahelian Centre (ISC) in Niger uitgevoerd. De invloed van windhagen in een gierstgewas op licht-, water- en nutriëntenvoorziening, gewasgroei en microclimaat van het gewas is experimenteel onderzocht. Gierst, een tropische C_4 graansoort,

is de voornaamste voedselbron in Niger, uitstekend aangepast aan de hoge temperaturen, nutriëntenarme gronden en de lage neerslag. De windhagen waren noord-zuid gericht dus loodrecht op de inkomende (storm)winden uit het oosten en het gewas ter westerzijde beschermend. Het agroforestry systeem bestond uit meerdere velden (plots) met windhagen van verschillende soorten. Ter vergelijking hadden enkele velden geen windhaag (controle). Straling, windsnelheid, relatieve luchtvochtigheid en luchttemperatuur werden doorlopend gemeten. Bodemtemperaturen werden van tijd tot tijd in een *Bauhinia rufescens* (een van de boomsoorten voor de windhaag) veld gemeten. Deze Bauhinia windhagen waren aan het begin van het groeiseizoen 2 meter hoog en hadden een porositeit van 0.9. Aan het eind van het groeiseizoen waren ze 3 meter hoog met een porositeit van 0.2.

De gewasopbrengsten grenzend aan zeven windhaagsoorten en in de controlevelden zijn van twee relatief natte groeiseizoenen bepaald. De totale obprengst van beschermde velden was steeds hoger dan van de velden zonder windhaag. Tot een afstand van ca. 2.5 keer de hoogte van de windhaag (H) werd echter een lagere opbrengst gevonden dan in het midden van het veld.

De groeireductie in de nabijheid van een windhaag werd, gemiddeld over alle velden, meer dan gecompenseerd door de verhoogde produktie in het midden van het veld. Experimenteel werd geen verbetering van het microklimaat gevonden, zodat de oorzaak van de opbrengstverhoging onzeker bleef. Temperatuur en luchtvochtigheid (aan de bovenkant van het gewas) bleken constant met de afstand tot de Bauhinia windhaag, ondanks de gevonden verlaging van de windsnelheid tot een afstand van 5 H. De schaduw van de windhagen leidde weliswaar tot lagere bodemtemperaturen, maar dit had geen invloed op de gewasontwikkeling. Het is mogelijk dat de combinatie van lagere windsnelheden en beschaduwing elkaar in de individuele effecten opheft.

Een sterke opbrengstverlaging werd gevonden in de zone 0.5 - 1.5 H grenzend aan de windhaag. Dit komt overeen met de zone waarin de sterkste reductie in straling en bodemvocht gevonden werd en duidt dus op competitie. Om meer inzicht in deze competitie-effecten tussen gewas en windhaag te verkrijgen werden de bodemvocht- en nutriëntentoestand op verschillende afstanden van de windhagen en in de controlevelden gemeten. In de nutriëntentoestand werd geen noemenswaardig verschil gevonden. Daarentegen werd een sterke reductie in bodemvocht in de nabijheid van de windhaag gemetem gedurende droge perioden. Aangezien de bomenwortels geen toegang tot het grondwater hadden was competitie voor bodemvocht tussen de windhaag en het gewas te verwachten. Interessant is dat deze competitie optrad ondanks het feit dat in beide jaren de totale neerslag relatief hoog was. Uit eerdere experimenten was geconcludeerd dat in droge jaren de competitie om bodemvocht hoger zou

zijn dan in natte jaren. Dat dit niet noodzakelijkerwijs het geval hoeft te zijn is in dit proefschrift door middel van een simulatiestudie aangetoond.

Competitie om licht en water, als ook de reductie in de windsnelheid in de zone van 0 tot 5 H van de windhaag zijn de belangrijkste studieobjecten in dit agroforestry experiment (Deel A van dit proefschrift). Derhalve dienen deze effecten met het oog op de agronomische haalbaarheid van windhagen in de Sahel gekwantificeerd te worden. Het bestuderen van deze competitieeffecten is gecompliceerd omdat de ondergrondse competitie moeilijk is te meten en ook vanwege de interacties met andere boom-gewas wisselwerkingen. Een modelmatige aanpak kan hierbij behulpzaam zijn doordat individuele effecten gekwantificeerd en met elkaar in verband gebracht kunnen worden. Bij begin van deze studie waren geen windhaag-gewas modellen beschikbaar. Bestaande gewasgroeimodellen konden geen horizontale heterogeniteit simuleren en de gebruikte tijdsintervallen waren te lang voor agroforestry modelling. Gedurende het hier beschreven onderzoek is een model, WIMISA (WIndbreak-MIllet-SAhel), ontwikkeld dat op een combinatie van bestaande modellen en nieuwe concepten berust. Vooral de vereiste hoge resolutie in tijd en ruimte heeft hierbij een grote rol gespeeld.

WIMISA simuleert de groei van een aantal parallel aan de windhaag geplaatste plantrijen simultaan op basis van lokale bodemvochtgehaltes en straling. Bodemvocht en stralingsintensiteit worden berekend door de onderliggende processen met kleine tijdstappen te integreren. De groei van de windhaag zelf wordt niet gesimuleerd, maar de karakteristieke grootheden worden als input gegeven. Voor deze eenvoudige benadering is gekozen om het aantal aannamen in de beschrijving van competitieeffecten te beperken. De windsnelheidsreductie wordt beschreven via een empirische faktor toegepast op de eerste 5 H. De lichtcompetitie is beschreven als lichtinterceptie door een twee-dimensionale windhaagbarrière met een gedurende het seizoen toenemende hoogte en dichtheid. WIMISA berekent de momentane directe en diffuse invallende straling voor iedere plantrij apart met tijdsintervallen van 6 minuten. Dit tijdsinterval werd ook toegepast in de berekening van de CO_2 assimilatie. Waterstroming in de bodem wordt in twee dimensies gesimuleerd om met horizontale gradiënten, die door horizontaal variërende evopotranspiratie onstaan, rekening te kunnen houden. De bodemwater module voert de simulatie uit voor een fijn rooster bestaande uit compartimenten. De tijdstap voor integratie van de bodemwaterstroming wordt endogeen bepaald op grond van de stroomsnelheid en compartimentgrootte. Competitie om water wordt in het model beschreven door het lokaal beschikbare bodemvocht tussen windhaag en gewas te verdelen in evenredigheid naar de opnamesnelheden in een niet competitieve situatie. De wateropnamesnelheden door de vegetatie worden berekend op basis van de worteldichtheidsverdeling in de bodem.

WIMISA is geparameteriseerd voor gierst, de boomsoort Bauhinia en de bodemkarakteristieken van ISC. Specifieke gewasparameters voor het model zijn bepaald in een giertsperceel zonder windhaaginvloeden. De simulatieresultaten voor stroo- en korrelopbrengsten kwamen redelijk overeen met de experimentele gegevens uit de groeiseizoenen 1992 en 1993, vooral wanneer de hoge ruimtelijke variabiliteit in aanmerking genomen wordt en het feit dat de invloed van nutriëntengebrek niet in het model is opgenomen. De korrelopbrengst op afstanden van meer dan 3 m van de windhaag werd onderschat, wellicht doordat windhaageffecten opgetreden zijn die niet in het model zijn verwerkt. Op grond van de goede overeenkomst tussen gesimuleerde en gemeten stralingsintensiteiten en bodemvochtgehaltes, in afhankelijkheid van tijd en afstand tot de windhaag, en de opbrengstreducties gestandaardiseerd tot die op 10 m kan aangenomen worden dat de processen voor water- en lichtcompetitie in de juiste verhouding gesimuleerd worden.

In het onderzochte gierst-windhaag systeem was het gebruik van de natuurlijke hulpbronnen meer competitief dan complementair. Dit veroorzaakte een vermindering van de opbrengst in de 0.5 tot 2 m zone grenzend aan de windhaag. De gesimuleerde invloedsfeer komt goed overeen met de experimenteel gevonden waarde en met resultaten uit andere windhaag-gewas experimenten in de Sahel. In verschillende scenario's is onderscheid gemaakt tussen de competitie om licht en water door één van beide effecten uit te schakelen in de simulaties voor 1987, 1992 en 1993. De competitie om water was het sterkst in het natte jaar 1992, intermediair in het droge jaar 1987 en het zwakst in het natte jaar 1993. Op plaatsen waar de bomen geen toegang tot het grondwater hebben is competitie om water zeer waarschijnlijk het sterkst aan het begin van het regenseizoen wanneer het beschikbare bodemvocht beperkt is tot de allerbovenste bodemlagen en de transpiratie van de windhaag hoger is dan die van het gewas. Noch de horizontale waterstroming, noch de door beschaduwing verminderde evaporatie konden de wateropname door de windhaag compenseren. Gedurende ernstige droogteperioden was water de belangrijkste competitiefaktor (1992), in andere omstandigheden was licht van gelijk belang of zelfs belangrijker (1987 en 1993). De simulatieresultaten laten zien dat de mate van licht- en watercompetitie ook afhangt van de neerslagverdeling over het groeiseizoen en van de lengte van de periode tussen de start van boomgroei en gewasgroei.

Het model is geschikt om de relatieve invloed van competitie om licht en water in een gedefineerd windhaag-gierst system te kwantificeren. Sommige processen eisen echter een meer gedetailleerde beschrijving en/of verdere evaluatie, voordat het model ook betrouwbaar in andere omgevingen toegepast kan worden. Indien nutriënten-, temperatuur- en erosiemodules in WIMISA worden ingebouwd, kan het model toegepast worden voor verkennend onderzoek aan windhaag-gewas systemen en vooral voor het evalueren van beleidsmaatregelen ten aanzien van agroforestry systemen.

REFERENCES

Aase, J.K., 1978. Relationship between leaf area and dry matter in winter wheat. Agron. J. 70: 563-565.

Alvenäs, G. and Jansson, P.-E., 1997. Model for evaporation, moisture and temperature of bare soil: calibration and sensitivity analysis. Agric. For. Met. *(In press)*

Azam-Ali, S.N., Gregory, P.J. and Monteith, J.L., 1984. Effects of planting density on water use and productivity of pearl millet *(Pennisetum typhoides)* grown on stored water. 1. Growth of roots and shoots. Expl. Agric. 20: 203-214.

Banzhaf, J., 1988. Auswirkungen von Windschutzstreifen aus Brachlandvegetation auf Wachstum und Ertragsbildung von Perlhirse *(Pennisetum americanum* (L.) Leeke) und Cowpea *(Vigna unguiculata* (L.) Walp.) im südlichen Sahel Westafrikas. Ph.D. Thesis, University of Hohenheim, Hohenheim, Germany.

Banzhaf, J., Leihner, D.E., Buerkert, A. and Serafini, P.G., 1992. Soil tillage and windbreak effects on millet and cowpea: I. Wind speed, evaporation, and wind erosion. Agron. J. 84(6): 1056-1060.

Bationo, A., Chien, S.H., Henao, J., Christianson C.B. and Mokwunye, A.U., 1990. Agronomic evaluation of two unacidulated and partially acidulated phosphate rocks indigenous to Niger. Soil Sci. Soc. Am. J. 54: 1772-1777.

Batjes, N.H., 1996. Development of a world data set of soil water retention properties using pedotransfer rules. Geoderman 71: 31-52.

Bell, M.A. and Keulen, H. van, 1995. Soil pedotransfer functions for four Mexican soils. Soil Sci. Soc. Am. J. 59: 865-871.

Bergez, L.E., Balandier, P. and Etienne, M., 1997. Sensitivity analysis of the always silvopastoral simulation model across contrasting pedoclimatic conditions. p. 395-399. *In:* Agroforestry for sustainable Land-use. International workshop, 23-29 July 1997, Montpellier, France.

Bernardes, M.S., pers. comm., 1996. Dourado-Neto D. and Câmara G. M. de S., Department of Agriculture, ESALQ/USP-Brazil.

Bley, J., 1990. Experimentelle und modellanalytische Untersuchungen zum Wasser-und Nährstoffhaushalt von Perlhirse *(Pennisetum americanum* L.) im Südwest-Niger. Ph.D. Thesis, University of Hohenheim, Hohenheim, Germany.

Bley, J., Ploeg, R.R. van der, Sivakumar, M.V.K. and Allison, B.E., 1991. A risk-probability map for millet production in southwest Niger. p. 571-581. *In:* Sivakumar, M.V.K., Wallace, J.S., Renard, C. and Giroux, C. (eds.), Soil water balance in the Sudano-Sahelian zone. Proceedings of the Niamey workshop, February 1991. IAHS Publ. No.199:

Bognetteau-Verlinden, E., 1980. Study on impact of windbreaks in Majjia Valley, Niger. Ms.C. Thesis, Agricultural University Wageningen, Wageningen, The Netherlands.

Breman, H. and Kessler, J.J., 1995. Woody plants in agro-ecosytems of semi-arid regions. Advanced Series in Agricultural Sciences 23. Springer-Verlag, Berlin Heidelberg, Germany.

Brenner, A.J., 1991. Tree-crop interactions within a Sahelian windbreak system. Ph.D. Thesis, University of Edinburgh, Edinburgh, UK.

Brenner, A.J., Beldt, R.J. van den and Jarvis, P.G., 1993. Tree-crop interface competition in a semi-arid Sahelian Windbreak. Paper presented to the 4th International Symposium on Windbreaks and Agroforestry, 26-30 July 1993, Viborg, Denmark.

Brenner, A.J., Jarvis, P.G., and Beldt, R.J. van den, 1995a. Windbreak-crop interactions in the Sahel. 1. Dependence of shelter on field conditions. Agric. For. Meteorol. 75: 215-234.

Brenner, A.J., Jarvis, P.G. and Beldt, R.J. van den, 1995b. Windbreak-crop interactions in the Sahel. 2. Growth response of millet in shelter. Agric. For. Meteorol. 75: 235-262.

Brookes, R.H. and Corey, A.T., 1964. Hydraulic properties of porous media. Hydrology Papers No. 3., Civil Engineering Dep., Colorado State Univ., Fort Collins, Co. USA.

Brouwer, J. et Bouma, J., 1997. La variabilité du sol et da la croissance des cultures au Sahel: points saillants de la recherche (1990-95) au Centre sahélien de l'ICRISAT. Bulletin d'information No.49 ICRISAT, Andrah Pradesh, Inde et Université agricole de Wageningen, Wageningen, Pays-Bas.

Brouwer, J., Fussel, L.K. and Herrmann, L., 1993. Soil and crop growth micro-variability in the West African semi-arid tropics: a possible risk-reducing factor for subsistence farmers. Agric. Ecosys. Environ. 45: 229-238.

Buerkert, A., Lamers, J.P.A., Marschner, H. and Bationo, A., 1996. Inputs of mineral nutrients and surface mulch reduce wind erosion on millet in the Sahel. p. 145-160. In: Buerkert, B., Allison, B. and Oppen, M. van (eds.), Wind erosion in West Africa: The problem and its control. 5-7 December 1994, Stuttgart-Hohenheim, Germany.

Caldwell, R.M., 1997. Common ground for comparing models and datasets. Agroforestry Forum 8(2): 4-7.

Campbell, G.S., 1974. A simple method for determining unsaturated conductivity from moisture retention data. Soil Sci. 117(6): 311-314.

Campbell, G.S., 1985. Soil physics with BASIC: transport models for soil-plant systems. Elsevier Science Publishers B.V. Amsterdam, The Netherlands.

Cannell, M.G.R., Noordwijk, M. van, and Ong, C.K., 1996. The central agroforestry hypothesis: the tree must acquire resources that the crop would not otherwise acquire. Agroforestry systems 34: 27-31.

Carberry, P.S., Campbell, L.C. and Bidinger, F.R., 1985. The growth and development of pearl millet as affected by plant population. Field Crop Res. 11: 193-205.

Chepil, W.S. and Woodruff, N.P., 1963. The physics of wind erosion and its control. Advances in Agron. 15: 211-302.

Christianson, C.B., Bationo, A. and Baethgen, W.E., 1990a. The effect of soil tillage and fertilizer use on pearl millet yields in Niger. Plant Soil 123: 51-58.

Christianson, C.B., Bationo, A., Henao, J. and Vlek, P.L.G., 1990b. Fate and efficiency of N fertilizer applied to pearl millet in Niger. Plant Soil 125: 221-231.

Coaldrake, P.D. and Pearson, C.J., 1985. Development and dry weight accumulation of pearl millet as affected by nitrogen supply. Field Crop Res. 11: 171-184.

Conijn, J.G., 1995. RECAFS: a model for resource competition and cycling in agroforestry systems. Model description and user manual. Production Soudano-Sahelienne (PSS). Rapports PSS No.12. AB-DLO, Wageningen, The Netherlands.

Cook, C.C. and Grut, M., 1989. Agroforestry in Sub-Saharan Africa, a farmer's perspective. World Bank Technical Paper 112, The World Bank, Washington, D.C., USA.

Corlett, J.E., Black, C.R., Ong, C.K. and Monteith, J.L., 1992. Above- and below-ground

interactions in a leucaena/millet alley cropping system. II Light interception and dry matter production. Agric. For. Meteorol. 60: 73-91.

Dancette, C. and Poulain, J.F., 1969. Influence of *Acacia albida* on pedoclimatic factors and crop yields. Afr. Soils 14: 143-184.

Dierckx, J., Belmans, C. and Pauwels, P., 1986. SWATRER. A Computer Package for Modelling the Field Water Balance. Laboratory of Soil and Water Engineering, KU. Leuven, Leuven, Belgium.

Dijksterhuis and Willigen, de, pers. comm., 1995. Research Institute for Agrobiological and Soil Fertility (AB-DLO), Haren, The Netherlands.

Duivenbooden, N. van, and Cissé, L., 1989. L'amélioration de l'alimentation hydrique par des techniques culturales liées à l'interaction eau/ fertilisation azotée. Rapport No.117. Centre de Recherche Agrobiologiques, Wageningen, Pays-Bas.

Duivenbooden, N. van, and Cissé, L., 1992. Fertilization of millet cv. Souna III in Senegal: dry matter production and nutrient uptake. Fert. Research.

Dupraz, C., pers. comm., 1998. Institut National de la Recherche Agronomique (INRA), LEPSE, 2 Place Pierre Viala, Montpellier, France.

Durar, A.A. and Skidmore, L.E., 1995. Hydrology Submodel. p. H1- H64. *In*: Hagen, L.J. et al. (eds.), Wind Erosion Prediction system (WEPS). User Manual. Technical Documentation, Kansas State University, Manhattan, USA.

Eastham, J. and Rose, C.W., 1990. Tree/pasture interactions under three tree spacings in an agroforestry experiment. I. Rooting patterns. Aust. J. Agric. Res. 41: 683-695.

Eimern, J.van, Karschon, R., Razumova, L.A. and Robertson, G.W., 1964. Windbreaks and shelterbelts. WMO. Technical Note No. 59, Secretariat of WMO, Geneva, Switzerland.

Erenstein, O., 1990. Simulation of water-limited yields of sorghum, millet and cowpea for the 5th region of Mali in the framework of quantitative land evaluation. Department of Theoretical Production Ecology, Wageningen Agricultural University, Wageningen, The Netherlands.

FAO, 1984. Guidelines for predicting crop water requirements. Vol. 1. Irrigation and drainage paper, no. 24. FAO, Rome, Italy.

FAO, 1992. Production yearbook. FAO, Rome, Italy.

Fechter, J., 1993. The simulation of pearl millet (*Pennisetum Glaucum* L.) growth under the environmental conditions of South-west Niger, West Africa. Ph.D. Thesis, University of Hohenheim, Hohenheimer Bodenkundliche Hefte No. 10, Germany.

Fechter, J.E., Allison, B.E., Sivakumar, M.V.K., Ploeg van der, R.R., and Bley, J., 1991. An evaluation of the SWATRER and CERES-Millet models for the southwest Niger. p. 505-513. *In*: Sivakumar, M.V.K., Wallace, J.S., Renard, C. and Giroux, C. (eds.), Soil water balance in the Sudano-Sahelian zone. Proceedings of the Niamey workshop, February 1991. IAHS Publ. No.199.

Feddes, R.A., Kowalik, P.J. and Zaradny, H., 1978. Simulation of field water use and crop yield. Simulation Monographs, Pudoc, Wageningen, The Netherlands.

Feddes, R.A., 1982. Simulation of field water use and crop yield. p. 194-209. *In*: Penning de Vries, F.W.T. and Laar, H.H. van (eds.), Simulation Monographs. Pudoc, Wageningen, The Netherlands.

Feddes, R.A. and Koopmans, R.W.R., 1995. Agrohydrology. Lecture notes no. 06141109, Wageningen University, Wageningen, The Netherlands.

Frank, A.B., Harris, D.G. and Willis, W.O., 1974. Windbreak influences on water relations,

growth, and yield of soybeans. Crop Sci. 14: 761-765.

Garba, M., and Renard, C., 1991. Biomass production, yields and water use efficiency in some pearl millet/legume cropping systems at Sadoré, Niger. p. 431-439. *In:* Sivakumar, M.V.K., Wallace, J.S., Renard, C. and Giroux, C. (eds.), Soil and water balance in the Sudano-Sahelian Zone. IAHS Press: Wallingford, UK.

Gardner, W.R., 1960. Dynamic aspects of water availability to plants. Soil Sci. 89: 63-73.

Gaze, S.R., Simmonds, L.P., Brouwer, J. and Bouma, J., 1997. Measurement of surface redistribution of rainfall modelling its effect on water balance calculations of a millet field on sandy soil in Niger. J. of Hydrol. 188-189: 267-284.

Genuchten, M. Th. van, 1987. A numerical model for water and solute movement in and below the root zone. Research report 121, USDA, Agricultural service, US salinity laboratory, Riverside, California, USA.

Goudriaan, J., 1977. Crop micrometeorology: a simulation study. Ph.D. Thesis. Wageningen Agricultural University. Simulation Monographs, Pudoc, Wageningen, The Netherlands.

Goudriaan, J., 1982. Potential production processes. p. 98-113. *In:* Penning de Vries, F.W.T. and Laar, H.H. van (eds.), Simulation of plant growth and crop production. Simulation Monographs, Pudoc, Wageningen, The Netherlands.

Goudriaan, J., 1986. A simple and fast numerical method for the computation of daily totals of crop photosynthesis. Agric. For. Meteorol. 38: 249-254.

Green, W.H. and Ampt, G.A., 1911. Studies on soil physics. 1. The flow of air and water through soils. J. Agric. Sci. 4: 1-24.

Groot, J.J.R., pers. comm., 1996. Institute for Agrobiological and Soil Fertility Research (AB-DLO), Bornsesteeg 47, 6708 PD Wageningen, The Netherlands.

Godwin, D.C., Jones, C.A., Ritchie, J.T., Vlek, P.L.G. and Youngdahl, L.J., 1984. The water and nitrogen components of the CERES models. p. 101-106. *In:* Proceedings of the International Symposium on Minimum Data Set for Agrotechnology Transfer (ICRISAT, March 1983). ICRISAT Center Patancheru, AP 502324, India.

Hafner, H., Bley, J., Bationo, A., Martin, P. and Marschner, H., 1992. Long-term nitrogen balance for pearl millet (*Pennisetum glaucum* L.) in an acid sandy soil of Niger. Z. Pflanzenernähr. Bodenk. 156: 169-176.

Hagen, L.J., 1991. A wind erosion prediction system to meet user needs. J. Soil Water Conserv. 46(2): 106-111.

Hairiah, K. and van Noordwijk, M., 1986. Root studies on a tropical Ultisol in relation to nitrogen management. Rapport 7-86. Research Institute for Agrobiological and Soil Fertility (AB-DLO), Haren, The Netherlands.

Hall, A.E. and Dancette, C., 1978. Analysis of fallow farming systems in semi-arid Africa using a model to simulate hydraulic budget. Agron. J. 70: 816-823.

Heemst, H.D.J., 1988. Plant data values required for simple crop growth simulation models: review and bibliography. Simulation Report CABO-TT Nr. 17. Department of Theoretical Production Ecology, Agricultural University Wageningen, Wageningen, The Netherlands.

Heijer, R.P. den, 1990. Trees tame the wind. The use of wind-breaks in the Sahel. ATSource Vol.18 (2): 9-13.

Heinen, M and de Willigen, P., 1992. FUSSIM2. A simulation model for two-dimensional flow of water in unsaturated soil. Nota 260, Institute for Agrobiological and Soil

Fertility Research (AB-DLO), Haren, The Netherlands.

Heinen, M., 1997. Dynamics of water and nutrients in closed, recirculating cropping systems in glasshouse horticulture. With special attention to lettuce grown in irrigated sand beds. Ph.D. Thesis, Agricultural University of Wageningen, Wageningen, The Netherlands.

Heisler, G.M. and Dewalle, D.R., 1988. 2. Effects of windbreak structure on wind flow. Agric., Ecosys. and Environ. 22/23: 41-69.

Hellmers, H. Horton, J.S., Juhren, G. and O'Keefe, J., 1955. Root systems of some chaparral plants in southern California. Ecology 36: 667-678.

Hermann, L. Stahr, K and Sivakumar, M.V.K., 1996. Dust deposition on soils of southwest Niger. p. 35-47. *In:* Buerkert, B., Allison, B. and Oppen, M. van (eds.), Wind erosion in West Africa: The problem and its control. 5-7 December 1994, Stuttgart-Hohenheim, Germany.

Hermann, L. and Sterk, G., 1996. Towards a Regional Mass Budget of Eolian Transported Material in a Sahelian Environment. p. 319-326. *In:* Buerkert, B., Allison, B. and Oppen, M. van (eds.), Wind erosion in West Africa: The problem and its control. 5-7 December 1994, Stuttgart-Hohenheim, Germany.

Hillel, D., 1975. Some criteria for comprehensive modeling of transport phenomena in the soil-plant atmosphere continuum. p.121-132. *In:* Vansteenkiste, G.C. (ed.), Computer simulation of water resources systems. Proceedings of the IFIP Working Conference, North-Holland Publishing Company, Amsterdam, The Netherlands.

Hillel, D., Krentos, V.D., Stylianou Y., 1972. Procedure and test of an internal drainage method for measuring soil hydraulic characteristics in situ. Soil. Sci. 114: 395-400.

Hoogmoed, W.B. and Stroosnijder, L., 1984. Crust formation on sandy soils in the Sahel. I. Rainfall and infiltration. Soil Till Res. 4: 5-23.

Horie, T., Wit, C.T. de, Goudriaan, J. and Bensink, J., 1979. A formal template for the development of cumcumber in its vegetative stage. Proceedings of the Koninlijke Nederlandse Akademie van Wetenschapen Series C, Vol. 82(4): 433-479.

Huda, A.K.S., Sivakumar, M.V.K., Virmani, S.M., Sekaran, J.G., and Singh, S., 1982. Role of simulation Models in Yield Predictions. Icrisat Experience in Modellling Sorghum and Development. Proceedings of IRAT-ICRISAT Workshop on Water Management and Crop Production, 3-6 May 1982, Montpellier, France.

Huxley, P., 1996. Biological factors affecting form and function in woody-non-woody plant mixtures. p. 235-298. *In:* Ong, C.K. and Huxley, P. (eds.), Tree-crop interactions. A physiological approach. CAB International, Wallingford, UK.

Ibrahim, Y.M., Marcarian, V. and Dobrenz, A.K., 1985. Evaluation of Drought Tolerance in Pearl Millet *(Pennisetum Americanum* (L.) Leeke) under a Sprinkler Irrigation Gradient. Field Crop Res. 11: 233-240.

ICRISAT (1984-1990). West African programs. Annual reports. ICRISAT Sahelian Center. B.P. 12404, Niamey, Niger.

ICRISAT Annual Report 1994. ICRISAT and collaborative programs Western and Central African Region. ICRISAT Sahelian Center. B.P. 12404, Niamey, Niger.

Jackson, R.D., 1972. On the calculation of hydraulic conductivity. Soil Sci. Soc. Amer. Proc. 36: 380-382.

Jacobs, A.F.G., pers. comm., 1992. Dep. of Meteoreology, Wageningen Agricultural University (WAU), P.O. Box 9101, 6700 HB Wageningen, The Netherlands.

Jansen, D.M. and Gosseye, P., 1986. Simulation of growth of millet *(Pennisetum*

Americanum) as influenced by water stress. Simulation Reports CABO-TT.10. Agricultural University Wageningen, Wageningen, The Netherlands.

Jarvis, P.G. and McNaughton, K.G., 1986. Stomatal control of transpiration: scaling up from leaf to region. Adv. Ecol. Res. 15: 1-49.

Jayne, T.S., Day, J.C. and Dregne, H.E., 1989. Technology and Agricultural Productivity in the Sahel. Agricultural Economic Report No. 612. Resources and Technology Division, Economic Research Service, U.S. Department of Agriculture, USA.

Jetten, V.G., 1994. Modelling the effects of logging on the water balance of a tropical rain forest. A study in Guyana. Tropenbos series 6. Ph.D. Thesis, University of Utrecht, Utrecht, The Netherlands.

Jones, C.A., Ritchie, J.T., Kiniry, J.R. and Godwin, D.C. 1986. Subroutine Structure. p. 49-111. *In:* Jones, C.A. and Kiniry, J.R. (eds.), CERES-Maize. A simulation model of Maize Growth and Development. Texas A & M University Press, USA.

Keesman, K. and Straten, G., van, 1998. Uncertainty modelling and analysis. Manual of a Postgraduate Course at the Wageningen Agricultural University, Wageningen, The Netherlands.

Kessler, J.J., 1992. The influence of karité (*Vitellaria paradoxa)* and néré (*Parkia biglobosa*) trees on sorghum production in Burkina Faso. Agrofor. Syst. 17: 97-118.

Keulen, H. van, pers. comm., 1997. Institute for Agrobiological and Soil Fertility Research (AB-DLO), Bornsesteeg 65, 6708 PD Wageningen, The Netherlands.

Keulen, H. van, 1975. Simulation of water use and herbage growth in arid regions. Ph.D. Thesis, Wageningen Agriculture University, Simulation Monographs, Pudoc, Wageningen, The Netherlands.

Keulen, H. van, 1976. Evaluation of models. p. 22-29. *In:* Arnold, G.W. and Wit, C.T., de (eds.), Critical evaluation of systems analysis in ecosystems research and management. Simulation Monographs, Pudoc, Wageningen, The Netherlands.

Keulen, H. van, and Seligman, N.G., 1987. Simulation of water use, nitrogen nutrition and growth of a spring wheat crop. Simulation Monographs, Pudoc, Wageningen, The Netherlands.

Keulen, H. van, and Seligman, N.G., 1992. Moisture, nutrition availbaility and plant production in the semi-arid region. p. 25- . *In:* Alberda, Th. H., Keulen, H., van, Seligman, N.G. and Wit, C.T., de (eds.), Food from dry lands. An integrated approach to planning of agricultural development. Systems Approaches for Sustainable Agricultural Development Vol. I, Kluwer Acad. Publ. Dordrecht, The Netherlands.

Keulen, H. van and Stol, W., 1991. Quantitative aspects of nitrogen nutrient in crops. Fert Res. 27: 151-160.

Konaté, M., 1984. Climate of the sorghum and millet cultivation zones of the semi-arid tropical regions of West-Africa. Agrometeorology of sorghum and millet in the semi-arid tropics. Proceedings of the International Symposium, 15-20 Nov, 1982, ICRISAT Center, India. Patancheru, A.P. 502 324, India.

Kort, J., 1988. Benefits of windbreaks to field and forage crops. Agric. Ecosys. Environ. 22/23: 165-190.

Kraalingen, D.W.G. van and Keulen, H. van, 1988. Model development and application for the 'Projet pilote en agrométéorologie'. Report prepared for submission to World Meteorological Organisation. University of Wageningen and Institute of Agrobiological and Soil Fertility Research (AB-DLO), Wageningen, The Netherlands.

Kropff, M.J., 1993. Mechanism of competition for light. p. 33-61 *In:* Kropff, M.J. and Laar, H.H. van (eds.), Modelling crop-weed interactions. CAB International, Wallingford, UK.

Kropff, M.J. and Laar, H.H. van, 1993. Modelling crop-weed interactions. CAB International, Wallingford, UK.

Lambert, C., 1983. L'irat et l'amelioration de mil. Agron. trop. 38 (1): 78-88.

Lamers, J.P.A., 1995. An assessment of wind erosion control techniques in Niger. Financial and economic analyses of windbreaks and millet crop residues. Ph.D. Thesis, University of Hohenheim, Hohenheim, Germany.

Lamers, J.P.A. and Feil, P.R., 1995. Farmers's knowledge and management of spatial soil and crop growth variability. Netherlands J. Agric. Sci. 43: 375-389.

Le Hoerou, H.N., 1989. The grazing land ecosystems of the African Sahel. Ecological Studies. Vol 75. Springer-Verlag, Berlin, Germany.

Livesley, S.J., Gregory, P.J. and Buresh, R.J., 1997. Approaches to modelling root growth and the uptake of water and nutrients. Agroforestry Forum 8(2): 24-27.

Leihner, D.E, Buerkert, A., Banzhaf, J. and Serafini P.G., 1993. Soil tillage and windbreak effects on millet and cowpea. II Dry matter and grain yield. Agron. J. 85 (2): 400-405.

Loeffler, A.E., Gordon, A.M. and Gillespie, T.J., 1992. Optical porosity and windspeed reduction by coniferous windbreaks in Southern Ontario. Agrofor. Systs. 17: 119-133.

Long, S.P., 1989. Influence of Neem windbreaks on yield, microclimate, and water use of Millet and Sorghum in Niger, West Africa. Ms.C. Thesis. Texas A&M University, Texas, USA.

Long, S.P. and Persaud, N., 1988. Influence of Neem (*Azadirachta indica*) windbreaks on millet yield, microclimate, and water use in Niger, West Africa. *In:* International Conference on Dryland Agriculture, 18-22 Aug, Bushland/Amarillo, Texas, USA.

Lott, J.E., Black, C.R. and Ong, C.K., 1997. Resource use and growth in semi-arid agroforestry systems. Agroforestry Forum 8(2): 33-37.

Lövenstein, H.M., Berliner P.R. and Keulen, H. van, 1991. Runoff agroforestry in arid lands. Forest Ecol Manage. 45: 59-70.

Lundgren, B.O. and Raintree, J.B., 1982. Sustainable agroforestry. p. 37-49. *In:* Nestle, B. (ed.), Agricultural Research for Development: Potential and Challenges in Asia. ISNAR, The Hague, The Netherlands.

Lyles, L., Tatarko, J. and Dickerson, J.D., 1984. Windbreak effects on soil water and wheat yield. Trans ASAE. 27(1): 69-72.

Mahalakshmi, V., Bidinger, F. R. and Raju, D.S., 1987. Effect of timing of water deficit on pearl millet (*Pennisetum americanum*). Field Crop Res. 15: 327-339.

Maiti, R.K. and Bidinger, F.R., 1981. Growth and development of the pearl millet plant. Research Bulletin No.6. ICRISAT, Pantancheru, India.

Mando, A., 1997. The role of termites and mulch in the rehabilitation of crusted Sahelian soils. Ph.D. Thesis, Wageningen Agricultural University, Wageningen, The Netherlands.

McCown, R.L., Hammer, G.L., Hargreaves, J.N.G., Holzworth, D.P. and Freebairn, D.M., 1996. APSIM: A novel software system for model development, model testing, and simulation in agricultural research. Agric. Syst. 50: 255-271.

McLean, E.O., 1982. Soil pH and lime requirements. *In:* Page A.L. et al. (eds.), Methods of soil analysis, Part 2. Agron. Monographs. 9. ASA and SSSA, Madison: 199-224.

McNaughton, K.G., pers. comm., 1992. Plant Physiology Division, Dept. of Scientific and

Industrial Research, (DSIR) Palmerston North, New Zealand.

McNaughton, K.G., 1988. Effects of windbreaks on turbulent transport and microclimate. Agric. Ecosys. Environ. 22/23: 17-39.

Mellouli, H.J., 1989. Etude de la concurrence hydrique entre brise-vent et une culture irriguée. Annales de l'INRAT, 1989. Numero Special: 157-171.

Meinke, H., 1996. Improving wheat simulation capabilities in Australia from a cropping systems perspective. Ph.D. Thesis, Wageningen Agricultural University, Wageningen, The Netherlands.

Michels, K., 1990. Influence of wind erosion and water barriers on millet growth, development, soil water content and yield. Ms.C. Thesis, University of Hohenheim, Hohenheim, Germany.

Michels, K., 1994. Wind erosion in the southern Sahelian zone. Ph.D. Thesis, University of Hohenheim, Hohenheim, Germany.

Michels, K., Sivakumar, M.V.K. and Allison, B.E., 1993. Wind erosion in the southern Sahelian zone and induced constraints to pearl millet production. Agric. For. Meteorol. 67: 65 - 77.

Michels, K., Sivakumar, M.V.K. and Allison, B.E., 1994. Wind erosion control using crop residue. I. Effects on soil flux and soil properties. Field Crop Res. 40: 101-110.

Mobbs, D.C., Crout, N.M.J., Lawson, G.J. and Cannell, M.G.R., 1997. Structure and applications of the HyPAR model. Agroforestry Forum 8(2): 10-14.

Monteith, J.L., 1981. Climatic variation and the growth of crops. Q.J.R. Meteorol. Soc. 107: 749-773.

Monteith, J.L., 1991. Weather and water in the Sudano-Sahelian zone. p 11-31. *In:* Sivakumar; M.V.K., Wallace, J.S., Renard, C. and Giroux, C. (eds.), Soil Water Balance in the Sudano-Sahelian Zone. Proceedings of the Niamey Workshop, February 1991. IAHS Publ. no. 199.

Monteith, J.L., 1997. Agroforestry modelling: a view from the touchline. Agroforestry Forum 8(2): 52-54.

Mutezefeldt, R.I. and Sinclair, F.L., 1993. Ecological modelling of agroforestry systems. Agroforestry Abstracts 6: 207-247.

Nair, P.K., 1993. An introduction to agroforestry. Kluwer Academic, Dorderecht, The Netherlands.

Noordwijk, M. van, Lawson, G., Soumaré A., Groot, J.J.R., and Hairiah, K., 1996. Root distribution of trees and crops: Competition and/ or complementarity. p. 319-364. *In:* Ong, C.K. and Huxley, P. (eds.), Tree-crop interactions. A physiological approach. CAB International, Wallingford, UK.

Noordwijk, M. van and Lusiana, B., 1997. WaNuLCAS- a model of light, water and nutrient capture in agroforestry systems. *In:* Agroforestry for sustainable Land-use. International workshop, 23- 29 July 1997, Montpellier, France.

Ntare, B.R., Serafini, P.G. and Fussell, L.K., 1989. Recent developments in pearl millet/ cowpea cropping systems for low-rainfall areas of the Sudano-Sahelian zone of West Africa. p. 277-289. *In:* Soil, crop and water management in the Sudano-Ahelian Zone. Proceedings of an International Workshop, 11-16 January 1987, ICRISAT, Niamey, Niger.

ODA, 1987. Microclimatology in tropical agriculture, Vol 1. Final Report, Research schemes R3208 and R3819. Overseas Development Administration, London, UK.

Olsen, S.R. and Sommer, L.E., 1982. Phosphorus. p. 403-430. *In:* Page, A.L. et al. (eds.) Methods of soil analysis. Part 2. Agron. Monographs. 9. ASA and SSSA, Madison, USA.

Ong, C.K., 1983. Response to temperature in a stand of pearl millet (*Pennisetum typhoides* S.& H.). J. of Experimental Botany. 34(140): 322-336.

Ong, C.K., 1996. A framework for quantifying the various effects of tree-crop interactions. p. 1-23. *In:* Ong, C.K. and Huxley, P. (eds.), Tree-crop interactions. A physiological approach. CAB International, Wallingford, UK.

Ong, C.K. and Monteith, J.L., 1985. Response of pearl millet to light and temperature. Field Crop Res. 11: 141-160.

Ong, C.K. and Sinclair, F.L., 1997. The need for a fundamental understanding of agroforestry systems. p. 13-19. *In:* Agroforestry for sustainable Land-use. International workshop, 23-29 July 1997, Montpellier, France.

Ong, C.K., Subrahmanyam, P. and Khan, A.A.H., 1991. The microclimate and productivity of a groundnut/millet intercrop during the rainy season. Agric. For. Meteorol. 56: 49-66.

Ong, C.K., Black, C.R., Marschall, F.M. and Corlett, J.E., 1996. Principles of resource capture and utilization of light and water. p. 73-158. *In:* Ong, C.K. and Huxley, P. (eds.), Tree-crop interactions. A physiological approach. CAB International, Wallingford, UK.

Onyewotu, L.O.Z., Ogigirigi, M.A. and Stigter, C.J., 1994. A study of competitive effects between *Eucalyptus camaldulensis* shelterbelt and adjacent millet (*Pennisetum typhoides*) crop. Agric. Ecosys. Environ. 51: 281-286.

Onyewotu, L.O.Z., pers. comm., 1996. Forestry Research Institute of Nigeria, P.M.B. 3239, Kano, Nigeria.

Payne, W.A., 1990. Growth and transpirational water use efficiency of Pearl Millet in response to water and phosphorus supply. Ph.D. Thesis, Texas A&M University, Texas, USA.

Payne, W.A., Wendt, C.W. and Lascano, R.J., 1990. Root zone water balance of three low-input millet fields in Niger, West Africa. Agron. J. 82: 813-819.

Payne, W.A., Lascano, R.J., Hossner, L.R., Wendt, C.W. and Onken, A.B., 1991a. Pearl millet as affected by phosphorus and water. Agron. J. 83: 942-948.

Payne, W.A., Lascano, R.J. and Wendt, C.W., 1991b. Physical and hydrological characterization of three sandy millet fields in Niger. p. 199-207. *In:* Sivakumar, M.V.K., Wallace, J.S., Renard, C. and Giroux, C. (eds.), Soil Water Balance in the Sudano-Sahelian Zone. Proceedings of the Niamey Workshop, February 1991. IAHS Publ. no. 199.

Payne, W.A., Lascano, R.J. and Wendt, C.W., 1991c. Annual soil water balance of cropped and fallowed millet fields in Niger. p. 401-411. *In:* Sivakumar, M.V.K., Wallace, J.S., Renard, C. and Giroux, C. (eds.), Soil Water Balance in the Sudano-Sahelian Zone. Proceedings of the Niamey Workshop, February 1991. IAHS Publ. no. 199.

Pearson, C.J., 1985. Editorial: Research and development for yield of pearl millet. Field Crop Res. 11: 113-121.

Penman, H.L., 1948. Natural evaporation from open water, bare soil, and grass. Proc. R. Soc. London Series A, 193: 120-146.

Penman, H.L., 1956. Evaporation: An introductory survey. Neth J Agr Sci 4: 9-29.

Penning de Vries, F.W.T., 1975. The cost of maintenance processes in plant cells. Ann. Bot.

39: 77-92.

Penning de Vries, F.W.T., 1982. Modelling growth and production. p. 68 B17. *In:* New Enceclopedia of plant physiology, Springer Verlag, Berlin-Heidelberg, Germany.

Penning de Vries, F.W.T. and Laar, van, H.H. (eds.), 1982. Simulation of plant growth and crop production. Simulation Monographs, Pudoc, Wageningen, The Netherlands.

Penning de Vries, F.W.T. and Keulen, H. van, 1982. The actual productivity and the role of nitrogen and phosphorus. p. 196-226. *In:* Penning de Vries, F.W.T. and Dijtèye, A.M. (eds.) La productivité des pâturages Sahéliens. Une étude des sols, des végétations et de l'expoitation de cette ressource naturelle. Agr. Res. Rep. 918, Pudoc, Wageningen, Pays-Bas.

Piro, B., 1993. Genotypische Unterschiede in der Phosphateffizienz von Kolbenhirsesorten unter besonderer Berücksichtigung von Wurzelmerkmalen. Ms.C. Thesis, University of Kiel, Kiel, Germany.

Plentinger, M.C. and Penning de Vries, F.W.T. (eds.), 1995. CAMASE. Register of Agro-ecosystems models. Version I.

Poethke, H. J., Oertel D. and Seitz, A., 1994. Parameter sensitivity and the quality of model predictions. p. 389-397. *In:* Grasman, J. and Straten, G. van (eds.), Predictability and non-linear modelling in natural sciences and economics. Kluwer Academics Publishers, The Netherlands.

Press, H.W, Flannery, B.P., Teukolsky, S.A. and Vetterling, W.T., 1990. Numerical recipes in C. The art of scientific computing. Cambridge University Press. USA.

Proton, H., Ndikumagenge, C. Bousquet, F. and Guizol, P.H., 1997. La modélisation multi-agent: un outil pour analyser les dynamiques de passage entre formations forestièrs et agroforestières à l'échelle d'une région. p. 443-447. *In:* Agroforestry for sustainable Land-use. International workshop, 23- 29 July 1997, Montpellier, France.

Rawls, W. J., Brakensiek, D. L. and Saxton, K.E., 1982. Estimation of soil water properties. Trans. ASAE. 25(5): 1316-1328.

Rebafka, F.P., 1993. Deficiency of phosphorus and molybdenum as major growth limiting factors of pearl millet and groundnut on an acid sandy soil in Niger, West Africa. Ph.D. Thesis, University of Hohenheim, Hohenheimer Bodenkundliche Hefte no. 9, Germany.

Reffye, P. de, Houllier, F., Blaise, F., Barthelemy, D., Dauzat, J. and Auclair, D., 1995. A model simulating above- and below-ground tree architecture with agroforestry applications. Agric. Syst 30: 175-197.

Renard, C. and Vandenbeldt, R.J., 1990. Bordures d'*Andropogon gayanus* Kunth comme moyen de lutte contre l'érosion éolienne au Sahel. L'agronomie Tropicale 45 (3): 227-231.

Ridder, N., de, Keulen, H. van, Breman, H. and Uithol, P.W.J., 1991. III.2. La production végétale. p. 293-355. *In:* Breman, H. and Ridder, N. (eds.), Manuel sur les paturages des pays Saheliens. ACCT- CTA-KARTHALA.

Rockström, J., Jansson, P-E. and Andersson, J. On-farm rainfall partitioning under runon and runoff conditions on sandy soil in Niger - On-farm measurements and water balance modelling. Submitted to J. Hydrol. *In:* Rockström, J., 1997 Ph.D. Thesis, Stockholm University, Stockholm, Sweden.

Rosenberg, N.J., 1974. Microclimate: The biological Environment. Microclimate: The Biological Environment. John Wiley and Sons, Inc., New York, USA.

Ross, J., 1981. In Task for vegetation sciences 3. The radiation regime and architecture of plant stands by J.Ross. Dr W. Junk Publishers.

Salim, M.H., Todd, G.W. and Schlehuber, A.M., 1965. Root development of wheat, oats, and barely under conditions of soil moisture stress. Agron. J. 57: 603-607.

SAS Institute, 1988. SAS/STAT Guide for Personal Computers, V.6. Cary, NC, USA.

Sivakumar, M.V.K., 1986. Climate of Niamey. Progress Report 1. ICRISAT Sahelian Center B.P. 12404 Niamey, Niger.

Sivakumar, M.V.K., 1988. Predicting rainy season potential from the onset of rains in the Southern Sahelian and Sudanian climatic zones of West Africa. Agric. For. Meteorol. 42: 295-305.

Sivakumar, M.V.K., 1989. Agroclimatic aspects of rainfed agriculture in the Sudano-Sahelian Zone. p. 17-38. *In:* Renard, C., Van den Beldt, R.J. and Parr, J.F. (eds.), Soil, Crop and Water management systems for rainfed agriculture in the Suadano-Sahelian Zone. Proceedings of the international workshop, 11-16 January 1987, ICRISAT, Niamey, Niger.

Sivakumar, M.V.K., 1992. Climatic change and implications to agriculture in Niger. Climatic Change 20: 297-312.

Sivakumar, M.V.K. and Wallace, J.S., 1991. Soil water balance in the Sudano-Sahelian Zone: need, relevance and objectives of the workshop. p. 3-10. *In:* Sivakumar, M.V.K., Wallace, J.S., Renard, C. and Giroux, C. (eds.), Soil Water Balance in the Sudano-Sahelian Zone. Proceedings of the Niamey Workshop, February 1991. IAHS Publ.no. 199.

Sivakumar, M.V.K., Maidoukia , A. and Stern, R.D., 1993. Agroclimatology of West Africa: Niger, 2nd edition. ICRISAT Information Bulletin No.5. International Crops Research Institute for the Semi-Arid Tropics, Patancheru, A.P., India.

Smith, D.M., 1995. Water use by windbreak trees in the Sahel. Ph.D. Thesis, University of Edinburgh, Edinburgh, UK.

Smith, D.M., pers. comm., 1996. Institute of Hydrology, Wallingford, Oxon OX10 8BB,UK.

Smith, D.M., Jarvis, P.G., and Odongo, J.C.W., 1996a. Sources of water used by trees and millet in Sahelian windbreak systems. J. Hydrol. 189: 140-153.

Smith, D.M., Jarvis, P.G., and Odongo, J.C.W., 1996b. Energy budgets of windbreak canopies in the Sahel. Agric. For. Meteorol. 86: 33-49.

Soumaré, A., Groot, J.J.R., Koné, D. and Radersma, S., 1994. Structure spatial du système racinaire de deux arbres du Sahel: *Acacia seyal* et *Sclerocarya birrea*. Rapports PSS no. 5. AB-DLO Wageningen, Pays-Bas.

Spencer, D.S.C. and Sivakumar, M.V.K., 1987. Pearl millet in african agriculture. Proceedings of the International Pearl Millet Worksop, 7-11 April 1986, ICRISAT Center India, Pantancheru, India.

Spiertz, J.H.J. and Sibma, 1982. cited in van Keulen and Seligman (1987)

Spiertz, J.H.J. and Keulen, H. van, 1980. Effects of nitrogen and water supply on growth and grain yield of wheat. Proceedings 3rd International Wheat Conference, Madrid, Spain: 595-610.

Spitters, C.J.T, 1982. Grondslagen Plantaardige Produktie. Algemene Plantenteelt 1. Lecture notes. Department of Theoretical Production Ecology, Wageningen Agricultural University Wageningen, The Netherlands.

Spitters, C.J.T., 1990. Crop growth models: Their usefulness and limitations. Acta

Horticulturae. 267: 349-368.

Spitters, C.J.T. and Keulen v.H., 1990. Toepassing van Simulatie en Systeemanalyse: Stand van Zaken en Knelpunten. Cabo-Verslag nr.128.

Spitters, C.J.T., Toussiant, H.A.M. and Goudriaan, J., 1986. Separating the diffuse and direct component of global radiation and its implications for modeling canopy photosynthesis. Part I. Components of incoming radiation. Agric. For. Meteorol. 38: 217-229.

Squire, G.R., Ong, C.K. and Monteith, J.L., 1987. Crop growth in semi-arid environments. In ICRISAT Annual Report 1987. p. 219-232.

Sterk, G., 1997. Wind erosion in the Sahelian Zone of Niger: Processes, models and control techniques. Ph.D. Thesis, Wageningen Agricultural University, Wageningen, The Netherlands.

Sterk, G., Herrmann, L. and Bationo, A., 1996. Wind-blown nutrient transport and soil productivity changes in southwest Niger. Land Degradation Developm. 7: 325-335.

Sterk, G. and Spaan, W.P., 1997. Wind erosion with crop residues in the Sahel. Soil Sci. Soc. Am. J. 61(3): 911-917.

Stigter, C.J., Kainkwa, R.M.R., A. El-Tayeb Mohamed and Onyewotu, L.O.Z., 1993. Essentials and cases of wind protection from scattered trees and shelterbelts. Paper presented at the International Symposium on Agroforestry Parklands, 25-27 Oct.1993, Ougadougou, Burkina Faso.

Stroosnijder, L., 1982. Simulation of soil water balance. p. 175-193. In: Penning de Vries, F.W.T. and Laar, H.H. van (eds.), Simulation Monographs. Pudoc, Wageningen, The Netherlands.

Stroosnijder, L. and Hoogmoed, W.B., 1984. Crust formation on sandy soils in the Sahel. II. Tillage and its effect on the water balance. Soil Till Res. 4: 321-337.

Sturrock, J.W., 1975. Wind effects and their amelioration in crop production. In: GUPTA, U.S. (ed.), 1975: Physiological aspects of dryland farming: 282313, Oxford and IBH Publishing Co., New Dehli, Bombay and Calcutta.

Tauer, W. and Humborg, G., 1992. Runoff irrigation in the Sahel Zone. Remote sensing and geographical information systems for determining potential sites. Technical Centre for Agricultural and Rural Cooperation, Verlag Josef Margraf, Germany.

Terry, N., Waldron, L.J. and Taylor, S.E., 1983. Environmental influences on leaf expansion. In: Dale, J.E. and Milthorpe, F.L. (eds.), The growth and functioning of leaves. Proceedings of a Symposium held prior to the 13th International Botanical Congress at the University of Sidney 18-20 August 1981. Cambridge University Press, USA.

Tibke, G., 1988. Basic principles of wind ersoiopn control. Agric. Ecosys. Environ. 22/23: 103-122.

Ujah, J.E. and Adeoye, K.B., 1984. Effects of shelterbelts in the sudan savana zone of Nigeria on microclimate and yield of millet. Agric. For. Meteorol. 33: 99-107.

Unger, P.W., Stewart B.A. Parr J.F. and Singh, R.P., 1991. Crop residue management and tillage methods for conserving soil water in semi-arid regions. Soil Till Res. 20: 210-240.

Vandenbeldt, R.J. 1990. Agroforestry in the semiarid tropics. p. 150-194. In: MacDicken, K.G. and Vergara, N.T. (eds.), Agroforestry: classification and management. John Wiley and Sons, Inc., New York, USA.

Vandenbeldt, R.J. and Williams, J.H., 1992. The effect of soil surface temperature on the

growth of millet in relation to the effect of *Faidherbia albida* trees. Agric. For. Meteorol. 60: 93-100.

Veihmeyer, F.J. and Hendrickson, A.H., 1950. Soil moisture in relation to plant growth. Ann. Rev. Plant Physiol. 1: 285-304.

Verberne, E., Dijksterhuis, G., Jongschaap, R., Bazi, H., Sanou, A. and Bonzi, M., 1995. Simulation des cultures pluviales au Burkina Faso (CP-BKF3): sorgho, mil et mais. Institute for Agrobiological and Soil Fertility Research (AB-DLO), Wageningen, The Netherlands, Bureau National des Sols INERA and Intstitut d'Etudes et de Recherches Agricoles, Burkina Faso. Nota 18.

Walkley, A. and Black, I.A., 1934. An examination of the Degtjareff methods for determining soil organic matter and a proposed modification of the chromic acid titration method. Soil Sci. 37: 29-38.

Wallace, J.S., 1991. The measurement and modelling of evaporation from semiarid land. p. 131-148. *In:* Sivakumar, M.V.K., Wallace, J.S., Renard, C. and Giroux, C. (eds.), Soil Water Balance in the Sudano-Sahelian Zone. Proceedings of the Niamey Workshop, February 1991. IAHS Publ. no. 199.

Wallace, J.S., Roberts, J.M. and Sivakumar, M.V.K., 1990. The estimation of transpiration from sparse dryland millet using stomatal conductance and vegetation area indices. Agric. For. Meteorol. 51: 35-49.

Wallace, J.S., Lloyd, C.R. and Sivakumar, M.V.K., 1993. Measurements of soil, plant, and total evaporation from millet in Niger. Agric. For. Meteorol. 63: 149-169.

Weihong, L., 1996. Simulation and measurements of leaf wetness formation in paddy rice crops. Ph.D. Thesis, Wageningen Agricultural University, Wageningen, The Netherlands.

West, L.T., Wilding, L.P., Landeck, J.K. and Calhoun, F.G., 1984. Soil survey of the ICRISAT Sahelian Center, Niger, West Africa. Bulletin of Soil and Crop Science Department/Trop Soils, Texas A&M University, USA.

Williams, J.R., Dyke, P.T., Fuchs, W.W., Benson, V.W., Rice, O.W. and Taylor, E.D., 1990. EPIC-Erosion/Productivity Impact Calculator: 2. User Manual. A.N. Sharply and Williams, J.R. (eds.), Technical Bulletin No. 1768., U.S. Department of Agriculture, USA.

Wit, C.T., 1958. Transpiration and crop yields. Versl. Landbouwkund. Onderz. (Agr. Res. Rep.) 64.6, Pudoc, Wageningen, The Netherlands.

Wit, C.T. de, and Penning de Vries, F.W.T., 1982. L'analyse des sytèmes de production primaire. p. 20-23. *In:* La productivité de pâturages, Sahéliens. Penning de Vries, F.W.T. and Dijteye, M.A. (eds.), Agr. Res. Rep.918, Pudoc, Wageningen, The Netherlands.

Wit, C.T. de et al., 1978. Simulation of assimilation, respiration and transpiration of crops. Simulation Monographs. Pudoc, Wageningen, The Netherlands.

WMO. 1964. Windbreaks and shelterbelts. Technical Note no.59. Geneva, Switzerland: WMO.

Appendix A1: Results from experiment and review

The following data were derived from our agroforestry experiment (Part A), in an accompanying study by Michels (1994) and in preliminary studies by Michels (1990) and Banzhaf et al.(1992), all performed at ISC. The data were used for discussion of the experimental results (Chapter 3) and for model development (Chapter 5).

1   Wind speed

In a preliminary study in 1990, Michels (1990) measured wind speed during storms in all three Bauhinia and control plots of the windbreak-millet experiment. Experimental design and treatments were the same as described in Chapter 2 of this thesis, except that: (i) residues of the previous year were incorporated into the soil before sowing and (ii) millet was sown in rows with 0.75 and 0.4 m between and within rows, respectively. Wind speed was measured with cup anemometers 0.3 and 0.7 m above the cropped soil at a distance of 3 and 10 m from the windbreak. Winds approaching more or less from the east (controlled by a windvane) were recorded ervery 20 seconds and averaged over 2 minutes. From the 6th of June (one week after sowing) till the end of July seven easter wind storms occured and had been reduced at least up to 10 m upwinded from the windbreak (Table A1-1).

Table A1-1   Average wind speed in the lee of Bauhinia as percentage of speeds in unsheltered (control) plots during more or less easter storms at ISC, Niger, in June and July, 1990. Standard error (SE) is given between brackets (Source: Michels, 1990).

Distance from windbreak line (m)	Measurement height			
	0.3 m	(SE)	0.7 m	(SE)
3	71.2	(2.1)	65.9	(2.1)
10	69.5	(1.5)	67.6	(1.2)

An intensive study on wind speed profiles was performed by Banzhaf et al. (1992) in an agroforestry experiment with approximately 0.6 m high windbreaks of natural bush savanna at four different WB spacings (i.e. naturally growing fallow vegetation was left in place and additional trees were afforested). Dominant species in the natural vegetation were: the two

annuals *Cenchrus biflorus* Roxb. and *Cassisa mimosoides* L., and the perennials *Stylosanthes* spp., *Tephrosia* spp., *Guirea senegalensis* (J. Gmelin), and *Andropogon gayanus* Kunth. Afforested species were: *Acacia albida* Del., *Acacia nilotica* (L.) Willd. ex Del and *Bauhinia rufescens* (Lam.). The field research was conducted from 1985 to 1987 at ISC. Wind speed was measured with cup anemometers at 0.3 m above the bare soil 5 days before millet planting. To compute the relative wind speed a control measurement was taken at 0.1 m above the savanna vegetation of the most upwind windbreak. The results are summarized in Figure A1-1.
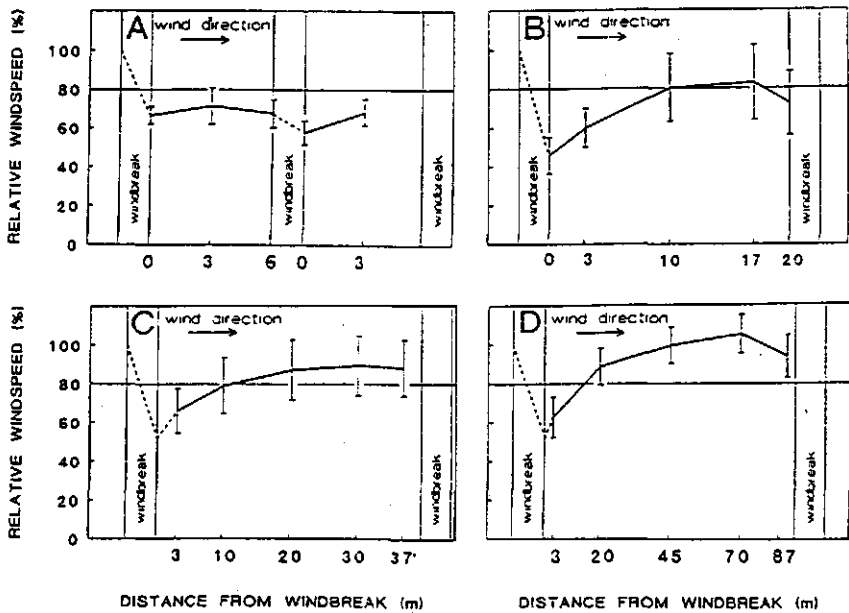
Figure A1-1 Wind speed profiles within windbreaks of natural bush savanna with different windbreak spacings: A) 6 m, B) 20 m, C) 40 m, and D) 90 m. Data are means of repeated measurements taken at 0.3 m height above a flat bare soil surface. Bar intervals indicate one standard deviation (Banzhaf et. al, 1992).

2   Chemical soil analysis

The statistical analysis and presentation of soil chemical properties was performed by Michels (1994) and are reproduced below.

Table A1-2   Univariate ANOVA with 2 repeated-measures factors (soil depth; distance from windbreak (WB) or windbreak line) for soil chemical properties in WB-millet systems, without crop residue application, 1991 and 1993 (Michels, 1994).

Source of variation	pH	Org. C	Total N	Bray1-P	Na	K	Ca	Mg	Al
1991					Pr > F				
WB species	0.236	0.428	0.554	0.920	0.083	0.168	0.215	0.142	n.a.
Distance	0.147	0.129	0.195	0.068	0.869	0.017	0.306	0.032	n.a.
Depth	<0.001	<0.001	<0.001	<0.001	0.042	<0.001	<0.001	<0.001	n.a.
WB x Distance	0.748	0.360	0.480	0.467	0.945	0.558	0.448	0.370	n.a.
WB x Depth	0.153	0.537	0.690	0.940	0.917	0.064	0.221	0.006	n.a.
Distance x Depth	0.793	0.003	<0.001	0.007	0.654	<0.001	0.660	0.037	n.a.
WB x Distance x Depth	0.481	0.075	0.311	0.322	0.243	0.910	0.207	0.529	n.a.
Contrasts									
A. gayanus vs Control	0.728	0.534	0.669	0.749	0.066	0.316	0.689	0.730	n.a.
A. gayanus vs Control x Distance	0.669	0.163	0.214	0.504	0.893	0.368	0.384	0.151	n.a.
A. gayanus vs Control x Depth	0.827	0.630	0.708	0.717	0.897	0.949	0.298	0.004	n.a.
B. rufescens vs Control	0.192	0.483	0.520	0.730	0.730	0.274	0.183	0.075	n.a.
B. rufescens vs Control x Distance	0.841	0.576	0.735	0.208	0.812	0.935	0.572	0.637	n.a.
B. rufescens vs Control x Depth	0.120	0.390	0.567	0.829	0.818	0.052	0.132	0.004	n.a.
1993									
WB species	0.427	0.298	0.302	0.193	0.627	0.316	0.152	0.069	0.205
Distance	0.875	0.112	0.485	0.417	0.461	0.041	0.827	0.161	0.346
Depth	<0.001	<0.001	<0.001	<0.001	0.448	0.092	<0.001	<0.001	<0.001
WB x Distance	0.735	0.626	0.694	0.282	0.523	0.518	0.713	0.544	0.669
WB x Depth	0.149	0.021	0.021	0.249	0.440	0.430	0.062	0.083	0.026
Distance x Depth	0.362	0.002	0.289	0.292	0.340	0.228	0.001	<0.001	0.570
WB x Distance x Depth	0.176	0.028	0.171	0.020	0.443	0.610	0.115	<0.001	0.301
Contrasts									
A. gayanus vs Control	0.905	0.567	0.298	0.318	0.363	0.736	0.216	0.073	0.990
A. gayanus vs Control x Distance	0.873	0.401	0.392	0.680	0.293	0.774	0.496	0.529	0.564
A. gayanus vs Control x Depth	0.097	0.016	0.017	0.590	0.271	0.960	0.025	0.023	0.011
B. rufescens vs Control	0.299	0.147	0.151	0.087	0.656	0.169	0.068	0.032	0.131
B. rufescens vs Control x Distance	0.414	0.442	0.623	0.210	0.365	0.429	0.675	0.426	0.533
B. rufescens vs Control x Depth	0.304	0.016	0.022	0.217	0.235	0.278	0.083	0.253	0.121
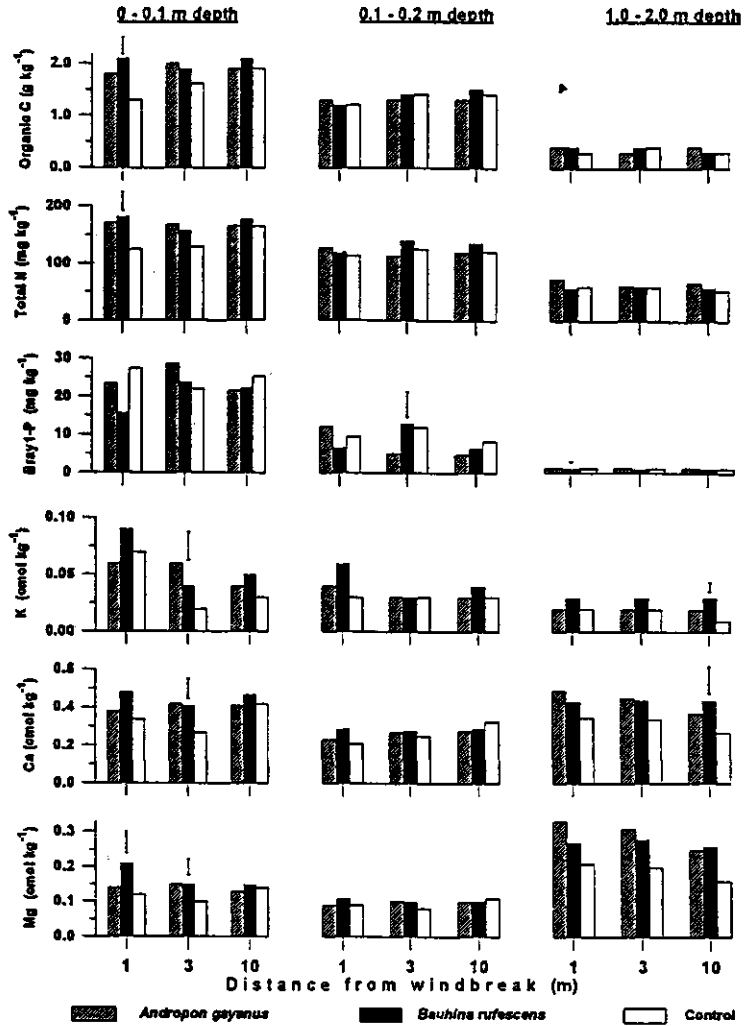
Figure A1-2 Soil chemical properties as affected by windbreak species, at 3 distances and 3 soil depths (without crop residue application), 1993. Error bars represent LSD (0.1) when ANOVA indicated significant effects (Michels, 1994).

3   Millet dry matter

In 1992 and 1993, final millet dry matter and grain yield were determined for seven windbreak species and the control plots by Michels (1994). The biomass production was quantified for each millet row parallel to the windbreak as mean value over three replicates. In Figure A1-3 straw dry matter for the plots with crop residues is presented as function of the distance from the windbreak. To show spatial heterogeneity the results are presented per block. Statistical analysis was performed on total plot biomass (Table A1-3).

Table A1-3   ANOVA for millet dry matter, grain yield, and number of established pockets as affected by windbreak (WB) species, crop residue (CR) application, and year, 1992-1993 (Source: Michels, 1994).

	Straw DM	Grain yield	Potential[†] grain yield	Number of pockets[‡] (1992 / 1993)
			— P > F—	
WB species	0.284	0.489	0.341	0.284 / 0.677
CR application	<0.001	<0.001	<0.001	<0.001 / <0.001
Year	<0.001	<0.001	--	n.a.
WB x CR	0.573	0.547	0.752	0.035 / 0.866
Year x WB	0.002	0.008	--	n.a.
Year x CR	0.001	0.330	--	n.a.
Year x WB x CR	0.279	0.990	--	n.a.
Contrasts				
WB vs Control	0.233	0.681	--	n.a.
Year x *WBs vs Control*	0.007	0.742	--	n.a.
1992: *WBs vs Control*	0.884	0.854	--	n.a.
1993: *WBs vs Control*	0.026	0.489	0.112	0.058 / n.a.

[†] Potential grain yield was calculated due to strong pest damage in the 1993 season.

[‡] Due to missing values the pocket numbers were analyzed for each year separately.

Straw weight per row (kg ha⁻¹)
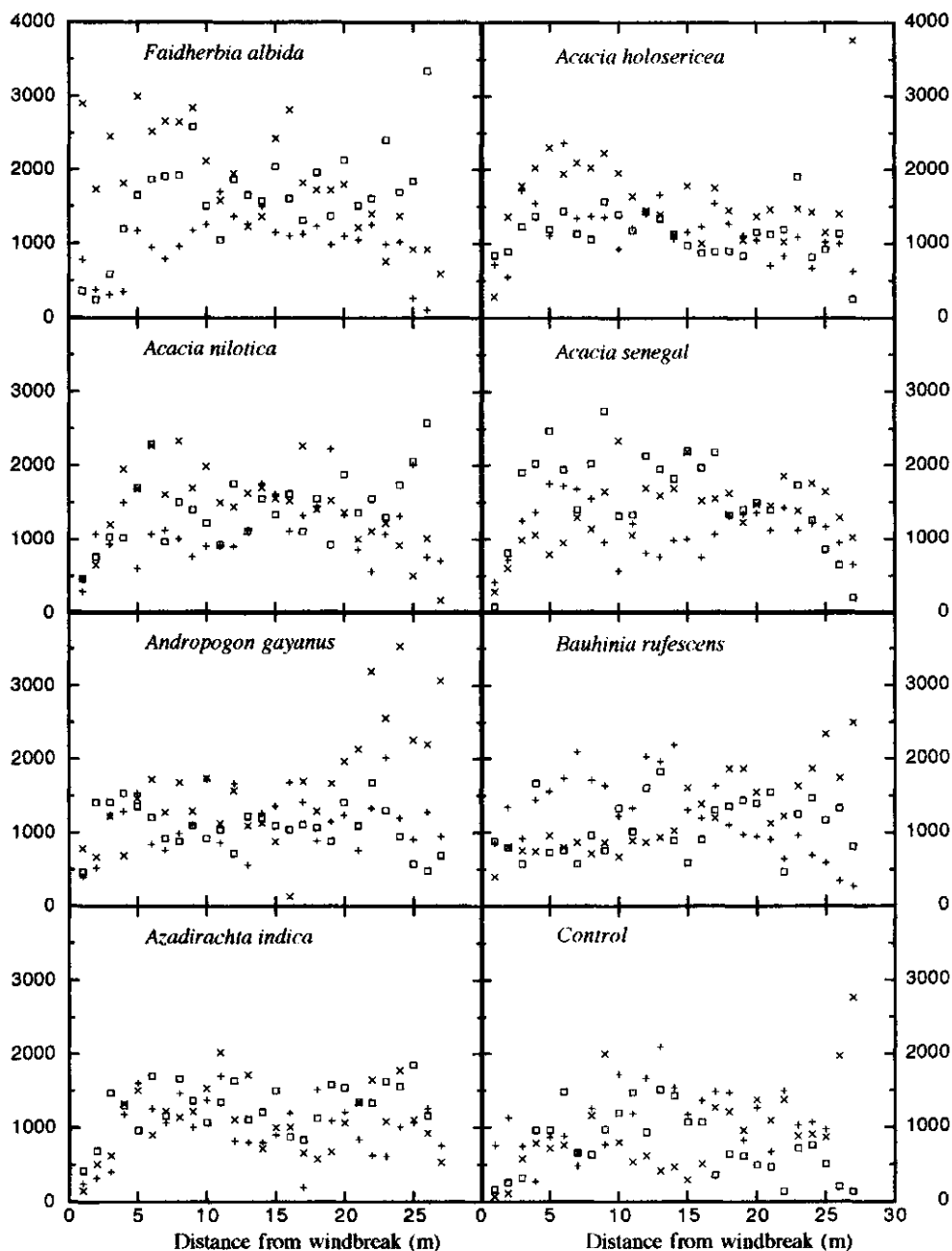
Figure A1-3 Millet straw dry matter in plots with crop residues adjacent 7 windbreak pecies and in the control plot at ISC, Niger, 1993. Biomass is given for block 1 (o), block 2 (×) and block 3 (+).

Appendix B1: Additional equations used in the model

1 Reference evapotranspiration

The Penman (1948) equation to calculate reference evapotranspiration (Eqs. 4.16 and 4.17) consists of a radiation and an aerodynamic term.

The radiation term is calculated according to:

$$R_n = \left(1 - \rho_g\right) \bullet I_g - R_b \tag{B1-1}$$

$$R_b = \sigma_{sb}\left[T_{ae} + 273\right]^4 \bullet \left(0.56 - 0.079\sqrt{e_a}\right) \bullet \left(1 + 0.9\,f_o\right) \tag{B1-2}$$

$$T_{ae} = \frac{T_{max} + T_{min}}{2} \tag{B1-3}$$

with

I_g incoming total global radiation (J m^{-2} soil d^{-1})

R_n net radiation (J m^{-2} soil d^{-1})

R_b net outgoing long wave radiation, according to Penman similar to the one of Brunt (1932) (J m^{-2} soil d^{-1})

ρ_g reflection coefficient of the vegetation for global radiation (albedo), with values of 0.05, 0.15, 0.12 and 0.25 for open water, bare sandy soil, windbreak trees and millet (-), respectively.

σ_{sb} Stefan-Boltzman constant (J m^{-2} soil d^{-1} K^{-4})

f_o fraction of day that the sky is overcast, estimated from the Ångstrom formula (-)

T_{ae} average daytime air temperature (°C)

T_{max} daily maximum air temperature (°C)

T_{min} daily minimum air temperature (°C)

e_a actual vapour pressure during daytime (kPa)

The aerodynamic term of the Penman reference evapotranspiration contains a wind function, e_s and s:

$$e_s = 6.11 \bullet \exp\left(\frac{17.4\,T_{ae}}{T_{ae} + 239}\right) \tag{B1-4}$$

$$s = 239. \bullet 17.4 \bullet \frac{e_s}{\left(T_{ae} + 239.\right)^2} \tag{B1-5}$$

with

e_s saturated vapour pressure during daytime, empirical function after Goudriaan (1977) (kPa)

s the slope of the saturated vapour pressure curve (kPa K^{-1})

In the Penman equation wind functions are often empirically that are implicitly parameterized for effects of roughness of the surface and atmospheric stability. For open water and soil surface we use:

$$f(u) = 0.263 \left(0.5 + BU \bullet u\right) \tag{B1-6}$$

and, for a short, closed grass canopy:

$$f'(u) = 0.263 \left(1 + BU \bullet u\right) \tag{B1-7}$$

with

$f(u)$, $f'(u)$ the wind function after Penman (1956) for open water and short grass canopy, respectively (kg m^{-2} s^{-1} kPa^{-1})

u wind speed (m s^{-1})

BU an empirical coefficient:

$$BU = 0.54 + 0.35\, T_l \tag{B1-8}$$

where the second term corrects for high T_{dif}, i.e. the difference in T_{max} and T_{min} (^oC)

$$T_l = \begin{cases} 0, & \text{if}\left(\dfrac{T_{dif} - 12}{4}\right) < 0 \\[2mm] 1, & \text{if}\left(\dfrac{T_{dif} - 12}{4}\right) > 1 \end{cases} \tag{B1-9}$$

2   Root length distribution function

Integration of the distribution function for root length $\psi(x,z,t)$, Eq. 4.48, is given in detail:

$$\int\limits_{z_0}^{z_0+D(t)} \int\limits_{x_0-\frac{1}{2}W(t)}^{x_0+\frac{1}{2}W(t)} \Psi(x,z,t)\,dxdz = W(t) \int\limits_{z_0}^{z_0+D(t)} \Psi(z,t)\,dz \qquad (B1\text{-}10)$$

with

$$\int\limits_{z_0}^{z_0+D(t)} \Psi(z,t)\,dz = \int\limits_{z_0}^{z_0+D(t)} C\exp\left[-\frac{z-z_0}{p(t)}\right]$$

$$= \left[-\frac{C}{p(t)}\exp\left[-\frac{z-z_0}{p(t)}\right]\right]_{z_0}^{z_0+D(t)}$$

$$= -\frac{C}{p(t)}\exp\left[-\frac{D(t)}{p(t)}\right] + \frac{C}{p(t)}\exp[-0] \qquad (B1\text{-}11)$$

$$= \frac{C}{p(t)}\left\{1-\exp\left[-\frac{D(t)}{p(t)}\right]\right\}$$

so that

$$\int\limits_{z_0}^{z_0+D(t)} \int\limits_{x_0-\frac{1}{2}W(t)}^{x_0+\frac{1}{2}W(t)} \Psi(x,z,t)\,dxdz = \frac{CW(t)}{p(t)}\left\{1-\exp\left[-\frac{D(t)}{p(t)}\right]\right\} \qquad (B1\text{-}12)$$

Appendix B2: Input data for the WIMISA model

Values for the input parameters were derived from experiments at the ICRISAT Sahelian Center (ISC) in Niger and from literature. Many values for crop characteristics could be taken from the input dataset of CP-BKF3 (Verberne et al., 1995), a model developed and calibrated for millet in the Sahel. Those values are marked with (‡) in the corresponding comments of the following input data list. Input parameters, mentioned in Chapter 4 and 5 are given their corresponding symbol names in the comment lines. The input is organized in one file for each subsystem (submodel: e.g. CROP.INP) and a control input file with environmental and management parameters and output specifications. The input list is given in the format of the model source code. The positions of the system components (e.g. of windbreak canopy and roots) are given relative to the left edge of the bare soil part (Fig. 4.4). The keyword "linear" at the end of each table indicates applied type of interpolation.

```
* * * *      CONTROL.INP
*
*            File containing the control parameter settings
* * * *
```

** CONTROL SETTINGS FOR SIMULATION OUTPUT

```
*       output is given when file_name_output = 1, but no output if file_name_output = 0
crop_output = 1
roots_output = 0
soil_water_output = 1
evaporation_output = 1
infiltration_output = 1
drainage_output = 1
micro_climate_output = 0
weather_output = 0
windbreak_output = 1
```

** ENVIRONMENTAL SETTINGS

```
*       If a windbreak is present at the field edge set the following parameter equal to 1 and otherwise
*       equal to zero.
windbreak_present = 0
```

```
*       Latitude (degrees) and altitude (m) of the field to be simulated
latitude = 13.15
altitude = 221.0
```

** OTHER CONTROL SETTINGS here for the year 1993

```
*       First and last day of year for simulation run
first_day = 140
last_day = 265
```

*   *Day of year at which sowing takes place*
day_of_sowing = 157

*   *Depth of sowing , z_0, (m)*
depth_of_sowing = 0.05

*   *Simulation time steps in hours:*
*   *assimilation_time_step :*
*   *Time step to be taken by the assimilation module and the microclimate updates for the*
*   *assimilation .*
*   *soil_water_time_step :*
*   *Maximum time step allowed for the soil water update.*
*   *Within this time step the microclimate is only updated once, but the soil water module is*
*   *automatically updated with smaller time steps if necessary. This time step must be*
*   *smaller than or equal to one hour.*
assimilation_time_step = 0.05
soil_water_time_step = 0.25

* * * *   **MICRO.INP**
*
*   **Input parameter settings for the MICROCLIMATE module**
* * * *

*   *Albedo of the crop and soil , ρ_g, (-)*
albedo_crop = 0.25
albedo_soil = 0.05

*   *Fraction diffuse light coming from other direction than through the windbreak for position*
*   *directly adjacent to the WB-barrier, f_{dif} (-)*
wb_diffuse_light_reduction = 0.5

*   *Relative distance with respect to the height of the windbreak at which wind speed is*
*   *affected,(m)*
wb_relative_distance = 5.0

*   *Reduction factor for wind speed reduction in the area*
*   *where it is affected by the windbreak*
windspeed_reduction_table = 0.0   0.8
                           4.0   0.8
                           4.0001   0.7
                           1000.0   0.7
                           linear

* * * *   **WINDBREAK.INP**
*
*   **Input parameters describing WINDBREAK characteristics needed for**
*   **the soil water balance and calculation of local radiation conditions.**
* * * *

** GEOMETRY

*   *Angle of the windbreak with the north axis , α_w, (degrees)*
angle = 0

* *Position of the left and right edge of the windbreak canopy and the position of the left edge of*
* *windbreak roots (m)*
left_position =   3.5
right_position = 7
roots_left_position = 0

** WINDBREAK PARAMETERS here for the year 1993

*   *Height of the Bauhinia windbreak , H_b, (m) as function of day of year. This is based on*
*   *experimental results at the beginning and end of each growing season in 1993 at ISC*
*   *(Section 3.4). With this parameter the influence of windbreak is switched on or off (set height*
*   *to zero for the whole season).*
tree_height =   1   0
                365   0
                linear
*   *or*
*tree_height = 1   2.0
*   150   2.0
*   161   2.0
*   250   3.0
*   365   3.5
*   linear

*   *Extinction coefficient for total global radiation of tree canopy , k, (-)*
k_extinction_tree = 0.7

*   *Porosity factor of the Bauhinia windbreak , ε_p, (-), as function of day of year (Estimated*
*   *from results of experiment ISC 1993, Section 5.3).*
porosity =   1   0.9
                100   0.9
                150   0.9
                161   0.8
                200   0.6
                250   0.2
                365   0.2
                linear

*   *Water use efficiency, E_w, (kg ha^{-1} mm^{-1}) as function of porosity (after Lövenstein et al.,*
*   *1991, Section 5.3).*
water_use_efficiency =   0   25.0
                             0.2   25.0
                             0.9   20.0
                             1.0   20.0
                                      linear

*   *Potential rate of dry matter production of Bauhinia trees P_{WB}, (kg ha^{-1} d^{-1}), as function of*
*   *day of year, Present version calculates these values as derivative of an approximated Bauhinia*
*   *growth curve (Experiment ISC, Source: Lamers , 1995; Section 5.3).*
potential_dm_rate =   100   0
                       135   29
                       182   1 06
                       245   79
                       275   33

                        linear

*   *Thickness (vertical) of Bauhinia tree root compartments (m) (after Soumaré et al. ,1994,*
*   *Section 5.3).*
roots_compartment_thickness =   1   0.1
                                       6   0.1
                                       linear

*   *Width of the horizontal tree areas (m). (Estimated from data of Soumaré et al., 1994,*
*   *Section 5.3).*
roots_compartment_width =   1   1.5
                               7   1.5
                               linear

*   *Root length density, ($l_R(x,z,t)$ / dx dy dz), (cm cm^{-3}) for 6 layers of the 7 distinguished tree*
*   *root areas (Estimated from data of Soumaré et al. 1994; Section 5.3).*
* *area 1 = a3:*
root_length_1 =   1   1
                       2   16.5
                       3   31.25
                       4   1
                       5   1.75
                       6   1.5
                       linear
* *area 2 = a_2+a_3:*
root_length_2 =   1   5.5
                       2   58
                       3   122.25
                       4   23
                       5   6.75
                       6   11
                       linear
* *area 3 = a_1+a_2:*
root_length_3 =   1   22
                       2   114.5
                       3   239.25
                       4   98.5
                       5   12.5
                       6   25.5
                       linear
* *area 4 = $2a_1$:*
root_length_4 =   1   35
                       2   146
                       3   296.5
                       4   153
                       5   15
                       6   32
                       linear
* *area 5 = a_1+a_2:*
root_length_5 =   1   22
                       2   114.5
                       3   239.25
                       4   98.5
                       5   12.5
                       6   25.5
                       linear
* *area 6 = a_2+a_3:*
root_length_6 =   1   5.5

2	58
3	122.25
4	23
5	6.75
6	11
linear	

area 7 = a_3:
root_length_7 =

1	1
2	16.5
3	31.25
4	1
5	1.75
6	1.5
linear	

*   *Leaf area index of Bauhinia LAI, (-) as a function of day of year (Estimated from*
*   *measured leaf weights of experiment ISC 1992-1993; Section 5.3).*

lai =

100	0.52
157	0.5
265	3.79
300	3.79
linear	

* * * *   **SOIL.INP**
*
*   **Input parameters used for calculation of the soil water balance**
* * * *

** GEOMETRY OF THE SOIL

*   *Field width in horizontal x-direction, W, (m)*
width = 1.0

*   *Distance between two neighboring grid points in horizontal x-direction, Δx,(m)*
deltax = 1.0

*   *Distance between two neighboring grid points in the vertical z-direction , Δz, (m)*

deltay =

1	0.02
2	0.03
3	0.05
4	0.05
5	0.05
6	0.05
7	0.05
8	0.10
9	0.10
10	0.10
11	0.10
12	0.10
13	0.10
14	0.10
15	0.25
16	0.25
17	0.25

```
       18   0.25
       19   0.50
       linear
```

** SOIL PHYSICAL CHARACTERISTICS

```
*        Volumetric soil water content at air dry and wilting, θ_ad and θ_wilt (m^3 m^-3), depending on z
*        index (soil depth) (Experiment ISC 1993 (Section 3.2) and literature (Section 5.4)).
theta_air_dry =  1      0.0167
                19      0.0167
                linear
theta_wilting =  1      0.030
                19      0.030
                linear
```

```
*        Volumetric soil water content at field capacity , θ_f (m^3 m^-3), depending on the z index (soil
*        depth) (Experiment ISC 1993 (Section 3.2) and literature (Section 5.4)).
theta_field  =   1      0.120
                20      0.120
                linear
```

```
*        Volumetric soil water content at saturation, θ_sat (m^3 m^-3), depending on the z index (soil
*        depth) (Bley, 1990, field at ISC).
theta_saturation =      1      0.395
                       20      0.395
                       linear
```

```
*        Initial values for volumetric soil water content, θ_i (m^3 m^-3), depending on the z index (soil
*        depth) (Experiment ISC 1993 (Section 3.2) and Bley, 1990, field at ISC).
theta =                 1      0.02
                        2      0.02
                        3      0.04
                       20      0.04
                       linear
```

```
*        Pressure head at air entry, h_ae (m), for a sandy soil texture class (USDA), depending on
*        the z index (soil depth) (Rawls et al., 1982).
h_air_entry =  1       0.163
              20       0.163
              linear
```

```
*        Power for the matric potential power law for a sandy soil texture class (USDA), C_b,
*        depending on the z index (soil depth) (Rawls et al., 1982).
Campbell_power =   1      1.44
                  20      1.44
                  linear
```

```
*        Power for the conductivity power law, C_k, depending on the z index (soil depth) (Rawls et
*        al., 1982).
conductivity_power =        1      5.88
                           20      5.88
                           linear
```

```
*        Hydraulic conductivity at saturation, K_sat (m s^-1), depending on the z index (soil depth)
*        (Bley, 1990; field at ISC).
```

conductivity_saturation =   1   0.8e-4
                              20   0.8e-4
                              linear

*   *Fraction of rain contributing to run-on. Run-on is not considered in this thesis and set to 0.*
runon_fraction_of_rain = 0.0

*   *Absorption capacity for water of the soil under reference conditions for a sandy soil*
*   *(mm min^{-1}). Reference condition is a completely dry soil. The absorption capacity varies with*
*   *texture class (Verberne et al., 1995). This factor is not considered in the version used for this*
*   *thesis, instead all rain infiltrates (Subsection 4.6.2).*
sorptivity_ref = 7.0

* * * *   **CROP.INP**
*
*   **Input parameter settings for the (millet) CROP module for L2**
* * * *

*   *Table containing for each millet crop row (first column) its distance (m) perpendicular to*
*   *the canopy edge of the windbreak (second column).*
*   *Implicitly the total number of crop rows to be simulated is defined by this table. In the*
*   *geometry of the WB-cropping system the position where the crop field starts is 7 m.*
x_position =   1   7
                 n   (7+n)
                 linear

*   *Crop coefficient for potential transpiration, k_c, (-) (Verberne et al., 1995). (‡)*
transpiration_coefficient = 0.7

*   *Crop row height of millet, h_m, (m) as function of DVS (Experiment ISC 1993).*
crop_height = 0.000 0
               0.185 0.094
               0.197 0.155
               0.215 0.278
               0.268 0.463
               0.306 0.664
               0.332 1.192
               0.511 1.475
               0.793 1.844
               1.156 1.887
               1.293 1.918
               1.407 1.938
               1.564 1.875
               2.000 1.870
               linear

*   *Days from sowing till emergence (Experiment ISC 1993: range of 2-4 days; for*
*   *years with unknown period a value of 4 should be selected).*
days_of_germination = 3
*   *Threshold value of volumetric soil water content ($m^3 m^{-3}$), above which germination*
*   *proceeds. This value corresponds to pF = 4.0 , i.e. just above wilting point (Verberne et al.,*
*   *1995). (‡)*
theta_germination = 0.04

*   *Initial weight of above-ground biomass (DM_0) for every crop row (kg ha^{-1}) (where n denotes*
*   *crop row number) (Experiment ISC 1993 and theory of Carberry et al. (1985), Section 5.5).*

```
initial_dm =    1        30
                2        30
                    ...
                n        30
                linear
```

*   *Development rates d^{-1} for the pre-anthesis (DVR1) and post-anthesis period (DVR2)*
*   *(Experiment ISC 1993, and Verberne et al .(1995), Section 5.5).*

```
dvr_pre_anthesis  = 0.0141
dvr_post_anthesis = 0.0305
```

*   *Correction factor for development rates as function of temperature (Van Kraalingen and*
*   *van Keulen, 1988). (‡)*

```
temp_reduction_dvr_pre =     10.0     0.0
                             25.0     1.0
                             30.0     1.0
                             40.0     1.2
                             linear
temp_reduction_dvr_post =    10.0     0.0
                             25.0     1.0
                             35.0     1.0
                             45.0     0.0
                             linear
```

*   *Reduction factor for dvr_pre_anthesis as function of daylength. (‡)*

```
daylength_reduction_dvr_pr =      0.0     1.0
                                 13.6     1.0
                                 14.3     0.65
                                 24.0     0.10
                                 linear
```

*   *Fraction of assimilates allocated to the various plant organs, F_x (-), as function of*
*   *development stage (Verberne et al., 1995). Using these values results in a distribution of*
*   *aerial dry matter that agrees well with the results of experiment ISC 1993 (Section 5.5). (‡)*

```
fraction_dm_roots =   0.00     0.50
                      0.25     0.50
                      0.50     0.30
                      0.85     0.20
                      1.10     0.00
                      2.10     0.00
                      linear
fraction_dm_shoot =            0.00     0.50
                               0.25     0.50
                               0.50     0.70
                               0.85     0.80
                               1.10     1.00
                               2.10     1.00
                               linear
fraction_dm_leaves =           0.00     0.75
                               0.25     0.65
                               0.50     0.55
                               0.75     0.30
                               0.85     0.20
                               1.00     0.05
                               1.10     0.00
                               2.10     0.00
```

		linear
fraction_dm_stem =	0.00	0.25
	0.25	0.35
	0.50	0.45
	0.75	0.55
	0.85	0.55
	1.00	0.35
	1.10	0.15
	1.20	0.00
	2.10	0.00
		linear

fraction_dm_stem_reserves =	0.00	0.00
	0.50	0.00
	0.75	0.10
	0.85	0.15
	1.00	0.25
	1.10	0.15
	1.20	0.10
	1.30	0.00
	2.10	0.00
		linear

fraction_dm_grain =	0.00	0.00
	1.00	0.00
	1.10	0.30
	1.20	0.55
	1.30	0.75
	1.50	1.00
	2.10	1.00
		linear

fraction_dm_comb =	0.00	0.00
	0.50	0.00
	0.75	0.05
	0.85	0.10
	1.00	0.35
	1.10	0.40
	1.20	0.35
	1.30	0.25
	1.50	0.00
	2.10	0.00
		linear

*   *Reduction factors for the distribution of assimilates to aerial dry matter as function of water*
*   *stress factor, f_{part},(-),(Verberne et al., 1995). (‡)*

water_stress_mass_reduction =	-1.0	0.5
	0.00	0.5
	0.25	0.6
	0.60	1.0
	1.00	1.0
	2.00	1.0
		linear

** CHARACTERISTICS OF INTERCEPTION OF RADIATION AND ASSIMILATION

*   *Extinction coefficient of the crop canopy for diffuse radiation, K_{dif}, (-) (Verberne et*
*   *al., 1955). (‡)*
k_diffuse = 0.53

*   *Extinction coefficient of the crop canopy for radiation, k, (-) (Verberne et al., 1995). (‡)*

k_extinction_crop = 0.50

*   *Initial light use efficiency, ε, $((kg\ CO_2\ ha^{-1}\ h^{-1})/(J\ m^{-2}s^{-1}))$ (McPherson and Slayter, 1973*
*   *cited in van Heemst, 1988). ($\ddagger$)*
light_use_efficiency = 0.38

*   *Reduction of initial light_use_efficiency as function of mean temperature (^oC) (Verberne et*
*   *al., 1995). ($\ddagger$)*
red_light_use_efficiency =   0.0   1.0
    40.0   1.0
    50.0   0.025
    linear

*   *Scattering coefficient of leaves. ($\ddagger$)*
scattering_coefficient = 0.20

*   *Specific leaf area, SLA, (ha kg^{-1}) as function of development stage (Experiment ISC 1993,*
*   *Section 5.5).*
specific_lai =   0.00 0.0022
    0.15 0.0020
    0.40 0.0018
    0.85 0.0014
    1.30 0.0010
    2.10 0.0010
    linear

*   *Specific surface area of stems (ha kg^{-1}) (Verberne et al., 1995). (Erenstein (1990) used*
*   *0.0007; needs further examination). ($\ddagger$)*
specific_lai_stem = 0.0004

*   *Maximum rate of photosynthesis, A_m, depends on the nitrogen concentration of leaves.*
*   *Van Duivenbooden and Cissé (1989) made a regression between A_m and N% leaves, with*
*   *the following slope and intercept: ($\ddagger$)*
assim_N_ratio = 1016.0
assim_N_intercept = -2.50

*   *Reduction factor for assimilation as function of DVS (related to leaf age) (Verberne et al.,*
*   *1995). ($\ddagger$)*
assim_leaf_age_reduction =   0.00   1.00
    1.00   0.80
    1.50   0.40
    2.00   0.00
    2.10   0.00
    linear

*   *Reduction factor for assimilation as function of air temperature (Vong and Murata, 1977; cited*
*   *in van Heemst, 1988). ($\ddagger$)*
assim_temp_reduction =   12.0   0.66
    18.0   0.83
    24.0   0.90
    30.0   1.00
    36.0   0.89
    42.0   0.75
    50.0   0.00
    linear

** MAINTENANCE RESPIRATION

*   *Reference temperature and Q10 for maintenance respiration (Verberne et al ., 1995). (‡)*
reference_temperature = 25.0
Q10 = 2.0

*   *Maintenance coefficients for the various organs, c_m, (kg CH_2O kg^{-1} d^{-1}) (Penning de Vries,*
*   *1975). (‡)*
maintenance_coefficient_leaves = 0.020
maintenance_coefficient_stem   = 0.010
maintenance_coefficient_grain = 0.007
maintenance_coefficient_comb   = 0.007
maintenance_coefficient_roots = 0.007

** GROWTH

*   *Assimilate requirement for the production of 1 kg carbohydrates (kg kg^{-1}) (Verberne et al.,*
*   *1995). (‡)*
effective_hydrocarbons_conversion =1.25

*   *Assimilate requirement for the production of 1 kg proteins (kg kg^{-1}) (Verberne et al.,*
*   *1995). (‡)*
effective_proteins_conversion = 2.25

*   *Leaf longevity in degree days , SPAN, (Experiment ISC 1993, Section 5.5).*
life_span_leaves = 800.0

*   *Base temperature (^oC) for assimilation of leaves (Ong, 1983; cited in van Heemst,*
*   *1988). (‡)*
base_temperature = 10.0

*   *Minimum number of grains per ha (Experiment ISC 1993).*
minimum_number_grain = 8.9E7

*   *Specific number of grains (number grains kg^{-1} aerial dry matter) (Experiment ISC 1993).*
specific_number_grain = 36842

*   *Time constant (d) for translocation of reserves as function of relative amount of reserves*
*   *(Verberne et al., 1995). (‡)*
reserves_translocation =   0.00   50
                                0.05   8
                                0.10   2
                                0.20   1
                                1.00   1
                                linear

*   *Potential growth rate of individual grains, P_G, (kg $grain^{-1}$ d^{-1}) as function of development rate*
*   *and correction factor for effect of temperature (-) (Van Duivenbooden and Cissé, 1989).*
*   *estimated with field data from Nioro du Rip, Senegal). (‡)*
dvs_growth_grain =   0.00   0.00
                     1.00   0.00
                     1.15   0.13
                     1.40   0.30
                     2.10   0.21
                     linear
temp_growth_grain =   20.0   0.90

```
                    30.0   1.00
                    40.0   0.90
                    linear
```

** DEATH

* *Relative death rate of leaves, PERDL, (d⁻¹)(calibrated), and proportionality factor for death*
* *rates of stem and roots (Verberne et al., 1995). For PERDL Verberne et al.(1995) used*
* *0.03.(‡)*

relative_mortality_leaves = 0.04
death_ratio_stem_leaves = 0.6
death_ratio_roots_leaves = 0.5

** DISTRIBUTION OF NITROGEN

* *Maximum nitrogen concentration (kg N kg⁻¹ DM) in the various plant organs as function of*
* *development stage and maximum nitrogen concentration in grains. (Van Duivenbooden and*
* *Cissé, 1989: estimated with field data from Nioro du Rip, Senegal). (‡)*

```
max_N_leaves =      0.00   0.059
                    0.40   0.047
                    1.00   0.036
                    2.00   0.024
                    2.10   0.024
                    linear
max_N_stem =        0.00   0.050
                    0.30   0.042
                    0.40   0.035
                    0.74   0.022
                    1.00   0.021
                    1.60   0.009
                    2.00   0.008
                    2.10   0.008
                    linear
max_N_roots =       0.00   0.020
                    2.00   0.010
                    2.10   0.010
                    linear
max_N_comb =        0.00   0.022
                    1.00   0.022
                    1.60   0.0091
                    2.10   0.0091
                    linear
max_N_grain = 0.025
```

* *Non- remobilizable nitrogen concentration (kg N kg⁻¹ DM) in the various plant organs and*
* *minimum nitrogen concentration in grains (Van Duivenbooden and Cissé, 1989: needs further*
* *examination from literature or field experiments). (‡)*

fixed_N_leaves = 0.005
fixed_N_stem = 0.0015
fixed_N_roots = 0.001
fixed_N_grain = 0.0025
fixed_N_comb = 0.009

* *Potential rate of nitrogen uptake (kg N ha⁻¹ d⁻¹) (Van Duivenbooden and Cissé, 1989: needs*
* *further examination from literature or field experiments). (‡)*

potential_N_uptake_rate = 6.0

*   *Definition of conversion factor from crop weight to root uptake capacity for nitrogen*
*   *(kg DM kg^{-1} N). (‡)*
N_uptake_mass_conversion = 200.0

* * * *   **ROOTS.INP**
*
*   **Inputs for root characteristics of millet**
* * * *

*   *Specific root length, $l_{R,spec}$, (m g^{-1}) (Verberne et al., 1995). (‡)*
specific_root_length = 100

*   *Root radius (cm) (Van Duivenbooden and Cissé, 1989). (‡)*
root_radius = 0.005

*   *Maximum soil water flux into millet roots, q_R, (cm^{-3} cm^{-2} d^{-1}) (Jordan and Sinclair,*
*   *1983). (‡)*
maximum_flux = 0.12

*   *Potential root extension rate, RE_p, (cm d^{-1}) (Azam-Ali et al., 1984).*
potential_rooting_rate = 4.5

*   *Ratio: (2*horizontal root extension) / (vertical root extension) in (cm cm^{-1}), based on Piro*
*   *(1994).*
rooting_extension_ratio = 0.4

*   *Initial rooting depth below sowing depth, z_0, (cm).*
initial_rooting_depth = 0.5

*   *Maximum rooting depth, counted from the soil surface (cm) (Azam-Ali et al., 1984). (‡)*
maximum_rooting_depth = 220

*   *Water uptake reduction factor, $f_{up,C(n)}$, (-), depending on the pF value of the soil. (Van*
*   *Keulen and Seligman, 1987)*
uptake_reduction_table =   0.0   0.00
                              0.5   1.00
                              3.0   1.00
                              4.2   0.00
                              10.0   0.00
                              linear

Appendix B3: Additional simulation results and data

1   Actual soil evaporation in an unshielded millet field

In an unshielded crop field actual soil evaporation was highest in the beginning of the rainy season when the soil has recently been wetted and crop canopy cover was still low.
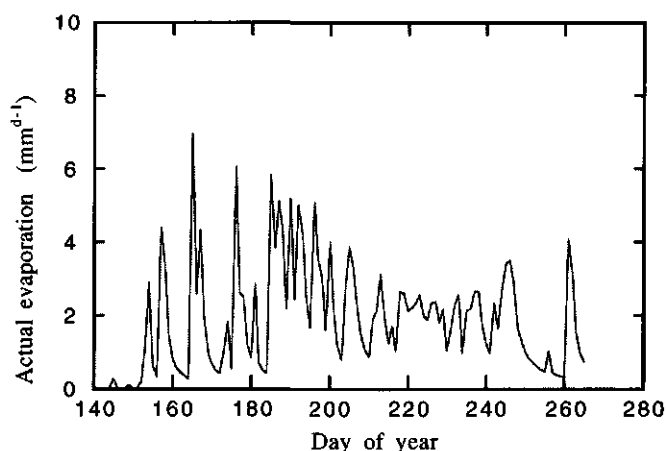
Figure B3-1   Simulated daily actual soil evaporation (E_a) in 1993 at ISC, Niger. For simulation run input dataset of production level 3 (L3) was used.

2.1   Actual transpiration of Bauhinia trees

In an accompanying study on 'water use by windbreak trees in the Sahel' Smith (1995) measured tree transpiration using the heat-pulse technique in *Acacia indica* and *Acacia holosericea* of the windbreak field. Such measurements were not performed on Bauhinia trees, because the method to calibrate the heat-pulse technique did, for unknown reason, not work on the Bauhinia trunk. In this thesis, actual transpiration of Bauhinia (Fig. 6.15), therefore, was compared with transpiration measurements of *Acacia indica* and *Acacia holosericea* (Fig. B3-2).

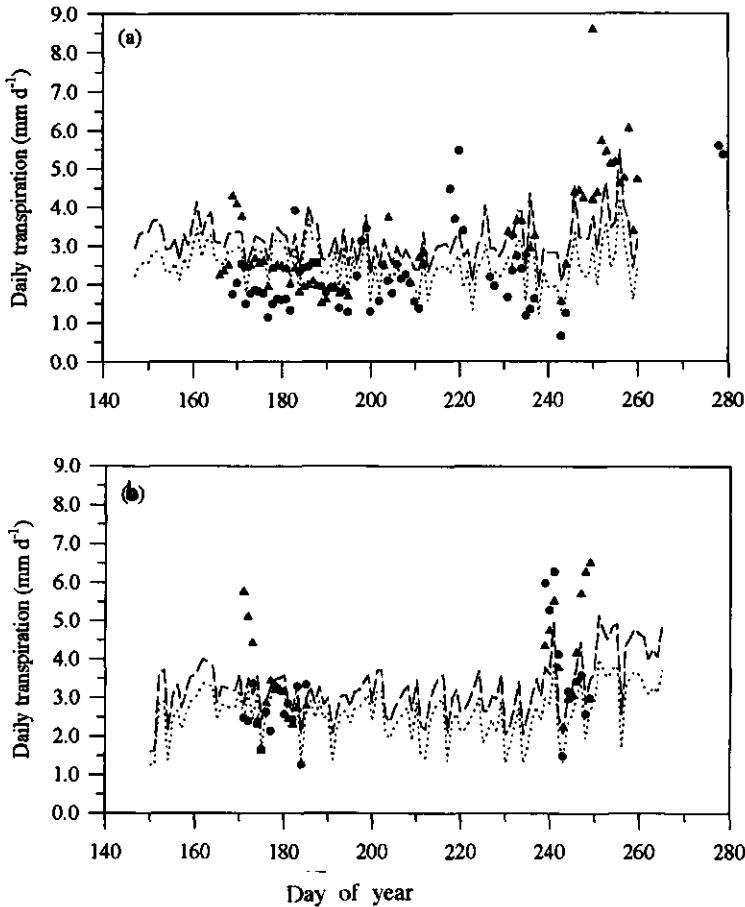**Figure B3-2** Estimated (lines) and measured (symbols) actual daily transpiration for *Acacia indica* (•••; •) and *Acacia holosericea* (---; ▲) for the 1992 (a) and 1993 (b) cropping season, Niger. (Smith, 1995).

Simulation runs with a water use efficiency (E_W) varying from 20 to 25 kg ha^{-1} mm^{-1} during the season showed best results with respect to total seasonal transpiration and maximum daily transpiration (Section 5.3 and 6.4). However, at the onset and end of the season simulated daily transpiration rates ($T_{a,WB}$) differed from the values measured for *Acacia indica* and *Acacia holosericea*. Due to lack of better information on Bauhinia water use or other tree characteristics, no modifications in WIMISA were done. Largest discrepancy between WIMISA estimates and results reported by Smith (1995) was found towards the end of the cropping season: actual transpiration rates of *Acacia indica* and *Acacia holosericea were* enhanced as a result of increasing vapour pressure deficit and expansion of LAI, whereas

Bauhinia showed a strong decrease. WIMISA $T_{a,WB}$ was decreasing due to a combination of decreasing potential rate of Bauhinia dry matter production (P_{WB}) and increasing E_W towards the end of the cropping season (Section 5.3). Whether the assumptions on the time course of P_{WB} are realistic needs further investigations in field experiments. Early in the cropping season, the amount of daily transpiration was generally low (despite the high evaporative demand of the atmosphere), because LAI of trees was low and probably also due to low amount of plant available soil water.

2.2   Competition for water

The influence of tree species on water content
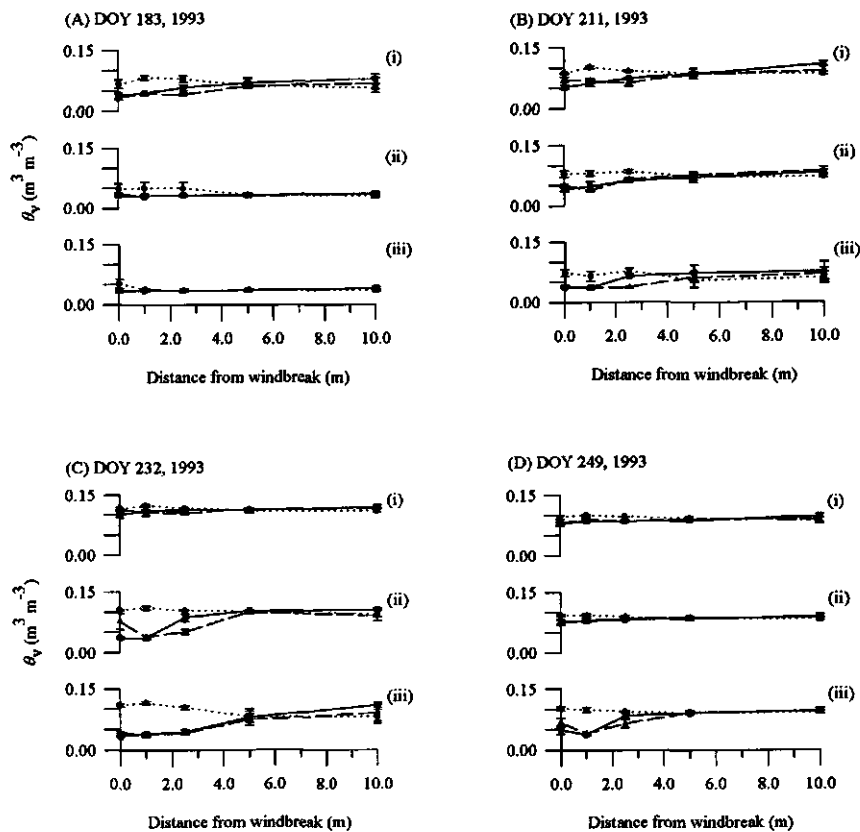
Figure B3-3   Volumetric water content (θ_v) at 0.4, 1.0 and 1.6 m soil depth at several distances from the trunks of *Acacia nilotica* (■—■), *Azadirachta indica* (●···●), *Acacia holosericea* (▲--▲) trees, in windbreaks at ISC, Niger, on selected days from the cropping season 1993. Bars show +-1 S.E.

The influence of tree species on adjacent crop yields
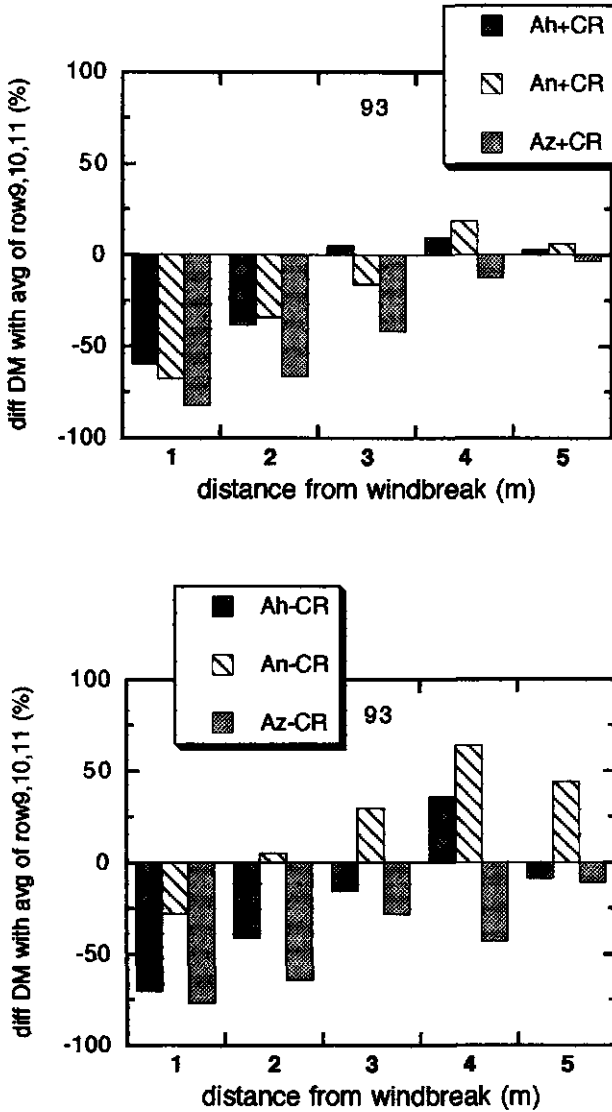
Figure B3-4   Percentage yield reduction at several distances from *Acacia holosericea* (Ah), *Acacia nilotica* (An) and *Acacia indica* (Az) windbreaks in plots A) with (+CR) and B) without (-CR) crop residues at ISC, Niger, 1993. Yields at 1, 2, 3, 4, and 5 m are normalized with respect to yields averaged over the zone 9 - 11 m from the windbreak.

3   Soil water contents in a windbreak-shielded millet field

Time course of volumetric soil water contents (θ_v's) at 1.0 and 1.9 m soil depth are presented
for the rainy season of 1993 at ISC, Niger.
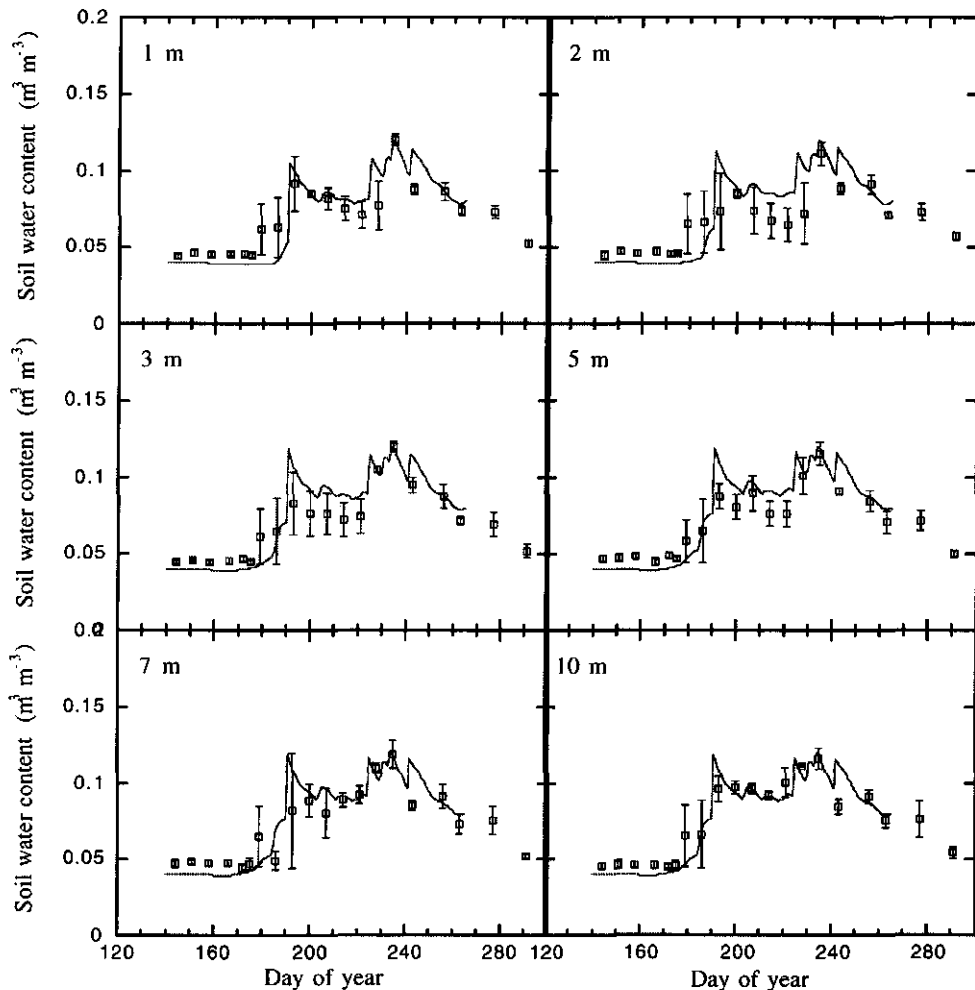
Figure B3-5   Simulated (line) and measured (dots) volumetric soil water content (θ_v) in 1.0
m depth at a distance of 1, 2, 3, 5, 7, and 10 m from the trunk of the WB
trees, 1993 growing season at ISC, Niger. Bars show standard error of
means.
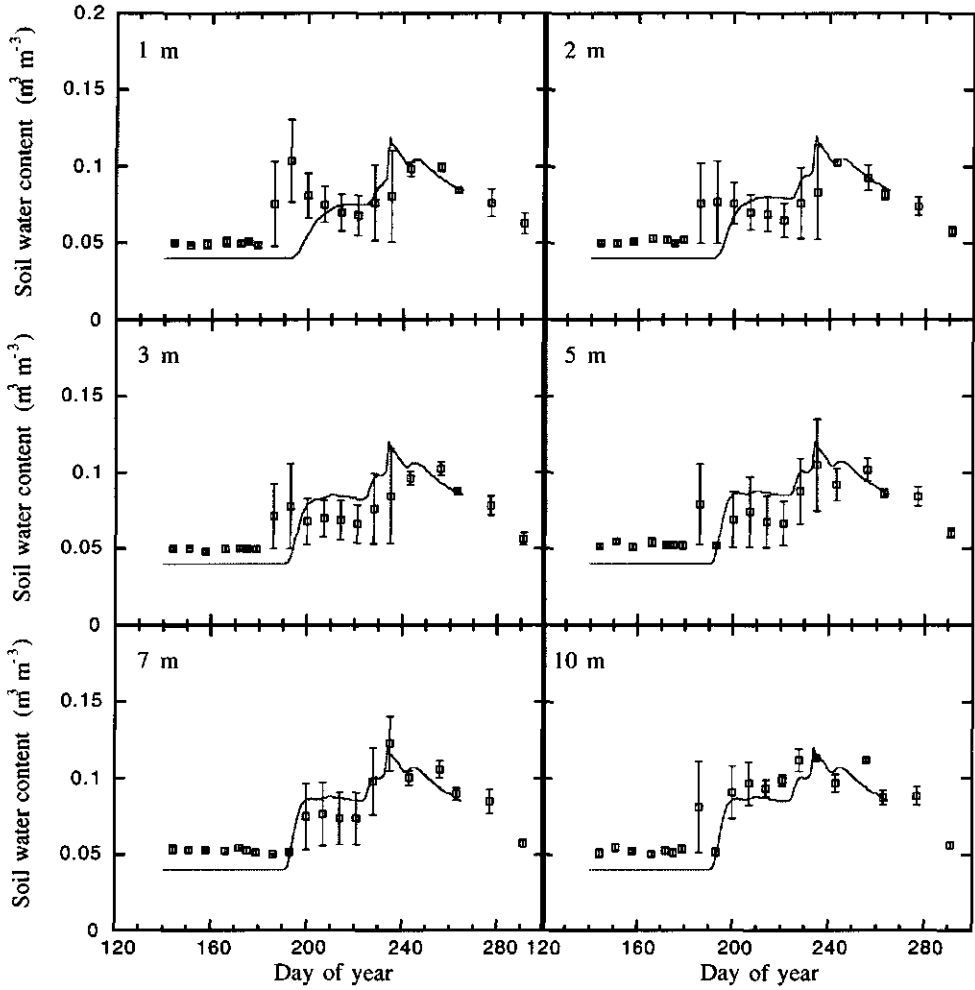
Figure B3-6 Simulated (line) and measured (dots) volumetric soil water content (θ_v) in 1.9 m depth at a distance of 1, 2, 3, 5, 7, and 10 m from the trunk of the WB trees, 1993 growing season at ISC, Niger. Bars show standard error of means.

4   Horizontal water flow q
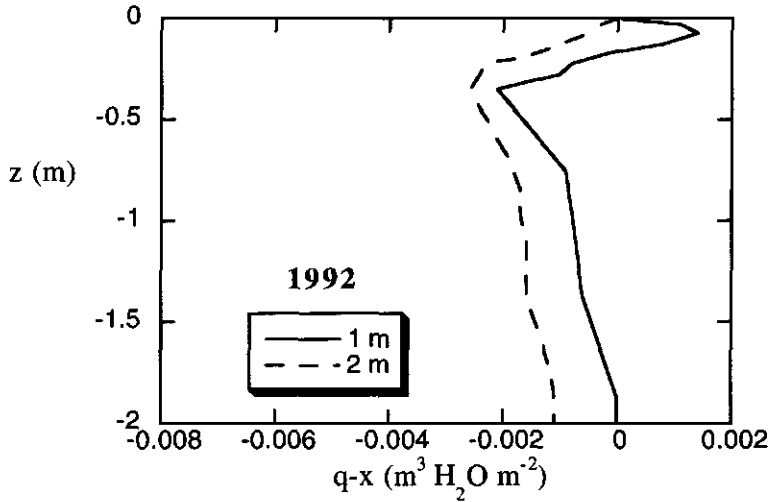
Figure B3-7   Simulated seasonal horizontal water flow **q** with increasing soil depth (z) at a distance of 1 and 2 m from the trunk of the WB trees, 1992, ISC, Niger.
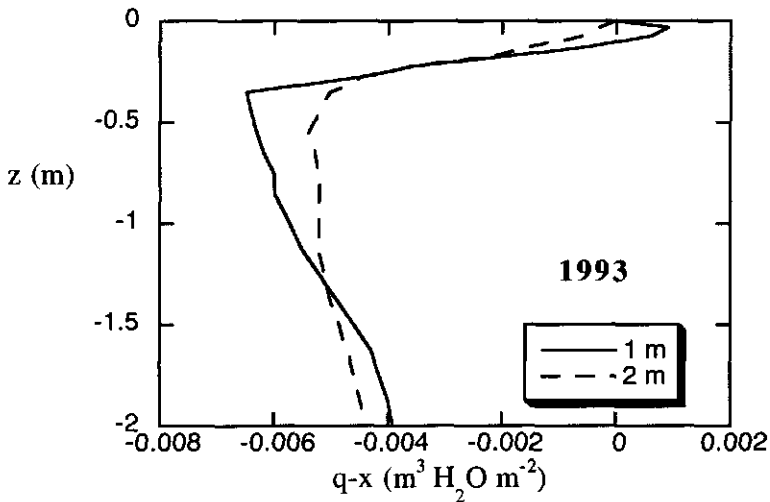
Figure B3-8   Simulated seasonal horizontal water flow **q** with increasing soil depth (z) at a distance of 1 and 2 m from the trunk of the WB trees, 1993, ISC, Niger.

5 WIMISA tested against data from Bley (1990)

WIMISA results for unshielded millet with ISC weather data of 1987 and 1988 were tested against millet field data of Bley (1990). Bley measured biomass production under poor and good soil fertility in the dry year of 1987 and the wet year of 1988. These conditions correspond to the model production level L1, L2 or L3. As described in Section 6.1 input values for DM_0, SPAN, SLA, SSA and LUE have been chosen in correspondence to growth conditions. First simulations runs showed that the values of input parameters needed to be refined to correspond better to the field situation and to approximate the yields found by Bley (1990). Thus, intermediate production levels were defined and a further parameter was added: For L1 the standard value of SSA was replaced by a higher value as used in the millet model of Erenstein (1990) (SSA: 0.0006-0.00083 in ha kg^{-1}) (Table B3-1).

Table B3-1 Suggested sets of parameter values for simulation of production level 1, 2 and 3: initial biomass (DM_0), maximum relative death rate of leaves (PERDL), leaf longevity (SPAN), specific leaf area (SLA), specific stem area (SSA), and initial light use efficiency (LUE).

Production level	Input parameter					
	DM_0	PERDL	SPAN	SSA	SLA	LUE
	kg ha^{-1}	d^{-1}	$^oC d^{-1}$	ha kg^{-1}	ha kg^{-1}	kg CO_2 ha^{-1} $h^{-1}/$ $J\,m^2\,s^{-1}$
water & N limited						
L3	16	0.05	800	0.0004	0.0022 - 0.0010	0.38
L3+	18	0.05	800	0.0004	0.0022 - 0.0010	0.38
water or N limited						
L2	30	0.05	800	0.0004	0.0022 - 0.0010	0.38
L2+	30	0.05	900	0.0004	0.0022 - 0.0010	0.38
L2++	30	0.05	1000	0.0004	0.0022 - 0.0010	0.38
potential-Sahel						
L1-F[1]	30	0.03	1000	0.0004	0.0024 - 0.0013	0.40
L1-F[1]*	30	0.03	1000	0.0007	0.0024 - 0.0013	0.40
L1-E[2]	30	0.03	1000	0.0004	0.0035 - 0.0018	0.40

[1] SLA values reported by Fechter (1993) for CIVT in Tara, Niger. [2] SLA values found by Erenstein (1990) for short and long cycle millet in the 5th region of Mali. * SSA reported by Erenstein (1990).

On the whole, simulations agree reasonable with field data, in particular for -F+CR in 1987 (Table B3-2). In case of a rather good growth situation, (e.g. +F+CR) simulated LAI and total aerial dry matter are somewhat underestimated, while grain yield is overestimated. It appeared that with increasing biomass WIMISA gives increasing HI values, while in the field the opposite was found. Obviously, dry matter distribution functions need to be reconsidered for high production levels.

Table B3-2 Simulated (WIMISA) and measured (Bley, 1990) final harvest results and maximum LAI for several production levels (between L3 and L1-) for the dry year 1987 and wet year 1988 at the ISC. Input values for the various levels are given in table 6.3.

Year, (rain) Production level: WIMISA, Bley		Total aerial dry matter $(kg\ ha^{-1})$		Grain yield $(kg\ ha^{-1})$		LAI $(m^2\ m^{-2})$	
		simulated	measured	simulated	measured	simulated	measured
1987 (411 mm)							
L3,	-F+CR	1921.3	1647	370.2	369	0.54	0.68
	+F-CR		1496		251		0.69
L2++,	+F+CR	3222.7	3953	643.1	777	0.96	1.45
1988 (613 mm)							
L2+,	-F+CR	2682.6	2958	588.5	448	0.73	0.83
	+F-CR		2398		375		0.85
L1-,	+F+CR	5355.4	6018	1185.1	883	1.62	2.45

F denotes fertilizer: 30 kg N, 30 kg P_2O_5 as super phosphate and 30 kg K_2O as kaliumchlorid), + CR denotes crop residues (straw from the year before left on the field): ca. 1.5 - 3 t ha^{-1} in 1987 and ca. 1.5 t ha^{-1} for -F+CR/ +F-CR and ca 3.9 t ha^{-1} for +F+CR in 1988.

6 Actual crop transpiration and water stress

Actual crop transpiration and water stress for unshielded millet increases with production level:
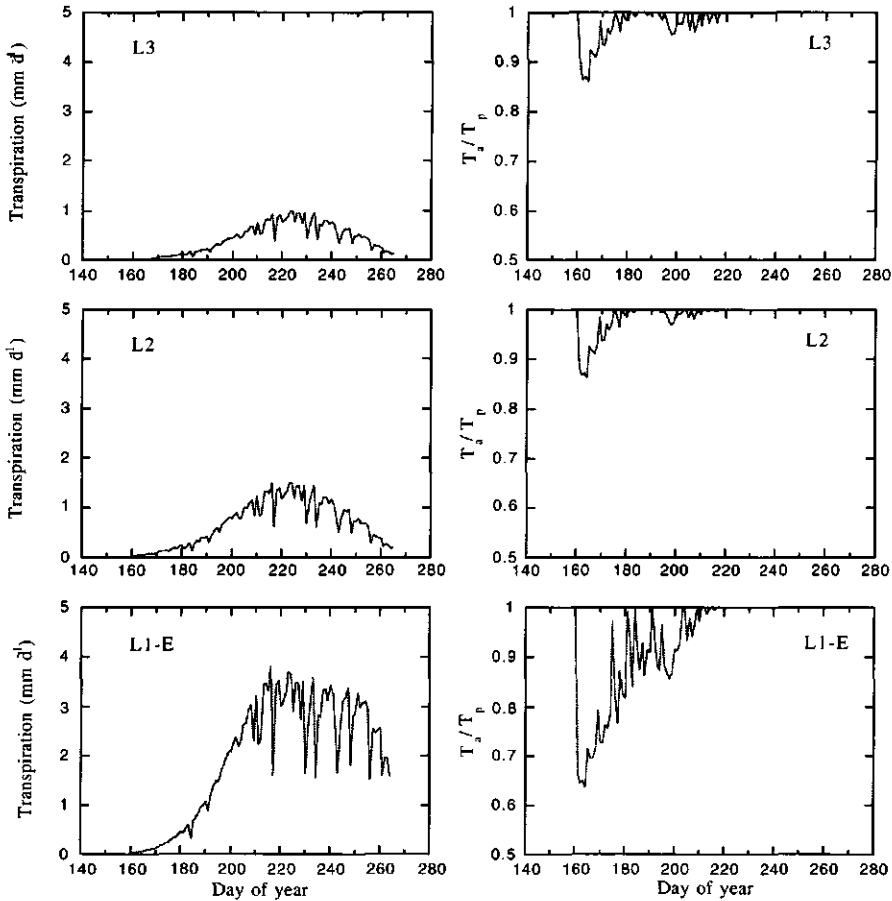
Figure B3-9 Simulated transpiration of millet at production level L3, L2 and L1-E and the corresponding water stress factor T_a/T_p for unshielded crop in 1993.

7   Leaf area index and assimilate production per unit leaf area
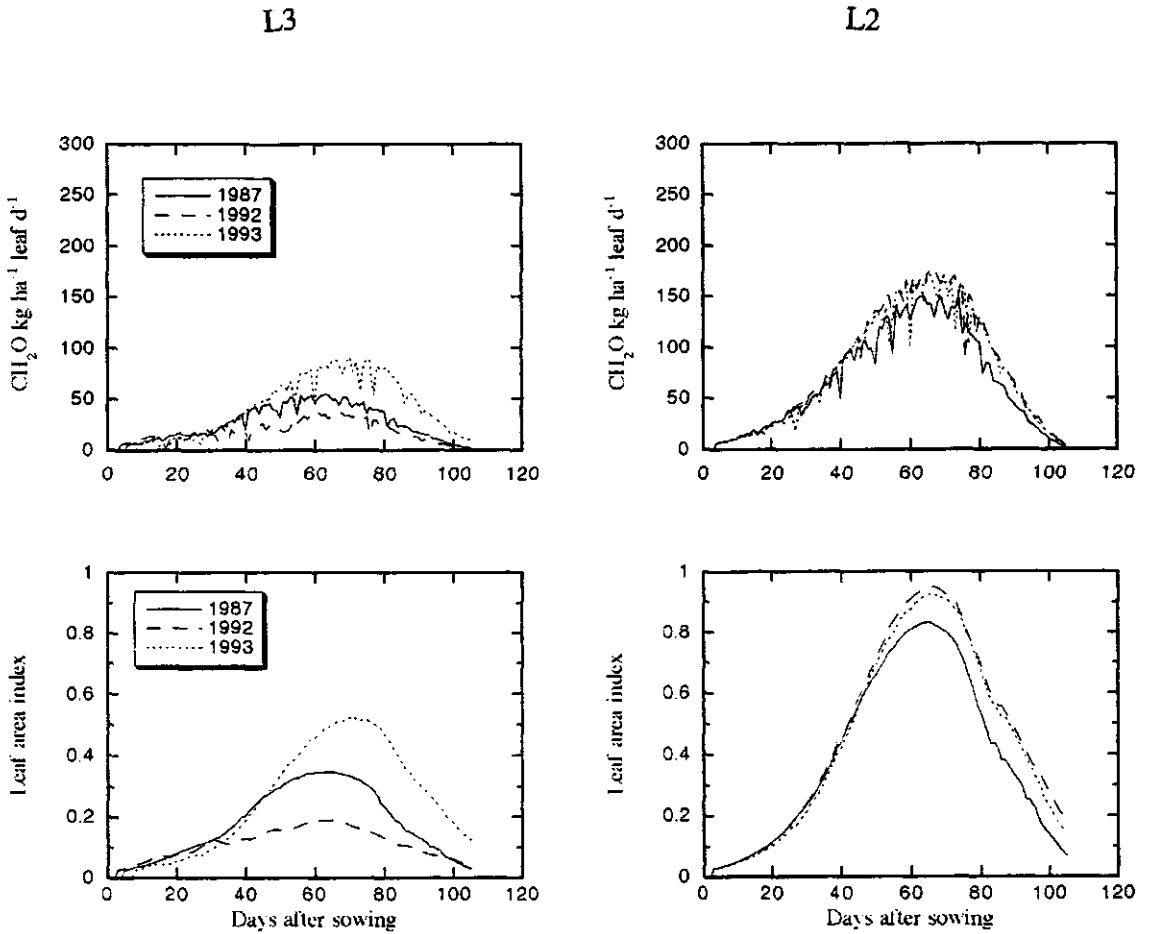
L3   L2

Figure B3-10   Simulated assimilate production per unit leaf and leaf area index of millet at production level L3 and L2 of shielded millet in 1987, 1992 and 1993.

List of abbreviations

Abbreviation	Definition
A	*Andropogon gayanus*
AB-DLO	Research Institute for AgroBiological and Soil Fertility
ANSI C	C standard of the American National Standards Institute
APSIM	Agricultural Production Systems sIMulator
B	*Bauhinia rufescens*
C	Control
CERES	Crop Environmental and REsource Simulation (model)
CIVT	Composite -Inter-Variétal de Tarna: improved variety of pearl millet
CP-BKF3	Cultures Pluviales-Burkina Faso version 3 (model)
+CR	With crop residues
-CR	Without crop residues
DAE	Days After Emergence
DAS	Days After Sowing
DBS	Days Before Sowing
DOY	Day Of Year
DSIR	Department of Scientific and Industrial Research
DVR1, DVR2	DeVelopment Rate pre-anthesis and post-anthesis
DVS	DeVelopment Stage
EPIC	Erosion Productivity Impact Calculator (model)
FUSSIM2	two-dimensional SImulation Model for Flow of water in Unsaturated Soil
H	multiples of the Height of the windbreak
HI	Harvest Index
ICRAF	International Centre for Research in AgroForestry
ICRISAT	International Crops Research Institute for the Semi-Arid Tropics
INTERCOM	simulation model for crop-weed INTERspecific COMpetition
ISC	ICRISAT Sahelian Center
LAI	Leaf Area Index
L1, L2, L3	Production Level 1, 2, and 3
LUE	Light Use Efficiency
PAR	Photosynthetic Active Radiation
PERDL	maximum relative death rate of leaves
RECAFS	model for REsource Competition and cycling in AgroForestry Systems
RH	Relative Humidity
SLA	Specific Leaf Area

SPAN	Leaf longevity
SSP	Simple Super Phosphate
SUCROS	Simple and Universal CROp growth Simulator
SWATRER	Soil Water and Actual TRanspiration simulation Extended
USDA	
WAU	Wageningen Agricultural University
WB(s)	Windbreak(s)
WEPS	Wind Erosion Prediction System (model)
WIMISA	WIndbreak-MIllet SAhel (model)
WaNuLCAS	model for Light, Water and Nutrient CApture in agroforestry Systems

List of symbols

In the list below the equation or subsection number of first occurrence are given in [] and ()
parenthesis, respectively. Vectors are noted with small, bold letters and dimensionless is noted by (-).

Symbol	Definition	Unit	Equation
a	coefficient	(-)	[4.9]
a_R	specific root surface	m^2 root m^{-1} root	[4.53]
at	atmospheric transmission coefficient	(-)	[4.7]
A_m	maximum CO_2 assimilation rate at light saturation	kg CO_2 ha^{-1} h^{-1}	(4.3.1)
b	coefficient	(-)	[4.9]
c_G	carbohydrate demand for grain growth	kg CH_2O ha^{-1}d^{-1}	[4.2]
c_{mx}	maintenance coefficient per unit DM at maximum N-concentration and reference temperature for each plant organ x	kg CH_2O kg^{-1} DM	[4.1]
cv_G	conversion efficiency for carbohydrates into grains	kg CH_2O kg^{-1} DM	[4.2]
C	normalisation constant	(-)	[4.47]
C_b	Campbell's power value for retention curve	(-)	[4.25]
C_k	power value for hydraulic conductivity	(-)	[4.26]
D	depth of millet root compartment	m	[4.48]
D_s	depth below the soil surface	m	(4.6.1)
D_L	death rate of leaves due to water stress	kg DM ha^{-1} d^{-1}	[4.5]
DM_L	dry matter of leaves	kg DM ha^{-1}	[4.5]

DM_R	dry matter of roots	kg DM m^{-2} soil	[4.47]
DM_{WB}	dry matter weight of windbreak	kg DM ha^{-1}	[5.2]
DM_x	dry matter weight of organ x	kg DM ha^{-1}	[4.1]
DVR1	pre-anthesis development rate	d^{-1}	(4.3.1)
DVR2	post-anthesis development rate	d^{-1}	(4.3.1)
DVS	development stage	(-)	[4.4]
e_a	actual vapour pressure	kPa	[4.16]
es	saturated vapour pressure	kPa	[4.16]
E_o	evaporation from open water	m^3 H$_2$O m^{-2} soil s^{-1}	[4.16]
E_{max}	maximum soil evaporation rate	m^3 H$_2$O m^{-2} soil s^{-1}	[4.42]]
E_p	potential soil evaporation rate	m^3 H$_2$O m^{-2} soil s^{-1}	[4.18]
ET_o	potential evapotranspiration rate for a short grass canopy	m^3 H$_2$O m^{-2} soil s^{-1}	[4.17]
E_w	water use efficiency for DM production of trees	kg DM ha^{-1} (m^3 H$_2$O m^{-2} soil s^{-1})$^{-1}$	[4.20]
f(u)	wind function	kg m^{-2} s^{-1} kPa^{-1}	[4.10]
f_o	fraction of the day that the sky is overcast	(-)	[B1-2]
f_{dif}	fraction diffuse radiation coming from other directions than that from the windbreak	(-)	[4.14]
f_{mt}	factor accounting for the influence of temperature on maintenance respiration	(-)	[4.1]
f_{part}	reduction factor for allocation of assimilates to shoots due to water stress	(-)	[4.4]
f_{up}	reduction factor for water uptake due to pF $\geq$ 4.2	(-)	(4.7.3)
$f_{up,C}$	reduction factor for water uptake of the crop	(-)	[4.53]
$f_{up,WB}$	reduction factor for water uptake of the windbreak	(-)	[4.57]
F_{RT}	fraction assimilates allocated to roots	(-)	[4.4]
F_{SH}	fraction assimilates allocated to shoots	(-)	[4.4]
G_a	actual rate of gross assimilation	kg CH$_2$O ha^{-1} d^{-1}	[4.3]
G_p	potential rate of gross assimilation	kg CH$_2$O ha^{-1} d^{-1}	[4.3]
h	soil water pressure head	m	[4.24]
hae	pressure head at air-entry	m	[4.25]
h_m	height of crop row	m	[4.13]
h_s	height of the shadow	m	[4.12]
H	hydraulic head	m	[4.23]
H_b	height of the windbreak	m	[4.11]
I	infiltration rate	m^3 H$_2$O s^{-1}	[4.21]
I_0	total theoretical radiation outside the atmosphere	J m^{-2} soil s^{-1}	(4.4.1)

$I_{0,td}$	total theoretical radiation outside the atmosphere per day	J m^{-2} soil d^{-1}	[4.15]
I_{dif}	diffuse flux of global radiation	J m^{-2} soil s-1	[4.7]
I_{dir}	direct flux of global radiation	J m^{-2} soil s^{-1}	[4.13]
I_g	total measured global radiation	J m^{-2} soil s^{-1}	[4.7]
$I_{g,td}$	total global radiation measured per day	J m^{-2} soil d^{-1}	(4.4.1)
I_i	incident radiation	J m^{-2} soil s^{-1}	[4.8]
$I_{par,dif}$	diffuse flux of PAR	J m^{-2} soil s^{-1}	(4.4.1)
$I_{par,dir}$	direct flux of PAR	J m^{-2} soil s^{-1}	(4.4.1)
I_t	sum of transmitted and reflected radiation	J m^{-2} soil s^{-1}	[4.8]
k	extinction factor for soil cover	(-)	[4.18]
k_c	crop coefficient to relate ET_0 to crop	(-)	[4.19]
K	soil hydraulic conductivity	m s^{-1}	[4.23]
K_{dif}	extinction coefficient for diffuse radiation	(-)	[4.19]
K_{sat}	soil hydraulic conductivity at saturation	m s^{-1}	[4.26]
l_R	root length	m	[4.46]
$l_{R,spec}$	specific root length	m root kg^{-1} root	[4.47]
$l_{R,tot}$	total root length	m	[4.46]
l_s	length of the shadow	m	[4.11]
L_s	length of the soil system	m	(4.6)
LAI	leaf area index	m^2 leaf m^{-2} soil	[4.18]
m	coefficient for van Genuchten equation	(-)	[4.58]
N_G	number of grains per ha	no. grains ha^{-1}	[4.2]
p	proportionality factor for distribution function of root length	m	[4.48]
P_G	potential growth rate of grains	kg DM grain^{-1} d^{-1}	[4.2]
P_{WB}	potential rate of tree dry matter production	kg DM ha^{-1} d^{-1}	[4.20]
PAR	intensity of photosynthetically active radiation	J m^{-2} soil s^{-1}	(4.3.1)
$\mathbf{q}$	rate of water flow	m^3 H$_2$O m^{-2} soil s^{-1}	[4.22]
$\mathbf{q_x, q_y, q_z}$	rate of water flow in x-, y-, z-direction, respectively	m^3 H$_2$O m^{-2} soil s^{-1}	[4.37]
q_R	water flux into roots	m^3 H$_2$O m^{-2} root s^{-1}	[4.53]
r_{mx}	maintenance respiration of organ x	kg CH$_2$O ha^{-1} d^{-1}	[4.1]
R_b	net outgoing long-wave radiation	J m^{-2} soil d^{-1}	[B1-1]
R_n	net radiation	J m^{-2} soil s^{-1}	[4.16]
RD_L	relative death rate of leaves	d^{-1}	[4.5]
RE	root extension rate	m d^{-1}	[4.6]
RE_p	potential extension rate of roots	m d^{-1}	[4.6]
s	slope of the saturated vapour pressure curve at		

	surface temperature	kPa K^{-1}	[4.16]
sink	sum of all sink terms in the soil system	m^3 H$_2$O m^{-3} soil	[4.22]
sink$_{dp}$	sink term deep percolation in the soil system	m^3 H$_2$O m^{-3} soil	[4.36]
sink$_{ev}$	sink term evaporation in the soil system	m^3 H$_2$O m^{-3} soil	[4.34]
sink$_{up}$	sink term root water uptake in the soil system	m^3 H$_2$O m^{-3} soil	[4.35]
source	sum of all source terms in the soil system	m^3 H$_2$O m^{-3} soil	[4.22]
S$_{dp}$	deep percolation	m^3 H$_2$O s^{-1}	[4.21]
S$_{ev}$	evaporation	m^3 H$_2$O s^{-1}	[4.21]
S$_{up}$	root water uptake	m^3 H$_2$O s^{-1}	[4.21]
SW	total amount of water in soil system	m^3 H$_2$O	[4.21]
t$_d$	time, day of the year	(-)	[4.10]
t$_h$	solar time	h	[4.9]
T	soil temperature	°C	[2.1]
T$_a$	actual rate of transpiration	m^3 H$_2$O m^{-2} soil s^{-1}	[4.3]
T$_a$	actual soil temperature at location x$_i$	°C	(2.4.1)
T$_{ae}$	average daytime air temperature	°C	[B1-2]
T$_{dif}$	difference between T$_{max}$ and T$_{min}$	°C	[B1-9]
T$_{max}$	daily maximum air temperature	°C	[B1-3]
T$_{min}$	daily minimum air temperature	°C	[B1-3]
T$_t$	soil temperature averaged over transect	°C	(2.4.1)
T$_p$	potential rate of transpiration	m^3 H$_2$O m^{-2} soil s^{-1}	[4.3]
T$_{p,C}$	potential transpiration rate from the crop canopy	m^3 H$_2$O m^{-2} soil s^{-1}	[4.19]
T$_{p,WB}$	potential transpiration rate from the windbreak canopy	m^3 H$_2$O m^{-2} soil s^{-1}	[4.20]
u	wind speed at 2 m height	m s^{-1}	[B1-6]
U	total root water uptake rate	m^3 H$_2$O m^{-3} soil s^{-1}	[4.44]
U$_C$	root water uptake rate of the crop	m^3 H$_2$O m^{-3} soil s^{-1}	[4.55]
U$_{max}$	maximum root water uptake rate	m^3 H$_2$O m^{-3} soil s^{-1}	[4.53]
U$_{max,C(n)}$	maximum root water uptake rate of crop row n	m^3 H$_2$O m^{-3} soil s^{-1}	[4.53]
U$_{WB}$	root water uptake rate of windbreak	m^3 H$_2$O m^{-3} soil s^{-1}	[4.57]
vol	volume of soil cell	m^3	[4.40]
W	width of root compartment	m	[4.48]
W$_{C(n)}$	width of crop row n	m	[4.56]
W$_s$	width of soil system	m	(4.6)
W$_{WB}$	width of the windbreak	m	[4.57]
x	horizontal coordinate with direction perpendicular to windbreak above and within the soil	m	[4.12]
x$_0$	horizontal coordinate in the center of a crop row	m	[4.48]

x_n	horizontal distance of plant row n from the WB	m	[4.13]
y	horizontal coordinate with direction parallel to windbreak above and within the soil	m	[4.22]
z	elevation head	m	[4.24]
z	vertical coordinate negative downwards	m	[4.22]
z_0	soil depth were root growth starts	m	[4.48]
α	reduction factor for potential crop transpiration due to water availability	(-)	[4.55]
β	solar elevation	degrees	[4.7]
δ	solar declination	degrees	[4.10]
ε	initial light use efficiency of leaf CO_2 assimilation	kg CO_2 ha^{-1} leaf h^{-1}/ (J m^{-2} leaf s^{-1})	[4.8]
ε_p	porosity of the windbreak	(-)	[4.13]
ϕ_{upper}	fluxes across upper cell surface	m^3 H_2O s^{-1}	[4.41]
ϕ_{lower}	fluxes across lower cell surface	m^3 H_2O s^{-1}	[4.41]
ϕ_{left}	fluxes across the left side cell surface	m^3 H_2O s^{-1}	[4.41]
ϕ_{right}	fluxes across the right side cell surface	m^3 H_2O s^1	[4.41]
γ	psychrometric constant	kPa K^{-1}	[4.16]
γ_b	angle of the sun beam with the windbreak line	degrees	[4.11]
λ	latent heat of vaporization of water	J kg^{-1}	[4.16]
λ_a	geographical latitude of the location	degrees	(4.4.2)
σ_{sb}	Stefan-Boltzmann constant	J m^{-2} soil d^{-1} K^{-4}	[B1-2]
θ	soil moisture content	m^3 H_2O m^{-3} soil	[4.22]
θ_{ad}	soil moisture content at air dry conditions	m^3 H_2O m^{-3} soil	[4.22]
θ_f	soil moisture content at field capacity	m^3 H_2O m^{-3} soil	[]
θ_{sat}	soil moisture content at saturation	m^3 H_2O m^{-3} soil	[4.25]
θ_{wilt}	soil moisture content at wilting point	m^3 H_2O m^{-3} soil	[4.61]
ρ_g	reflection coefficient of the surface for global radiation or the albedo	(-)	[B1-2]
ρ_{H2O}	mass density of water	kg H_2O m^{-3}	[4.16]
σ_{sb}	Stefan-Boltzmann constant	J m^{-2} d^{-1} K^{-4}	[B1-2]
ψ	distribution function for root length	(-)	[4.46]
ζ	reduction coefficient for time step	(-)	[4.45]

Curriculum Vitae

Martina Mayus was born on 28 July 1962 in Kranenburg, Germany. She obtained the M.Sc. degree in Agronomy from the Wageningen Agricultural University with specification in Grassland in 1990. During the summer of 1988 she did a practical training at the Scotland Macaulay Land Use Research Institute (Department of Grazing Ecology) Edinburgh, United Kingdom. After a short period, in which she was employed by the City of Amsterdam for developing a project proposal for testing alternative methods of weed managment, she was employed by the University of Hohenheim (Department of Tropical and Subtropical Plant Production), Stuttgart, Germany. Here, she worked on an agroforestry project from 1991 to 1994 for which she did field experiments at the International Crops Research Institute for the Semi-Arid Tropics (ICRISAT), Niger, during the rainy seasons of 1991, 1992 and 1993. Part of that work has been used for this thesis. From September 1994 onwards she worked for her Ph.D. degree at the Erosion and Soil and Water Conservation Group of the Wageningen Agricultural University and developed during this period the simulation model WIMISA.